On the use of sampling methods and spectral signatures to identify defects in inhomogeneous media

Kevish Napal

université PARIS-SACLAY

NNT : 2019SACLX102

Thèse de doctorat

Sur l'utilisation de méthodes d'échantillonnages et des signatures spectrales pour la résolution de problèmes inverses en diffraction

Thèse de doctorat de l'Université Paris-Saclay
préparée à L'École Polytechnique

École doctorale n°574 mathématique Hadamard (EDMH)
Spécialité de doctorat : mathématiques appliquées

Thèse présentée et soutenue à Palaiseau, le 17/12/2019, par

KEVISH NAPAL

Composition du Jury :

Marion Darbas Maître de Conférence HDR, Université de Picardie (LAMFA CNRS)	Rapporteuse
Guanghui Hu Professeur associé, BCSR	Rapporteur
Laurent Bourgeois Enseignant-Chercheur, ENSTA (UMA)	Examinateur
Josselin Garnier Professeur, École Polytechnique (CMAP)	Président
Maya de Buhan Chargée de recherche CNRS, Université Paris Descartes (MAPS)	Examinatrice
Michel Kern Chargé de recherche INRIA, Université Paris-Est (CERMICS)	Examinateur
Houssem Haddar Directeur de recherche INRIA, École Polytechnique (CMAP)	Directeur de thèse
Lucas Chesnel Chargé de recherche INRIA, École Polytechnique (CMAP)	Invité (co-directeur)
Lorenzo Audibert Ingénieur de recherche, EDF (PRISME)	Invité (co-directeur)

Remerciements

Tout au long de cette thèse, j'ai été épaulé par trois personnes qui m'ont été d'une aide précieuse. Je tiens à leur exprimer en ces quelques lignes ma profonde gratitude. Houssem, Lucas, Lorenzo, merci! J'ai eu beaucoup de chance de pouvoir compter sur vous pendant ces trois dernières années. Merci Houssem pour la confiance que tu m'as accordée pendant la thèse. Travailler avec toi m'a permis de développer d'avantage mes intuitions mais aussi de les poser sur papier avec plus de rigueur. Merci Lucas pour ta générosité et ta bienveillance. Tu n'as jamais hésité à mettre la main à la pâte aux moments les plus intenses et je t'en suis très reconnaissant. Merci Lorenzo pour tes conseils sur la partie numérique de ma thèse ainsi que le temps que tu m'as accordé pour déboguer mon code.

Je remercie Marion Darbas et Guanghui Hu d'avoir accepté de rapporter cette thèse. Il m'a été très agréable de retrouver dans vos rapports les moindres petites remarques que j'avais jetées telle une bouteille à la mer dans mon manuscrit.

Je suis honoré que Laurent Bourgeois, Josselin Garnier, Maya de Buhan et Michel Kern aient accepté de faire partie de mon jury. J'espère que vous parviendrez à venir sans encombre jusqu'au lieu de la soutenance malgré les grèves en cours.

Travailler au CMAP a été une expérience très agréable. J'y ai rencontré des personnes passionnées avec qui il a été très stimulant d'échanger. Il y règne aussi une grande camaraderie entre les doctorants. Merci à vous tous pour l'atmosphère chaleureuse que vous apportez en ce labo. Je remercie également Nasséra, Alexandra, Marie et Hanadi qui m'ont toujours guidé avec patience dans mes démarches administratives.

Je remercie mes colocs Eugène, Céline, Heythem et Frédéric pour les bons moments et les fous rires que nous avons eu ensemble. Refaire le monde autour d'un dîner, parties endiablées de FIFA, les délires Ginosajiques, les plantations désastreuses de tomates et de piments, le chat d'Ambra, notre boulangerie adorée, la vie des ballons, l'étude détaillée de la combustibilité des différents rhums pour de meilleures bananes flambées... sont autant de bons souvenirs que je garderai de mes trois années passées avec vous au 78 ter.

Je remercie mes professeurs qui ont entretenus mon intérêt pour les mathématiques et qui m'ont également soutenu lors de mon cursus, je pense à Mme Thieullen, M. Moussa et M. Adelman en écrivant ces mots.

Je remercie Mathieu qui m'a si souvent offert le gîte et le couvert après avoir vadrouillé jusque tard sur Paris en compagnie des infatigables Flavio, Philippe et Xavier. Certains savent à quel point je lui dois bien plus que ça...

Je remercie Rémi pour sa présence aux moments où j'en avais le plus besoins. Nous avons été dans le même bateau depuis notre rencontre aux journées de cohésions des doctorants. Surmonter ensemble les difficultés de la thèse m'a été d'une grande aide.

Je remercie Frédéric de m'avoir transmis son amour pour l'escalade, nos multiples séances communes, accompagnées de ses conseils avisés me seront d'une grande utilité pour gravir les Rocky Mountains.

Je remercie Fedor qui ne m'a jamais refusé une pause en salle café. Les moments que j'y ai passé à discuter de mathématiques avec lui ou bien à l'écouter raconter des anecdotes croustillantes sur Dumas, Pouchkine et bien d'autres, à toujours été un vrai plaisir.

Je remercie Florian d'avoir partagé avec moi sa passion pour le yoga. Promis, notre voyage annulé pour l'Inde n'est que partie remise!

Je remercie Charlotte pour les répétions de blues que nous avons faites ensemble, ces moments ont été pour moi de vrais échappatoires.

Je remercie mes amis d'enfance Baptiste, Marie-Anne et Damien qui ont toujours répondu présent lorsque je rentrais au bercail.

Je remercie la team Mauricienne, Guillaume, Natasha, Kishan B., Trishka, Kishan N., Evans, Davis, Sébastien, Rubina, Warren. Nos immanquables rendez-vous me permettent de vivre notre culture et de perpétuer nos traditions.

Enfin je remercie ma famille qui a toujours été présente pour moi; mon grand frère et sa femme qui ont été de très bon conseil pour mes choix d'avenir; mon père et ma mère qui sont toujours aux petits soins; et enfin ma soeur qui a si souvent fait mine d'être intéressée lorsque je lui parlais de mathématiques.

Contents

General introduction

English version

State of the art

Research related to inverse acoustic and electromagnetic scattering problems has undergone several developments since the first work on sonar and radar in the early 20th century. These two techniques, that allow to detect a target and estimate its position, became quite well mastered during the inter-war period. Subsequently, the possibility of determining the nature of the target, for example to distinguish a submarine from a whale, was quickly considered. First attempts in this direction encountered several difficulties. Firstly, this identification problem is non-linear due to possible multiple reflections (reflections between the components of the target, diffusion, etc.). A second complication lies in the ill-posedness of the problem. For instance small differences in the noise level in the data may lead to very different solutions. These difficulties have been overcome on the one hand thanks to technical advances in the computer industry facilitating access to increasingly high-performance computing machines, and on the other hand thanks to the development of the mathematical theory of inverse problems since the 1960s. Among the long list of contributors to the theory of inverse problems we mention Tikhonov [118, 117], D.L. Phillips [107] and Keith Miller [100]. These advances have provided the opportunity to develop a myriad of inversion techniques that have had an impact in various fields such as geophysics, medicine and non-destructive testing [17, 2, 48, 50].

The physical theory of scattering problems was already at maturity before the invention of the radar and the sonar. The illumination of an object with an incident wave produces a scattered field which is fully described by the Maxwell equations in the case of electromagnetic waves, and by the Helmholtz equation in the case of acoustic waves. More precisely the scattered field is the solution to a Partial Differential Equation (PDE) with the incident field as right hand side. The PDE depends on parameters related to the physical properties of the obstacle such as the shape and according to the problem under consideration, the refractive index, the Lamé coefficients, the conductivity, the permittivity, etc. The problem of determining the scattered field for a given incident wave and from the knowledge of the obstacle and its physical parameters, or in other words solving the PDE, is referred to as the direct problem. The direct problem is well posed and there are many ways to solve it numerically. One of the most efficient numerical approximation, the boundary elements method, is based on so-called integral equation methods. The integral equation methods consist in reformulating the PDE, which is initially formulated in the whole space, into an integral equation defined on the obstacle boundary. We refer the reader to [102] for an overview of integral equation methods. Implementations of the boundary elements method can be found in [40] for both acoustic and electromagnetic problems. Conversely to the direct problem, when the physical parameters are unknown, the problem of retrieving the latter from at least one pair of the solution and the corresponding right hand side of the PDE, is referred to as the inverse problem. The active procedure allowing to collect the data to solve the inverse problem is simple: interrogative waves are sent into the probed domain and the

resulting scattered fields are measured via receivers. When the distance between the receiver and the target is of the order of the wavelength, then the measurements are referred to as near field data. If the distance is large enough, we rather use the far field pattern, a coefficient which appears in the first order of the asymptotic development of the scattered field with respect to the distance to the source location. The far field depends on the direction of observation. If we moreover consider the far fields obtained for incident plane waves, it is obtained a data which hence depends on two variables on the unit sphere. There are also other possibilities for placing the receivers, for example they can be arranged on a plane or on the surface of the probed domain (while probing waveguides for instance). The primary issue before trying to solve the inverse problem is to know if the accessible data allows to characterize the parameters of interest. Positive answers are given for the problem of finding the shape of the obstacle, the refractive index, but also for many other problems [115, 75, 84, 108, 58, 97]. In the following, we review some inversion methods using far field pattern.

For a long time, because of the difficulty of the problem, it has been more convenient to distinguish two categories of inverse problems. The inverse obstacle problem which is dedicated to inverse problems related to impenetrable obstacle, and the inverse medium problem which is devoted to inverse problems related to penetrable inhomogeneities. This distinction is due to the fact that the first inversion algorithms were strongly based on the mathematical model describing the scattering problem. A first approach has been to linearize the problem, reducing it to the problem of solving a linear integral equation of the first kind. This approach is known as the Kirschoff and the physical optics approximation for the inverse obstacle problem, and as the Born and Rytov approximation for the inverse medium problem. These approximations are attractive because of their mathematical simplicity, and have proved to be efficient for many applications such as tomography [14, 39, 52, 91] and synthetic aperture radar [36, 16]. However, the linearized models have an important weak point: since the nonlinearity of the scattering problem is ignored, they are not guaranteed to be acceptable in complex media. Among the first works preserving the non linearity of the inverse problem we can mention [74, 120], which have been followed by many others that moreover addressed the ill-posedeness nature of the inverse problem [64, 78, 67, 65, 98, 57]. All of the proposed techniques in these works belongs to the class of iterative methods which require to solve the direct problem several times, by implementing optimization techniques such as least squares methods [116], Newton's method [68, 69, 70], quasi-Newton methods [51], level set methods [21]. More precisely, starting from some initial guess for the target, updates of this guess are obtained by solving multiple times the direct problem in order to fit to the observable data. Although these techniques give good results, it is difficult to use them for industrial applications. Indeed, they are very expensive in terms of cpu time and hence cannot be used in real-time imaging applications e.g. monitoring the evolution of a material, medical application that requires the presence of the patient, etc. Another major disadvantage of these methods is that their implementation requires strong a priori information on the object, such as the number of connected components, in order to choose a good parameterization and initialization. A new class of inversion techniques, such as the sampling and probe methods, tried to relax the required a priori information and reduce the computational cost, at the price of extracting less information from the probed material. Typically, these methods do not require to solve the direct problem. Instead, they define some indicator function which provides information on the location, shape and properties of the unknown object. To mention some of these methods, we can cite the probe method [73], the singular-source method [12] and the Linear Sampling Method (LSM) [46]. A survey of these methods can be found in [109].

We are interested in more recent techniques that have improved the first version of the LSM while extending its range of applications. The LSM can be referred to point sampling methods;

it provides a scheme to decide if a chosen point $z \in \mathbb{R}^3$ is in the interior of the scatterer or not. The original formulation of the LSM is based on the knowledge of the far field operator F, an integral operator with the far field pattern being its kernel. According to the uniqueness results mentioned above, F contains all the information on the probed object. The LSM more particularly intends to extract these information from the spectrum of F. In a few words, it relies on the solvability of the far field equation, a linear ill-posed equation involving F and whose right hand side depends on the parameter $z \in \mathbb{R}^3$. The study of this equation yields an indicator function for the support of the obstacle. However, the numerical implementation of this method, relying on a Tikhonov regularization of the far field equation, does not give access to the exact predicted indicator function. Despite this weak point, the LSM has been attractive because various numerical simulations proved it can be reliable in a first approach to localize an inhomogeneity and/or determine the number of its connected components. Furthermore, the fact that the described algorithm can be used regardless to the nature of the probed domain is also a significant advantage over optimization methods. The theoretical weak point of the LSM is addressed by the well known Factorization Method [79, 80]. It roughly consists in replacing the far field equation by another one, which yields to a numerically tractable indicator function. FM first proved its effectiveness for impenetrable obstacles [79], then for inhomogeneous media [80, 81]. Since then, FM has been extended to numerous academical inverse problems [83]. More recently, many works contributed to justify FM for more complex backgrounds, allowing one to implement it in practical applications such as geophysics or nondestructive testing [72, 71]. We also mention the articles [86, 15, 122] where scatterers made of both impenetrable obstacles and inhomogeneous medium are considered. These works raise new questions concerning the possibility to distinguish the impenetrable obstacle from the inhomogeneous medium. More recently, an alternative solution to overcome the weak point of the LSM has been provided by the Generalized Linear Sampling Method [10]. The classical Tikhonov regularization of the far field equation is replaced by new regularization schemes which provides an exact characterization of the support of the obstacle. Furthermore, the GLSM has also broaden the application of the LSM by identifying the appearance of defects in a material [9, 8].

From the beginning of the LSM, which was first studied for Dirichlet obstacles, it was pointed out that some specific values of the wavenumber k should be avoided. Indeed, the justification of the method requires that at the considered wavenumber, all far fields obtained for all incident plane waves must be dense in the space of the square integrable functions on the unit sphere of $\mathbb{R}^3$. It is shown in [46] that this result is only valid when k^2 is not a Dirichlet eigenvalue for the Laplace operator in the obstacle support. We illustrate in Figure 1 the fact that this restriction on the wavenumber is not superfluous. For a Dirichlet obstacle made of two non intersecting disks of radius $r_1 = 1$ and $r_2 = 2$, we generated two set of far field data respectively obtained with slightly different wavenumbers. The image on the left shows the LSM results for $k_1 = 4$ and the one on the right for $k_2 = 4.33$. According to the principle that waves with wavelength $\lambda = 2\pi/k$ should allow to recover obstacles that have dimensions of the same order of λ, the presented results are doubly striking. First, in the image on the right, the small disk is better recovered than the large disk. Secondly, in the image on the left, the reconstruction of the obstacle is sharper while the wavelength used is larger. This undesired effect is due to the fact that k_2^2 corresponds to a Dirichlet eigenvalue of the Laplace operator on the disk of radius $r_2 = 2$. The adaptation of the LSM to penetrable obstacles [47, 77] led in a similar way to a restriction on the wavenumber. The latter must be chosen so that the so-called Interior Transmission Problem (ITP), a boundary value problem coupling two PDEs on a domain corresponding to the support of the inhomogeneity, is well posed. Thus the equivalent of Dirichlet eigenvalues for a penetrable medium correspond to the spectrum of the ITP which are referred to as Transmission Eigenvalues (TEs). Therefore, one of the main issues was to show that the set of TEs is at most

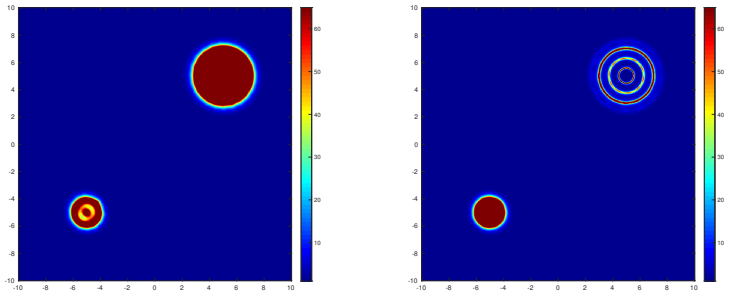

Figure 1: Implementation of the LSM to find a Dirichlet obstacle consisting of two non intersecting disks $r_1 = 1$ and $r_2 = 2$. The reconstruction is conducted for two sets of far fields generated at different wavenumbers $k_1 = 4$ (left) and $k_2 = 4.33$ (right). k_2^2 corresponds to the first Dirichlet eigenvalue of the large disc (to the nearest hundredth). In the image on the right, the inclusion in the top right is abnormally poorly reconstructed.

discrete in order to ensure the efficiency of the LSM at almost every frequency. This has first been proved for spherically stratified media [47], for which the problem can be studied through algebraic equations involving Bessel functions. This result has then been proved in a more general case in [43, 113]. The question of the existence of TEs was considered much later and for a long time, the only known result was that real TEs do not exist for dissipative media (i.e. with complex valued refractive index). Answering the question of existence is not easy since the ITP is neither elliptic nor self-adjoint. Moreover, the discrete nature of the TEs was sufficient to accredit the use of the LSM. Some recent works brought the need for showing the existence of TEs: it has been established the possibility of computing TEs from far field data [28] and obtaining qualitative information on the physical properties of the material surveyed from the knowledge of TEs [31, 25]. Proof of the existence of at least one real TE in the general case is provided in 2008 by Päivärinta and Sylvester [104] assuming that the refractive index is sufficiently large. This result is complemented in the work of Cakoni, Gintides and Haddar [33], where it is demonstrated the existence of an infinity of real TEs while removing the condition on the refractive index.

After these results, a growing attention has been given to TEs and also to their use for solving the inverse problem. The assumption on the refractive index have been constantly relaxed. For long time, it has been required to exclude material with changing sign contrast, whereas such problems arise in practical application, for instance in thermoacoustic tomography [61]. The study of ITP with cavities [26] has been the first to cope with this difficulty. The use of the notion of T-Coercivity which have been initially developed for problems involving metamaterials [38] has significantly weakened the condition on the contrast. Indeed, it has been shown in [37] the discreteness property of TEs with the only condition that the contrast does not change in a vicinity of the boundary. The same assumption is made in [112] where the refractive index is moreover allowed to be complex valued. In the latter work, a complete characterization of the whole spectrum of the ITP (including complex TEs) is made. To conclude on the properties of TEs, we also mention the Weyl-type asymptotic estimates for the counting function [111, 56, 89, 90, 105] and the results on the localization of TEs in the complex plane [60, 89, 106]. Finally, the different developed frameworks to study ITP problems have been extended to the Maxwell equations [53, 35, 49]. In parallel to all these works, several contributions have proven the relevance of using TEs to solve the inverse problem. First of all, the theoretical justification of the determination of TEs which have been relying on the LSM was not satisfactory because of the mentioned inherent weak point of the LSM. The determination of TEs has been enhanced by new methods such as the GLSM and the inside-outside duality [10, 85, 93, 94, 95]. Secondly, many works proposed techniques using TEs to find estimates on the material properties

[22, 31, 63, 66, 32]. We also mention the interesting work on invisibility [54] which makes use of the existence of TEs to propose applications in stealth technology. The physical coefficients of a material are prescribed in order to make it invisible to any observer trying to detect it with far field measurements. The recent works on the use of TEs for the inverse problem has focused on simplifying the link between TEs and the physical parameters. This initiative is explained by the fact that recovering sharp information from TEs is not an easy task, and hence limits the information that can be obtained. The main difficulty of using TEs relies in the fact that they cannot be viewed as the spectrum of a selfadjoint operator. To overcome this difficulty, it was suggested in [6, 30, 5, 41] to rather consider a modified spectrum that we refer to as Relative Transmission Eigenvalues (RTEs) and that can still be computed from far field data. The idea consists in introducing an artificial background that can be chosen by the observer. The RTEs correspond to the spectrum of a new transmission problem, the Relative Transmission Problem (RTP), which indicates that at RTEs, there exists an incident field such that the far field resulting from the effective background and the one resulting from the artificial background are arbitrarily close. The advantage of using RTEs is that they depend on the artificial background which can be fit as desired, in accordance with the problem under consideration. Hence choosing the appropriate setting for the artificial background components, such as the position, the geometry, whether they are penetrable or not and the corresponding refractive index or boundary conditions, can greatly simplify the link between the RTEs and the parameters of interest.

Outline of the thesis

We are interested in the use of ultrasound to detect and localize the presence of undesired inclusions in an investigated material. This issue has its importance in various fields. To cite some relevant examples, we can mention the monitoring of the level of degradation of certain structures from civil engineering such as bridges, buildings, rails; the detection of anomalies in biological tissues in order to diagnostic diseases; the probing of soils when searching for instance natural or anthropogenic cavities, networks, buried objects or underground anomalies. Many scattering problems can be modeled by the equation of linear elasticity, which is usually valid when strains and stress levels are small. Considering only the longitudinal waves, the elasticity equation can be simplified into the Helmholtz equation. We rely on the latter equation and measurements of the far field operator to develop inversion algorithms for our monitoring problem. The types of defect we are interested in are impenetrable obstacles. Both cases when the latter has a non empty interior and when it has an empty interior are considered. More attention is paid to sound hard defects which correspond to obstacles with Neumann boundary conditions since it is a rather realistic model for cracks. The chosen working frequency depends on the size of the defect we want to detect, in order to capture the signature of the defect in the measured data. A classical difficulty while imaging heterogeneous media is that in case of high contrast or presence of inclusions before the degradation, it is difficult to distinguish the contribution of the defect in the collected data. A solution to this difficulty has been proposed by the Differential Linear Sampling Method (DLSM) [9]. This method has originally been set up to identify a modification in the refractive index in an inhomogeneity, and reasonably rely on differential measurements, i.e. both measurements before and after the appearance of the defect. We adapt the DLSM for our purpose in chapter 2 where sound hard defects of empty interior are considered, and in chapter 4 where sound hard defects of non empty interior are considered. The DLSM relies on the results of the GLSM whose proper performance, as stated above, requires the well posedness of the ITP. Consequently, the adaptation of the DLSM to our problem has led us to study two different ITPs. The first ITP corresponds to inhomogeneities

with sound hard obstacles of empty interior which is studied in 3. The second ITP corresponds to inhomogeneities with sound hard obstacles of non empty interior which is studied in 5. In a final chapter 6, we develop two techniques allowing to monitor highly damaged backgrounds made of small crack networks. We more precisely provide a way to estimate what we define as local crack density. Our first approach uses the spectrum of a RTP and require far field data measurements at multiple frequencies. However this first technique is expensive in terms of required data but also in cpu time. Therefore we suggest another alternative which mixed ideas from the DLSM and the use of artificial backgrounds.

Chapter 1 : Sampling methods

In this chapter, we provide a brief overview of the Linear Sampling Method and two versions of its generalization, namely the Factorization Method and the Generalized Linear Sampling Method. We introduce the far field operator and while presenting the mentioned sampling methods, we insist on the fact that they mainly deal with the spectrum of F to recover the shape of the inhomogeneity. The Interior Transmission Problem which is closely related to these methods is also introduced and we present the method provided by the GLSM to compute the transmission eigenvalues. We illustrate these concepts on the simple case where the inhomogeneity embedded in $\mathbb{R}^2$ has a constant refractive index and whose support is a disk D. This setting allows one to carry explicit computations involving Bessel functions. Consequently, an exact description of the spectral properties of F can be derived, allowing one to explicitly write the indicator functions of D provided by the different considered sampling methods. Therefore it is possible to compare the accuracy of these methods (at least numerically). We also recall the two advances provided by the GLSM towards the possibility of retrieving information from ITP. Firstly, GLSM provides an exact determination of TEs from far field data. Secondly, the regularized solution of the far field equation which is defined in the framework of the GLSM, converges to the solution of ITP. Relating the error made in the computation of TEs with respect to the noise level seems challenging, although important because of the increasing interest in using TEs to solve the inverse problem. Determining the rate of convergence of the regularized solution of the GLSM to the solution of the transmission problem seems also to be a difficult task. This information is important as it would allow a better understanding of the behavior of the DLSM (choice of the the regularization parameter with respect to noise, interpretation of the produced images). For the particular example studied in this chapter, we provide a lower bound of this rate of convergence.

Chapter 2 : Detecting sound-hard cracks in isotropic inhomogeneities

We consider the problem of detecting the presence of sound-hard cracks in a non homogeneous reference medium from the measurement of multi-static far field data. First, we provide a factorization of the far field operator in order to implement the Generalized Linear Sampling Method (GLSM). The justification of the analysis is also based on the study of a special interior transmission problem. This technique allows us to recover the support of the inhomogeneity of the medium but fails to locate cracks. In a second step, we consider a medium with a multiply connected inhomogeneity assuming that we know the far field data at one given frequency both before and after the appearance of cracks. Using the Differential Linear Sampling Method (DLSM), we explain how to identify the component(s) of the inhomogeneity where cracks have emerged. The theoretical justification of the procedure relies on the comparison of the solutions of the corresponding interior transmission problems without and with cracks. Finally we illustrate the GLSM and the DLSM providing numerical results in 2D. In particular, we show that

our method is reliable for different scenarios simulating the appearance of cracks between two measurements campaigns.

Chapter 3 : The interior transmission problem for penetrable obstacles with sound-hard cracks

In this chapter we investigate the ITP for isotropic inhomogeneities with sound-hard cracks inside. This problem has been introduced in Chapter 2 while extending the Generalized Linear Sampling Method to isotropic inhomogeneities containing sound-hard cracks. Following the same approach proposed in [33], we show the existence of a discrete infinite set of real TEs, provided that the refractive index $n \in L^\infty(D)$ is bounded and satisfies $n > 1$. In this case we also derive Faber-Krahn type inequalities for the TEs. When $n < 1$, the framework we develop do not allow to show the Fredholm property of the ITP, preventing us to answer the question of the discreteness properties nor the existence of TEs. We point out that in the paper [32], where the case of inhomogeneities containing sound soft obstacles is studied, a similar restriction on the refractive index occurred as their developed framework allowed to study the case $n < 1$ but not the case $n > 1$. Similarly to more classical situations, we also show that real TEs do not exist if the considered isotropic medium containing the sound-hard crack is dissipative.

Chapter 4 : Detection of sound-hard obstacles in inhomogeneous media

We consider the problem of identifying sound-hard defects of non empty interior inside an unknown inhomogeneous medium from far field data at fixed frequency. As mentioned, we adapt for this purpose the results of the DLSM which requires two set of measurements done before and after the occurrence of the defect. The theoretical justification of the DLSM relies on the comparison of the solutions of two Interior Transmission Problem, the one corresponding to the healthy material and the one corresponding to the damaged material. The use of the DLSM in practice also requires to compute these solutions from the data. The latter can be done by the use of the Generalized Linear Sampling Method (GLSM) [10], which consists in approximating solutions of the far field equation with a particular penalty term. On the one hand, the GLSM requires a factorization of the far field operator, similar to the one used for the Linear Sampling Method. On the other hand, it requires the penalty term to be equivalent to the Herglotz operator and to satisfy a convexity property. Therefore we have chosen to use the $F_\sharp$ operator in the penalty term which is shown to satisfy the factorization similar to the one required for the so called $F_\sharp$ Method. Furthermore it should be noted that since $F_\sharp$ is positive definite, the optimization of the cost functional is greatly simplified and do not require any iterative method. As a product of our analysis, we have also extended the factorization method to this setting which yields a reconstruction procedure for the whole background. The same remark stands for the use of GLSM.

Chapter 5 : The Interior Transmission Problem for inhomogeneities with sound hard inclusions

In this chapter is studied the interior transmission problem for isotropic inhomogeneities containing sound hard obstacles. This chapter differs from chapter 3 in that the obstacles considered are now of non empty interior. We investigate the classical issues related to the study of interior transmission problems that are the Fredholm property, the discreteness of the set of transmission eigenvalues and the existence of positive transmission eigenvalues. The first approach we consider relies a fourth order formulation of the interior transmission problem. This approach has been introduced in [113] for the study of isotropic inhomogeneities and has been successfully used

in many other works [33, 34, 104, 32]. However we have encountered several difficulties with this approach. Finding the right weak formulation has not been easy and we have been compelled to set a variational space which depends on the parameter k. We treated this situation by adapting the works [26] which first introduced such formulations when studying the ITP with cavities. We notice that such difficulty did not arise in the study of ITP related to inhomogeneities with sound soft inclusions inside [32]. The developed framework allows us to prove that the set of TEs is at most discrete, but only if the inclusion is big enough and provided that the refractive index n satisfies $n > 1$. However we could not conclude about the existence of TEs with this framework and we explain why our various attempts failed. We propose another approach in order to relax the assumption on n and remove the condition on the size of the inclusion to obtain the discreteness of the set of TEs. The latter approach relies on the properties of the Dirichlet-to-Neumann operator.

Chapter 6 : Local estimates of crack densities in crack networks

We consider the problem of identifying a set of cracks Γ embedded in some homogeneous background from measured far field data at multiple frequencies generated by acoustic waves. First of all we point out that this framework do not allow to define usual TEs since a crack has empty interior. Working with an artificial sound-soft (resp. sound-hard) obstacle Ω, we show that it is possible to define RTEs. The latter mainly correspond to the Dirichlet eigenvalues (DEs) (resp. Neumann eigenvalues (NEs)) for the Laplace operator in Ω, with the exception that the corresponding eigenfunction u satisfies the additional condition $\sigma(u) = 0$ on Γ, where σ denotes the boundary conditions on Γ. Hence, each RTE is a perturbation $\delta(\Omega, \Gamma)$ of a DE (resp. NE) which encodes the additional condition satisfied by the associated eigenfunction. In addition to this, we show that RTEs can be determined from the data. For this purpose, we adapt the framework of the use of GLSM to compute TEs [10]. Consequently, it is possible to measure the difference $\delta(\Omega, \Gamma)$ between the computed RTEs and the known DEs (resp. NEs). In the case of sound-soft cracks, sound-hard cracks or impedance cracks, we prove that $\Gamma \mapsto \delta(\Omega, \Gamma)$ is monotonous with respect to $\Gamma \cap \Omega$ for the inclusion order. This result led us to use $\delta(\Omega, \Gamma)$ as an estimator of $|\Gamma \cap \Omega|$: we refer this quantity to the localized crack density in Ω. At last, an indicator function of the local crack density at each point is obtained by repeating this process and computing $(\delta(\Omega + t, \Gamma))_t$ for a collection of artificial backgrounds $(\Omega + t)_{t \in A \subset \mathbb{R}^3}$, made of translations of Ω, which scans the probed area. The resolution of this method is fixed by the size of Ω. Numerical simulations carried in the a two dimensional setting validates expected behavior of this indicator function.

A weak point to the method described above is the high numerical cost of the computations of the RTEs associated to one artificial background. Since increasing the resolution (reduce the size of Ω) requires to increase the number of considered artificial backgrounds, imaging with high resolution may be prohibitive. To bypass this drawback, we suggest another method which requires to deal with far field data at only one fixed frequency. This alternative approach mix the notion of artificial background with the ideas of the Differential Linear Sampling Method [9]. Indeed we consider the same Ω of the previous paragraph and compare two functions u and $\widetilde{u}$ which are the solutions of two different problems. $\widetilde{u}$ is the solution of the Helmholtz equation in Ω whereas u is the solution of RTP, which is the Helmholtz equation on $\Omega \setminus \overline{\Gamma}$. On the one hand, $\widetilde{u}$ can be computed independently to the data. On the other hand, we show that when the wavenumber is not a RTE, the GLSM can be used to approximate u. Consequently it is possible to detect the presence of the crack by computing the difference between u and $\widetilde{u}$ which is non zero when $\Gamma \cap \Omega \neq \emptyset$. Repeating this procedure for a collection of artificial backgrounds allow in principle to determine the position of the crack. On the presented numerical simulation, it seems that this indicator moreover reveals the crack density of the probed medium.

Version française

État de l'art

La recherche liée aux problèmes inverses de diffraction acoustique et électromagnétique a été très active depuis les premiers travaux sur le sonar et le radar au début du XX^{e} siècle. Ces deux techniques permettent de détecter une cible et d'estimer sa position. Toutes deux ont été plutôt bien maîtrisées pendant l'entre-deux-guerres. Par la suite, le problème de savoir s'il était possible d'identifier la cible, pour distinguer un sous-marin d'une baleine par exemple, a été tout naturellement envisagé. Les premières tentatives de réponse se sont heurtées à plusieurs difficultés. Premièrement, ce problème d'identification est non linéaire en raison des éventuelles réflexions multiples (réflexions entre les différentes composantes de la cible, diffusion, etc). Deuxièmement, le problème est mal posé, dans le sens où de légères différences sur les données, liées aux incertitudes des mesures par exemple, peuvent conduire à des solutions très différentes. Ces difficultés ont été surmontées d'une part grâce aux progrès techniques de l'industrie informatique facilitant l'accès à des machines de calcul de plus en plus performantes, et d'autre part grâce au développement de la théorie mathématique des problèmes inverses depuis les années 1960. Pour ne citer que quelques uns des contributeurs de cette théorie, nous mentionnons Tikhonov [118, 117], D.L. Phillips [107] et Keith Miller [100]. Ces avancées ont permis de développer une myriade de techniques d'inversions qui ont eu un impact dans divers domaines tels que la géophysique, la médecine et le contrôle non destructif [17, 2, 48, 50].

Les lois qui régissent le phénomène de diffraction étaient déjà bien établies avant l'invention du radar et du sonar. Lorsqu'une onde dite incidente rencontre un obstacle, il résulte de leur interaction un champ diffracté. Ce dernier est entièrement décrit par les équations de Maxwell dans le cas des ondes électromagnétiques et par l'équation de Helmholtz dans le cas des ondes acoustiques. Plus précisément, le champ diffracté est la solution d'une équation aux dérivées partielles (EDP) ayant pour terme source le champ incident. L'EDP dépend de plusieurs paramètres qui sont liés aux propriétés physiques de l'obstacle tels que sa forme et selon le problème considéré, l'indice de réfraction, les coefficients de Lamé, la conductivité, la permittivité, etc. Le problème consistant à déterminer le champ diffracté résultant d'une onde incidente donnée tout en connaissant les paramètres physiques de l'obstacle, ou en d'autres termes résoudre l'EDP, est qualifié de problème direct. Ce problème est bien posé et il existe de nombreuses approches qui permettent de le résoudre numériquement. L'une des approximations numériques les plus efficaces est la méthode des éléments finis de frontière. Elle est basée sur la théorie des équations intégrales, théorie qui a pour but de reformuler l'EDP, initialement formulée dans tout l'espace, en une équation intégrale posée sur le bord de l'obstacle uniquement. Nous référons le lecteur à [102] pour un aperçu sur les méthodes d'équations intégrales. Aussi des exemples d'implémentation de la méthode des éléments finis de frontière pourront être trouvées dans [40] pour la résolution de divers problèmes en électromagnétisme. Lorsque les paramètres physiques de l'obstacle sont inconnus, le problème de retrouver ces derniers à partir d'au moins une paire formée d'une solution de l'EDP et du terme source correspondant, est lui qualifié de problème inverse. La procédure à suivre pour collecter les données permettant de résoudre le problème inverse est simple: le domaine sondé est soumis à une onde incidente, puis le champ diffracté résultant est mesuré par des récepteurs. Cette opération peut éventuellement être répétée pour plusieurs ondes incidentes différentes afin d'enrichir les données. Lorsque la distance entre les récepteurs et la cible est de l'ordre de la longueur d'onde des ondes incidentes, les mesures sont qualifiées de données de champ proche. En revanche, lorsque cette distance est suffisamment grande, on utilise plutôt la donnée de champ lointain, une quantité qui apparaît dans le premier ordre du développement asymptotique du champ diffracté par rapport à la distance à l'emplacement de sa source (l'obstacle). Le champ lointain dépend de la direction de l'observation. Si l'on con-

sidère de surcroît l'ensemble des champs lointains générés par les ondes planes, on obtient un jeu de données paramétré par deux variables: la direction d'observation ainsi que la direction de propagation de l'onde plane incidente. Plusieurs méthodes d'inversions utilisent ce type de données, dont la Linear Sampling Method qui sera décrite ci-après. Il existe également d'autres possibilités pour placer les récepteurs, par exemple ils peuvent être disposés sur un plan ou sur la surface du domaine sondé (pour sonder des guides d'ondes par exemple). La première question à se poser avant d'essayer de résoudre le problème inverse est de savoir si les données collectées permettent de caractériser les paramètres que l'on cherche à déterminer. Des réponses ont été apportées en ce sens pour les problèmes de détermination de la forme de l'obstacle, de son indice de réfraction, mais aussi pour de nombreux autres problèmes [115, 75, 84, 108, 58, 97]. Dans la suite, nous passons en revue quelques méthodes d'inversion qui utilisent les données de champs lointains.

Sans doute en raison de la difficulté du problème, il a pendant longtemps été d'usage de traiter séparément deux types de problèmes inverses. Le premier regroupe les problèmes inverses liés à un obstacle impénétrable, le deuxième ceux qui sont liés à une inhomogénéité pénétrable. Cette distinction est due au fait que les premiers algorithmes d'inversion reposaient fortement sur le modèle mathématique décrivant le problème de diffraction. Dans les deux cas, une linéarisation du problème a été proposé en première approche, la ramenant à un problème d'équation intégrale de première espèce. Cette approche est connue sous le nom d'approximation de Kirschoff et d'optique physique pour le problème avec obstacle impénétrable, et sous le nom d'approximation de Born et Rytov pour le problème avec inhomogénéité pénétrable. Ces approximations sont intéressantes en raison de leur simplicité mathématique, et ont prouvé leur efficacité pour de nombreuses applications telles que la tomographie [14, 39, 52, 91] et le radar à synthèse d'ouverture [36, 16]. Cependant, les modèles linéarisés présentent un point faible important: la non-linéarité du problème de diffraction étant ignorée, leur validité n'est pas garantie pour des milieux complexes. Parmi les premiers travaux préservant la non-linéarité du problème inverse, on peut citer [74, 120], ils ont été complétés par de nombreux autres travaux qui ont de plus abordé le caractère mal posé du problème inverse [64, 78, 67, 65, 98, 57]. Les techniques proposées dans ces premiers travaux appartiennent toutes à une classe des méthodes dites itératives. Elles nécessitent de résoudre plusieurs fois le problème direct, en mettant en œuvre des techniques d'optimisations telles que les méthodes des moindres carrés [116], la méthode de Newton [68, 69, 70], les méthodes quasi Newton [51], les méthodes level set [21]. Plus précisément, à partir d'une estimation initiale de la cible, des mises à jour de cette dernière sont effectuées en résolvant le problème direct à plusieurs reprises, jusqu'à ce que son comportement soit suffisamment fidèle aux mesures. Bien que ces techniques donnent de bons résultats, il est difficile de les utiliser pour des applications industrielles. En effet, elles sont très coûteuses en temps de calcul et ne peuvent donc pas être utilisées dans des applications d'imagerie en temps réel, par exemple pour contrôler l'évolution d'un matériau, ou bien pour l'utilisation en milieu médical nécessitant la présence du patient, etc. Un autre inconvénient majeur de ces méthodes est que leurs mises en œuvre nécessitent d'importantes informations a priori sur l'objet, par exemple sa nature ou bien le nombre de composantes connexes, afin de choisir un bon paramétrage et une bonne initialisation. Une nouvelle classe de techniques d'inversions, dites d'échantillonnages offrent une alternative aux méthodes itératives. Elles permettent de réduire la quantité d'informations requises au préalable ainsi que les coûts en temps de calcul, mais au prix certes d'extraire moins d'informations sur le matériau sondé. En général, ces méthodes ne nécessitent pas de résoudre le problème direct. Elles définissent plutôt une fonction indicatrice qui fournit des informations sur l'emplacement, la forme et les propriétés de l'objet sondé. Pour mentionner quelques unes de ces méthodes, nous pouvons citer la méthode de sondage [73], la méthode de source unique [12] et la Linear Sampling Method (LSM) [46]. Un aperçu de ces méthodes peut être trouvé

dans [109].

Nous nous intéressons à des techniques plus récentes qui ont permis d'améliorer la première version de la LSM tout en élargissant son champ d'application. La LSM fait partie des méthodes d'échantillonnages ponctuelles; ces dernières fournissent un procédé permettant de déterminer si un point d'échantillonnage $z \in \mathbb{R}^3$ est à l'intérieur de l'obstacle ou non. La formulation de la LSM repose sur la connaissance de l'opérateur de champ lointain F, un opérateur intégral dont le noyau est constitué du champ lointain. Selon les résultats d'unicité mentionnés ci-dessus, F contient toutes les informations sur l'objet sondé. La LSM permet d'extraire une partie de ces informations du spectre de F. En quelques mots, elle s'appuie sur les propriétés de l'équation de champ lointain, une équation linéaire mal posée impliquant F et dont le membre de droite dépend du point d'échantillonnage z. L'étude de cette équation permet de définir une fonction de la variable z qui est une indicatrice du support de l'obstacle. Cependant, l'implémentation numérique de cette méthode, qui repose sur une régularisation de Tikhonov de l'équation de champ lointain, fournit une certaine fonction qui n'est pas exactement la fonction indicatrice prédite par la théorie. Malgré ce point faible, diverses simulations numériques attestent néanmoins que la LSM reste fiable en première approche pour localiser un obstacle et/ou déterminer le nombre de ses composantes connexes. En outre, l'algorithme décrit ci-dessus peut être utilisé indépendamment de la nature du domaine sondé, lui conférant un avantage significatif sur les méthodes d'optimisations. Le point faible théorique de la LSM est finalement levée grâce à la célèbre Factorization Method (FM) [79, 80]. Cette méthode consiste à remplacer l'équation de champ lointain par une autre, ce qui fournit une nouvelle fonction indicatrice de l'obstacle, qui elle est accessible à partir des données. La FM a d'abord prouvé son efficacité pour les obstacles impénétrables [79], puis pour les milieux inhomogènes [80, 81]. Depuis lors, la FM a été étendue à divers problèmes académiques [83]. Plus récemment, de nombreux travaux ont contribué à justifier la FM pour des milieux plus complexes, accréditant ainsi sa mise en œuvre dans des applications réelles telles que la géophysique ou le contrôle non destructif [72, 71]. Nous mentionnons également les articles [86, 15, 122] où des matériaux constitués à la fois d'obstacles impénétrables et d'inhomogénéités sont considérés. Ces travaux soulèvent de nouvelles questions concernant la possibilité de distinguer l'obstacle impénétrable de l'inhomogénéité. Plus récemment, la Generalized Linear Sampling Method (GLSM) a été proposée en autre alternative à la LSM [10]. Contrairement à la FM, l'équation de champs lointain est conservée mais sa régularisation classique de Tikhonov est remplacée par de nouveaux schémas de régularisations qui fournissent une caractérisation exacte du support de l'obstacle. Un point important à noter est que la GLSM a aussi abouti à des méthodes permettant d'identifier l'apparition de défauts dans un matériau [9, 8].

La LSM a initialement été étudiée pour les obstacles de Dirichlet. Il a alors été constaté que son bon fonctionnement requiert une certaine condition sur le nombre d'onde k des ondes incidentes utilisées. En effet, la justification de la méthode nécessite que l'ensemble des champs lointains générés par les ondes planes soient denses dans l'espace des fonctions de carré intégrable sur la sphère unité de $\mathbb{R}^3$. Ce résultat n'est valable que lorsque k^2 n'est pas une valeur propre de Dirichlet (VPD) pour l'opérateur de Laplace à l'intérieur de l'obstacle [46]. La figure 2 illustre le fait que cette restriction sur le nombre d'onde est effective. Pour un obstacle de Dirichlet constitué de deux disques disjoints de rayon $r_1 = 1$ et $r_2 = 2$, nous avons généré deux jeux de données de champs lointains respectivement obtenus avec des nombres d'onde légèrement différents. L'image de gauche montre les résultats de la LSM pour $k_1 = 4$ et celle de droite pour $k_2 = 4,33$. Suivant le principe que des ondes de longueur d'onde $\lambda = 2\pi/k$ devraient permettre de détecter des obstacles ayant des dimensions du même ordre de grandeur que λ, les résultats présentés sont doublement frappants. Tout d'abord, sur l'image de droite, le petit disque est mieux reconstitué que le grand disque. Deuxièmement, sur l'image de gauche, la reconstruction

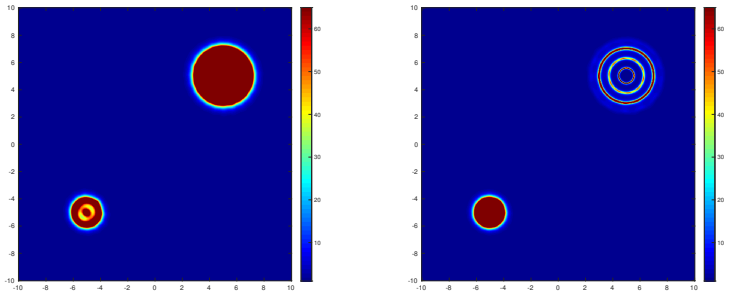

Figure 2: Performance de la LSM lors de la détection d'un obstacle de Dirichlet constitué de deux disques disjoints de rayons $r_1 = 1$ et $r_2 = 2$. La reconstruction est menée avec deux jeux de données de champs lointains générés à des nombres d'ondes différents $k_1 = 4$ (gauche) et $k_2 = 4.33$ (droite). k_2^2 correspond à la première valeur propre de Dirichlet du grand disque (au centième près). Sur l'image de droite, l'inclusion en haut à droite est anormalement mal reconstruite.

de l'obstacle est plus nette alors que la longueur d'onde utilisée est plus grande. Cet effet non désiré est dû au fait que k_2^2 correspond à une VPD pour l'opérateur de Laplace sur le disque de rayon $r_2 = 2$. Notons qu'une telle manifestation des VPD est rare en pratique, car ces dernières sont en quantité discrète. L'adaptation de la LSM aux obstacles pénétrables [47, 77] a conduit de manière similaire à une restriction sur le nombre d'onde. Ce dernier doit être choisi de sorte que le problème dit de transmission intérieur (PTI), un problème de Cauchy couplant deux équations aux dérivées partielles sur un domaine correspondant au support de l'obstacle, soit bien posé. Ainsi, l'équivalent des VPD pour un milieu pénétrable correspond au spectre du PTI dont les éléments sont les valeurs propres de transmissions (VPTs). Par conséquent, démontrer que les VPTs sont au plus en quantité discrète, tout comme les valeurs propres de Dirichlet, a été un enjeu majeur pour pouvoir assurer la validité de la LSM à presque toutes les fréquences. Cela a d'abord été prouvé dans le cas de milieux stratifiés à symétrie sphériques [47], situation pour laquelle il est possible de mener des calculs impliquant des équations algébriques où apparaissent naturellement les fonctions de Bessel. Peu après, ce résultat a été prouvé dans un cas plus général [43, 113]. En revanche, la question de l'existence des VPTs a été considérée beaucoup plus tard. Pendant longtemps, le seul résultat connu fut qu'il n'y a pas de VPTs réelles lorsque l'indice de réfraction a une partie imaginaire non nulle. Cette absence de résultats s'explique d'une part par la difficulté d'étudier le PTI, qui est ni elliptique ni auto-adjoint, avec les outils de l'époque. D'autre part, la nature discrète des VPTs étant suffisante pour justifier l'utilisation de la LSM en pratique, la question de l'existence était dépourvue d'intérêt. Récemment, des travaux ont remis la question de l'existence des VPTs au goût du jour: il est possible de calculer les VPTs à partir de données de champs lointains [28] et de les utiliser pour obtenir des informations qualitatives sur les propriétés physiques du matériau sondé [31, 25]. Päivärinta et Sylvester ont démontré en 2008 l'existence d'au moins une VPT réelle quelque soit la géométrie de l'obstacle [104], la preuve requiert néanmoins que l'indice de réfraction soit suffisamment grand. Ce résultat est complété par les travaux de Cakoni, Gintides et Haddar [33], où il est démontré l'existence d'une infinité de VPTs réels tout en supprimant la condition sur l'indice de réfraction.

Suite à ces résultats, une attention croissante a été accordée aux VPTs et à leur utilisation pour résoudre le problème inverse. Les hypothèses sur l'indice de réfraction ont été constamment affaiblies. Pendant longtemps, il a été nécessaire d'exclure les matériaux ayant un contraste qui change de signe, alors que de telles situations se présentent en pratique, nous citons la tomographie thermoacoustique à titre d'exemple [61]. L'étude du PTI avec cavités a été la première à faire face à cette difficulté [26]. Par la suite, l'utilisation de la notion de T-Coercivité, outil initialement développée pour les problèmes impliquant des métamatériaux, a considérablement affaibli les conditions sur le contraste [38]. En effet, l'utilisation de la T-Coercivité a permis de

prouver le caractère discret des VPTs sous la seule condition que le contraste ne change pas de signe sur le bord de l'obstacle [37]. Des travaux reprennent cette hypothèse pour traiter le cas de milieux dont l'indice de réfraction est autorisé à prendre des valeurs complexes [112]. Dans ce dernier travail, une caractérisation complète de l'ensemble du spectre du PTI est effectuée (y compris les VPTs complexes). Pour conclure sur les propriétés des VPTs, nous mentionnons également les estimations asymptotiques de type Weyl pour la fonction de comptage des VPTs [111, 56, 89, 90, 105] et les résultats sur la localisation des VPTs dans le plan complexe [60, 89, 106]. Enfin, les différents cadres développés pour étudier le PTI ont été étendus aux équations de Maxwell [53, 35, 49]. Parallèlement à tous ces travaux, plusieurs contributions ont étayé l'utilisation des VPTs pour résoudre le problème inverse. Tout d'abord, les méthodes de calculs des VPTs ont été grandement améliorées. Auparavant, la justification du calcul des VPTs s'appuyait sur la LSM, mais ceci n'était pas satisfaisant en raison des points faibles de la LSM mentionnés ci-dessus. De nouvelles méthodes telles que la GLSM et la dualité intérieur-extérieur règlent ce problème [10, 85, 93, 94, 95]. Par ailleurs, de nombreux travaux ont proposé des techniques recourant aux VPTs pour établir des estimations sur les propriétés des matériaux sondés [22, 31, 63, 66, 32]. Nous mentionnons également une application intéressante des VPTs permettant de concevoir des matériaux peu détectables par des mesures de champ lointain [54]. De récents travaux se sont donnés pour nouvelle tâche de simplifier le lien entre les VPTs et les paramètres physiques du matériau sondé. Cette initiative s'explique du fait que la restitution d'informations précises à partir des VPTs n'est pas aisée, ce qui limite considérablement les informations pouvant être obtenues. Une des raisons pour laquelle il est compliqué d'utiliser les VPTs est qu'elles n'apparaissent pas comme étant le spectre d'un quelconque opérateur auto-adjoint. Pour surmonter cette difficulté, certains travaux suggèrent de considérer plutôt un spectre modifié, dont les éléments dénommées valeurs propres de transmission relatives (VPTRs) peuvent aussi être calculé à partir des données de champ lointain [6, 30, 5, 41]. L'idée consiste à introduire un obstacle artificiel qui peut être choisi par l'observateur. Les VPTRs correspondent alors au spectre d'un nouveau problème de transmission, le problème de transmission relatif (PTR), qui indique qu'aux VPTRs, il existe un champ incident tel que le champ lointain résultant du milieu effectif et celui résultant du milieu artificiel sont arbitrairement proches. L'utilisation des VPTRs présente un autre avantage, elles dépendent de l'obstacle artificiel qui peut être ajusté à volonté, en fonction du problème considéré. Ainsi, le choix du paramétrage approprié des composantes de l'obstacle artificiel, comme sa position, sa géométrie, sa nature (pénétrable ou non) peut simplifier considérablement le lien entre les VPTRs et les paramètres d'intérêts.

Plan de la thèse

Nous nous intéressons à l'utilisation des ultrasons pour détecter et localiser la présence de défauts au sein d'un matériau. Cette question a son importance dans divers domaines. Pour citer quelques exemples, mentionnons le contrôle du niveau de dégradation de certaines structures du génie civil telles que les ponts, les bâtiments, les rails; la détection d'anomalies dans les tissus biologiques afin de diagnostiquer des maladies; l'exploration des sols lors de la recherche de cavités naturelles ou anthropogéniques, de réseaux, d'objets enterrés ou d'anomalies souterraines. De nombreux problèmes de diffusions peuvent être modélisés par l'équation d'élasticité linéaire, elle est généralement valable lorsque les déformations et contraintes sont faibles. En considérant uniquement les ondes longitudinales, l'équation d'élasticité peut être simplifiée en l'équation de Helmholtz. Nous nous appuyons sur cette dernière équation et utilisons des mesures de champs lointains pour développer des méthodes d'inversions qui répondent à nos objectifs. Les types de défauts qui nous intéressent sont des obstacles impénétrables. Ils peuvent être soit d'intérieurs non vide, soit d'intérieurs vide (on parle alors de fissures). Ces deux différents cas requièrent

chacun un traitement particulier et seront considérés séparément. Une plus grande attention est accordée aux défauts correspondant à des obstacles avec des conditions aux limites de types Neumann, car il s'agit d'un modèle assez réaliste pour les fissures. Pour que la présence d'un obstacle soit perceptible sur les données mesurées, la fréquence de travail doit être du même ordre de grandeur que la taille du défaut recherché. Une difficulté classique lors de l'imagerie de milieux hétérogènes est qu'en cas de contraste élevé ou de présence d'inclusions avant la dégradation, il est difficile de distinguer la contribution du défaut sur les mesures. La Differential Linear Sampling Method (DLSM) apporte une solution à cette difficulté [9]. Cette méthode a été initialement mise en place pour identifier une modification de l'indice de réfraction dans une inhomogénéité. Elle repose sur des mesures différentielles, c'est-à-dire des mesures prises à la fois avant et après l'apparition du défaut. Nous adaptons la DLSM à notre problème de détection dans les chapitres 2 et 4. Le chapitre 2 traite le cas des fissures de type Neumann tandis que le chapitre 4 traite le cas de défauts de type Neumann d'intérieurs non vide. La DLSM s'appuie sur les résultats de la Generalized Linear Sampling Method (GLSM) dont la mise en œuvre nécessite que le problème de transmission intérieur (PTI) soit bien posé. Par conséquent, l'adaptation de la DLSM à notre problème nous a aussi conduit à étudier deux PTI. Le premier PTI correspond à des inhomogénéités contenant des fissures, il est étudié dans le chapitre 3. Le second PTI correspond à des inhomogénéités contenant des obstacles d'intérieurs non vide, il est étudié dans le chapitre 5. Dans un dernier chapitre (chapitre 6), nous développons deux techniques permettant de sonder des milieux très endommagés comportants des réseaux de fissures. Nous définissons une densité locale de fissures et fournissons un moyen d'estimer cette quantité à partir des données. Deux différentes approches sont proposées. La première approche utilise le spectre d'un problème de transmission particulier dit relatif et nécessite des données de champ lointain mesurées à plusieurs fréquences différentes. Cependant, cette première technique est coûteuse en quantité de données requises ainsi qu'en temps de calculs. C'est pourquoi nous proposons une méthode alternative qui elle ne requiert pas de mesures multi-fréquentielles. Cette dernière méthode combine les idées de la DLSM et l'utilisation de milieux artificiels.

Chapitre 1 : Les méthodes d'échantillonages

Dans ce chapitre, nous proposons un bref aperçu de la Linear Sampling Method (LSM) et deux versions de ses généralisations, à savoir la Factorization Method (FM) et la Generalized Linear Sampling Method (GLSM). Ces trois méthodes d'échantillonnages permettent de retrouver le support d'un obstacle à partir de l'opérateur de champ lointain F dont nous rappelons la définition. Nous insistons sur le fait qu'elles extraient en particulier des informations du spectre de F. Nous introduisons également le problème de transmission intérieur (PTI), un problème de Cauchy qui est étroitement lié à ces méthodes. Plus précisément, le spectre de ce problème, dont les éléments sont appelés valeurs propres de transmissions (VPTs), indique les fréquences auxquels les méthodes mentionnées ne sont pas valides. Nous présentons une méthode fournie par le GLSM qui permet de calculer les VPTs. Ces concepts sont illustrés sur un cas simple en dimension 2, l'obstacle considéré est un disque pénétrable d'indice constant. Ce cadre offre la possibilité de mener des calculs impliquant des fonctions de Bessel. Par conséquent, une description exacte des propriétés spectrales de F peut être établie, ce qui permet d'écrire explicitement les fonctions indicatrices du disque, fournies par chacune des trois méthodes d'échantillonnages. Il est donc possible de comparer la précision de ces méthodes (au moins numériquement). La GLSM permet non seulement de déterminer les VPTs, mais aussi d'approximer certaines solutions du PTI. Relier l'erreur commise dans le calcul des VPTs au bruit semble être une tâche ardue, bien qu'importante en raison de l'intérêt croissant pour l'utilisation des VPTs dans la résolution du problème inverse. De même, il semble difficile de déterminer la vitesse de convergence de la solution régularisée de la GLSM vers la solution du problème de transmission dans

le cas général. Cette information est importante car permettrait une meilleure compréhension du comportement de la DLSM (choix du paramètre de régularisation par rapport au bruit et interprétation des images produites). Pour le cas particulier étudié dans ce chapitre, nous fournissons une borne inférieure de cette vitesse de convergence.

Chapitre 2 : Détection de fissures de type Neumann dans une inhomogénéité isotrope

Nous considérons le problème de détection de fissures de type Neumann dans un milieu de référence non homogène à partir de données multistatiques de champs lointains. Nous fournissons la factorisation adéquate de l'opérateur de champ lointain, nécessaire à la mise en œuvre de la Generalized Linear Sampling Method (GLSM). La justification de l'analyse est également basée sur l'étude d'un problème de transmission intérieur particulier. Cette technique nous permet dans un premier temps de retrouver le support de l'inhomogénéité, cependant elle ne permet pas de distinguer les fissures qu'elle contient. Dans un deuxième temps, nous justifions l'utilisation de la Differential Linear Sampling Method (DLSM) pour identifier la composante de l'inhomogénéité qui a été sujette à l'apparition de fissures, à partir de mesures effectuées avant et après l'endommagement. La justification théorique de cette méthode repose sur la comparaison des solutions de deux problèmes de transmission intérieurs différents, le premier problème étant associé au matériau sain et le deuxième au matériau endommagé. Enfin, nous illustrons la GLSM et la DLSM en fournissant des résultats numériques effectués en dimension 2. En particulier, nous montrons que notre méthode est fiable pour différents scénarios simulant l'apparition de fissures entre deux collectes de mesures.

Chapitre 3 : Le problème de transmission intérieur pour des inhomogénéités contenant des fissures de type Neumann.

Dans ce chapitre, nous étudions le problème de transmission intérieur (PTI) pour des d'inhomogénéités isotropes contenant des fissures de type Neumann. Ce problème a été introduit dans le chapitre 2 où nous avons étendu le domaine de validité de la Generalised Linear Sampling Method à ce type de milieux. Nous adaptons la méthode utilisée dans le cas sans fissures [33] pour prouver que l'ensemble des valeurs propres de transmissions (VPTs) réelles est infini, discret et sans points d'accumulations. Nous établissons également des inégalités de type Faber-Krahn pour les VPTs. Cette étude nécessite que l'indice de réfraction $n \in L^\infty(D)$ soit à valeurs réelles et minorée par 1. Dans le cas contraire, le cadre que nous développons ne permet pas de prouver que le PTI vérifie la propriété de Fredholm, ce qui empêche d'établir le caractère discret des VPTs ainsi que leur existence. Nous soulignons qu'une difficulté similaire apparaît dans l'analyse du PTI pour des inhomogénéités contenant des obstacles de Dirichlet [32]. Plus précisément, le cas $n < 1$ a pu être traité mais pas le cas $n > 1$. Enfin nous montrons que tout comme pour le PTI classique, il n'y a pas de VPTs réelles lorsque le milieu est absorbant.

Chapitre 4 : Détection d'inclusions de type Neumann dans des milieux hétérogènes

Nous considérons le problème d'identification de défauts de type Neumann d'intérieurs non vide au sein d'une hétérogénéité inconnue. Nous utilisons pour cela des données de champs lointains mesurées à une certaine fréquence que nous fixons. Nous adaptons les résultats de la Differential Linear Sampling Method (DLSM) [9] dont la mise en oeuvre requiert deux séries de mesures, l'une effectuée avant l'apparition du défaut et l'autre après. La justification théorique de la DLSM repose sur la comparaison des solutions de deux problèmes de transmission intérieurs différents. Le premier problème est associé au matériau sain alors que le second est associé au

matériau endommagé. Exploiter ces résultats en pratique requiert le calcul de ces deux solutions à partir des données. Ceci peut être effectué grâce à la Generalized Linear Sampling Method (GLSM) [10]. Cette dernière méthode consiste à approximer les solutions de l'équation de champ lointain en utilisant une pénalisation particulière. La justification de la GLSM nécessite d'une part une factorisation de l'opérateur de champ lointain, similaire à celle utilisée pour la Linear Sampling Method (LSM). D'autre part, la pénalisation utilisée doit être équivalente à l'opérateur de Herglotz et doit de plus satisfaire une certaine propriété de convexité. L'opérateur $F_\sharp$, utilisé dans la seconde version de la Factorization Method (FM) est un bon candidat pour une telle pénalisation. En outre, il convient de noter que les solutions de l'équation de champ lointain sont calculées via l'optimisation d'une fonction coût et que cette dernière étape est grandement simplifiée du fait que l'opérateur $F_\sharp$ est défini positif. Enfin nous mentionnons que notre analyse apporte également les éléments théoriques qui permettent d'étendre la validité de la FM ainsi que de la GLSM aux milieux hétérogènes contenant des inclusions de types Neumann, offrant ainsi une procédure de reconstruction du support de ce type d'obstacles.

Chapitre 5 : Le problème de transmission intérieur pour des inhomogénéités contenant des inclusions de type Neumann

Nous étudions dans ce chapitre le problème de transmission intérieur (PTI) pour des inhomogénéités isotropes contenant des inclusions de type Neumann. Ce chapitre diffère du chapitre 3 du fait que les inclusions considérées sont ici d'intérieurs non vide. Nous étudions les questions classiques liées à l'étude des problèmes de transmission intérieurs, à savoir la propriété de Fredholm, le caractère discret de l'ensemble des valeurs propres de transmissions (VPTs) et l'existence de VPTs positives. La première approche que nous considérons repose sur une formulation du quatrième ordre du PTI. Cette approche a été introduite dans [113] pour l'étude des inhomogénéités isotropes et utilisée avec succès dans de nombreux autres travaux : [33, 34, 104, 32]. Cependant, nous avons rencontré plusieurs difficultés avec cette approche. Tout d'abord, trouver la bonne formulation faible a été une tâche délicate et nous avons été contraints de définir un espace variationnel qui dépend du paramètre k. Nous avons traité cette situation en adaptant les travaux portant sur l'étude du PTI avec des cavités [26], où une telle formulation est utilisée. Nous précisons que cette difficulté ne s'est pas manifestée dans l'étude du PTI lorsque les inclusions sont de type Dirichlet [32] plutôt que de type Neumann. Le cadre que nous développons permet de prouver le caractère discret des VPTs sous certaines conditions, portant sur l'indice de réfraction mais aussi sur la taille de l'inclusion. La question de l'existence des VPTs reste quant à elle ouverte, nous expliquons pourquoi nos différentes tentatives pour répondre à cette question ont échouées. Dans une dernière partie, nous proposons une autre approche permettant d'établir le caractère discret de l'ensemble des VPTs tout en relaxant l'hypothèse faite sur l'indice de réfraction et en supprimant de surcroît la condition portant sur la taille de l'inclusion. Cette dernière approche repose sur les propriétés de l'opérateur de Dirichlet-to-Neumann.

Chapitre 6 : Estimation des densités locales de fissures dans des milieux fortement endommagés

Nous considérons le problème d'identification de fissures incluses dans un milieu homogène à partir de données multi-fréquentielles de champs lointains générées par des ondes acoustiques planes. Tout d'abord, nous faisons remarquer que cette configuration ne permet pas de définir un problème de transmission intérieur au sens usuel car l'ensemble des fissures Γ est d'intérieur vide. Cependant, en travaillant avec un obstacle artificiel de type Dirichlet Ω, nous montrons qu'il est possible de définir un problème de transmission relatif (PTR) dont le spectre est constitué des valeurs propres de transmissions relatives (VPTRs). Ces dernières ont une caractérisation qui est

proche de celle des valeurs propres de Dirichlet (VPD) pour l'opérateur de Laplace dans Ω. Les fonctions propres u correspondant aux VPTRs doivent satisfaire à la condition supplémentaire $\sigma(u) = 0$ sur $\Gamma \cap \Omega$, où σ indique les conditions aux limites sur Γ. Chaque VPTR peut donc être considérée comme étant une perturbation d'une VPD et la comparaison de ces deux valeurs propres pourrait apporter une information sur $\Gamma \cap \Omega$. En outre, nous montrons que les VPTRs peuvent être déterminées à partir des données. Nous adaptons à cet fin la Generalized Linear Sampling Method (GLSM) qui a déjà fait ces preuves pour le calcul des valeurs propres de transmissions classiques [10]. Les VPD peuvent elles aussi être déterminées car la géométrie de Ω nous est connue. Par conséquent, il est possible de mesurer les différences $\delta(\Omega, \Gamma)$ entre les VPTRs et les VPD à partir des données. De plus, nous montrons que la fonction $\Gamma \mapsto \delta(\Omega, \Gamma)$ est monotone par rapport à $\Gamma \cap \Omega$ pour l'ordre de l'inclusion, ceci étant valide quelque soit les conditions aux limites sur Γ (Dirichlet, Neumann, impédance). Ce résultat nous a conduit à utiliser $\delta(\Omega, \Gamma)$ comme estimateur de $|\Gamma \cap \Omega|$, quantité que nous avons désignée par densité de fissures localisées en Ω. Enfin, la densité de fissures est obtenue en tout points en répétant ce processus avec une collection d'obstacles artificiels $(\Omega + t)_{t \in A \subset \mathbb{R}^3}$, constituée de translations de Ω, qui balayent la zone sondée. La résolution de cette méthode est fixée par la taille de Ω.

La méthode décrite ci-dessus présente cependant un point faible. En effet, déterminer les VPTRs associées à un obstacle artificiel est très couteux en temps de calculs. La production d'images en haute résolution devient alors difficile car nécessite d'utiliser d'avantage d'obstacles artificiels (qui sont alors de taille plus petite). Pour contourner cet inconvénient, nous proposons une autre méthode qui ne requiert pas de données multi-fréquentielles. Cette nouvelle approche combine la notion de milieu artificiel aux résultats de la Differential Linear Sampling Method [9]. Au lieu de comparer les spectres, nous comparons plutôt les solutions du PTR à ceux de l'équation de Helmholtz dans Ω. Ceci permet de détecter la présence éventuelle de fissures à l'intérieur de Ω, car en effet les solutions coïncident lorsque $\Gamma \cap \Omega = \emptyset$ et diffèrent (en général) lorsque $\Gamma \cap \Omega \neq \emptyset$. Ce critère peut être utilisé en pratique grâce à la GLSM qui fournit une méthode pour calculer les solutions du PTR à partir des données. Les solutions de l'équation de Helmholtz sur Ω peuvent quant à elles être calculées avec une méthode d'approximation numérique car la géométrie de Ω nous est connue. On pourra par exemple utiliser la méthode des éléments finis. Enfin, en balayant la zone sondée par un obstacle artificiel Ω, il est possible de déduire la position des fissures. Cette méthode est valide pour des fissures ayant des conditions aux limites de type Dirichlet, Neumann, ou bien d'impédance. La précision est fixée comme pour la première méthode par la taille de Ω. Sur les simulations numériques présentées, il semble que cet indicateur révèle aussi la densité de fissures du milieu sondé, bien que ce résultat ne soit pas établi.

Chapter 1

Sampling methods

Contents

1.1 Introduction

Inverse scattering theory aims to determine the physical properties of the scattering medium from measurements of the scattered waves. This field is rich of numerous inversion techniques and has many applications, e.g. tomography, medical imaging, non destructive testing. We refer the reader to [45] for a state of the art on the mathematical theory of inverse scattering theory.

The sampling methods, which is the main topic of this chapter, is a wide class of inversion methods which finds a compromise between the physical parameters that can be retrieved and the required a priori knowledge on the obstacle. Indeed they only allow to reconstruct the shape of the obstacle without indicating the nature of the latter, but the flexibility of the method enables it to be implemented for a large range of problems [83]. The sampling methods rely on the knowledge of the far field pattern, a quantity that is obtained by measuring the amplitude of the resulting scattered wave far from the obstacle, repeatedly for every incident plane waves. The far field operator F which is an integral operator with the far field pattern being its kernel, contains all the information on the obstacle according to the uniqueness results [44]. The knowledge of the far field operator is indeed the starting point of the sampling method: they somehow more particularly deal with the spectrum of the latter. This last point will be highlighted in the present chapter. A famous method among the sampling methods is the Linear Sampling Method. It relies on the solvability of the far field equation, a linear ill-posed equation involving F. The far field equation depends on a parameter $z \in \mathbb{R}^3$, and the Tikhonov regularization of

this equation is used with a parameter α. In practice the far field operator is corrupted with noise and α is fixed by the a posteriori choice prescribed by the Morozov discrepancy principle [119]. The theory indicates that the support D should be identified by abnormal blow up of the norm of a certain linear function of the regularized solution when z is outside of D. However this function is not accessible and replaced by the regularized solution itself, which constitutes the main weak point of the LSM theory. The Factorization Method (FM) has been developed in order to bypass this weak point. The data fidelity term is modified in order to obtain a theoretical guarantee with a similar Tikhonov regularization. The first version of the FM was quite restrictive. The operator F was required to be normal, thus excluding the possibility to solve the inverse problem for dissipative medium. A second version of the FM has been proposed in order to weaken this restriction. More recently, an alternative solution to overcome the weak point of the LSM has been provided by the Generalized Linear Sampling Method [10]. The classical Tikhonov regularization of the far field equation is replaced by new regularization schemes which provides an exact characterization of the support of the obstacle.

In this chapter, we provide a brief overview of the Linear Sampling Method and two versions of its generalization, namely the Factorization Method and the Generalized Linear Sampling Method. We introduce the far field operator and while presenting the mentioned sampling methods, we insist on the fact that they mainly deal with the spectrum of F to recover the shape of the inhomogeneity. The Interior Transmission Problem which is closely related to these methods is also introduced and we present the method provided by the GLSM to compute the transmission eigenvalues. We illustrate these concepts on the simple case where the inhomogeneity embedded in $\mathbb{R}^2$ has a constant refractive index and whose support is a disk D. This setting allows one to carry explicit computations involving Bessel functions. Consequently, an exact description of the spectral properties of F can be derived, allowing one to explicitly write the indicator functions of D provided by the different considered sampling methods. Therefore it is possible to compare the accuracy of these methods (at least numerically). We also recall the two advances provided by the GLSM towards the possibility of retrieving information from ITP. Firstly, GLSM provides an exact determination of TEs from far field data. Secondly, the regularized solution of the far field equation which is defined in the framework of the GLSM, converges to the solution of ITP. Relating the error made in the computation of TEs with respect to the noise level seems challenging, although important because of the increasing interest in using TEs to solve the inverse problem. Determining the rate of convergence of the regularized solution of the GLSM to the solution of the transmission problem seems also to be a difficult task. This information is important as it would allow a better understanding of the behavior of the DLSM (choice of the the regularization parameter with respect to noise, interpretation of the produced images). For the particular example studied in this chapter, we provide a lower bound of this rate of convergence.

1.2 The basics of acoustic scattering theory

We consider an isotropic inhomogeneity embedded in $\mathbb{R}^d$, $d = 2$ or 3. We assume that the propagation of waves in time harmonic regime is governed by the Helmholtz equation

$$\Delta u + k^2 n u = 0 \text{ in } \mathbb{R}^d$$

where $k > 0$ is the wave number and $n \in L^\infty(\mathbb{R}^d)$ is the refractive index of the medium. We assume that n is a complex valued function such that the support of $n - 1$ is equal to a set $\overline{D}$ corresponding to the shape of the inhomogeneity. The domain D is bounded, its boundary is Lipschitz and $\mathbb{R}^d \setminus D$ is connected. For physical considerations, n is moreover assumed to be

satisfying $\Im\mathfrak{m}(n) \geq 0$ in $\mathbb{R}^d$. Given an incident wave u_i which solves the Helmholtz equation in free space, that is $\Delta u_i + k^2 u_i = 0$ in $\mathbb{R}^2$, the scattered field

$$u_s := u - u_i$$

then satisfies

$$\Delta u_s + k^2 n u_s = -k^2(n-1)u_i \text{ in } \mathbb{R}^d. \tag{1.1}$$

Moreover we impose that u_s satisfies the Sommerfeld radiation condition

$$\lim_{r\to+\infty} r^{\frac{d-1}{2}} \left(\frac{\partial u_s}{\partial r} - iku_s \right) = 0. \tag{1.2}$$

The scattered field $u_s \in H^2_{loc}(\mathbb{R}^d)$ is uniquely determined by (1.1)-(1.2) [44]. Furthermore, it can be shown that the Sommerfeld radiation condition implies following asymptotic expansion for the scattered field,

$$u_s(x) = \frac{e^{ik|x|}}{|x|^{\frac{d-1}{2}}} \left(u_s^\infty(\widehat{x}) + O(1/|x|) \right) \tag{1.3}$$

as $|x| \to +\infty$, uniformly in $\widehat{x} = x/|x| \in \mathbb{S}^{d-1}$, which denotes the unit sphere of $\mathbb{R}^d$. The function $u_s^\infty : \mathbb{S}^{d-1} \to \mathbb{C}$, is called the far field pattern associated with u_i. We are interested in far field patterns associated with a particular class of incident waves called Herglotz wave functions defined for $g \in L^2(\mathbb{S}^{d-1})$ by

$$v_g := \int_{\mathbb{S}^{d-1}} g(\theta) e^{ik\theta\cdot x} \, \mathrm{ds}(\theta). \tag{1.4}$$

We denote by $u_s^\infty(\theta, \widehat{x})$ the far field pattern associated to $u_i(\theta, \cdot) := e^{ik\theta\cdot x}$ for $\theta \in \mathbb{S}^{d-1}$ (incident plane wave of direction θ), thanks to the linearity of the scattering problem (1.1)-(1.2), the far field pattern associated to the Herglotz wave v_g is given by

$$(Fg)(\widehat{x}) = \int_{\mathbb{S}^{d-1}} g(\theta)\, u_s^\infty(\theta, \widehat{x}) \, \mathrm{ds}(\theta). \tag{1.5}$$

This defines the so called far field operator $F : L^2(\mathbb{S}^{d-1}) \to L^2(\mathbb{S}^{d-1})$ which constitutes the data of the inverse scattering problem where one is interested in recovering qualitative or even quantitative information on the refractive index n. In the next section, we present three methods allowing one to recover the shape of D from the knowledge of F, namely the Linear Sampling Method (LSM), the Factorization Method (FM) and the Generalized Linear Sampling Method (GLSM). These methods belong to the class of sampling methods which consist in constructing an indicator function depending on a parameter $z \in \mathbb{R}^d$ that is only bounded for z in D, the support of $n - 1$.

1.3 An overwiew of some sampling methods

1.3.1 The linear sampling method

We begin with the LSM which is the earliest sampling method and also the starting point of FM and GLSM. It was first introduced by Colton and Kirsch in 1996 [42]. For $z \in \mathbb{R}^d$ we denote by Φ_z the fundamental solution of (1.1)-(1.2) defined by

$$\Phi_z(x) = \frac{i}{4}H_0(k|x-z|) \text{ if } d=2 \qquad \text{and} \qquad \Phi_z(x) = \frac{1}{4\pi}\frac{e^{ik|x-z|}}{|x-z|} \text{ if } d=3 \tag{1.6}$$

where H_0 is the Bessel function of first kind of order 0. The far field pattern of Φ_z^∞ is given by

$$\Phi_z^\infty(\widehat{x}) = \eta_d e^{-ik\widehat{x}\cdot z}, \tag{1.7}$$

where the constant η_d is equal to $e^{i\frac{\pi}{4}}/\sqrt{8\pi k}$ for $d=2$, and to $1/(4\pi)$ for $d=3$. The main idea behind the LSM is that Φ_z^∞ can be approached by a sequence of far fields associated to Herglotz waves if and only if $z \in D$. In this case, the chosen sequence of Herglotz waves converges to some limit $u_i \in L^2(D)$ (which is not a Herglotz wave in general). Furthermore, the far field associated with u_i is Φ_z^∞. A more rigorous description of this result requires a particular factorization of the far field operator which is explained hereafter. We define the Herglotz operator $H : L^2(\mathbb{S}^{d-1}) \to L^2(D)$ by

$$Hg := v_{g|D}, \tag{1.8}$$

the closure of the range of H is given by [44]

$$\overline{R(H)} = \{v \in L^2(D) \,|\, \Delta v + k^2 v = 0 \text{ in } D\}. \tag{1.9}$$

Then we define the operator $G : \overline{R(H)} \to L^2(\mathbb{S}^{d-1})$ by

$$Gv := u_s^\infty \tag{1.10}$$

where u_s^∞ is the far field of the solution u_s of (1.1)-(1.2) with $u_{i|D} = v$. Notice from (1.1) that u_s only depends on $u_{i|D}$. Then the following equality is straightforward

$$F = GH. \tag{1.11}$$

With these notations, the mentioned main result can be reformulated as follows: $z \in D$ if and only if there exists $v \in \overline{R(H)}$ such that $Gv = \Phi_z^\infty$. At this point, it is important to mention that this assertion is true under a particular assumption on the wavenumber k. Indeed, consider such an incident field v for $z \in D$ and let u_s be the associated scattered field. By definition of G, we have that $u_s^\infty = \Phi_z^\infty$. But according to the Rellich lemma [29, Lemma 1.6] (two outgoing solutions of the homogeneous Helmholtz equation outside a ball that have the same far field patterns are equal outside the ball) and the unique continuation principle, $u_s = \Phi_z$ in $\mathbb{R}^d \setminus D$. Now $u := u_s + v$ is easily seen to be satisfying $\Delta u + k^2 n u = 0$ in D. Moreover the H^2 regularity of u_s implies the two transmission conditions $u - v = \Phi_z$ and $\partial_\nu(u-v) = \partial_\nu \Phi_z$ on ∂D. In short, a solution $v \in \overline{R(H)}$ of $Gv = \Phi_z^\infty$ must satisfies the interior transmission problem (ITP) below with $f = \Phi_{z|\partial D}$ and $g = \partial_\nu \Phi_{z|\partial D}$.

The Interior Transmission Problem
For given $f \in H^{3/2}(\partial D)$ and $g \in H^{1/2}(\partial D)$, find $(u, v) \in L^2(D) \times L^2(D)$ such that $u - v \in H^2(D)$ and

$$\left|\begin{array}{rcll} \Delta u + k^2 n\, u &=& 0 & \text{in } D \\ \Delta v + k^2\, v &=& 0 & \text{in } D \\ u - v &=& f & \text{on } \partial D \\ \partial_\nu(u-v) &=& g & \text{on } \partial D. \end{array}\right. \tag{ITP}$$

For instance, in the case where $(n-1)^{-1} \in L^\infty(\mathbb{R}^d)$ and $\mathfrak{Re}(n-1)$ is positive definite or negative definite, it is known that problem (ITP) is well posed for all $k \in \mathbb{R}$ except a countable set without any finite accumulation point [43]. We now have all the ingredients to outline the theoretical result of LSM.

Theorem 1.3.1. *Assume that* (ITP) *is well posed. Then* $\Phi_z^\infty \in R(G)$ *if and only if* $z \in D$.

Proof. The proof for $z \in D$ is already outlined above. If $z \notin D$ then by the Rellich lemma and the unique continuation principle, $u_s = \Phi_z^\infty$ in $\mathbb{R}^d \setminus \{D \cup \{z\}\}$ where u_s is as in the discussion above. This gives a contradiction since $u_s \in H^2(B)$ while $\Phi_z \notin H^2(B)$ with $B \subset \mathbb{R}^d$ being a neighborhood of z. □

A direct consequence from the definition of G and (1.11) is:

Corollary 1.3.2. *Assume that* k *is such that* (ITP) *is well posed then*

- *If* $z \in D$ *then there exists* g_z^α *such that* $\|Fg_z^\alpha - \Phi_z^\infty\| < \alpha$ *and* $\lim_{\alpha \to 0} \|Hg_z^\alpha\|_{L^2(D)} < +\infty$.
- *If* $z \notin D$ *then for all* g_z^α *such that* $\|Fg_z^\alpha - \Phi_z^\infty\| < \alpha$, $\lim_{\alpha \to 0} \|Hg_z^\alpha\|_{L^2(D)} = +\infty$.

This result gives a first possibility to recover D by the use of the indicator $z \mapsto \|Hg_z^\alpha\|_{L^2(D)}$ for small values of α but this is not of practical interest. Indeed, a first weak point is that it does not indicate how to construct the sequence $(g_z^\alpha)_{\alpha>0}$. In practice, one uses the Tikhonov regularization of the equation $Fg = \Phi_z^\infty$, i.e the solution of

$$(F^\star F + \alpha I) g_z^\alpha = F^\star \Phi_z^\infty.$$

Since F has dense range, this provides a sequence g_z^α such that $\|Fg_z^\alpha - \Phi_z^\infty\| \to 0$ when $\alpha \to 0$. In the case $\Im\mathfrak{m}(n) = 0$, it has been shown that the solution of Tikhonov regularization satisfies the first point of the theorem (see [3, 4]). A second weak point of this method is that the quantity $\|Hg_z^\alpha\|_{L^2(D)}$ cannot be computed since D is unknown. For numerical implementations, the quantity $\|g_z^\alpha\|_{L^2(\mathbb{S}^{d-1})}$ is computed instead and generally provides satisfactory results.

1.3.2 The factorization method

The Factorization Method introduced by Kirsch [80] avoids the drawbacks of the LSM as it gives an exact characterization of D in terms of F. The main idea is to define a new operator that can be computed from the far field operator and that has the same range of G. Then the operator G is replaced by this new operator in the LSM theoretical result, Theorem 1.3.1. This leads to a more explicit characterization of the belonging of z to D.

The $(\mathbf{F^\star F})^{\frac{1}{4}}$ method

The $(F^\star F)^{\frac{1}{4}}$ is the first version of FM. It relies on a second factorization of the far field operator F which is

$$F = H^\star T H. \tag{1.12}$$

The operator $T : \overline{R(H)} \subset L^2(D) \to L^2(D)$ is defined by

$$Tv := k^2(n-1)(v + u_s) \tag{1.13}$$

with u_s being the solution of (1.1) with $u_{i|D} = v$. Under some specific conditions on the refractive index n, it can be shown that $R((F^\star F)^{\frac{1}{4}}) = R(G)$. These conditions ensures that the middle

operator T can be decomposed as $T = T_0 + K$ where T_0 is coercive and K is compact non negative.

Theorem 1.3.3. *Assume that $\Im\mathfrak{m}(n) = 0$, that either $\Re\mathfrak{e}(n-1)$ or $\Re\mathfrak{e}(1-n)$ is definite positive, and that problem (ITP) is well posed. Then $z \in D$ if and only if Φ_z^∞ is in the range of $(F^\star F)^{\frac{1}{4}}$.*

The hypothesis $\Im\mathfrak{m}(n) = 0$ is required to ensure that F is normal ([29], Theorem 1.14 & Theorem 2.25) but also to guarantee that T satisfies some technical properties ([29] Lemma 2.26 & Theorem 2.27). To use this result in practice, one could for example invoke Picard theorem to characterize D: for $p \geq 1$, let λ_p and e_p be the eigenvalues and eigenfunctions of F, observing that $(F^\star F)^{\frac{1}{4}}$ has for singular system $(\sqrt{|\lambda_p|}, e_p, e_p)$, we get from Picard theorem that $z \in D$ if and only if

$$\sum_{p=1}^{+\infty} \frac{|\langle \Phi_z^\infty, e_p \rangle|^2}{|\lambda_p|} < +\infty, \tag{1.14}$$

and the solution to $(F^\star F)^{\frac{1}{4}} g_z = \Phi_z^\infty$ is given by

$$g_z = \sum_{p=1}^{+\infty} \frac{\langle \Phi_z^\infty, e_p \rangle}{|\lambda_p|^{\frac{1}{2}}} e_p. \tag{1.15}$$

In practice this infinite series is truncated so that sensitivity to noise is reduced. Another possibility is to define the sequence g_z^α as solution with Tikonov regularization, namely

$$((F^\star F)^{\frac{1}{2}} + \alpha I) g_z^\alpha = (F^\star F)^{\frac{1}{4}} \Phi_z^\infty \tag{1.16}$$

which allows to deal with noisy measurements by adapting α to the noise. The solution is given by

$$g_z^\alpha = \sum_{p=1}^{+\infty} \frac{|\lambda_p|^{\frac{1}{2}}}{|\lambda_p| + \alpha} \langle \Phi_z^\infty, e_p \rangle e_p \tag{1.17}$$

and we have the following, $z \in D$ if and only if $\lim_{\alpha \to 0} \|g_z^\alpha\|_{L^2(\mathbb{S}^{d-1})} = +\infty$.

The $\mathbf{F_\sharp}$ method

The $F_\sharp$ method is a second version of the factorization that does not require F to be normal, hence it allows to weaken the assumptions of the theorem above on the refractive index. It also relies on the second factorization of F. Defining the operator $F_\sharp^\theta := |\Re\mathfrak{e}(e^{i\theta} F)| + |\Im\mathfrak{m}(F)|$ for $\theta \in [0, \pi]$, it can be shown that

Theorem 1.3.4. *Assume that $\Im\mathfrak{m}(n) \geq 0$ and that there exists $\theta \in [0, \pi]$ such that $\Re\mathfrak{e}\left(e^{i\theta}(n-1)\right) > \epsilon > 0$ in D for some constant ϵ. Assume in addition that (ITP) is well posed. Then $z \in D$ if and only if Φ_z^∞ is in the range of $(F_\sharp^\theta)^{\frac{1}{2}}$.*

As for the $(F^\star F)^{\frac{1}{4}}$ method, one can use Picard Theorem or a Tikhonov regularization, for this, (λ_p, e_p) has only to be replaced by the pairs of eigenvalues and eigenfunctions of the self-adjoint and positive operator $F_\sharp^\theta$.

1.3.3 The generalized linear sampling method

Presentation of the method

A more recent method, the Generalized Linear Sampling Method introduced by Audibert-Haddar [10], also gives an exact characterization of D in terms of F but also relaxes the assumption of Theorem 1.3.3 concerning the refractive index n. Inspired by the LSM it is also based on the solvability of the far field equation $Fg = \Phi_z^\infty$, the difference being that the regularization of the latter equation uses a penalty term that controls $\|Hg_z^\alpha\|^2_{L^2(D)}$ instead of the classical Tikhonov regularization. For this, it is assumed that $\mathfrak{Re}(n-1)+\mu\mathfrak{Im}(n)$ or $\mathfrak{Re}(1-n)+\mu\mathfrak{Im}(n)$ is positive definite on D for some constant $\mu > 0$. Then the operator T is coercive in the following sense:

$$\exists C > 0,\ \forall \varphi \in \overline{R(H)}, \qquad |\langle T\varphi, \varphi\rangle_{L^2(D)}| \geq \|\varphi\|^2_{L^2(D)}. \tag{1.18}$$

Consequently, according to the second factorization (1.12), the quantities $\|Hg_z^\alpha\|^2_{L^2(D)}$ and $|\langle Fg, g\rangle_{L^2(\mathbb{S}^{d-1})}|$ are equivalent. Hence $|\langle Fg, g\rangle_{L^2(D)}|$ can be used as a penalty term to the far field equation. Therefore we define

$$J_z^\alpha(g) = \alpha|\langle Fg, g\rangle_{L^2(\mathbb{S}^{d-1})}| + \|Fg - \Phi_z^\infty\|^2_{L^2(\mathbb{S}^{d-1})}. \tag{1.19}$$

Let g_z^α be a minimizing sequence of J_z^α that satisfies

$$J_z^\alpha(g_z^\alpha) \leq \inf_{g\in L^2(\mathbb{S}^{d-1})} J_z^\alpha(g) + C\alpha. \tag{1.20}$$

We then have the following result,

Theorem 1.3.5. *Assume that k is such that (ITP) is well posed and that $\mathfrak{Re}(n-1)+\mu\mathfrak{Im}(n)$ or $\mathfrak{Re}(1-n)+\mu\mathfrak{Im}(n)$ is positive definite on D for some constant $\mu > 0$. Then $z \in D$ if and only if $\limsup_{\alpha\to 0} |\langle Fg, g\rangle_{L^2(\mathbb{S}^{d-1})}| < +\infty$.*

The penalty term $|\langle Fg, g\rangle|$ can be replaced by any other quantity that is equivalent to $\|Hg_z^\alpha\|^2_{L^2(D)}$ (and that can be computed from F). For instance the penalty $|\langle (F^\star F)^{\frac{1}{4}} g, g\rangle|$ is valid and leads to the factorization method indicator. Another possibility is to choose $|\langle F_\sharp g, g\rangle|$ as a penalty term where $F_\sharp = |\frac{1}{2}(F + F^\star)| + |\frac{1}{2i}(F - F^\star)|$.

Determination of transmission eigenvalues from far field data

The failure of the reconstruction algorithms at wave numbers k that are transmission eigenvalues have eventually led to the development of ways to determine transmission eigenvalues from far field data. This first result stems from the LSM. It allows to detect transmission eigenvalues k that are not non-scattering wave numbers, that are more specific transmission eigenvalues for which the eigenfunction v is moreover a Herglotz wave function.

Theorem 1.3.6. *Assume that $(n-1)$ is positive definite or negative definite on D, that k is not a non-scattering wave number. Then for any ball $B \subset D$, $\lim_{\alpha\to 0} \|Hg_z^\alpha\|_{L^2(D)}$ is bounded for a.e $z \in B$ if and only if k is not a transmission eigenvalue.*

The first weak point of this result is the assumption made on k. On this issue we mention that the set of non-scattering wave numbers has been shown to be empty [13] when the scattering object has corners and that the only known case for which the set of non scattering

wave number is non-empty is the sphere with constant refractive index. Once again the quantity $\lim_{\alpha\to 0} \|Hg_z^\alpha\|_{L^2(D)}$ cannot be computed since the operator H is unknown and is replaced by $\lim_{\alpha\to 0} \|g_z^\alpha\|_{L^2(\mathbb{S}^{d-1})}$ in practice, and transmission eigenvalues are detected by peaks in the curve

$$k \mapsto \int_B \|g_z^\alpha\|_{L^2(\mathbb{S}^{d-1})} \, \mathrm{d}z \tag{1.21}$$

for small values of α. Another possibility could be to first determine the shape D with some sampling method which would give access to the right quantity $\lim_{\alpha\to 0} \|Hg_z^\alpha\|_{L^2(D)}$. However, the GLSM framework provides a more direct characterization of TEs which is stated by the following theorem.

Theorem 1.3.7. *Assume that $(n-1)$ is positive definite or negative definite on D, that k is not a non-scattering wave number. Then for any ball $B \subset D$, $\lim_{\alpha\to 0} \langle F_\sharp g_z^\alpha, g_z^\alpha \rangle_{L^2(D)}$ is bounded for a.e $z \in B$ if and only if k is not a transmission eigenvalue.*

In the next section, the three mentioned methods, LSM, FM and GLSM, are explicited in a particular setting.

1.4 Explicit computations in a simple case

In this section, we consider the scattering problem in a particular setting of the two dimensional case, where the medium is delimited by a disk and has a constant refractive index. This setting allows to compute the eigenvalues of the far field operator, and to write explicitly the different indicator functions of D given by the sampling methods. We retrieve through these computations the theoretical results of the previous section and also discuss the optimality of the assumptions on the refractive index.

1.4.1 Expression of the scattered field for a disk

We consider the particular scattering problem by a disk shaped medium centered at the origin and of radius $R > 0$ and of constant refractive index. The index $n(x)$ is then defined by $n(x) = 1$ for $|x| \geq R$ and $n(x) = n_0 \in \mathbb{C} \setminus \{1\}$ for $|x| < R$. In all this section, for the sake of readability, n will refer to the constant n_0. For an incident field u_i satisfying the homogeneous Helmholtz equation in $\mathbb{R}^2$ we would like to find the Fourier expansion of the scattered field $u_s \in H^2_{loc}(\mathbb{R}^2)$ solution of (1.1)-(1.2) in the form

$$u_s(x) = \sum_{p\in\mathbb{Z}} f_p(k|x|)e^{ip\widehat{x}} \text{ for } |x| > R \tag{1.22}$$

where $\widehat{x} = x/|x|$. From $\Delta u_s + k^2 u_s$ for $|x| > R$ we obtain that for all $p \in \mathbb{Z}$, f_p is a solution of the Bessel equation

$$t^2 f_p'' + t f_p'(t) + (t^2 - p^2) f_p(t) = 0 \tag{1.23}$$

which admits two linearly independent solutions, the Bessel function of first kind J_p and of second kind Y_p. These functions have been massively studied in the literature, all the properties used in this chapter are listed in [1]; for a deeper study we refer to [62]. From the asymptotic behavior of these functions ([1] 9.2.1-9.2.2), the only possible combination of them allowing to obtain the right asymptotic behavior (1.3) is $H_p := J_p + iY_p$, this function is called the Hankel function of first kind. At this point we have that the functions f_p appearing in the Fourier decomposition of u_s are of the form

$$f_p = b_p H_p, \tag{1.24}$$

where b_p are complex numbers that will be linked to the incident field u_i next. Samely to u_s, we obtain the following expansion for u_i (the functions Y_p do not appear because they have a singularity at 0 while any entire solution of Helmholtz equation is smooth),

$$u_i(x) = \sum_{p\in\mathbb{Z}} a_p J_p(k|x|)e^{ip\widehat{x}} \quad \forall x \in \mathbb{R}^2, \tag{1.25}$$

where a_p are complex numbers. In the same way the total field is also a sum of Bessel functions in D,

$$u(x) = \sum_{p\in\mathbb{Z}} c_p J_p(k\sqrt{n}|x|)e^{ip\widehat{x}} \quad \forall x \in D.$$

The regularity of $u_s = u - u_i$ through ∂D implies the following Cauchy conditions on ∂D,

$$\left|\begin{array}{rcll} -u_s + u & = & u_i & \text{on } \partial D \\ -\partial_\nu u_s + \partial_\nu u & = & \partial_\nu u_i & \text{on } \partial D. \end{array}\right. \tag{1.26}$$

The latter implies the following relations between the Fourier coefficients of u, u_i and u_s,

$$\begin{pmatrix} -H_p(kR) & J_p(k\sqrt{n}R) \\ -H_p'(kR) & \sqrt{n}J_p'(k\sqrt{n}R) \end{pmatrix} \begin{pmatrix} b_p \\ c_p \end{pmatrix} = a_p \begin{pmatrix} J_p(kR) \\ J_p'(kR) \end{pmatrix}.$$

The coefficient b_p which appears in the decomposition of u_s can be obtained by the use of the Cramer formula,

$$b_p = a_p \frac{\sqrt{n}J_p(kR)J_p'(k\sqrt{n}R) - J_p'(kR)J_p(k\sqrt{n}R)}{J_p(k\sqrt{n}R)H_p'(kR) - \sqrt{n}J_p'(k\sqrt{n}R)H_p(kR)}.$$

We now simplify the latter expression by using the recurrence relation formulas satisfied by the Bessel functions (see [62] 2.12 p.17)

$$\mathcal{C}_p'(z) = \mathcal{C}_{p-1}(z) - \frac{p}{z}\mathcal{C}_p(z)$$

where $\mathcal{C}_p$ denotes J_p, Y_p or H_p. The numerator of b_p can be simplified with

$$\sqrt{n}J_p(kR)J_p'(k\sqrt{n}R) - J_p'(kR)J_p(k\sqrt{n}R) = \sqrt{n}J_p(kR)J_{p-1}(k\sqrt{n}R) - J_{p-1}(kR)J_p(k\sqrt{n}R)$$

and it's denominator with

$$J_p(k\sqrt{n}R)H_p'(kR) - \sqrt{n}J_p'(k\sqrt{n}R)H_p(kR) = J_p(k\sqrt{n}R)H_{p-1}(kR) - \sqrt{n}J_{p-1}(k\sqrt{n}R)H_p(kR).$$

Finally we have

$$b_p = a_p \frac{\sqrt{n}J_p(kR)J_{p-1}(k\sqrt{n}R) - J_{p-1}(kR)J_p(k\sqrt{n}R)}{J_p(k\sqrt{n}R)H_{p-1}(kR) - \sqrt{n}J_{p-1}(k\sqrt{n}R)H_p(kR)}.$$

To summarize, for a given incident field in the form (1.25) the resulting scattered field is given with

$$u_s(x) = \sum_{p\in\mathbb{Z}} a_p B_p(k,n,R) H_p(k|x|) e^{ip\widehat{x}} \text{ for } |x| > R, \tag{1.27}$$

where the coefficient $B_p(k,n,R)$ is given by

$$B_p(k,n,R) := \frac{\sqrt{n}J_p(kR)J_{p-1}(k\sqrt{n}R) - J_{p-1}(kR)J_p(k\sqrt{n}R)}{J_p(k\sqrt{n}R)H_{p-1}(kR) - \sqrt{n}J_{p-1}(k\sqrt{n}R)H_p(kR)}. \tag{1.28}$$

From the formulas $\mathcal{C}_{-p}(x) = (-1)^p \mathcal{C}_p(x)$ and $\mathcal{C}_{p+1} = \frac{2p}{x}\mathcal{C}_p(x) - \mathcal{C}_{p-1}(x)$ we decuce that $B_{-p} = B_p$ and when $n \in \mathbb{R}$ simple computations shows that $|B_p(k,n,R)| \leq 1$.

We finish this paragraph by linking the coefficient c_p appearing in the Fourier expansion of u to a_p. Once again the Cramer formula gives

$$c_p = a_p \frac{J_p(kR)H_p'(kR) - J_p'(kR)H_p(kR)}{J_p(k\sqrt{n}R)H_{p-1}(kR) - \sqrt{n}J_{p-1}(k\sqrt{n}R)H_p(kR)}.$$

Using the following wronskian formula,

$$J_p(x)Y_p'(x) - J_p'(x)Y_p(x) = \frac{2}{\pi x},$$

the numerator of c_p can be simplified as follows,

$$J_p(kR)H_p'(kR) - J_p'(kR)H_p(kR) = J_p(kR)Y_p'(kR) - J_p'(kR)Y_p(kR) = \frac{2i}{\pi kR}.$$

Finally

$$c_p = \frac{2ia_p}{\pi kR\left(J_p(k\sqrt{n}R)H_{p-1}(kR) - \sqrt{n}J_{p-1}(k\sqrt{n}R)H_p(kR)\right)}.$$

1.4.2 Spectral properties of the far field operator

In this section the far field operator is shown to be diagonalizable in the Fourier basis of $L^2([0,2\pi])$. After being computed, the asymptotic behavior of the sequence of eigenvalues is established.

Diagonalization of the far field operator

Following the previous notations we recall that the polar coordinates of $x \in \mathbb{R}^2 \setminus \{0_{\mathbb{R}^2}\}$ are denoted $(|x|, \widehat{x}) \in \mathbb{R}_+^\star \times \mathbb{S}^1$. The set $\mathbb{S}^1$ is identified with $[0, 2\pi[$ and we denote the canonical orthonormal basis of $L^2([0,2\pi])$ with

$$e_p(\theta) = \frac{1}{\sqrt{2\pi}} e^{ip\theta} \quad \forall \theta \in [0,2\pi].$$

Using Jacobi-Anger formula,

$$e^{izcos(\alpha)} = \sum_{p\in\mathbb{Z}} i^p J_p(z) e^{ip\alpha} \quad \forall z \in \mathbb{C},\ \forall \alpha \in \mathbb{R}, \tag{1.29}$$

the following decomposition is obtained for an incident plane wave of direction $d \in \mathbb{S}^1$ defined by $u_i(d,x) = e^{ikx.d}$,

$$u_i(d,x) = e^{ik|x|cos(\widehat{x}-d)} = \sum_{p\in\mathbb{Z}} i^p J_p(k|x|)2\pi e_p(-d)e_p(\widehat{x}). \tag{1.30}$$

According to (1.27) the associated scattered field to $u_i(d,\cdot)$ is

$$u_s(d,x) = \sum_{p\in\mathbb{Z}} i^p B_p(k,n,R)H_p(k|x|)2\pi e_p(-d)e_p(\widehat{x}).$$

Then the asymptotic behavior of the Hankel functions implies

$$u_\infty(d,\widehat{x}) = \sqrt{\frac{8\pi}{k}}e^{-\frac{i\pi}{4}}\sum_{p\in\mathbb{Z}} B_p(k,n,R)e_p(-d)e_p(\widehat{x}).$$

Finally from definition of the far field operator we obtain

$$(Fe_p)(\widehat{x}) = \int_{\mathbb{S}^1} e_p(d)u_\infty(d,x)\,\mathrm{d}(d) = \sqrt{\frac{8\pi}{k}}e^{-\frac{i\pi}{4}}B_p(k,n,R)e_p(\widehat{x}).$$

Hence F is diagonal in the basis $(e_p)_{p\in\mathbb{Z}}$ and the associated eigenvalues are

$$\lambda_p = \sqrt{\frac{8\pi}{k}}e^{-\frac{i\pi}{4}}B_p(k,n,R). \tag{1.31}$$

Whether the refractive index has an imaginary part or not, the far field operator is always normal in this setting. However, as it is known for the general case, the hypothesis of real refractive index is required for the scattering operator $S := I + \frac{2ike^{-\frac{i\pi}{4}}}{\sqrt{8\pi k}}F$ to be unitary. Indeed first observing that

$$B_p(k,n,R) = \frac{\alpha_p}{i\beta_p - \alpha_p} \tag{1.32}$$

with

$$\alpha_p = \sqrt{n}J_p(kR)J_{p-1}(\sqrt{n}kR) - J_{p-1}(kR)J_p(\sqrt{n}kR) \tag{1.33}$$

and

$$\beta_p = J_p(k\sqrt{n}R)Y_{p-1}(kR) - \sqrt{n}J_{p-1}(k\sqrt{n}R)Y_p(kR) \tag{1.34}$$

one obtains the following for the eigenvalues σ_p of the scattering operator,

$$\sigma_p := 1 + \frac{2ike^{-\frac{i\pi}{4}}}{\sqrt{8\pi k}}\lambda_p = 1 + 2B_p(k,n,R) = 1 + 2\frac{\alpha_p}{-\alpha_p + i\beta_p} = \frac{\alpha_p + i\beta_p}{-\alpha_p + i\beta_p}. \tag{1.35}$$

The hypothesis $\Im\mathfrak{m}(n) = 0$ guarantees that $\alpha_p, \beta_p \in \mathbb{R}$ so that $|\sigma_p| = 1$. This result is illustrated in the following figures.

We finish this paragraph by mentioning that F is injective with dense range if and only if $\lambda_p(k,n,R) \neq 0$ for all $p \in \mathbb{Z}$. Since $k \mapsto \lambda_p(k)$ is analytic, this always holds true except for a countable set of k, which will be shown be closely related to the well posedness of problem (1.71) in a next section. This set of k will be linked to the interior transmission problem in a next section.

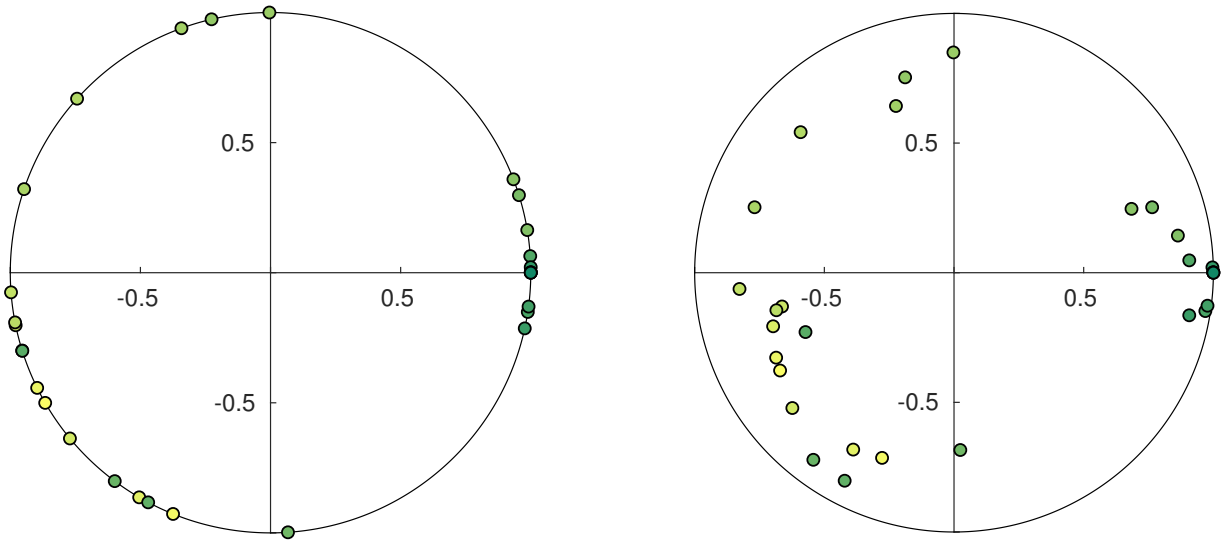

Figure 1.1: 30 first values of $\sigma_p(k,n,R)$ for $k=10$, $R=2$, $n=2$ (left) and $n=2+0.02i$ (right).

Asymptotic behaviour of the far field eigenvalues

We now establish the asymptotic behavior of λ_p when $p \to +\infty$. The knowledge of the result will be significant to understand the indicator functions of D proposed by the sampling methods. In view of (1.31), it is sufficient to study the behavior of the coefficient $B_p(k,n,R)$ defined at (1.28). To this end are introduced the two following quantities for $x>0$,

$$\mathcal{N}_p(x) = \sqrt{n}J_p(x)J_{p-1}(\sqrt{n}x) - J_{p-1}(x)J_p(\sqrt{n}x) \tag{1.36}$$

and

$$\mathcal{D}_p(x) = J_p(\sqrt{n}x)H_{p-1}(x) - \sqrt{n}J_{p-1}(\sqrt{n}x)H_p(x) \tag{1.37}$$

so that

$$B_p(k,n,R) = \frac{\mathcal{N}_p(kR)}{\mathcal{D}_p(kR)}. \tag{1.38}$$

We first turn our attention to $(\mathcal{N}_p)_{p\geq 0}$. Seeking for an equivalent with formula (1.41) would amount to zero. We recall the series expansion of Bessel functions,

$$J_p(x) = \sum_{j=0}^{+\infty} \frac{(-1)^j}{j!(p+j)!}\left(\frac{x}{2}\right)^{p+2j}, \quad x>0 \tag{1.39}$$

Denoting $s_p^j = \frac{(-1)^j}{j!(p+j)!}\left(\frac{x}{2}\right)^{p+2j}$ the general term of the series above and splitting the sum for $r \geq 0$ gives,

$$J_p(x) = \sum_{j=0}^{r} s_p^j + \sum_{j\geq 1} s_p^{j+r} = \sum_{j=0}^{r} s_p^j + s_p^r \sum_{j\geq 1}(-1)^j \left(\frac{x}{2}\right)^{2j} \frac{r!(p+r)!}{(j+r)!(p+j+r)!},$$

the second term of the last equation is $\underset{p\to+\infty}{o}\left(s_p^r\right)$, indeed for p sufficiently large

$$\left|\sum_{j\geq 1}(-1)^j \left(\frac{x}{2}\right)^{2j} \frac{r!(p+r)!}{(j+r)!(p+j+r)!}\right| \leq \frac{1}{p+r}\sum_{j\geq 1}\left(\frac{|x|}{2}\right)^{2j}\frac{1}{(p+r)^{j-1}}.$$

D'Alembert criteria for convergence of series guarantees that the right hand side of the above estimate goes to zero as p goes to infinity. Finally for $r \in \mathbb{N}^*$, $J_p(x)$ satisfies the following Taylor expansion,

$$J_p(x) = \sum_{j=0}^{r} s_p^j + \underset{p\to+\infty}{o}\left(s_p^r\right).$$

Applying this result to $\mathcal{N}_p(x)$ gives,

$$\begin{aligned}\mathcal{N}_p(x) = n^{\frac{1}{2}}\left(s_p^0 + s_p^1 + \underset{p\to+\infty}{o}\left(s_p^1\right)\right)\left(n^{\frac{p-1}{2}}s_{p-1}^0 + n^{\frac{p+1}{2}}s_{p-1}^1 + \underset{p\to+\infty}{o}\left(n^{\frac{p+1}{2}}s_{p-1}^1\right)\right)\\ - \left(s_{p-1}^0 + s_{p-1}^1 + \underset{p\to+\infty}{o}\left(s_{p-1}^1\right)\right)\left(n^{\frac{p}{2}}s_p^0 + n^{\frac{p+2}{2}}s_p^1 + \underset{p\to+\infty}{o}\left(n^{\frac{p+2}{2}}s_p^1\right)\right).\end{aligned}$$

Keeping only the leading term gives

$$\mathcal{N}_p(x) \underset{p\to+\infty}{\sim} n^{\frac{p}{2}}(n-1)(s_p^0 s_{p-1}^1 - s_p^1 s_{p-1}^0) = -n^{\frac{p}{2}}(n-1)\left(\frac{x}{2}\right)^{2p+1}\frac{1}{p!(p+1)!}. \tag{1.40}$$

We now turn our attention to $\mathcal{D}_p(x)$. From the behaviour of Bessel functions for large order

$$J_p(x) \underset{p\to+\infty}{\sim} \frac{1}{p!}\left(\frac{x}{2}\right)^p \quad \text{and} \quad Y_p(x) \underset{p\to+\infty}{\sim} -\frac{(p-1)!}{\pi}\left(\frac{x}{2}\right)^{-p}, \tag{1.41}$$

the following asymptotics are easily derived,

$$J_p(\sqrt{n}x)Y_{p-1}(x) \underset{p\to+\infty}{\sim} -\frac{n^{\frac{p}{2}}x}{2\pi p^2} \quad \text{and} \quad \sqrt{n}J_{p-1}(\sqrt{n}x)Y_p(x) \underset{p\to+\infty}{\sim} -\frac{2n^{\frac{p}{2}}}{\pi x}. \tag{1.42}$$

From (1.41)-(1.42) it is obvious that when p is large, the quantity $\sqrt{n}J_{p-1}(\sqrt{n}x)Y_p(x)$ dominates the three terms $J_p(\sqrt{n}x)Y_{p-1}(x)$, $J_p(\sqrt{n}x)J_{p-1}(x)$ and $\sqrt{n}J_{p-1}(\sqrt{n}x)J_p(x)$. Consequently,

$$\mathcal{D}_p(x) \underset{p\to+\infty}{\sim} -i\sqrt{n}J_{p-1}(\sqrt{n}x)Y_p(x) \underset{p\to+\infty}{\sim} \frac{2in^{\frac{p}{2}}}{\pi x}. \tag{1.43}$$

Finally from (1.40) and (1.43) we deduce that

$$B_p(k,n,R) = \frac{\mathcal{N}_p(kR)}{\mathcal{D}_p(kR)} \underset{p\to+\infty}{\sim} i\pi(n-1)\left(\frac{kR}{2}\right)^{2(p+1)}\frac{1}{p!(p+1)!}. \tag{1.44}$$

Hence from (1.31) and (1.44), the following asymptotics for the eigenvalues of the far field operator is straightforward,

$$\lambda_p \underset{p\to+\infty}{\sim} \sqrt{\frac{8\pi^3}{k}}(n-1)e^{i\frac{\pi}{4}}\left(\frac{kR}{2}\right)^{2(p+1)}\frac{1}{p!(p+1)!}. \tag{1.45}$$

This result will be useful for the study of the sampling methods. Before doing so we point out that the equivalent (1.45) for λ_p can be used to determine the refractive index of a material having a circular shape, provided that the radius R is known.

1.4.3 Study of the sampling methods

Now that has been determined a basis on which F is diagonal and the associated eigenvalues, the indicator functions of the sampling methods for D can be computed. The explicit formulas in this situation gives the possibility to seek for more precise estimates such as the speed of blow up of the indicators when $\alpha \to 0$ for $z \notin D$; speed of blow up of the indicator when $z \to \partial D^-$; determine the most optimal indicator of the presented method; more challenging, find an optimal way to choose α for noisy measurements. To simplify the computations, the constant η_2 in (4.22) is dropped. We define ϕ_z by

$$\phi_z(\widehat{x}) := e^{-ikz\cdot\widehat{x}}. \tag{1.46}$$

and consider the far field equation

$$Fg = \phi_z. \tag{1.47}$$

This does not change the theoretical results and affect the following computations only by the multiplicative constant η_2.

The Linear Sampling Method

Let $z \in \mathbb{R}^2$ and denote by g_z^α the solution of the Tikhonov regularization of the far field equation $Fg = \phi_z$. It can be shown that g_z^α is given by [82]

$$g_z^\alpha = (F^\star F + \alpha I)^{-1} F^\star \phi_z.$$

By using the basis of eigenvectors of F, the function g_z^α can easily be written as follows,

$$g_z^\alpha = \sum_{p\in\mathbb{Z}} \frac{\overline{\lambda_p}}{|\lambda_p|^2 + \alpha} \langle \phi_z, e_p\rangle e_p. \tag{1.48}$$

On the one hand, from the definition of H (1.8) and formula (1.30), we obtain that for all $x \in \mathbb{R}^2$,

$$(He_p)(x) = \int_{\mathbb{S}^1} \frac{e^{ipd}}{\sqrt{2\pi}} e^{ikx.d}\, \mathrm{d}(d) = \int_{\mathbb{S}^1} \frac{e^{ipd}}{\sqrt{2\pi}} \sum_{q\in\mathbb{Z}} i^q J_q(k|x|) e^{iq(\widehat{x}-d)}\, \mathrm{d}(d).$$

Consequently,

$$(He_p)(x) = 2\pi i^p J_p(k|x|) e_p(\widehat{x}). \tag{1.49}$$

On the other hand the conjugation of Jacobi-Anger formula gives,

$$\phi_z(\widehat{x}) = \sum_{q\in\mathbb{Z}} (-i)^q e^{iq\widehat{x}} J_q(k|z|) e^{-iq\widehat{z}}$$

so that (after integrating with respect to $\widehat{x}$)

$$\langle \phi_z, e_p\rangle = \sqrt{2\pi}(-i)^p J_p(k|z|) e^{-ip\widehat{z}}. \tag{1.50}$$

The combination of (1.48),(1.49) and (1.50) leads to

$$Hg_z^\alpha(x) = (2\pi)^{\frac{3}{2}} \sum_{p\in\mathbb{Z}} \frac{\overline{\lambda_p} J_p(k|x|) J_p(k|z|) e^{-ip\widehat{z}}}{|\lambda_p|^2 + \alpha} e_p(\widehat{x}),$$

from which we easily obtain

$$\|Hg_z^\alpha\|^2_{L^2(D)} = \int_0^R |x|\ \mathrm{d}|x| \int_{\mathbb{S}^1} Hg_z^\alpha(x)\overline{Hg_z^\alpha(x)}\ \mathrm{d}\widehat{x}$$
$$= (2\pi)^3 \int_0^R |x|\ \mathrm{d}|x| \left(\sum_{p\in\mathbb{Z}} \frac{|\lambda_p|^2 J_p(k|x|)^2 J_p(k|z|)^2}{(|\lambda_p|^2+\alpha)^2} \right).$$

We finally deduce after a change of variable in the integral above that

$$\|Hg_z^\alpha\|^2_{L^2(D)} = \frac{(2\pi)^3}{k^2} \sum_{p\in\mathbb{Z}} \frac{|\lambda_p|^2 J_p(k|z|)^2}{(|\lambda_p|^2+\alpha)^2} \int_0^{kR} J_p(r)^2 r\ \mathrm{d}r. \tag{1.51}$$

We now study the convergence of $(\|Hg_z^\alpha\|^2_{L^2(D)})_{\alpha>0}$ when α goes to zero, the result will depend as expected on $|z|$. The absolute convergence of series (1.39) allows to write the following with the previous notations for s_p^j

$$J_p(x)^2 = \sum_{(j,m)\in\mathbb{N}^2} s_p^j s_p^m = \sum_{l\in\mathbb{N}} \sum_{j+m=l} \frac{(-1)^l}{j!m!(p+j)!(p+m)!} \left(\frac{x}{2}\right)^{2(p+l)}$$

Then

$$\int_0^{kR} J_p(x)^2 x\,\mathrm{d}x = \sum_{l\in\mathbb{N}} \sum_{j+m=l} \frac{(-1)^l \times 2}{j!m!(p+j)!(p+m)!(p+l+1)} \left(\frac{kR}{2}\right)^{2(p+l+1)}$$
$$= \frac{2}{p!(p+1)!} \left(\frac{kR}{2}\right)^{2(p+1)} (1+\epsilon(p)).$$

We have

$$|\epsilon(p)| = \sum_{l\in\mathbb{N}^\star} \sum_{j+m=l} \frac{p!^2(p+1)}{j!m!(p+j)!(p+m)!(p+l+1)} \left(\frac{kR}{2}\right)^{2l}$$
$$\leq \frac{1}{(p+1)} \sum_{l\in\mathbb{N}^\star} \frac{l+1}{(p+1)^{l-1}} \left(\frac{kR}{2}\right)^{2l}.$$

The d'Alembert criteria implies that $\epsilon(p) \to 0$ when $p \to +\infty$. Consequently

$$\int_0^{kR} J_p^2(r) r\,\mathrm{d}r \underset{p\to+\infty}{\sim} \frac{2}{p!(p+1)!} \left(\frac{kR}{2}\right)^{2p+2}.$$

Now for $\alpha > 0$ the series (1.51) is easily seen to be convergent whereas for $\alpha = 0$, its general term satisfies

$$\frac{J_p(k|z|)^2}{|\lambda_p|^2} \int_0^{kR} J_p(r)^2 r\ \mathrm{d}r \underset{p\to+\infty}{\sim} \frac{p+1}{k\pi^3 R^2 |n-1|^2} \left(\frac{|z|}{R}\right)^{2p}.$$

We recover the result of the LSM, $\|Hg_z^\alpha\|^2_{L^2(D)}$ converges when $\alpha \to 0$ iff $|z| < R$ and the limit $l(z)$ is

$$\forall z \in B(0,R), \quad l(z) = \frac{(2\pi)^3}{k^2} \sum_{p\in\mathbb{Z}} \frac{J_p(k|z|)^2}{|\lambda_p|^2} \int_0^{kR} J_p(r)^2 r\ \mathrm{d}r.$$

As mentionned before, one does not have access to the operator H and rather compute $\|g_z^\alpha\|^2_{L^2(\mathbb{S}^1)}$ for small value of α given by

$$\|g_z^\alpha\|^2_{L^2(\mathbb{S}^1)} = 2\pi \sum_{p\in\mathbb{Z}} \frac{|\lambda_p|^2 J_p^2(k|z|)}{(|\lambda_p|^2+\alpha)^2}. \tag{1.52}$$

This quantity is defined for all $z \in \mathbb{R}^2$ and it's behavior with respect to z is not clear. Furthermore the limit when α goes to zero never exists, formally one can obtain from (1.48) that

$$\lim_{\alpha\to 0} \|g_z^\alpha\|^2_{L^2(\mathbb{S}^1)} = 2\pi \sum_{p\in\mathbb{Z}} \frac{J_p^2(k|z|)}{|\lambda_p|^2}, \tag{1.53}$$

the general term of this series decreases less rapidly than the one of the original indicator $l(z)$. More precisely, with the use of (1.41) and (1.45),

$$\frac{J_p^2(k|z|)}{|\lambda_p|^2} \underset{p\to+\infty}{\sim} \frac{k(p+1)!^2}{(2\pi)^3|n-1|^2}\left(\frac{2}{kR}\right)^4\left(\frac{2|z|}{kR^2}\right)^{2p}.$$

This series never converges (except for $z=0$) indicating that a solution to the far field equation $Fg = \phi_z$ that would be given by

$$\sum_{p\in\mathbb{Z}} \frac{\langle \phi_z, e_p\rangle}{\lambda_p} e_p \tag{1.54}$$

never exists.

Despite this weak point, LSM remains a quick and simple method and numerical results show that it is reliable in a first approach to localize an inhomogeneity and/or determine number of connected components of an inhomogeneity. We carry on the investigation of the factorization method and GLSM.

The Factorization Method

The factorization method consists in solving the equation $(F^\star F)^{\frac{1}{4}} g = \phi_z$. Since $(F^\star F)^{\frac{1}{4}}$ is diagonalizable in the basis $(e_p)_{p\in\mathbb{Z}}$ with the corresponding eigenvalues $\sqrt{|\lambda_p|}$. According to the Picard theorem, there exist a solution to this equation if and only if

$$\varphi_z := \sum_{p=1}^{+\infty} \frac{|\langle \phi_z, e_p\rangle|^2}{|\lambda_p|} < +\infty. \tag{1.55}$$

By using the relation (1.50), the expression of φ_z can be simplified as follows,

$$\varphi_z = 2\pi \sum_{p=1}^{+\infty} \frac{J_p^2(k|z|)}{|\lambda_p|}. \tag{1.56}$$

Compared to the series (1.53), the general term of the series above goes (quite rapidly) to zero, more precisely it has the following asymptotic,

$$\frac{J_p^2(k|z|)}{|\lambda_p|} \underset{p\to+\infty}{\sim} \frac{\sqrt{k}(p+1)}{\sqrt{2\pi}|n-1|}\left(\frac{kR}{2}\right)^2\left(\frac{|z|}{R}\right)^{2p} \tag{1.57}$$

Consequently we obtain the expected result, $\varphi_z < +\infty$ if and only if $z \in D$. As mentioned above, one can rather use a Tikhonov regularization of $(F^\star F)^{\frac{1}{4}} g = \phi_z$ which consists in minimizing the cost function

$$J_z^\alpha = \alpha \|g\|^2_{L^2(\mathbb{S}^1)} + \|(F^\star F)^{\frac{1}{4}} g - \phi\|^2_{L^2(\mathbb{S}^1)}. \tag{1.58}$$

The minimizer g_z^α of J_z^α satisfies the following normal equation associated to J_z^α,

$$(F^\star F)^{\frac{1}{2}} g_z^\alpha + \alpha g_z^\alpha = (F^\star F)^{\frac{1}{4}} \phi_z, \tag{1.59}$$

and

$$g_z^\alpha = ((F^\star F)^{\frac{1}{2}} + \alpha I)^{-1} (F^\star F)^{\frac{1}{4}} \phi_z. \tag{1.60}$$

We deduce that

$$g_z^\alpha = \sum_{p \in \mathbb{Z}} \frac{|\lambda_p|^{\frac{1}{2}}}{|\lambda_p| + \alpha} \langle \phi, e_p \rangle e_p \tag{1.61}$$

and

$$\|g_z^\alpha\|^2_{L^2(\mathbb{S}^1)} = 2\pi \sum_{p \in \mathbb{Z}} \frac{|\lambda_p| J_p^2(k|z|)}{(|\lambda_p| + \alpha)^2} \tag{1.62}$$

Since $\lim_{\alpha \to 0} \|g_z^\alpha\|^2_{L^2(\mathbb{S}^1)} = \varphi_z$ (see (1.56)), the use of the Tikhonov regularization provides exactly the same indicator function for D, that we recall in terms of $\lim_{\alpha \to 0} \|g_z^\alpha\|^2_{L^2(\mathbb{S}^1)} = \varphi_z$:

$$\lim_{\alpha \to 0} \|g_z^\alpha\|^2_{L^2(\mathbb{S}^1)} < +\infty \iff z \in D. \tag{1.63}$$

Note that the $(F^\star F)^{\frac{1}{4}}$ method works in our setting even if n has an imaginary part, although F is not normal in this case.

The Generalized Linear Sampling Method

To simplify the computations, we opted for the presentation of the regularization of the far field equation with the penalty term $|\langle F^\sharp g, g \rangle|$ where $F^\sharp = |\frac{1}{2}(F + F^\star)| + |\frac{1}{2i}(F - F^\star)|$ or equivalently by

$$F^\sharp g = \sum_{p \in \mathbb{Z}} \sigma_p \langle g, e_p \rangle_{L^2(\mathbb{S}^1)} e_p, \quad \forall g \in L^2(\mathbb{S}^1), \tag{1.64}$$

where $\sigma_p = |\mathfrak{Re}(\lambda_p)| + |\mathfrak{Im}(\lambda_p)|$. The functional

$$J_z^\alpha(g) = \alpha \langle F^\sharp g, g \rangle_{L^2(\mathbb{S}^{d-1})} + \|Fg - \phi_z\|^2_{L^2(\mathbb{S}^{d-1})}. \tag{1.65}$$

has a minimizer which is given by

$$g_z^\alpha = \sum_{p \in \mathbb{Z}} \frac{\overline{\lambda_p} \langle \phi_z, e_p \rangle}{|\lambda_p|^2 + \alpha \sigma_p} e_p \tag{1.66}$$

and

$$\langle F^\sharp g_z^\alpha, g_z^\alpha \rangle_{L^2(\mathbb{S}^{d-1})} = \sum_{p \in \mathbb{Z}} \frac{\sigma_p |\lambda_p|^2 J_p^2(k|z|)}{(|\lambda_p|^2 + \alpha \sigma_p)^2}. \tag{1.67}$$

Since $|\lambda_p| \leq \sigma_p \leq \sqrt{2}|\lambda_p|$, the general term of this series satisfies for $\alpha = 0$,

$$\frac{J_p^2(k|z|)}{|\lambda_p|} \leq \frac{\sigma_p J_p^2(k|z|)}{|\lambda_p|^2} \leq \sqrt{2}\frac{J_p^2(k|z|)}{|\lambda_p|} \tag{1.68}$$

Consequently the quantity $\lim_{\alpha\to 0}\langle F^\sharp g_z^\alpha, g_z^\alpha\rangle_{L^2(\mathbb{S}^{d-1})}$ is equivalent to the quantity φ_z defined by (1.55), and is bounded if and only if $z \in D$ according to the study of the factorization method in the previous paragraph. Once again we point out that the hypothesis on the refractive index is not required.

For later use we mention that the quantity Hg_z^α is known to be converging to the solution of (ITP) with $(f, g) = (\Phi_{z|\partial\Omega}, \partial_\nu \Phi_{z|\partial\Omega})$. By using relations (1.49) and (1.50), we first obtain

$$Hg_z^\alpha = (2\pi)^{\frac{3}{2}} \sum_{p\in\mathbb{Z}} \frac{\overline{\lambda_p} J_p(k|\cdot|)J_p(k|z|)e^{-ip\widehat{z}}}{|\lambda_p|^2 + \alpha\sigma_p} e_p, \tag{1.69}$$

Then letting $\alpha \to 0$, we obtain for $|z| < R$,

$$\lim_{\alpha\to 0} Hg_z^\alpha = (2\pi)^{\frac{3}{2}} \sum_{p\in\mathbb{Z}} \frac{J_p(k|\cdot|)J_p(k|z|)e^{-ip\widehat{z}}}{\lambda_p} e_p \tag{1.70}$$

1.4.4 The interior transmission problem

Transmission eigenvalues

The interior transmission problem in the setting of a disk of radius R denoted B_R and constant refractive index n is the following: for given $f \in H^{3/2}(\partial B_R)$ and $g \in H^{1/2}(\partial B_R)$, find $(u, v) \in L^2(B_R) \times L^2(B_R)$ such that $u - v \in H^2(D)$ and

$$\left|\begin{array}{rcll} \Delta u + k^2 n u &=& 0 & \text{in } B_R \\ \Delta v + k^2 v &=& 0 & \text{in } B_R \\ u - v &=& f & \text{on } \partial B_R \\ \partial_\nu(u - v) &=& g & \text{on } \partial B_R. \end{array}\right. \tag{1.71}$$

As we will see this problem always admits a unique couple of solution (u, v) except for particular values of k, more precisely and at is will be clearer later, when k belongs to the set of transmission eigenvalues defined by the following.

Definition 1.4.1. *$k > 0$ is said to be a transmission eigenvalue if and only if there exist a non trivial solution to (1.71) for $f = g = 0$.*

As in the previous section it can be shown that the solutions u and v can be decomposed as a sum of Bessel functions by the following means,

$$\left|\begin{array}{rcll} v(x) &=& \sum_{p\in\mathbb{Z}} v_p J_p(k|x|)e^{ip\widehat{x}} & \forall x \in B_R \\ u(x) &=& \sum_{p\in\mathbb{Z}} u_p J_p(k\sqrt{n}|x|)e^{ip\widehat{x}} & \forall x \in B_R. \end{array}\right. \tag{1.72}$$

Denoting

$$f_p = \int_0^{2\pi} f(R, \widehat{x})\overline{e_p(\widehat{x})}\,\mathrm{d}\widehat{x} \quad \text{and} \quad g_p = \int_0^{2\pi} g(R, \widehat{x})\overline{e_p(\widehat{x})}\,\mathrm{d}\widehat{x}, \tag{1.73}$$

the transmission conditions in (1.71) give

$$\begin{pmatrix} J_p(k\sqrt{n}R) & -J_p(kR) \\ k\sqrt{n}J_p'(k\sqrt{n}R) & -kJ_p'(kR) \end{pmatrix} \begin{pmatrix} u_p \\ v_p \end{pmatrix} = \begin{pmatrix} f_p \\ g_p \end{pmatrix}. \tag{1.74}$$

There exists a unique solution to the interior transmission problem (1.71) if and only if the couple (u_p, v_p) can be uniquely defined for all $p \in \mathbb{Z}$ by the above system or equivalently if

$$J_p(kR)\sqrt{n}J_p'(k\sqrt{n}R) - J_p(k\sqrt{n}R)J_p'(kR) \neq 0 \quad \forall p \in \mathbb{Z}. \tag{1.75}$$

This first indicates that

$$k \text{ is not a transmission eigenvalue} \Longleftrightarrow (1.71) \text{ is well posed.}$$

Now using the formula $J_p'(x) = J_{p-1}(x) - \frac{p}{x}J_p(x)$, the quantity (1.75) is seen to be equal to the numerator of $B_p(k, n, R)$ defined by (1.28). Consequently, the transmission eigenvalues correspond to the zeros of the function $k \mapsto B_p(k, n, R)$. Since the latter function is analytic, we first deduce that the set of transmission eigenvalues is discrete. Furthermore, since the eigenvalues $\lambda_p(k, n, R)$ of F are equal to $B_p(k, n, R)$ up to a nonzero multiplicative parameter (see (1.31)), we moreover have

$$k \text{ is not a transmission eigenvalue} \iff F \text{ is injective with dense range.}$$

This property is remarkable. It stipulates that all transmission eigenvalues correspond to values of k for which F is non injective. Yet it is known that F is not injective if and only if k is not a non scattering wavenumber [29, Theorem 1.43]. These are particular transmission eigenvalues k for which the associated eigenvector v solution to (1.71) with $f = g = 0$, can be extended to an entire solution to Helmholtz equation. Consequently, in the case of a disk of constant refractive index, every transmission eigenvalue is a non scattering wave number. We mention that this result is known to be true for any spherically stratified medium.

The far field equation

We turn back our attention to the far field equation, let $z \in B_R$ and consider Φ_z the fundamental solution of Helmholtz equation, given in the two dimensional case by,

$$\Phi_z(x) = \frac{i}{4}H_0(k|x - z|) \quad \forall x \in \mathbb{R}^2 \setminus \{z\}. \tag{1.76}$$

Assume that the interior transmission is well posed, as mentioned at the beginning of subsection 1.3.1, the solution v_z of the equation $Gv_z = \Phi_z^\infty$ is the solution of the interior transmission problem with $f = \Phi_z$ and $g = \partial_\nu \Phi_z$. To compute the coefficients f_p and g_p we use the addition formula,

$$H_0(k|x - z|) = \sum_{p\in\mathbb{Z}} J_p(k|z|)e^{-ip\widehat{z}}H_p(k|x|)e^{ip\widehat{x}} \tag{1.77}$$

we deduce that

$$f_p = \frac{i\sqrt{2\pi}}{4}J_p(k|z|)e^{-ip\widehat{z}}H_p(kR) \quad \text{and} \quad g_p = \frac{i\sqrt{2\pi}}{4}J_p(k|z|)e^{-ip\widehat{z}}kH_p'(kR). \tag{1.78}$$

We now search an expression for v_z in the form (1.72). Thanks to the system of equations (1.74), the coefficients v_p are given by

$$\begin{aligned} v_p &= \frac{J_p(k\sqrt{n}R)g_p - k\sqrt{n}J_p'(k\sqrt{n}R)f_p}{J_p(kR)k\sqrt{n}J_p'(k\sqrt{n}R) - J_p(k\sqrt{n}R)kJ_p'(kR)} \\ &= \frac{i\sqrt{2\pi}}{4}\frac{J_p(k\sqrt{n}R)H_p'(kR) - \sqrt{n}J_p'(k\sqrt{n}R)H_p(kR)}{J_p(kR)\sqrt{n}J_p'(k\sqrt{n}R) - J_p(k\sqrt{n}R)J_p'(kR)}J_p(k|z|)e^{-ip\widehat{z}} \\ &= \frac{i\sqrt{2\pi}}{4}\frac{1}{B_p(k,n,R)}J_p(k|z|)e^{-ip\widehat{z}} \\ &= \frac{\pi e^{\frac{i\pi}{4}}}{\sqrt{k}}\frac{1}{\lambda_p}J_p(k|z|)e^{-ip\widehat{z}}. \end{aligned} \tag{1.79}$$

We finally obtain

$$v_z = \eta_2(2\pi)^{\frac{3}{2}}\sum_{p\in\mathbb{Z}}\frac{J_p(k|z|)e^{-ip\widehat{z}}J_p(k|x|)}{\lambda_p}e^{ip\widehat{x}}. \tag{1.80}$$

We recognize the $L^2(D)$ limit of Hg_z^α where g_z^α is the solution of the GLSM regularization (1.70). The rate of convergence of Hg_z^α to v_z is important to understand while implementing the Differential Linear Sampling Method (DLSM) [9] which is based on the computation of the solution of the transmission problem to identify defects in a material. Even in our simple setting, establishing a sharp result on the rate of the convergence is not an easy task but we give a first answer to this issue. We more precisely show that the rate of convergence $\|v_z - Hg_z^\alpha\|_{L^2(D)}$ when $\alpha \to 0$ is slower than α. From (1.69) and (1.80) we obtain (up to a constant)

$$v_z - Hg_z^\alpha = \alpha\sum_{p\in\mathbb{Z}}\frac{\overline{\lambda_p}\sigma_p J_p(k|z|)e^{-ip\widehat{z}}J_p(k|x|)}{|\lambda_p|^2(|\lambda_p|^2+\alpha\sigma_p)}e^{ip\widehat{x}}, \tag{1.81}$$

then

$$\|v_z - Hg_z^\alpha\|^2_{L^2(D)} = \frac{\alpha^2}{k^2}\left\{\sum_{p\in\mathbb{Z}}\frac{|\lambda_p|^2|\sigma_p|^2J_p^2(k|z|)}{|\lambda_p|^4(|\lambda_p|^2+\alpha\sigma_p)^2}\int_0^{kR}J_p(r)^2 r\ \mathrm{d}r\right\}. \tag{1.82}$$

We show that the series appearing under the brackets goes to infinity when $\alpha \to 0$. Indeed, by using (1.45) and (1.4.3), we obtain the following asymptotic (we also recall that $\lambda_p \le \sigma_p \le \sqrt{2}\lambda_p$),

$$\frac{|\sigma_p|^2J_p^2(k|z|)}{|\lambda_p|^6}\int_0^{kR}J_p(r)^2 r\,dr \underset{p\to+\infty}{\sim} C(k,n)(p+1)^3p!^4\left(\frac{|z|}{R}\right)^{2p}. \tag{1.83}$$

We then conclude with the D'Alembert criteria. Finally we have shown that

$$\frac{\|v_z - Hg_z^\alpha\|}{\alpha} \underset{\alpha\to0}{\longrightarrow} +\infty. \tag{1.84}$$

Chapter 2

Detecting sound-hard cracks in isotropic inhomogeneities

Contents

2.1 Introduction

This work is a contribution to sampling methods in inverse scattering theory when the issue is to determine the shape of an unknown background from fixed frequency multi-static data. The Factorization Method (FM) and the Generalized Linear Sampling Method (GLSM), which are methods among the class of the sampling methods, have shown good results in solving this problem [83, 10]. The FM has been justified for different complex backgrounds, allowing one to implement it in practical applications such as geophysics or nondestructive testing. We mention for instance the papers [86, 15, 122] where backgrounds made of both impenetrable obstacles and inhomogeneous medium are considered. The GLSM implementation mainly requires two complementary factorizations of the far field operator, one used in the Linear Sampling Method (LSM) and another used in the FM. As a consequence, the GLSM can be used as soon as the use of the FM is valid. Furthermore, the GLSM has provided the possibility to identify changes of the refractive index in a given inhomogeneity. The method is described by the Differential Linear Sampling Method (DLSM) [9] which requires the knowledge of far field measurements collected before and after the occurrence of the degradation. A natural research perspective is to adapt the DLSM for the identification of emergence of impenetrable defects in a surveyed material.

We consider the problem of detecting the presence of sound-hard cracks in a non homogeneous reference medium from the measurement of multi-static far field data. First, we provide a factorization of the far field operator in order to implement the Generalized Linear Sampling

Method (GLSM). The justification of the analysis is also based on the study of a special interior transmission problem. This technique allows us to recover the support of the inhomogeneity of the medium but fails to locate cracks. In a second step, we consider a medium with a multiply connected inhomogeneity assuming that we know the far field data at one given frequency both before and after the appearance of cracks. Using the Differential Linear Sampling Method (DLSM), we explain how to identify the component(s) of the inhomogeneity where cracks have emerged. The theoretical justification of the procedure relies on the comparison of the solutions of the corresponding interior transmission problems without and with cracks. Finally we illustrate the GLSM and the DLSM providing numerical results in 2D. In particular, we show that our method is reliable for different scenarios simulating the appearance of cracks between two measurements campaigns.

2.2 The forward scattering problem

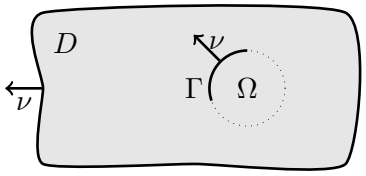

Figure 2.1: Example of setting in $\mathbb{R}^2$.

We consider an isotropic medium embedded in $\mathbb{R}^d$, $d = 2$ or 3, containing sound-hard cracks. Following [24], a crack Γ is defined as a portion of a smooth nonintersecting curve ($d = 2$) or surface ($d = 3$) that encloses a domain Ω, such that its boundary $\partial\Omega$ is smooth. We assume that Γ is an open set with respect to the induced topology on $\partial\Omega$. The normal vector ν on Γ is defined as the outward normal vector to Ω (see Fig. 6.1). To define traces and normal derivatives of functions on Γ, we use the following notation for all $x \in \Gamma$:

$$f^{\pm}(x) = \lim_{h\to 0^+} f(x \pm h\nu(x)) \quad \text{and} \quad \partial_\nu^{\pm} f(x) = \lim_{h\to 0^+} \nu(x).\nabla f(x \pm h\nu(x)).$$

We shall also work with the jump functions

$$[f] := f^+ - f^- \quad \text{and} \quad \left[\frac{\partial f}{\partial \nu}\right] := \partial_\nu^+ f - \partial_\nu^- f.$$

We assume that the propagation of waves in time harmonic regime in the reference medium is governed by the Helmholtz equation $\Delta u + k^2 u = 0$ in $\mathbb{R}^d$ where Δ stands for the Laplace operator of $\mathbb{R}^d$ and where k is the wave number. We assume that the cracks are embedded in a local perturbation of the reference medium. To model this perturbation, we introduce $n \in L^\infty(\mathbb{R}^d)$ a complex valued coefficient (the refractive index of the medium) such that $n = 1$ in $\mathbb{R}^d \setminus \overline{D}$ and $n \neq 1$ in D. Here $D \subset \mathbb{R}^d$ is a bounded domain with Lipschitz boundary ∂D such that $\mathbb{R}^d \setminus D$ is connected. We assume that $\Im\mathfrak{m}(n) \geq 0$ in $\mathbb{R}^d$ and that $\Gamma \subset D$. The scattering of the incident plane wave $u_i(\theta, \cdot) := e^{ik\theta\cdot x}$ of direction of propagation $\theta \in \mathbb{S}^{d-1}$ by the medium is described by the problem

$$\left|\begin{array}{l} \text{Find } u = u_i + u_s \text{ such that} \\ \Delta u + k^2 n\, u = 0 \quad \text{in } \mathbb{R}^d \setminus \overline{\Gamma} \\ \partial_\nu^{\pm} u = 0 \quad \text{on } \Gamma \\ \lim\limits_{r\to+\infty} r^{\frac{d-1}{2}} \left(\dfrac{\partial u_s}{\partial r} - iku_s\right) = 0, \end{array}\right. \tag{2.1}$$

with $u_i = u_i(\theta, \cdot)$. The last line of (2.1), where $r = |\boldsymbol{x}|$, is the Sommerfeld radiation condition which selects the outgoing scattered field and which is assumed to hold uniformly with respect to $\widehat{x} = x/|x| \in \mathbb{S}^{d-1}$. For all $k > 0$, Problem (2.1) has a unique solution u belonging to $H^1(\mathcal{O}\setminus\overline{\Gamma})$ for all bounded domain $\mathcal{O} \subset \mathbb{R}^d$. The scattered field $u_s(\theta, \cdot)$ has the expansion

$$u_s(\theta, x) = \eta_d e^{ikr} r^{-\frac{d-1}{2}} \left(u_s^\infty(\theta, \widehat{x}) + O(1/r) \right), \tag{2.2}$$

as $r \to +\infty$, uniformly in $\widehat{x} = x/|x| \in \mathbb{S}^{d-1}$. In (2.2) the constant η_d is given by $\eta_d = e^{i\frac{\pi}{4}}/\sqrt{8\pi k}$ for $d = 2$ and by $= 1/(4\pi)$ for $d = 3$. The function $u_s^\infty(\theta, \cdot) : \mathbb{S}^{d-1} \to \mathbb{C}$, is called the far field pattern associated with $u_i(\theta, \cdot)$. From the far field pattern, we can define the far field operator $F : L^2(\mathbb{S}^{d-1}) \to L^2(\mathbb{S}^{d-1})$ such that

$$(Fg)(\widehat{x}) = \int_{\mathbb{S}^{d-1}} g(\theta)\, u_s^\infty(\theta, \widehat{x})\ \mathrm{ds}(\theta). \tag{2.3}$$

By linearity, the function Fg corresponds to the far field pattern of the scattered field in (2.1) with

$$u_i = v_g := \int_{\mathbb{S}^{d-1}} g(\theta) e^{ik\theta\cdot x}\ \mathrm{ds}(\theta) \qquad \text{(Herglotz wave function)}. \tag{2.4}$$

2.3 Factorization of the far field operator

In this section we explain how to factorize the far field operator F defined in (2.3). From the Green representation theorem, computing the asymptotic behaviour of the Green's function as $r \to +\infty$ gives

$$u_s^\infty(\widehat{x}) = \left(k^2 \int_D (n(y) - 1) u(y) e^{-ik\widehat{x}y}\, \mathrm{d}y + \int_\Gamma [u(y)] \partial^+_{\nu(y)} e^{-ik\widehat{x}y}\, \mathrm{ds}(y) \right) \tag{2.5}$$

for the far field pattern of u_s in (2.2). A first step towards the factorization of F is to define the Herglotz operator $H : L^2(\mathbb{S}^{d-1}) \to L^2(D) \times L^2(\Gamma)$ such that

$$Hg = (v_{g|D}, \partial^+_\nu v_{g|\Gamma}). \tag{2.6}$$

We give in Proposition 2.3.1 below a characterization of the closure of the range of H. Set

$$\mathscr{H} = \left\{ v \in L^2(D) \,|\, \Delta v + k^2 v = 0 \text{ in } D \right\}. \tag{2.7}$$

and define the map $\Psi : \mathscr{H} \to L^2(D) \times L^2(\Gamma)$ such that

$$\Psi v = (v_{|D}, \partial^+_\nu v_{|\Gamma}). \tag{2.8}$$

Proposition 2.3.1. *The operator $H : L^2(\mathbb{S}^{d-1}) \to L^2(D) \times L^2(\Gamma)$ defined in (2.6) is injective and $\overline{R(H)} = \Psi(\mathscr{H})$.*

Proof. The proof of the injectivity of H follows a classical argument based on the Jacobi Anger expansion (apply [29, Lemma 2.1]). To establish the second part of the claim, first we note that v_g (defined in (2.4)) belongs to $\mathscr{H}$ so that $R(H) \subset \Psi(\mathscr{H})$. On the other hand, classical results of interior regularity ensure the existence of some constant $C > 0$ such that $\|\partial_\nu v\|_{L^2(\Gamma)} \leq C\|v\|_{L^2(D)}$ for all $v \in \mathscr{H}$. This in addition to $\|\Psi v\|_{L^2(D\setminus\overline{\Gamma})\times L^2(\Gamma)} \geq \|v\|_{L^2(D)}$ allows one to show that $\Psi(\mathscr{H})$ is a closed subspace of $L^2(D) \times L^2(\Gamma)$. The regularity result implies that $\Psi : (\mathscr{H}, \|\cdot\|_{L^2(D)}) \to L^2(D) \times L^2(\Gamma)$ is continuous. Since the set of Herglotz wave functions is dense in $(\mathscr{H}, \|\cdot\|_{L^2(D)})$, we deduce that $\overline{R(H)} = \Psi(\mathscr{H})$.

□

Next we define the operator $G : \overline{R(H)} \to L^2(\mathbb{S}^{d-1})$ such that

$$G(v, \partial_\nu^+ v) = u_s^\infty, \tag{2.9}$$

where u_s^∞ is the far field pattern of u_s, the outgoing scattered field which satisfies

$$\left| \begin{array}{rcll} \Delta u_s + k^2 n\, u_s & = & k^2(1-n)v & \text{in } \mathbb{R}^d \setminus \overline{\Gamma} \\ \partial_\nu^\pm u_s & = & -\partial_\nu^\pm v & \text{on } \Gamma. \end{array} \right. \tag{2.10}$$

Note that if $(v, \partial_\nu^+ v) \in \overline{R(H)}$ then interior regularity implies $\partial_\nu^+ v = \partial_\nu^- v$ on Γ. We also define the map $T : L^2(D \setminus \overline{\Gamma}) \times L^2(\Gamma) \to L^2(D \setminus \overline{\Gamma}) \times L^2(\Gamma)$ such that

$$T(v, \partial_\nu^+ v) = (k^2(n-1)(v + u_s), [v + u_s]). \tag{2.11}$$

Clearly we have $F = GH$. And one can check using (2.5) that $G = H^* T$ so that F admits the factorization

$$F = H^* T H. \tag{2.12}$$

The justification of the techniques we propose below to recover the cracks will depend on the properties of the operators G, T. And the latter are related to the solvability of the so-called interior transmission problem which in our situation states as follows: given $f \in H^{3/2}(\partial D), g \in H^{1/2}(\partial D)$

$$\left| \begin{array}{l} \text{Find } (u, v) \in L^2(D) \times L^2(D) \text{ such that} \\ u - v \in \{\varphi \in H^1(D \setminus \overline{\Gamma}) \,|\, \Delta\varphi \in L^2(D \setminus \overline{\Gamma})\} \\ \begin{array}{rcll} \Delta u + k^2 n\, u & = & 0 & \text{in } D \setminus \Gamma \\ \Delta v + k^2\, v & = & 0 & \text{in } D \\ \partial_\nu^\pm u & = & 0 & \text{on } \Gamma. \end{array} \qquad \begin{array}{rcll} u - v & = & f & \text{on } \partial D \\ \partial_\nu u - \partial_\nu v & = & g & \text{on } \partial D \end{array} \end{array} \right. \tag{2.13}$$

We shall say that $k > 0$ is a transmission eigenvalue if (2.13) with $f = g = 0$ admits a non zero solution. One can show for example that if the coefficient n is real and satisfies $1 < n_* < n < n^*$ for some constants n_*, n^* , then the set of transmission eigenvalues is discrete without accumulation point and that Problem (2.13) is uniquely solvable if and only if k is not a transmission eigenvalue (this will be part of a future work). We shall say that (2.13) is well-posed if it admits a unique solution for all $f \in H^{3/2}(\partial D), g \in H^{1/2}(\partial D)$.

Proposition 2.3.2. *Assume that $k > 0$ is not a transmission eigenvalue. Then the operator $G : \overline{R(H)} \to L^2(\mathbb{S}^{d-1})$ is compact, injective with dense range.*

Proof. First we show the injectivity of G. Let $V = (v, \partial_\nu^+ v) \in \overline{R(H)}$ such that $GV = 0$. Then from the Rellich lemma, the solution u_s of (2.10) is zero in $\mathbb{R}^d \setminus \overline{D}$. Therefore, if we define $u = v + u_s$, then the pair (u, v) satisfies the interior transmission problem (2.13) with $f = g = 0$. Since we assumed that $k > 0$ is not a transmission eigenvalue, we deduce that $v = 0$ and so $V = 0$.
Now we focus our attention on the denseness of the range of G. First we establish an identity of symmetry. Let $V_1 = (v_1, \partial_\nu^+ v_1)$, $V_2 = (v_2, \partial_\nu^+ v_2) \in \overline{R(H)}$. Denote w_1, w_2 the corresponding solutions to Problem (2.10). In particular we have

$$\Delta w_1 + k^2 n w_1 = k^2(1-n)v_1, \quad \Delta w_2 + k^2 n w_2 = k^2(1-n)v_2 \quad \text{in } \mathbb{R}^d \setminus \overline{\Gamma}. \tag{2.14}$$

Multiplying the first equation by w_2 and the second by w_1, integrating by parts the difference over B_R, the open ball of radius R centered at O, we obtain

$$k^2 \int_D (n-1)(v_1 w_2 - v_2 w_1)\,\mathrm{d}x \\ = \int_{\partial B_R} (\partial_\nu w_1 w_2 - w_1 \partial_\nu w_2)\,\mathrm{ds}(x) + \int_\Gamma ([w_2]\partial_\nu^+ v_1 - [w_1]\partial_\nu^+ v_2)\,\mathrm{ds}(x).$$

Taking the limit as $R \to +\infty$ and using that $\lim_{R\to+\infty} \int_{\partial B_R} (\partial_\nu w_1 w_2 - w_1 \partial_\nu w_2\,\mathrm{ds}(x) = 0$ (w_1 and w_2 satisfy the radiation condition), we find the identity

$$k^2 \int_D (n-1) v_1 w_2\,\mathrm{d}x + \int_\Gamma \partial_\nu^+ v_1 [w_2]\,\mathrm{ds}(x) = k^2 \int_D (n-1) v_2 w_1\,\mathrm{d}x + \int_\Gamma \partial_\nu^+ v_2 [w_1]\,\mathrm{ds}(x). \quad (2.15)$$

Using (2.15), we deduce that for ϕ, $g \in L^2(\mathbb{S}^{d-1})$, we have

$$\begin{aligned} & \langle G(H\phi), \overline{g}\rangle_{L^2(\mathbb{S}^{d-1})} \\ = \; & k^2 \int_D (n-1)(H\phi + u_s(\phi)) H g\,\mathrm{d}x + \int_\Gamma [H\phi + u_s(\phi)]\partial_\nu^+(Hg)\,\mathrm{ds}(x)s \\ = \; & k^2 \int_D (n-1)(Hg + u_s(g)) H\phi\,\mathrm{d}x + \int_\Gamma [Hg + u_s(g)]\partial_\nu^+(H\phi)\,\mathrm{ds}(x) \\ = \; & \langle G(Hg), \overline{\phi}\rangle_{L^2(\mathbb{S}^{d-1})}. \end{aligned}$$

Therefore if $\overline{g} \in R(G)^\perp$ then $G(Hg) = 0$. The injectivity of G and H imply that $g = 0$ which shows that G has dense range.
Finally, using again the estimate $\|\partial_\nu v\|_{L^2(\Gamma)} \le C\|v\|_{L^2(D)}$ for all $v \in \mathscr{H}$, results of interior regularity and the definition of H (see (2.6)), one can check that $H : L^2(\mathbb{S}^{d-1}) \to L^2(D) \times L^2(\Gamma)$ is compact. Since $G = H^*T$ and T is continuous, we deduce that $G : L^2(D) \times L^2(\Gamma) \to L^2(\mathbb{S}^{d-1})$ is compact. □

Proposition 2.3.3. *For all $V = (v, \partial_\nu^+ v) \in \overline{R(H)}$, we have the energy identity*

$$\Im\mathfrak{m}\left(\langle TV, V\rangle_{L^2(D\setminus\overline{\Gamma})\times L^2(\Gamma)}\right) = k^2 \int_D \Im\mathfrak{m}\,(n)|u_s + v|^2\,\mathrm{d}x + k\|GV\|^2_{L^2(\mathbb{S}^{d-1})}, \quad (2.16)$$

where u_s denotes the solution of (2.10). As a consequence if $\Im\mathfrak{m}(n) \ge 0$ a.e. in D and if k is not a transmission eigenvalue of (2.13), then T is injective.

Proof. Multiplying by $\overline{u_s}$ the equation $\Delta u_s + k^2 u_s = -k^2(n-1)(u_s + v)$ and integrating by parts over the ball B_R, we obtain

$$-k^2 \int_D (n-1)(u_s + v)\overline{u_s}\,\mathrm{d}x = \\ -\int_{B_R} (|\nabla u_s|^2 - k^2|u_s|^2)\,\mathrm{d}x + \int_{\partial B_R} \partial_\nu u_s \overline{u_s}\,\mathrm{ds}(x) - \int_\Gamma \partial_\nu^+ u_s [\overline{u_s}]\,\mathrm{ds}(x). \quad (2.17)$$

Using (2.17), then we find

$$\langle TV, V\rangle_{L^2(D\setminus\overline{\Gamma})\times L^2(\Gamma)} = k^2 \int_D (n-1)|u_s + v|^2\,\mathrm{d}x - \int_{B_R} (|\nabla u_s|^2 - k^2|u_s|^2)\,\mathrm{d}x \\ + \int_\Gamma [v + u_s]\partial_\nu^+ \overline{v}\,\mathrm{ds}(x) - \int_\Gamma \partial_\nu^+ u_s [\overline{u_s}]\,\mathrm{ds}(x) + \int_{\partial B_R} \partial_\nu u_s\,\overline{u_s}\,\mathrm{ds}(x).$$

Since $\partial_\nu^+ u_s = -\partial_\nu^+ v$ and $[v] = 0$ (interior regularity) on Γ, we deduce

$$\begin{aligned}\langle TV, V\rangle_{L^2(D\setminus\overline{\Gamma})\times L^2(\Gamma)} &= k^2\int_D (n-1)|u_s+v|^2\,\mathrm{d}x - \int_{B_R}(|\nabla u_s|^2 - k^2|u_s|^2)\,\mathrm{d}x \\ &\quad -2\Re\mathfrak{e}\left(\int_\Gamma [u_s]\partial_\nu^+\overline{u_s}\,\mathrm{ds}(x)\right) + \int_{\partial B_R}\partial_\nu u_s\overline{u_s}\,\mathrm{ds}(x).\end{aligned} \tag{2.18}$$

The radiation condition (see (2.1)) implies $\lim_{R\to\infty}\int_{\partial B_R}\partial_\nu u_s\overline{u_s}\,ds = ik\int_{\mathbb{S}^{d-1}}|u_s^\infty|^2 d\theta = ik\|GV\|^2_{L^2(\mathbb{S}^{d-1})}$. As a consequence, taking the imaginary part of (2.18) and letting R goes to infinity, we get identity (2.16). Now if $TV = 0$ and if $\Im\mathfrak{m}(n) \geq 0$ a.e. in D, then (2.16) gives $GV = 0$. Since G is injective when k is not a transmission eigenvalue of (2.13) (Proposition 2.3.2), we deduce that T is injective. □

2.4 Reconstruction algorithms

For $z \in \mathbb{R}^d$, we denote by $\Phi(.,z)$ the outgoing fundamental solution of the homogeneous Helmholtz equation such that

$$\Phi(x,z) = \frac{i}{4}H_0^{(1)}(k|x-z|) \text{ if } d=2 \qquad \text{and} \qquad \frac{e^{ik|x-z|}}{4\pi|x-z|} \text{ if } d=3. \tag{2.19}$$

Here $H_0^{(1)}$ stands for the Hankel function of first kind of order zero. The far field of $\Phi(.,z)$ is $\phi_z(\widehat{x}) = e^{-ikz.\widehat{x}}$. The GLSM uses the following theorem whose proof is classical [29].

Theorem 2.4.1. *Assume that the interior transmission problem (2.13) is well-posed. Then*

$$z \in D \qquad \textit{if and only if} \qquad \phi_z \in R(G).$$

The particularity of the GLSM is to build an approximate solution ($Fg \simeq \phi_z$) to the far field equation by minimizing the functional $J^\alpha(\phi_z,.) : L^2(\mathbb{S}^{d-1}) \to \mathbb{R}$ defined by

$$J^\alpha(\phi_z, g) = \alpha\langle F^\sharp g, g\rangle_{L^2(\mathbb{S}^{d-1})} + \|Fg - \phi_z\|^2_{L^2(\mathbb{S}^{d-1})}, \quad \forall g \in L^2(\mathbb{S}^{d-1}), \tag{2.20}$$

where $F^\sharp := |\frac{1}{2}(F+F^*)| + |\frac{1}{2i}(F-F^*)|$.

Theorem 2.4.2 (GLSM)**.** *Assume that the interior transmission problem (2.13) is well-posed, that the index n satisfies $[\,\Im\mathfrak{m}(n) \geq 0,\ \Re\mathfrak{e}(n-1) \geq n_*$ a.e. in $D\,]$ or $[\,\Im\mathfrak{m}(n) \geq 0,\ \Re\mathfrak{e}(1-n) \geq n_*$ a.e. in $D\,]$ for some constant $n_* > 0$. Let $g_z^\alpha \in L^2(\mathbb{S}^{d-1})$ be a minimizing sequence of $J^\alpha(\phi_z,.)$ such that*

$$J^\alpha(\phi_z, g_z^\alpha) \leq \inf_g J^\alpha(\phi_z, g) + p(\alpha), \tag{2.21}$$

where p is such that $\lim_{\alpha\to 0}\alpha^{-1}p(\alpha) = 0$. Then

- *$z \in D$ if and only if $\lim_{\alpha\to 0}\langle F^\sharp g_z^\alpha, g_z^\alpha\rangle_{L^2(\mathbb{S}^{d-1})} < +\infty$.*
- *If $z \in D$ then there exists $h \in \overline{R(H)}$ such that $\phi_z = Gh$ and Hg_z^α converges strongly to h as $\alpha \to 0$.*

Thus the GLSM, justified by this theorem, offers a way to recover D, that is to identify the perturbation in the reference background. Note that the GLSM, contrary to the LSM, provides an exact characterization of D. However it does not give any information on the location of the crack Γ.

Proof. We establish this theorem by applying the abstract result of [29, Theorem 2.10]. The latter requires that the following properties hold.

i) $F = GH = H^*TH$ is injective with dense range and G is compact.

ii) $F^\sharp$ factorizes as $F^\sharp = H^*T^\sharp H$ where $T^\sharp$ satisfies the coercivity property

$$\exists \mu > 0,\ \forall V \in \overline{R(H)}, \qquad |\langle T^\sharp V, V\rangle_{L^2(D\setminus\overline{\Gamma})\times L^2(\Gamma)}| \geq \mu \|V\|^2_{L^2(D\setminus\overline{\Gamma})\times L^2(\Gamma)}; \tag{2.22}$$

iii) $V \mapsto |\langle T^\sharp V, V\rangle_{L^2(D\setminus\overline{\Gamma})\times L^2(\Gamma)}|^{1/2}$ is uniformly convex on $\overline{R(H)}$.

Item *i)* is a consequence of Propositions 2.3.1, 2.3.2 and 2.3.3. Moreover, we deduce *iii)* from *ii)* and from the fact that $\langle F^\sharp g, g\rangle_{L^2(D\setminus\overline{\Gamma})\times L^2(\Gamma)} = \|(F^\sharp)^{1/2} g\|^2_{L^2(\mathbb{S}^{d-1})}$ (see e.g. [29]). Therefore, it remains to show *ii)*. To proceed, we use [29, Theorem 2.31] which guarantees that it is true if :

- T injective on $\overline{R(H)}$;
- $\Im\mathfrak{m}(\langle TV, V\rangle_{L^2(D\setminus\overline{\Gamma})\times L^2(\Gamma)}) \geq 0$ for all $V \in \overline{R(H)}$;
- $\Re\mathfrak{e}(T)$ decomposes as $\Re\mathfrak{e}(T) = T_0 + C$ where T_0 satisfies (2.22) and where C is compact on $\overline{R(H)}$.

The first two items have been proved in Proposition 2.3.3. Let us focus our attention on the last one. By definition, we have $TV = (k^2(n-1)(v+u_s), [v+u_s])$. Set $\tilde{C}V = (k^2(n-1)u_s, [v+u_s]) - \partial_\nu^+ v|_\Gamma)$. Using results of interior regularity, one can check that $C = \Re\mathfrak{e}(\tilde{C})$ is compact. Now, define $T_0 := \Re\mathfrak{e}(T) - C = (k^2\Re\mathfrak{e}(n-1)v, \partial_\nu^+ v|_\Gamma)$. Clearly one has $|\langle T_0 V, V\rangle_{L^2(D\setminus\overline{\Gamma})\times L^2(\Gamma)}| \geq n_* \|V\|^2_{L^2(D\setminus\overline{\Gamma})\times L^2(\Gamma)}$ when $\Re\mathfrak{e}(n-1) \geq n_*$. The case $\Re\mathfrak{e}(1-n) \geq n_*$ can be dealt in a similar way. □

When one has only acces to a noisy version F^δ of F, then $F^{\sharp,\delta}$ might not have the required factorization and the cost function (2.20) must be regularized. For this aspect, we refer the reader to [10, Section 5.2].
We now give the theoretical foundation of the DLSM which will allow us to localize the position of the crack Γ. The DLSM relies on the comparison of the solutions of the following interior transmission problems (without and with cracks).

$$\mathscr{P}(D)\left|\begin{array}{rcll} \Delta u_0 + k^2 n u_0 &=& 0 & \text{in } D \\ \Delta v_0 + k^2 v_0 &=& 0 & \text{in } D \\ u_0 - v_0 &=& \Phi_z & \text{on } \partial D \\ \partial_\nu u_0 - \partial_\nu v_0 &=& \partial_\nu \Phi_z & \text{on } \partial D, \end{array}\right. \qquad \mathscr{P}_\Gamma(D)\left|\begin{array}{rcll} \Delta u + k^2 n u &=& 0 & \text{in } D \\ \Delta v + k^2 v &=& 0 & \text{in } D \\ \partial_\nu^\pm u &=& 0 & \text{on } \Gamma \\ u - v &=& \Phi_z & \text{on } \partial D \\ \partial_\nu u - \partial_\nu v &=& \partial_\nu \Phi_z & \text{on } \partial D, \end{array}\right. \tag{2.23}$$

where u_0, v_0, u, $v \in L^2(D)$, $u_0 - v_0 \in H^2(D)$ and $u - v \in H^1(D\setminus\Gamma)$ is such that $\Delta(u-v) \in L^2(D\setminus\Gamma)$. We split the domain D into two kinds of connected components (see Fig. 2.2): The ones containing cracks are listed by $(D_\Gamma^j)_j$; others are listed by $(D_0^j)_j$. And we set $D_\Gamma := \cup_j D_\Gamma^j$ and $D_0 := \cup_j D_0^j$ so that $D = D_\Gamma \cup D_0$.

Theorem 2.4.3. *Assume that Γ is a part of the boundary of a domain Ω such that $\partial\Omega$ is analytic. Assume that n is analytic in D_Γ and does not vanish. Assume also that k is not a Neumann eigenvalue for $-n^{-1}\Delta$ in Ω and is such that both $\mathscr{P}(D)$ and $\mathscr{P}_\Gamma(D)$ (see (2.23)) are well-posed.*

i) If $z \in D_0$ then $v = v_0$ in D. *ii) If $z \in D_\Gamma$ then $v \neq v_0$ in D_Γ.*

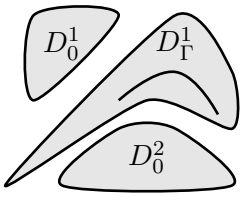

Figure 2.2: We split D into two families of connected components.

Proof. i) Let $z \in D_0$. In D_0, the equations for $\mathscr{P}(D)$ and $\mathscr{P}_\Gamma(D)$ coincide. By uniqueness of the solution for these problems, we deduce that $v = v_0$ in D_0. On the other hand, one observes that $(0, -\Phi_z)$ satisfies the equations of $\mathscr{P}(D)$ and $\mathscr{P}_\Gamma(D)$ in D_Γ. As a consequence, by uniqueness of the solution for these problems, we also have $v = v_0 = -\Phi_z$ in D_Γ.
ii) Now let $z \in D_\Gamma$. We wish to show that $v \neq v_0$ in D_Γ. We proceed by contradiction assuming that $v = v_0$ in D_Γ. Define U such that $U = u - u_0$ in $D_\Gamma \setminus \overline{\Gamma}$ and $U = 0$ in $\mathbb{R}^d \setminus \overline{D_\Gamma}$. Since $U = \partial_\nu U = 0$ on ∂D_Γ, from the unique continuation principle, we find $U = 0$ in $\mathbb{R}^d \setminus \overline{\Gamma}$ and so $\partial_\nu^\pm u_0 = 0$ on Γ (because $\partial_\nu^\pm u = 0$ on Γ). Furthermore the regularity of n implies that $\partial_\nu^\pm u_0$ is analytic on $\partial\Omega$ and we conclude that $\partial_\nu^\pm u_0 = 0$ on $\partial\Omega$. Since we assumed that k is not a Neumann eigenvalue for $-n^{-1}\Delta$ in Ω, we deduce that $u_0 = 0$ in Ω, and by unique continuation, $u_0 = 0$ in D_Γ. Thus we must have $v_0 = -\Phi_z$ in D_Γ which contradicts the fact that $u_0 - v_0 \in H^2(D)$. □

Now we consider a first heterogeneous medium without crack with a perturbation of the reference background supported in $\overline{D}$ modeled by some index n, and a second medium with the same n but with an additional crack inside D. The corresponding far field operators are denoted respectively F_0 and F_1. Then for $j = 0, 1$, let $g_{j,z}^\alpha$ refer to the sequences introduced in the statement of Theorem 2.4.2 with $F_j^\sharp = |\frac{1}{2}(F_j + F_j^*)| + |\frac{1}{2i}(F_j - F_j^*)|$. We also set for $j = 0, 1$

$$\mathcal{A}_j^\alpha(z) = \langle F_j^\sharp g_{j,z}^\alpha, g_{j,z}^\alpha \rangle_{L^2(\mathbb{S}^{d-1})};\ \mathcal{D}_j^\alpha(z) = \langle F_j^\sharp (g_{1,z}^\alpha - g_{0,z}^\alpha), (g_{1,z}^\alpha - g_{0,z}^\alpha) \rangle_{L^2(\mathbb{S}^{d-1})}. \tag{2.24}$$

The combination of Theorems 2.4.2 and 2.4.3 leads to the following result.

Theorem 2.4.4 (DLSM)**.** *Assume that k, n and Γ are as in Theorem 2.4.3 and that n also satisfies the assumptions of Theorem 2.4.2. Then for $j = 0$ or 1*

$$\big[\, z \in D_0 \,\big] \Rightarrow \big[\, \lim_{\alpha \to 0} \mathcal{D}_j^\alpha(z) = 0 \,\big] \quad \text{and} \quad \big[z \in D_\Gamma \big] \Rightarrow \big[\, 0 < \lim_{\alpha \to 0} \mathcal{D}_j^\alpha(z) < +\infty \,\big].$$

Proof. As explained in the proof of Theorem 2.4.2, $F_1^\sharp$ admits a factorization of the form $H^* T_1^\sharp H$ where $T_1^\sharp$ is continuous and $\langle T_1^\sharp \cdot, \cdot \rangle$ is coercive. According to the study of crack-free inhomogeneous medium a same factorization stands for F_0 involving an operator $T_0^\sharp$ that have the same properties of $T_1^\sharp$. This implies (for $j = 0$ or 1) the existence of two positive constants κ and K such that

$$\kappa \| H(g_{1,z}^\alpha - g_{0,z}^\alpha) \|_{L^2(D)}^2 \leq \mathcal{D}_j^\alpha(z) \leq K \| H(g_{1,z}^\alpha - g_{0,z}^\alpha) \|_{L^2(D)}^2. \tag{2.25}$$

Now for $z \in D$, if we denote (u_0, v_0) (resp. (u_1, v_1)) the solution of $\mathscr{P}(D)$ (resp. $\mathscr{P}_\Gamma(D)$), then Theorem 2.4.2 and the GLSM for the crack-free inhomogeneous medium (see the justification in [29]) guarantee that $\lim_{\alpha \to 0} \| H(g_{1,z}^\alpha - g_{0,z}^\alpha) \| = \| H(v - v_0) \|$. Then the result follows from Theorem 2.4.3. □

From Theorems 2.4.2 and 2.4.4, one can design indicators for D and D_Γ. Set for $j = 0$ or 1,

$$I^{\mathrm{GLSM}}(z) = \lim_{\alpha \to 0} \frac{1}{\mathcal{A}_1^\alpha(z)} \quad \text{and} \quad I_j^{\mathrm{DLSM}}(z) = \lim_{\alpha \to 0} \frac{1}{\mathcal{A}_0^\alpha(z) \Big(1 + \frac{\mathcal{A}_0^\alpha(z)}{\mathcal{D}_j^\alpha(z)} \Big)}. \tag{2.26}$$

For these indicators, one can show the following theorem which allows one to identify the connected components of D in which some cracks have appeared.

Corollary 2.4.5. *Under the assumptions of Theorem 2.4.4, we have for $j = 0$ or 1*

- $I^{\mathrm{GLSM}}(z) = 0$ *in* $\mathbb{R}^d \setminus D$ *and* $I^{\mathrm{GLSM}}(z) > 0$ *in* D.
- $I_j^{\mathrm{DLSM}}(z) = 0$ *in* $\mathbb{R}^d \setminus D_\Gamma$ *and* $I_j^{\mathrm{DLSM}}(z) > 0$ *in* D_Γ.

2.5 Numerical results

To conclude this work, we apply the GLSM and the DLSM on simulated backgrounds. All backgrounds have the same shape D constituted of three disjoint disks of radius 0.75 and of index $n = 1.5$. They differ from one to another in the distribution of cracks inside the disks. Admittedly, the straight cracks appearing in the backgrounds are not a portion of the boundary of an analytic domain. However, we expect that our algorithm remains robust when this theoretical assumption is not satisfied. For each background we generate a discretization of the far field operator F by solving numerically the direct problem for multiple incident fields $u_i(\theta_p)$ with wave number $k = 4\pi$. Then we compute the matrix $F = (u_s^\infty(\theta_p, \widehat{x_q}))_{p,q}$ for θ_p, $\widehat{x_q}$ in $\{\cos(\frac{2l\pi}{100}), \sin(\frac{2l\pi}{100}),\ l = 1..100\}$ (somehow we discretize $L^2(\mathbb{S}^1)$). Finally, we add random noise to the simulated F and obtain our final synthetic far field data F^δ with $F^\delta_{pq} = F_{pq}(1 + \sigma N)$. Here N is a complex random variable whose real and imaginary parts are uniformly chosen in $[-1, 1]^2$. The parameter $\sigma > 0$ is chosen so that $\|F^\delta - F\| = 0.05\|F^\delta\|$.

2.5.1 Reconstruction of the background

To handle the noise δ added on the far field data, we use a regularized version of the GLSM consisting in finding the minimizers $g_z^{\alpha,\delta}$ of the functional

$$g \mapsto J^{\alpha,\delta}(\phi_z, g) = \alpha(|\langle F^{\sharp\delta} g, g\rangle_{L^2(\mathbb{S}^{d-1})}| + \delta\|F^\delta\|\|g\|^2_{L^2(\mathbb{S}^2)}) + \|F^\delta g - \phi_z\|^2_{L^2(\mathbb{S}^{d-1})},$$

where $F^{\sharp\delta} := |\frac{1}{2}(F^\delta + F^{\delta *})| + |\frac{1}{2i}(F^\delta - F^{\delta *})|$. We fit α to δ according to [10, Section 5.2]. The new relevant indicator function for the regularized GLSM is then given by

$$I^{\alpha,\delta}_{\mathrm{GLSM}}(z) = \frac{1}{\mathcal{A}^{\alpha,\delta}(z)}$$

where $\mathcal{A}^{\alpha,\delta}(z) = \langle F^{\sharp\delta} g_z^{\alpha,\delta}, g_z^{\alpha,\delta}\rangle_{L^2(\mathbb{S}^{d-1})} + \delta\|F^\delta\|\|g_z^{\alpha,\delta}\|^2_{L^2(\mathbb{S}^{d-1})}$.

Fig. 2.3 shows the results of GLSM indicator function $z \mapsto I^{\alpha,\delta}_{\mathrm{GLSM}}(z)$ for two different configurations where the second one is obtained from the first one by adding a crack to the third component. The two other components contain the same crack. One observes that GLSM is capable of retrieving the domain D for each configuration. We also observe how the behavior of the indicator function is different inside the third component. This is somehow what the DLSM exploits to isolate the component where a defect appears and this is what is discussed next.

2.5.2 Identification of sound hard crack defects in inhomogeneities

Given two far field data F_0^δ and F_1^δ, we respectively define $F_0^{\sharp\delta}$, $g_{0,z}^{\alpha,\delta}$, $\mathcal{A}_0^{\alpha,\delta}(z)$ and $F_1^{\sharp\delta}$, $g_{1,z}^{\alpha,\delta}$, $\mathcal{A}_1^{\alpha,\delta}(z)$ associated to each data as described in the previous paragraph. We also define

$$\mathcal{D}^{\alpha,\delta}(z) = \langle F_0^\sharp(g_{1,z}^{\alpha,\delta} - g_{0,z}^{\alpha,\delta}), (g_{1,z}^{\alpha,\delta} - g_{0,z}^{\alpha,\delta})\rangle_{L^2(\mathbb{S}^{d-1})}.$$

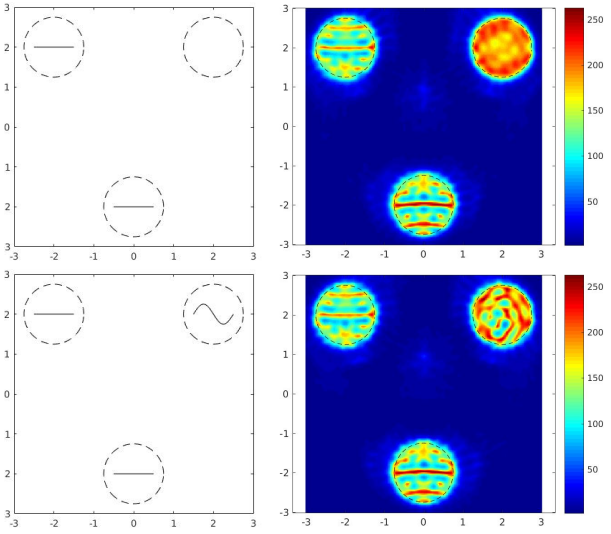

Figure 2.3: Simulated backgrounds on the left and associated GLSM indicator function $z \mapsto I^{\alpha,\delta}_{\mathrm{GLSM}}(z)$ on the right.

Then, according to (2.26), the DLSM indicator is given by

$$I^{\alpha,\delta}_{\mathrm{DLSM}}(z) = \frac{1}{\mathcal{A}^{\alpha,\delta}_0(z)\left(1 + \frac{\mathcal{A}^{\alpha,\delta}_0(z)}{\mathcal{D}^{\alpha,\delta}(z)}\right)}.$$

The behavior of the DLSM indicator function is illustrated below for several scenarios shown in Fig. 2.4-2.7. In each figure is presented from left to right, the initial background (associated with F^{δ}_0), the damaged background (associated with F^{δ}_1) and the DLSM indicator function $z \mapsto I^{\alpha,\delta}_{\mathrm{DLSM}}(z)$. As expected, the latter allows us to identify for all scenarios the component(s) D_Γ where (additional) cracks appeared. We also remark that it slightly accentuates the border of D_0. But this effect is not explained by our theory and it does not contradict it: Our theoretical result does not stipulate that the indicator function is "uniformly" close to 0 outside D_Γ.

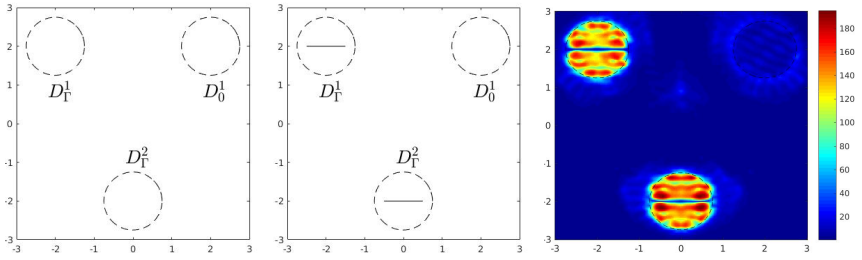

Figure 2.4: A scenario for DLSM simulating the emergence of cracks in two components of a defect free background.

2.6 Conclusion

We analyzed the DLSM to identify emergence of cracks embedded in an unknown background and image defective components from differential measurements of far field data at a fixed frequency. The analysis is based on the justification of the GLSM for backgrounds with cracks which necessitates the study of a special interior transmission problem and the derivation of

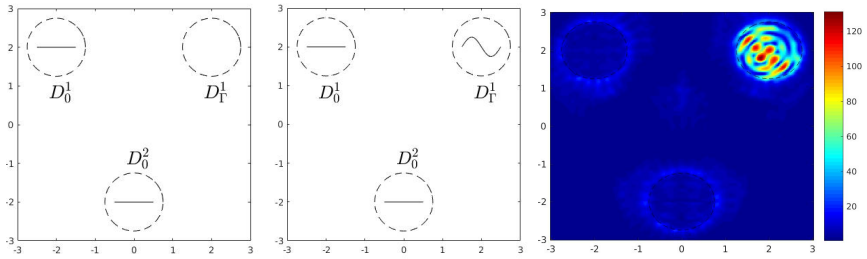

Figure 2.5: A scenario for DLSM simulating the emergence of a crack in a healthy component of an already damaged background.

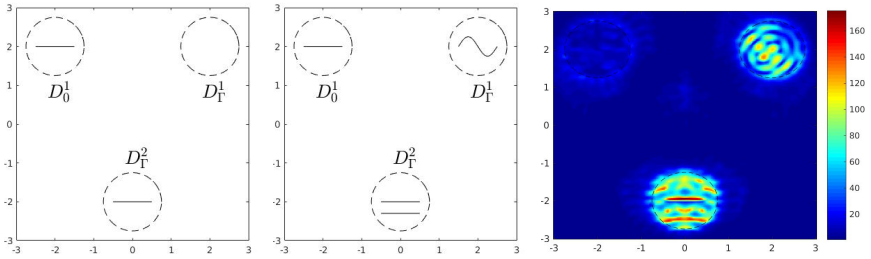

Figure 2.6: A scenario for DLSM simulating the emergence of additional cracks in a healthy and a damaged components of an already damaged background.

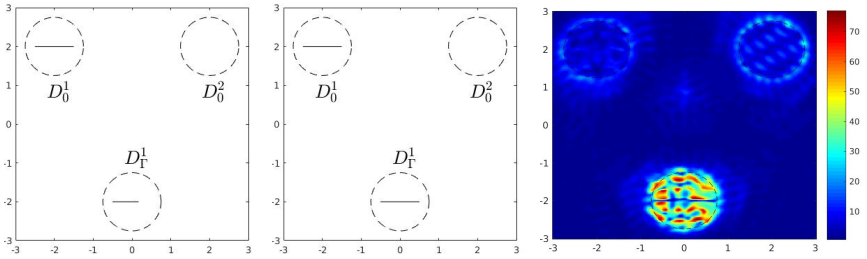

Figure 2.7: A scenario for DLSM simulating the increase of the crack size in one component of an already damaged background.

specific factorizations of the far field operator. The numerical tests on toy problems show that our method is reliable for different scenarios simulating the appearance of cracks between two measurements campaigns. This is a first step before addressing practical problems where the issues of limited aperture data and/or highly cluttered backgrounds should be solved.

Chapter 3

The interior transmission problem for penetrable obstacles with sound-hard cracks

Contents

3.1 Introduction

The Interior Transmission Problem (ITP) has first been mentioned when developing the Linear Sampling Method [47, 77] to retrieve the shape of penetrable inhomogeneities from far field measurements. In these papers it was pointed out that the chosen wavenumber of the interrogating waves should be different from the spectrum of the ITP which are referred as Transmission Eigenvalues (TEs). Recently, a series of works changed the status of the TEs, it has been established the possibility of computing TEs from far field data [28] and obtaining qualitative information on the physical properties of the material surveyed from the knowledge of TEs [31, 25]. Only after these results, the community has shown an interest in proving the existence of TEs which was deemed to be a difficult problem. Proof of the existence of at least one real TE in the general case is provided only in 2008 by Päivärinta and Sylvester [104] assuming that the refractive index is sufficiently large. This result is complemented in the work of Cakoni, Gintides and Haddar [33], where it is demonstrated the existence of an infinity of real TEs while removing the condition on the refractive index. After these striking results, a huge step forward has been made until now on the knowledge of TEs and also on their use for solving the inverse problem. For a long time it has been required to study only materials of fixed sign contrast. This assumption has been greatly relaxed in [37, 112], where the sign contrast is only required

to be fixed in a vicinity of the boundary. The different developed frameworks to study ITP problems has been extended to the Maxwell equations [53, 35, 49]. Furthermore, several contributions have proven the relevance of using TEs to solve the inverse problem. First of all, the theoretical justification of the determination of TEs which have been relying on the LSM was not satisfactory because of the mentioned inherent weak point of the LSM. The determination of TEs has been enhanced by new methods such as the GLSM and the inside-outside Duality [10, 85, 93, 94, 95]. Secondly, many works proposed techniques using TEs to find estimates of the material properties [22, 31, 63, 66, 32].

In this chapter we consider the ITP for isotropic inhomogeneities with sound-hard cracks inside. This problem has been introduced in Chapter 2 while extending the Generalized Linear Sampling Method to isotropic inhomogeneities containing sound-hard cracks. Following the same approach proposed in [33], we show the existence of a discrete infinite set of real TEs, provided that the refractive index $n \in L^2(D)$ is bounded and satisfies $n > 1$. In this case we also derive Faber-Krahn type inequalities for the TEs. When $n < 1$, the framework we develop do not allow to show the Fredholm property of the ITP, preventing us to answer the question of the discreteness properties nor the existence of TEs. We point out that in the paper [32], where the case of inhomogeneities containing sound soft obstacles is studied, a similar restriction on the refractive index occurred as their developed framework allowed to study the case $n < 1$ but not the case $n > 1$. Similarly to more classical situations, we also show that real TEs do not exist if the considered isotropic medium containing the sound-hard crack is dissipative.

3.2 Setting of the problem

We consider a penetrable obstacle containing sound hard cracks. The obstacle is delimited by a bounded domain of Lipschitz boundary D. We assume that the refractive index $n \in L^\infty(\mathbb{R}^d)$ satisfies $\mathrm{supp}(n-1) = \overline{D}$ and $\Im\mathfrak{m}(n) \geq 0$. The crack Γ is modelized by a non intersecting open arc/surface which is a portion of the boundary of a Lipschitz domain $\Omega \subset D$. The unit normal vector ν on Γ is chosen to coincide with the outward normal vector to $\partial\Omega$. For a function ψ defined on a neighborhood of Γ, we use the same notations $\psi^\pm{}_{|\Gamma}$, $\partial_\nu^\pm \psi_{|\Gamma}$, $[\psi]_{|\Gamma}$ and $[\partial_\nu \psi]_{|\Gamma}$ of the previous chapter. The propagation of waves in the time-harmonic regime is described by

$$\left| \begin{array}{rcll} \Delta u + k^2 n(x) u &=& 0 \quad \text{in} & \mathbb{R}^d \setminus \overline{\Gamma} \\ \partial_\nu^\pm u &=& 0 \quad \text{on} & \Gamma, \end{array} \right. \tag{3.1}$$

where the total field $u \in H^1_{loc}(\mathbb{R}^d \setminus \overline{\Gamma})$. Given an incident wave u_i that satisfies the homogeneous Helmholtz equation

$$\Delta u_i + k^2 u_i = 0 \text{ in } \mathbb{R}^d, \tag{3.2}$$

the scattered field defined in $\mathbb{R}^d \setminus \overline{\Gamma}$ by

$$u_s = u - u_i \tag{3.3}$$

satisfies

$$\left| \begin{array}{rcll} \Delta u_s + k^2 n u_s &=& -k^2(n-1)u_i \quad \text{in} & \mathbb{R}^d \setminus \overline{\Gamma} \\ \partial_\nu^\pm u_s &=& -\partial_\nu^\pm u_i \quad \text{on} & \Gamma. \end{array} \right. \tag{3.4}$$

along with the Sommerfield radiation condition

$$\lim_{r \to +\infty} \int_{|x|=r} \left| \frac{\partial u_s}{\partial r} - iku_s \right|^2 \mathrm{d}x = 0. \tag{3.5}$$

The scattered field $u_s \in H^2_{loc}(\mathbb{R}^d \setminus \overline{\Gamma})$ is uniquely determined by (3.4)-(3.5).

We are interested in the existence of incident waves defined on D such that the far field of the scattered wave u_s vanishes. Denoting v the incident field and $u = u_s + v$, Rellich lemma leads to the following system of equation for u and v,

$$\left|\begin{array}{rcll} \Delta u + k^2 n u &=& 0 \quad \text{in} & D \setminus \overline{\Gamma} \\ \Delta v + k^2 v &=& 0 \quad \text{in} & D \\ \partial_\nu^{\pm} u &=& 0 \quad \text{on} & \Gamma \\ u - v &=& 0 \quad \text{on} & \partial D \\ \frac{\partial u}{\partial \nu} - \frac{\partial v}{\partial \nu} &=& 0 \quad \text{on} & \partial D. \end{array}\right. \tag{3.6}$$

The purpose of this chapter is to study this problem that can be viewed as an eigenvalue problem, i.e find $k > 0$ such that there exists a non trivial couple of solution (u, v) whose regularity will be precised next.

3.3 Definition and properties of the interior transmission problem

To treat the interior eigenvalue problem (3.6), it is more convenient to understand it as a particular case of a boundary value problem that is defined and studied in this section.

3.3.1 A weak formulation

In order to study the interior transmission eigenvalue problem (3.6) is introduced the interior transmission problem, for given $f \in H^{\frac{1}{2}}(\partial D)$ and $g \in H^{-\frac{1}{2}}(\partial D)$, $v \in L^2(D)$ and $u \in L^2(D)$ such that $u - v \in H^1_\Delta(D \setminus \overline{\Gamma})$ and

$$\left|\begin{array}{rcll} \Delta u + k^2 n\, u &=& 0 \quad \text{in } D \setminus \overline{\Gamma} \\ \Delta v + k^2\, v &=& 0 \quad \text{in } D \\ \partial_\nu^{\pm} u &=& 0 \quad \text{on } \Gamma \end{array}\right. \qquad \left|\begin{array}{rcll} u - v &=& f \quad \text{on } \partial D \\ \partial_\nu u - \partial_\nu v &=& g \quad \text{on } \partial D, \end{array}\right. \tag{3.7}$$

where

$$H^1_\Delta(D \setminus \overline{\Gamma}) = \{w \in H^1(D \setminus \overline{\Gamma}) \text{ such that } \Delta w \in L^2(D)\}. \tag{3.8}$$

As we will see next, the only regularity that we can expect on $u - v$ with the variational formulation we propose is that it belongs to the space $H^1_\Delta(D \setminus \overline{\Gamma})$. A classical appoach is to define a new unknown $w := u - v$ in order to simplify the structure of the boundary conditions on ∂D which then reduces to

$$w = f \text{ on } \partial D \qquad \text{and} \qquad \partial_\nu w = g \text{ on } \partial D. \tag{3.9}$$

In view to reformulate the problem only in terms of w, we first observe, substracting the second equation from the first, that

$$(\Delta + k^2 n) w = -k^2 (n-1) v \quad \text{in} \quad D \setminus \overline{\Gamma}. \tag{3.10}$$

Finally, assuming that $\frac{1}{n-1} \in L^\infty(D)$ is obtained from the equation on v a fourth order equation for w,

$$(\Delta + k^2)(n-1)^{-1}(\Delta + k^2 n) w = 0 \quad \text{in} \quad D \setminus \overline{\Gamma}. \tag{3.11}$$

This fourth order equation has first been introduced in [113] and has been used in several works, for instance [34],[33] and [104]. Regarding the Neumann condition, it becomes

$$\partial_\nu^\pm w + \partial_\nu^\pm v = 0 \text{ on } \Gamma. \tag{3.12}$$

First note that the relation above gives sense to the original condition $\partial_\nu u = 0$. Secondly, since the interior regularity implies that $\partial_\nu v$ is smooth through Γ, one can derive

$$[\partial_\nu w] = 0 \text{ on } \Gamma. \tag{3.13}$$

The proposed weak formulation treats equation (3.11) variationally, the conditions (3.9) and (3.12) are included in the variational space defined below. We define

$$V = \left\{\varphi \in H^1(D \setminus \overline{\Gamma}) \mid \Delta\varphi \in L^2(D \setminus \overline{\Gamma}),\ [\partial_\nu\varphi]_\Gamma = 0,\ \varphi = \partial_\nu\varphi = 0 \text{ on } \partial D\right\}.$$

V is equipped with the induced scalar product of $H^1_\Delta(D \setminus \overline{\Gamma})$:

$$\langle \psi, \varphi\rangle_V = \int_D \psi\overline{\varphi}\,\mathrm{d}x + \int_D \nabla\psi\nabla\overline{\varphi}\,\mathrm{d}x + \int_D \Delta\psi\Delta\overline{\varphi}\,\mathrm{d}x, \tag{3.14}$$

and the associated euclidian norm $\|\cdot\|_V = \sqrt{\langle\cdot,\cdot\rangle_V}$. $(V, \|\cdot\|_V)$ is then a Hilbert space.

Let $\varphi \in V$, we integrate equation $\Delta v + k^2 v = 0$ on $D \setminus \overline{\Gamma}$ (or equivalently (3.11)) against $\overline{\varphi}$ and apply Green's second formula to obtain

$$\begin{aligned} 0 &= \int_D (\Delta v + k^2 v)\overline{\varphi}\,\mathrm{d}x \\ &= \int_D v(\Delta\overline{\varphi} + k^2\overline{\varphi})\,\mathrm{d}x - \int_\Gamma \partial_\nu v[\overline{\varphi}]\,\mathrm{ds}(x) \\ &= \int_D v(\Delta\overline{\varphi} + k^2 n\overline{\varphi})\,\mathrm{d}x + \int_D -k^2(n-1)v\overline{\varphi}\,\mathrm{d}x - \int_\Gamma \partial_\nu v[\overline{\varphi}]\,\mathrm{ds}(x). \end{aligned} \tag{3.15}$$

We now develop the second term of (3.15), v is replaced using expression (3.10) then we use Green's first formula

$$\begin{aligned} \int_D -k^2(n-1)v\overline{\varphi}\,\mathrm{d}x &= \int_D \Delta w\overline{\varphi}\,\mathrm{d}x + k^2\int_D nw\overline{\varphi}\,\mathrm{d}x \\ &= -\int_D \nabla w\nabla\overline{\varphi}\,\mathrm{d}x - \int_\Gamma \partial_\nu w[\overline{\varphi}]\,\mathrm{ds}(x) + k^2\int_D nw\overline{\varphi}\,\mathrm{d}x. \end{aligned} \tag{3.16}$$

Using (3.16), equation (3.15) becomes

$$\int_D v(\Delta\overline{\varphi} + k^2 n\overline{\varphi})\,\mathrm{d}x - \int_D \nabla w\nabla\overline{\varphi}\,\mathrm{d}x + k^2\int_D nw\overline{\varphi}\,\mathrm{d}x = 0 \tag{3.17}$$

by replacing v with expression (3.10) and multiplying by $-k^2$ we finally obtain

$$\int_D (n-1)^{-1}(\Delta w + k^2 nw)(\Delta\overline{\varphi} + k^2 n\overline{\varphi})\,\mathrm{d}x + k^2\int_D \nabla w\nabla\overline{\varphi}\,\mathrm{d}x - k^4\int_D nw\overline{\varphi}\,\mathrm{d}x = 0. \tag{3.18}$$

Now let $\theta \in H^2(D)$ be a lifting function such that $\theta = f$ and $\partial_\nu\theta = g$ on ∂D which moreover fulfills the two following conditions: $\theta = 0$ in D_0 such that $\Gamma \subset D_0 \subset D$ and

$$\|\theta\|_{H^2(D)} \leq \|f\|_{H^{\frac{1}{2}}(\partial D)} + \quad \|g\|_{H^{-\frac{1}{2}}(\partial D)}, \tag{3.19}$$

then the variational formulation amounts to find $w_0 = w - \theta \in V$ such that for all φ in V,

$$\begin{aligned}\int_D (n-1)^{-1}(\Delta w_0 + k^2 n w_0)(\Delta\overline{\varphi} + k^2 n\overline{\varphi})\,\mathrm{d}x + k^2\int_D \nabla w_0 \nabla\overline{\varphi}\,\mathrm{d}x - k^4\int_D n w_0\overline{\varphi}\,\mathrm{d}x \\ = \int_D (n-1)^{-1}(\Delta\theta + k^2 n\theta)(\Delta\overline{\varphi} + k^2 n\overline{\varphi})\,\mathrm{d}x + k^2\int_D \nabla\theta\nabla\overline{\varphi}\,\mathrm{d}x - k^4\int_D n\theta\overline{\varphi}\,\mathrm{d}x\end{aligned} \tag{3.20}$$

Theorem 3.3.1. *The existence of a unique pair of solution (u, v) to (3.7) is equivalent to the existence of a unique solution w_0 to the variational problem (3.20). Furthermore, denoting $w = w_0 + \theta$, we have the following relations on $L^2(D \setminus \overline{\Gamma})$,*

$$v = -\frac{1}{k^2(n-1)}(\Delta + k^2 n)w \quad \text{and} \quad u = -\frac{1}{k^2(n-1)}(\Delta + k^2)w. \tag{3.21}$$

Proof. According to the previous discussion, we only need to prove that the existence of a unique solution w_0 to the variational formulation (3.20) implies the existence of a unique pair of solution (u, v) given by (3.21) to (3.7). Let $w_0 \in V$ be a solution of (3.20), then $w := w_0 + \theta$ satisfies (3.18) for all $\varphi \in V$, by introducing the function

$$v := \frac{-1}{k^2(n-1)}(\Delta w + k^2 n w) \in L^2(D \setminus \overline{\Gamma}), \tag{3.22}$$

it can be written

$$-k^2\int_D v(\Delta\overline{\varphi} + k^2\overline{\varphi})\,\mathrm{d}x + k^2\int_D \Delta w\overline{\varphi}\,\mathrm{d}x + k^2\int_D \nabla w\nabla\overline{\varphi}\,\mathrm{d}x = 0. \tag{3.23}$$

Choosing $\varphi \in C_c^\infty(D \setminus \overline{\Gamma})$ we obtain after integrating by parts that v satisfies the following equation (in the classical sense since $v \in L^2(D \setminus \overline{\Gamma})$)

$$\Delta v + k^2 v = 0 \text{ in } D \setminus \overline{\Gamma}. \tag{3.24}$$

We now show that v satisfies Helmholtz equation in D, let $D_0 \subset D$ such that $\Gamma \subset D_0$ and that k^2 is not a Dirichlet eigenvalue for $-\Delta$ in D_0. Then for all $\varphi \in H_0^2(D)$ which moreover satisfies $\Delta\varphi + k^2\varphi = 0$ on D_0 is obtained from (3.23)-(3.24) that

$$\langle v, \partial_\nu\varphi\rangle_{H^{\frac{1}{2}}(\partial D_0), H^{-\frac{1}{2}}(\partial D_0)} - \langle \partial_\nu v, \varphi\rangle_{H^{-\frac{1}{2}}(\partial D_0), H^{\frac{1}{2}}(\partial D_0)} = 0. \tag{3.25}$$

Consequently there exists a unique $\widetilde{v} \in H^1(D_0)$ such that $\Delta\widetilde{v} + k^2\widetilde{v} = 0$ in D_0 and $(\widetilde{v}, \partial_\nu\widetilde{v}) = (v, \partial_\nu v)$ on D_0. Indeed let $\widetilde{v} \in H^1(D_0)$ be the unique solution of

$$\left|\begin{array}{rcll} \Delta\widetilde{v} + k^2\widetilde{v} & = & 0 \quad \text{in} & D_0 \\ \widetilde{v} & = & v \quad \text{on} & \partial D_0 \end{array}\right. \tag{3.26}$$

we obtain with Green formula

$$\langle \widetilde{v}, \partial_\nu\varphi\rangle_{H^{\frac{1}{2}}(\partial D_0), H^{-\frac{1}{2}}(\partial D_0)} - \langle \partial_\nu\widetilde{v}, \varphi\rangle_{H^{-\frac{1}{2}}(\partial D_0), H^{\frac{1}{2}}(\partial D_0)} = 0. \tag{3.27}$$

then

$$\langle \partial_\nu v - \partial_\nu\widetilde{v}, \varphi\rangle_{H^{-\frac{1}{2}}(\partial D_0), H^{\frac{1}{2}}(\partial D_0)} = 0. \tag{3.28}$$

Consequently $\partial_\nu v = \partial_\nu \widetilde{v}$. The unique continuation principle imples that $v = \widetilde{v}$ in D_0 hence v satisfies

$$\Delta v + k^2 v = 0 \text{ in } D. \tag{3.29}$$

The function $u := w + v \in L^2(D)$ is easily seen to be satisfying equation $\Delta u + k^2 n u = 0$ in $D \setminus \overline{\Gamma}$. We finish the proof showing that it satisfies Neumann condition on Γ. Let $\varphi \in V$, integrating (3.23) by parts and using the conditions $[\partial_\nu \varphi]_\Gamma = 0$ and $\varphi_{|D} = \partial_\nu \varphi_{|D} = 0$ we obtain the following equation,

$$-k^2 \int_\Gamma \partial_\nu^+ v \overline{\varphi}^+ \,\mathrm{ds}(x) + k^2 \int_\Gamma \partial_\nu^- v \overline{\varphi}^- \,\mathrm{ds}(x) - k^2 \int_\Gamma \partial_\nu w [\overline{\varphi}] \,\mathrm{ds}(x) = 0 \tag{3.30}$$

Interior regularity implies that $\partial_\nu^+ v = \partial_\nu^- v$, (3.30) then becomes,

$$\forall \varphi \in V, \quad \int_\Gamma (\partial_\nu w + \partial_\nu v)[\overline{\varphi}] \,\mathrm{ds}(x) = 0.$$

The jump $[\varphi]_{|\Gamma}$ can be chosen arbitrarly, we conclude that $\partial_\nu w + \partial_\nu v = \partial_\nu u = 0$ on Γ.

□

3.3.2 The Fredholm property

We now show that the interior transmission problem satisfies the Fredholm property, that is uniqueness of solutions for any (f, g) implies existence of solution for any (f, g). By linearity of the problem (3.7), if (u, v) and (u', v') are solutions then $(u - u', v - v')$ is a solution with zero right hand side (i.e $f = g = 0$), hence with the following definition it is equivalent to say that the problem is injective or that k is not a transmission eigenvalue.

Definition 3.3.2. *Values of $k > 0$ for which equation (3.7) with $f = g = 0$ has a non trivial solution are called transmission eigenvalues.*

Theorem 3.3.3. *Assume that there exists $\rho \in]-\frac{\pi}{2}, \frac{\pi}{2}[$ such that $\Re\mathfrak{e}(\frac{e^{i\rho}}{n-1}) > \alpha > 0$ and that $k > 0$ is not a transmission eigenvalue. Then for any $f \in H^{\frac{1}{2}}(\partial D)$, $g \in H^{-\frac{1}{2}}(\partial D)$, the interior transmission problem (3.7) has a unique solution $(u, v) \in L^2(D) \times L^2(D)$ and*

$$\|u\|_{L^2(D)} + \|v\|_{L^2(D)} \leq C \left(\|f\|_{H^{\frac{1}{2}}(\partial D)} + \|g\|_{H^{-\frac{1}{2}}(\partial D)} \right). \tag{3.31}$$

Proof. The function

$$F : \varphi \mapsto \int_D (n-1)^{-1} (\Delta\theta + k^2 n\theta)(\Delta\overline{\varphi} + k^2 n\overline{\varphi}) \,\mathrm{d}x + k^2 \int_D \nabla\theta \nabla\overline{\varphi} \,\mathrm{d}x - k^4 \int_D n\theta\overline{\varphi} \,\mathrm{d}x \tag{3.32}$$

is an antilinear continuous functional on V. According to the Riesz representation theorem, there exists a unique $l \in V$ such that $F(\varphi) = \langle l, \varphi \rangle_V$ for all $\varphi \in V$ and

$$\|l\|_V = \|F\| \leq C \|\theta\|_{H^2(D)}. \tag{3.33}$$

Samely are defined the two following operators on V,

$$\langle \mathbb{A}_k w, \varphi \rangle_V = \int_D \frac{1}{n-1} \Delta w \Delta\overline{\varphi} \,\mathrm{d}x + k^2 \int_D \nabla w \nabla\overline{\varphi} \,\mathrm{d}x \tag{3.34}$$

and

$$\langle \mathbb{B}_k w, \varphi \rangle_V = k^2 \int_D \frac{n}{n-1} (\Delta w \overline{\varphi} + w \Delta \overline{\varphi}) \, \mathrm{d}x + k^4 \int_D \frac{n}{n-1} w \overline{\varphi} \, \mathrm{d}x. \tag{3.35}$$

With these notations, a solution $w_0 \in V_k$ to (3.20) is equivalently a solution to equation

$$\mathbb{A}_k w_0 + \mathbb{B}_k w_0 = l. \tag{3.36}$$

It can be shown with the classical proof of Poincaré that

$$\forall \varphi \in V, \int_D \|\varphi\|^2 \, \mathrm{d}x \leq C_P \int_D \|\nabla \varphi\|^2 \, \mathrm{d}x \tag{3.37}$$

where

$$C_P := \sup_{w \in V \setminus \{0\}} \frac{\|w\|^2_{L^2(D)}}{\|\nabla w\|^2_{L^2(D)}} < +\infty \tag{3.38}$$

then the assumption on n implies that for all $\varphi \in V$, $|\langle \mathbb{A}_k \varphi, \varphi \rangle_V| > c \|\varphi\|^2_V$ and it can be shown by adapting the proof of Lax Milgram theorem that $\mathbb{A}_k$ is an isomorphism on V. The operator $\mathbb{B}_k$ is compact, the proof of this is classic, consider the part $\mathbb{B}^1_k$ of the operator $\mathbb{B}_k$ given by the first integral in (3.35), then

$$\forall \varphi \in V, \quad \|\mathbb{B}^1_k \varphi\|^2_V = k^2 \int_D \frac{n}{n-1} \Delta(\mathbb{B}^1_k \varphi) \overline{\varphi} \, \mathrm{d}x \leq C \|\varphi\|_{L^2(D)} \|\mathbb{B}^1_k \varphi\|_V \tag{3.39}$$

Consequently

$$\forall \varphi \in V, \quad \|\mathbb{B}^1_k \varphi\|_V \leq C \|\varphi\|_{L^2(D)} \tag{3.40}$$

The compact embedding of $H^1(D)$ in $L^2(D)$ then implies that $\mathbb{B}^1_k$ is compact. We proceed the same way to show that the other terms of $\mathbb{B}_k$ are compact. To conclude we use the Fredholm alternative, the hypothesis on k implies that the operator $(\mathbb{A}_k + \mathbb{B}_k)$ is injective consequently there exists a unique solution $w_0 \in V$ to equation (3.36) and $\|w_0\|_V \leq C \|l\|_V$. Theorem (3.3.1) implies that there exists a unique solution to (3.7) given by (u, v) defined by (3.21) where $w := w_0 + \theta$. Since u and v can be written with $w, \Delta w$, both of their L^2 norm on D are controlled by $\|w\|_V$. Finally we deduce with (3.33) and (3.19) the desired estimation (3.31).

□

We conclude this section by showing that in the case of dissipative medium, the set of real transmission eigenvalues is empty.

Theorem 3.3.4. *If $\Im\mathfrak{m}(n) > 0$ on a subset $\Omega \subset D$ of non empty interior, then there are no real transmission eigenvalues.*

Proof. Let $k^2 \in \mathbb{R}$ and w be a solution to (3.20) with $\theta = 0$, then regrouping the terms it is obtained that

$$\int_D (n-1)^{-1} (\Delta w + k^2 w)(\Delta \overline{w} + k^2 \overline{w}) \, \mathrm{d}x - k^4 \int_D |w|^2 \, \mathrm{d}x \\ + 2k^2 \int_D \Re\mathfrak{e}(w(\Delta \overline{w} + k^2 n \overline{w})) \, \mathrm{d}x + k^2 \int_D |\nabla w|^2 \, \mathrm{d}x = 0. \tag{3.41}$$

Taking the imaginary part gives

$$\int_D \Im\mathfrak{m}(n-1)^{-1}|\Delta w + k^2 w|^2 \,\mathrm{d}x = 0.$$

Since $\Im\mathfrak{m}(\frac{1}{n-1}) = -\Im\mathfrak{m}(n) < 0$ on Ω (and $-\Im\mathfrak{m}(n) \leq 0$ on D), we infer that

$$\Delta w + k^2 w = 0 \text{ on } \Omega,$$

consequently, from identity (3.21), $u = 0$ on Ω and the unique continuation principle implies that $u = 0$ in D. Finally equation (3.10) implies that $w = 0$ in $D \setminus \overline{\Gamma}$ and $u = v + w = 0$ in $D \setminus \overline{\Gamma}$. □

3.4 Transmission eigenvalues

We now consider the properties of transmission eigenvalues, as they do not exist when the refractive index has an imaginary part according to Theorem 3.3.4, it will be assumed that n is real valued. Furthermore, the approach we adopt requires that ITP satisfies the Fredholm property, that is $\mathbb{A}_k$ is coercive and $\mathbb{B}_k$ is compact. According to Theorem 3.3.3 the latter will require that the lower bound of the real refractive index is bigger that 1. Therefore from now on we do the following assumption

Assumption 3.4.1. *The refractive index $n \in L^\infty(D)$ is assumed to be a real valued function. With the following notations,*

$$n_* := \inf_{x\in D} n(x) \quad \textit{and} \quad n^* := \sup_{x\in D} n(x)$$

it is moreover assumed that $n_* > 1$.

3.4.1 Faber-Krahn inequalities for transmission eigenvalues

The following theorem enunciate that there are no real transmission eigenvalue near zero.

Lemma 3.4.2. *Any transmission eigenvalue $k > 0$ satisfies the following estimation*

$$k \geq \frac{1}{\sqrt{n^* C_P}} \tag{3.42}$$

where C_P is the Poincaré constant defined at (3.38).

Proof. We show that the interior transmission problem is uniquely solvable for all k under the bound given at (3.42). According to the previous section it is equivalent to show that the only solution to $(\mathbb{A}_k + \mathbb{B}_k)w = 0$ is zero for these values of k. Using Poincaré inequality and the assumptions on n we obtain that

$$\begin{aligned}\langle(\mathbb{A}_k + \mathbb{B}_k)w, w\rangle_V &= \int_D (n-1)^{-1}|\Delta w + k^2 n w|^2 \,\mathrm{d}x + k^2 \int_D |\nabla w|^2 \,\mathrm{d}x - k^4 \int_D n|w|^2 \,\mathrm{d}x \\ &\geq k^2 \|\nabla w\|^2_{L^2(D)} - k^4 n^* \|w\|^2_{L^2(D)} \\ &\geq (k^2 - k^4 n^* C_p^2)\|\nabla w\|^2_{L^2(D)}\end{aligned}$$

obviously $0 \leq k < \frac{1}{\sqrt{n^* C_p}}$ implies that $w = 0$, consequently every transmission eigenvalue satisfies the estimate of the theorem. □

For later use we will need the following sharper result which establish the coercivity of $\mathbb{A}_k+\mathbb{B}_k$ as soon as k is small enough.

Lemma 3.4.3. *Assume that n satisfies Assumption 3.4.1, then*

$$\langle(\mathbb{A}_k+\mathbb{B}_k)w,w\rangle_V \geq C\|w\|_V^2 \quad \text{for all} \quad k<\frac{n_*-1}{C_P n_*\sqrt{n^*-1}} \tag{3.43}$$

where C_P is the Poincaré constant defined at (3.38).

Proof. From the definitions of $\mathbb{A}_k$ and $\mathbb{B}_k$ (3.34)-(3.35), it is obtained that for all $w\in V$,

$$\begin{aligned}\langle(\mathbb{A}_k+\mathbb{B}_k)w,w\rangle_V &\geq \frac{1}{n^*-1}\|\Delta w\|^2_{L^2(D)}+k^2\|\nabla w\|^2_{L^2(D)}-2k^2\frac{n_*}{n_*-1}\|\Delta w\|_{L^2(D)}\|w\|_{L^2(D)}\\ &\geq \frac{1}{n^*-1}\|\Delta w\|^2_{L^2(D)}+k^2\|\nabla w\|^2_{L^2(D)}-2k^2\frac{C_P n_*}{n_*-1}\|\Delta w\|_{L^2(D)}\|\nabla w\|_{L^2(D)}\end{aligned}$$

We need to choose k such that $\frac{k^2}{n^*-1}>\left(k^2\frac{C_P n_*}{n_*-1}\right)^2$, which leads to the desired result. □

3.4.2 Discreteness of transmission eigenvalues

In this section, we show that the set of transmission eigenvalues is at most discrete. The proof relies on the analytic Fredholm theory, which concerns operator valued analytic functions defined by

Definition 3.4.4. *Let Ω be a domain in $\mathbb{C}$ and let $f:\Omega\to X$ be a function from Ω into the (complex) Banach space X. f is said to be analytic in Ω if for every $z_0\in\Omega$ there exists a power series expansion*

$$f(z)=\sum_{m=0}^{\infty}a_m(z-z_0)^m \tag{3.44}$$

that converges in the norm on X uniformly for all z in a neighborhood of z_0 and where the cofficients a_m are elements from X.

When X is more particularly $\mathcal{L}(E)$ for some Banach space E, we have the following result,

Theorem 3.4.5. *Let Ω be a domain in $\mathbb{C}$ and let $(\mathbb{T}_z)_{z\in\Omega}\subset\mathcal{L}(E)$ be a family of compact operators such that $z\mapsto\mathbb{T}_z$ is analytic in Ω. Then either*

a) $(I-\mathbb{T}_z)$ is not injective for any $z\in\Omega$ or

b) $(I-\mathbb{T}_z)$ is injective for all $z\in\Omega\setminus S$ where S is a discrete subset of Ω.

Theorem 3.4.6. *Assume that $n\in L^\infty(D)$ such that $\Im\mathfrak{m}(n)\geq 0$ and $\Re\mathfrak{e}(n)>\alpha+1$, then the set of transmission eigenvalues is at most discrete (possibly empty).*

Proof. We recall that k is a transmission eigenvalue if and only if $(\mathbb{A}_k+\mathbb{B}_k)$ is not injective. We reduce ourselves to the case of the theorem and uses the same notations. Choosing correctly Ω so that for all $k\in\Omega$ the operator $\mathbb{A}_k^{-1}$ exists (i), we can reformulate by defining the operator $\mathbb{T}_k:=\mathbb{A}_k^{-1}\mathbb{B}_k$ that k is a transmission eigenvalue if and only if $(I+\mathbb{T}_k)$ is not injective. The operator $\mathbb{T}_k$ is compact as well as $\mathbb{B}_k$ and $k\mapsto\mathbb{T}_k$ is analytic in Ω. $(\mathbb{T}_k)_{k\in\Omega}$ then satisfies the conditions of Theorem 3.4.5. Moreover taking care to include in Ω right elements which discriminates the first point of the theorem (ii), we deduce that $(I+\mathbb{T}_k)$ is injective except for

$k \in S$, a discrete subset of Ω. Then the set of real transmission eigenvalues simply given by $S \cap \mathbb{R}_+$ is discrete. A suitable set for Ω which both satisfies (i), (ii) and moreover contains the positive real axis is

$$\Omega = \left\{ k \in \mathbb{C} \text{ such that } \mathfrak{Re}(k) > 0 \text{ and } \mathfrak{Re}(k^2) > 0 \right\}. \tag{3.45}$$

Indeed $\mathbb{A}_k$ defined by (3.34) is coercive for all $k \in \Omega$ and Lemma 3.4.2 ensures that $(I + \mathbb{T}_k)$ is injective for real positive k sufficiently small. □

3.4.3 Existence of transmission eigenvalues

We now turn our attention on the existence of transmission eigenvalues, it is shown in this section that they form an infinite set with no accumulation point in $\mathbb{R}_+$. From the equivalence between the weak and the strong formulation of the interior transmission problem it is sufficient to show that k is a transmission eigenvalue if the nullspace of $\mathbb{A}_k + \mathbb{B}_k$ is not trivial. Since $\mathbb{A}_k$ is positive definite and self-adjoint, we can define [110] the operator $A_k^{-\frac{1}{2}}$ which is also bounded, positive definite and self-adjoint. Then defining the following self-adjoint compact operator on V,

$$\mathbb{U}_k := \mathbb{A}_k^{-\frac{1}{2}} \mathbb{B}_k \mathbb{A}_k^{-\frac{1}{2}}, \tag{3.46}$$

it is easily seen from the factorization $\mathbb{A}_k + \mathbb{B}_k = \mathbb{A}_k^{\frac{1}{2}}(I + \mathbb{U}_k)\mathbb{A}_k^{\frac{1}{2}}$ that k is a transmission eigenvalue if and only if $(I + \mathbb{U}_k)$ is not injective. The Hilbert-Schmidt theorem [110] implies the existence of a sequence of eigenvalues of $\mathbb{U}_k$ denoted $(\mu_j(k))_{j \geq 0}$ accumulating to 0 and ordered in the decreasing order for positive the eigenvalues and increasing order for negative eigenvalues. Finally we have that k is a transmission eigenvalue if and only if there exists $j \in \mathbb{N}$ such that $1 + \mu_j(k) = 0$. We use this last characterization of transmission eigenvalues to prove their existence and we rely on the following lemma which was first proved in [104].

Lemma 3.4.7. *Let H be an Hilbert space and $(\mathbb{U}_k)_{k \in \mathbb{R}} \subset \mathcal{L}(H)$ a family of self-adjoint compact operator such that $k \mapsto \mathbb{U}_k$ is continuous. Assume that*

1) there is a k_0 such that $I + \mathbb{U}_{k_0}$ is positive on H and

2) there is a $k_1 > k_0$ such that $I + \mathbb{U}_{k_1}$ is non positive on a p-dimensional subspace W of H

Then the equation $1 + \mu_j(k) = 0$ has p solutions in $[k_0, k_1]$ counting their multiplicity.

Proof. The Courant-Fischer min-max [92] principle gives the following characterization of the spectrum of $\mathbb{U}_k$,

$$\mu_j(k) = \min_{W \in H_j} \max_{u \in H_j \setminus \{0\}} \frac{\langle \mathbb{U}_k u, u \rangle_H}{\|u\|_H} \tag{3.47}$$

where H_j denotes the set of j-dimensional subspaces W of H. From this and the continuity of $\mathbb{U}_k$ with respect to k follows the continuity of $k \mapsto \mu_j(k)$ for all $j \in \mathbb{N}$. The conclusion of the lemma is then a simple consequence of the intermediate value theorem since the first point means that $\mu_j(k_0) > 1$ for all $j \in \mathbb{N}$ whereas the second point guaranties that $\mu_j(k_1) < 1$ for $j \in \mathcal{A}$, a p-element subset of $\mathbb{N}$.

□

Theorem 3.4.8. *Assume that the index n satisfies Assumption 3.4.1, then the set of transmission eigenvalues is infinite with no accumulation point in $\mathbb{R}_+$. Furthermore the multiplicity of each transmission eigenvalue is finite.*

Proof. We use the previous lemma to show that $1+\mu_j(k)=0$ has infinitely many solutions $k\in\mathbb{R}$ where $\mu_j(k)$ are the eigenvalues of $\mathbb{U}_k$ defined by (3.46). Observing that

$$\langle (I+\mathbb{U}_k)w,w\rangle_V = \langle (\mathbb{A}_k+\mathbb{B}_k)\mathbb{A}_k^{-\frac{1}{2}}w, \mathbb{A}_k^{-\frac{1}{2}}w\rangle_V \text{ for all } w\in V, \tag{3.48}$$

it is equivalent to deal with the operator $\mathbb{A}_k+\mathbb{B}_k$. The first assumption of the lemma is valid because of Lemma 3.4.3. We now prove the second assumption of Lemma 3.4.7 to be valid. Let $\epsilon>0$ be small enough such that $D\backslash\Gamma$ contains $m(\epsilon)\geq 1$ pairwise disjoint balls $B_\epsilon^1,\dots B_\epsilon^m \Subset D\backslash\Gamma$. We set each ball refractive index to be $n:=n_*$. We can show by a scaling argument that the interior transmission problem on each ball has in common the same transmission eigenvalue $k_\epsilon=\frac{k_1}{\epsilon}$, where k_1 is the first transmission eigenvalue for the unit ball with refractive index n_*. Then we denote by $u_\epsilon^j\in H_0^2(B_\epsilon^j)$ the associated eigenfunction of the problem on each ball, and by $\widetilde{u}^j$ the extension by zero of each u^j to the whole of $D\setminus\Gamma$. Each $\widetilde{u}_\epsilon^j$ is in the variational space V, and furthermore form an orthogonal family since they are of disjoint compact support. Note that for all j, $\widetilde{u}^j$ satisfies

$$\int_{B_\epsilon^j}\frac{1}{(n-1)}|\Delta\widetilde{u}^j+k_\epsilon^2\widetilde{u}^j|^2\,\mathrm{d}x - k_\epsilon^2\int_{B_\epsilon^j}|\nabla\widetilde{u}^j|^2\,\mathrm{d}x + k_\epsilon^4\int_{B_\epsilon^j}|\widetilde{u}^j|^2\,\mathrm{d}x = 0. \tag{3.49}$$

Now we show that $\mathbb{A}_k+\mathbb{B}_k$ is non positive on the $m(\epsilon)$-dimensional space $span(\widetilde{u}^1\dots\widetilde{u}^m)$

$$\begin{aligned}
\langle(\mathbb{A}_{k_\epsilon}+\mathbb{B}_{k_\epsilon})w,w\rangle_V &= \int_D\frac{1}{(n-1)}|\Delta\widetilde{u}^j+k_\epsilon^2 n\widetilde{u}^j|^2\,\mathrm{d}x + k_\epsilon^2\int_D|\nabla\widetilde{u}^j|^2\,\mathrm{d}x - k_\epsilon^4\int_D n|\widetilde{u}^j|^2\,\mathrm{d}x\\
&= \int_D\frac{1}{(n-1)}|\Delta\widetilde{u}^j+k_\epsilon^2\widetilde{u}^j|^2\,\mathrm{d}x + k_\epsilon^2\int_D|\nabla\widetilde{u}^j|^2\,\mathrm{d}x + k_\epsilon^4\int_D|\widetilde{u}^j|^2\,\mathrm{d}x\\
&+ k^2\int_{D\backslash\Gamma}(\Delta\widetilde{u}^j\overline{\widetilde{u}^j}+\widetilde{u}^j\Delta\overline{\widetilde{u}^j})\,\mathrm{d}x\\
&= \int_{B_\epsilon^j}\frac{1}{(n-1)}|\Delta\widetilde{u}^j+k_\epsilon^2\widetilde{u}^j|^2\,\mathrm{d}x + k_\epsilon^2\int_{B_\epsilon^j}|\nabla\widetilde{u}^j|^2\,\mathrm{d}x + k_\epsilon^4\int_{B_\epsilon^j}|\widetilde{u}^j|^2\,\mathrm{d}x\\
&+ k^2\int_{B_\epsilon^j}(\Delta\widetilde{u}^j\overline{\widetilde{u}^j}+\widetilde{u}^j\Delta\overline{\widetilde{u}^j})\,\mathrm{d}x\\
&= \int_{B_\epsilon^j}\frac{1}{(n-1)}|\Delta\widetilde{u}^j+k_\epsilon^2\widetilde{u}^j|^2\,\mathrm{d}x - k_\epsilon^2\int_{B_\epsilon^j}|\nabla\widetilde{u}^j|^2\,\mathrm{d}x + k_\epsilon^4\int_{B_\epsilon^j}|\widetilde{u}^j|^2\,\mathrm{d}x\\
&\leq \int_{B_\epsilon^j}\frac{1}{(n_*-1)}|\Delta\widetilde{u}^j+k_\epsilon^2\widetilde{u}^j|^2\,\mathrm{d}x - k_\epsilon^2\int_{B_\epsilon^j}|\nabla\widetilde{u}^j|^2\,\mathrm{d}x + k_\epsilon^4\int_{B_\epsilon^j}|\widetilde{u}^j|^2\,\mathrm{d}x\\
&= 0.
\end{aligned}$$

From Lemma 3.4.7, we conclude that there are $m(\epsilon)$ transmission eigenvalues contained in $[k_0,k_\epsilon]$. $m(\epsilon)$ and k_ϵ both go to infinity as $\epsilon\to\infty$. Since each non zero eigenvalue of of the compact operator $\mathbb{U}_k$ is isolated and of finite multiplicity hence we have shown by letting $\epsilon\to 0$, that there exists an infinite countable set of transmission eigenvalues of finite multiplicity and with no accumulation point in $\mathbb{R}_+$. □

Chapter 4

Detection of sound-hard obstacles in inhomogeneous media

Contents

4.1 Introduction

The primary issue in inverse scattering theory consists in recovering the shape of an unknown medium from collected measurements of scattered fields generated with given incident waves. The Factorization Method (FM) introduced by Kirsch, which is one method among the class of the sampling methods, has shown good results in solving this problem. It first proved its effectiveness for impenetrable obstacles [79], then to inhomogeneous media [80, 81]. Since then, FM has been extended to numerous academical inverse problems [83]. More recently, many works contributed to justify FM to more complex backgrounds, allowing one to implement it in practical applications such as geophysics or nondestructive testing. We mention for instance the papers [86, 15, 122] where scatterers made of both impenetrable obstacles and inhomogeneous medium are considered. These works raises new questions concerning the possibility to distinguish the impenetrable obstacle from the inhomogeneous medium. Several variants of this problem can be considered. Firstly, one can consider the feasibility of determining an obstacle inside a known inhomogeneous medium. This issue is treated in [101]. A second and more challenging problem is to do so with no a priori knowledge on the inhomogeneity. At last one can understand the obstacle as a defect which appeared in the inhomogeneity and consider the problem of detecting the position of the defect from measurements on both the healthy material and the damaged material. In this work, we treat this last issue by adapting the results of the Differential Linear

Sampling Method (DLSM) [9] which has originally been set up to identify a modification in the refractive index in an inhomogeneity.

More precisely, we consider the problem of identifying sound-hard defects of non empty interior inside an unknown inhomogeneous medium from far field data at fixed frequency. As mentioned, we adapt for this purpose the results of the DLSM which requires two set of measurements done before and after the occurrence of the defect. The theoretical justification of the DLSM relies on the comparison of the solutions of two Interior Transmission Problem, the one corresponding to the healthy material and the one corresponding to the damaged material. The use of the DLSM in practice also requires to compute these solutions from the data. The latter can be done by the use of the Generalized Linear Sampling Method (GLSM) [10], which consists in approximating solutions of the far field equation with a particular penalty term. On the one hand, the GLSM requires a factorization of the far field operator, similar to the one used for the Linear Sampling Method. On the other hand, it requires the penalty term to be equivalent to the Herglotz operator and to satisfy a convexity property. Therefore we have chosen to use the $F_\sharp$ operator in the penalty term which is shown to satisfy the factorization similar to the one required for the so called $F_\sharp$ Method. Furthermore it should be noted that since $F_\sharp$ is positive definite, the optimization of the cost functional is greatly simplified and do not require any iterative method. As a product of our analysis, we have also extended the factorization method to this setting which yields a reconstruction procedure for the whole background. The same remark stands for the use of GLSM.

The outline of this chapter is quite similar to Chapter 2 in which we have been considering sound-hard defects of empty interior referred as cracks. Consequently, and for the sake of making this chapter self contained, there are some repetitions for notations and settings in the introductory section and the numerical part. However, the study of these two problems differs in some technical aspects. For instance, in this chapter the regularity of the boundary of the non penetrable obstacle Ω is weaker than the one required for the cracks; but as a counterpart, the wave number is assumed not to be a Neumann eigenvalue for the Laplace operator in Ω. We also mention that this work has brought new difficulties such as the study of the corresponding interior transmission eigenvalue problem which is treated in a next chapter and for which the issue concerning the existence of transmission eigenvalue is not solved yet.

4.2 The forward scattering problem

We consider an isotropic inhomogeneous medium D embedded in $\mathbb{R}^d$ with $d = 2$ or 3, containing sound-hard obstacle $\Omega \subset D$. Both of the sets D and Ω are assumed to be domains of non empty interior, of Lipschitz boundary and of connected complement. The normal vector ν on ∂D and $\partial\Omega$ are respectively defined as the outward normal vector to D and Ω. In this setting, the total field $u \in H^1_{loc}(\mathbb{R}^d \setminus \overline{\Omega})$ satisfies

$$\left| \begin{array}{rcll} \Delta u + k^2 n\, u & = & 0 & \text{in } \mathbb{R}^d \setminus \overline{\Omega} \\ \partial_\nu u & = & 0 & \text{on } \partial\Omega \end{array} \right. \tag{4.1}$$

where $k > 0$ is the wave number and $n \in L^\infty(\mathbb{R}^d \setminus \overline{\Omega})$ the refractive index of the medium. We assume that $supp(n-1) = D \setminus \overline{\Omega}$ and $\Im\mathfrak{m}(n) \geq 0$ in $\mathbb{R}^d \setminus \overline{\Omega}$. Given an incident field u_i, the scattered field $u_s := u - u_i$ then satisfies

$$\left| \begin{array}{rcll} \Delta u_s + k^2 n\, u_s & = & -k^2(n-1)u_i & \text{in } \mathbb{R}^d \setminus \overline{\Omega} \\ \partial_\nu u_s & = & -\partial_\nu u_i & \text{on } \partial\Omega. \end{array} \right. \tag{4.2}$$

Moreover u_s is assumed to satisfy the Sommerfeld radiation condition,

$$\lim_{r\to+\infty} r^{\frac{d-1}{2}}\left(\frac{\partial u_s}{\partial r} - iku_s\right) = 0 \tag{4.3}$$

uniformly with respect to x/r with $r = |x|$. As a consequence, u_s has the following expansion

$$u_s(x) = e^{ik|x|}|x|^{-\frac{d-1}{2}}\left(u_s^\infty(\widehat{x}) + O(1/|x|)\right), \tag{4.4}$$

as $|x| \to +\infty$, uniformly in $\widehat{x} = x/|x| \in \mathbb{S}^{d-1}$, which denotes the unit sphere of $\mathbb{R}^d$. The function $u_s^\infty : \mathbb{S}^{d-1} \to \mathbb{C}$, is called the far field pattern associated with u_i. We are interested in far field patterns associated with a particular class of incident waves called Herglotz wave functions defined for $g \in L^2(\mathbb{S}^{d-1})$ by

$$v_g := \int_{\mathbb{S}^{d-1}} g(\theta)e^{ik\theta\cdot x}\,\mathrm{ds}(\theta). \tag{4.5}$$

We denote by $u_s^\infty(\theta,\widehat{x})$ the far field pattern associated to $u_i(\theta,\cdot) := e^{ik\theta\cdot x}$ for $\theta \in \mathbb{S}^{d-1}$ (incident plane wave of direction θ). Thanks to the linearity of the scattering problem (1.1)-(1.2), the far field pattern associated to the Herglotz wave v_g is given by

$$(Fg)(\widehat{x}) = \int_{\mathbb{S}^{d-1}} g(\theta)\, u_s^\infty(\theta,\widehat{x})\,\mathrm{ds}(\theta). \tag{4.6}$$

This defines the so-called far field operator $F : L^2(\mathbb{S}^{d-1}) \to L^2(\mathbb{S}^{d-1})$ which constitutes the data of the inverse scattering problem where one is interested in recovering qualitative or even quantitative information on the refractive index n and on Ω. In the next section is shown that the far field operator satisfies the needed properties allowing to apply the GLSM and the DLSM to this setting.

4.3 The far field operator

In this section we provide the two complementary factorizations of the far field operator which are required for the implementation of GLSM and DLSM. The first operator H involved in the factorization slightly differs from the classical Herglotz operator which appears in the study of more classical problem such as isotropic inhomogeneities. Indeed taking into account the contribution of the sound-hard obstacle into the far field while establishing the second factorization requires a second well chosen component in the definition of H. We also show all the results allowing to justify the use of the $F_\sharp$ method.

4.3.1 Factorization of the far field operator

For the reason that the scattered field u_s, determined by (4.2)-(4.3), only depends of the source term $(v_{|D\setminus\overline{\Omega}}, \partial_\nu v_{|\Omega})$ we define the following Herglotz operator by

$$\begin{array}{rccc} H: & L^2(\mathbb{S}^{d-1}) & \longrightarrow & L^2(D\setminus\overline{\Omega}) \times L^2(\partial\Omega) \\ & g & \longmapsto & (v_{g_{|D\setminus\overline{\Omega}}}, \partial_\nu v_{g_{|\partial\Omega}}) \end{array} \tag{4.7}$$

where v_g is defined by (4.5). As it will be clearer below, the second component in the definition of H is necessary to obtain the factorization (4.26).

Remark 4.3.1. *Another legitimate option would be to define*

$$\begin{array}{rccc} H_1: & L^2(\mathbb{S}^{d-1}) & \longrightarrow & L^2(D)\times L^2(\partial\Omega) \\ & g & \longmapsto & (v_{g|D}, \partial_\nu v_{g|\partial\Omega}) \end{array} \tag{4.8}$$

but there is no major difference between these two choices. Indeed the important point of our study relies on the space $\overline{R(H)}$ which is exactly, as we will see, restrictions of functions in the space $\overline{R(H_1)}$. We recall that the closure of Herglotz functions restricted to D for the $L^2(D)$ norm is [29, Lemma 2.1]

$$\mathscr{H} = \{v \in L^2(D) \,|\, \Delta v + k^2 v = 0 \text{ in } D\}. \tag{4.9}$$

It is well known that not all functions in $\mathscr{H}$ can be expanded to solution of Helmholtz equation on a set larger than D due to a lack of regularity of the traces on ∂D. However the situation is a bit different when we consider the closure of Herglotz functions restricted to an annulus such as $D\setminus\overline{\Omega}$. It will be shown in Proposition 4.3.3, that functions in the closure of Herglotz waves for the $L^2(D\setminus\overline{\Omega})$ norm have a specific trace reguarity on $\partial\Omega$, more precisely they are restriction to $D\setminus\overline{\Omega}$ of functions in $\mathscr{H}$.

Lemma 4.3.2. *Let $\widetilde{\Omega}\subset D$ be an open domain. There exists a constant $C_0>0$ depending only on D and $\widetilde{\Omega}$ such that for all v satisfying the Helmholtz equation on D,*

$$\|v\|_{H^2(\widetilde{\Omega})} \leq C_0 \|v\|_{L^2(D\setminus\widetilde{\Omega})}. \tag{4.10}$$

Proof. In this proof C refers to a non negative real number independant of v and whose value can differ from one line to another. We consider two domains of regular boundaries A, B such that $\widetilde{\Omega}\Subset A\Subset B\Subset D$. From the first set inclusion we have that for all $v\in\mathscr{H}$,

$$\|v\|_{H^2(\widetilde{\Omega})} \leq \|v\|_{H^2(A)}. \tag{4.11}$$

Then from the well posedness of the following boundary problem of finding $\varphi\in H^2(A)$ such that

$$\left|\begin{array}{rcll} \Delta\varphi + k^2\varphi & = & 0 & \text{in } A \\ \frac{\partial\varphi}{\partial\nu} + i\varphi & = & f & \text{on } \partial A \end{array}\right.$$

for $f\in H^{\frac{1}{2}}(\partial A)$, we infer the existence of a constant $C>0$ depending only on A such that

$$\|v\|_{H^2(A)} \leq C\|\partial_\nu v + iv\|_{H^{\frac{1}{2}}(\partial A)}. \tag{4.12}$$

From the trace regularity and the interior regularity theorem we deduce that

$$\|\partial_\nu v + iv\|_{H^{\frac{1}{2}}(\partial A)} \leq C\|v\|_{H^2(A\setminus B)} \leq C\|v\|_{L^2(D\setminus\widetilde{\Omega})}. \tag{4.13}$$

We finally combine (4.11), (4.12) and (4.13) to obtain the desired result. □

Proposition 4.3.3. *We have the following characterization for the closure of the range of H,*

$$\overline{R(H)} = \{(v_{|D\setminus\overline{\Omega}}, \partial_\nu v_{|\partial\Omega}) \text{ such that } v\in\mathscr{H}\}.$$

Proof. Let $v\in\overline{R(H)}$ and $(v_n)_{n\in\mathbb{N}}$ a sequence of Herglotz functions converging to v in $L^2(D\setminus\overline{\Omega})$. Let $X\subset D$ such that $\Omega\Subset X$. From Lemma (4.3.2) we have that $\forall m,n\in\mathbb{N}$,

$$\|v_n - v_m\|_{H^2(X)} \leq C_0\|v_n - v_m\|_{L^2(D\setminus\overline{\Omega})}. \tag{4.14}$$

Consequently $(v_n)_{n\in\mathbb{N}}$ is a Cauchy sequence in $H^2(X)$ and converges to some $\widetilde{v} \in H^2(X)$ which moreover satisfies Helmholtz equation in X. Note that $v = \widetilde{v}$ on $X \setminus \overline{\Omega}$. We conclude that v extended by $\widetilde{v}$ in Ω is an element of $\mathscr{H}$. □

We now define the operator $G : \overline{R(H)} \to L^2(\mathbb{S}^{d-1})$ by

$$G(v, \partial_\nu v) := u_s^\infty, \tag{4.15}$$

where u_s^∞ is the far field pattern of the solution u_s of equations (4.2)-(4.3) with $u_i = v$. The following first factorization of the far field operator is then obvious:

$$F = GH. \tag{4.16}$$

We now establish the second factorization of F. For $x \in \mathbb{R}^d$, we denote by $\Phi(x, \cdot)$ the outgoing solution of

$$\Delta\Phi(x, \cdot) + k^2\Phi(x, \cdot) = -\delta_x. \tag{4.17}$$

Φ is given by the following formulas,

$$\Phi(x, y) = \frac{i}{4} H_0(k|x - y|) \text{ if } d = 2 \qquad \text{and} \qquad \Phi(x, y) = \frac{1}{4\pi} \frac{e^{ik|x-y|}}{|x - y|} \text{ if } d = 3. \tag{4.18}$$

Let $u \in H^1_{loc}(\mathbb{R}^d \setminus \overline{\Omega})$ be the solution of (4.1)-(4.3) for a given incident wave in $\overline{R(H)}$. Let $x \in \mathbb{R}^d \setminus \overline{\Omega}$ and B a ball containing x and D. Then Green's second formula implies that

$$u(x) = k^2 \int_{B\setminus\overline{\Omega}} (n - 1)u(y)\Phi(x, y)\, \mathrm{d}y - \int_{\partial B} u(y)\partial_\nu\Phi(x, y)\, \mathrm{ds}(y) + \int_{\partial B} \partial_\nu u(y)\Phi(x, y)\, \mathrm{ds}(y) + \int_{\partial\Omega} u(y)\partial_\nu\Phi(x, y)\, \mathrm{ds}(y)$$

and

$$u_i(x) = -\int_{\partial B} u_i(y)\partial_\nu\Phi(x, y)\, \mathrm{ds}(y) + \int_{\partial B} \partial_\nu u_i(y)\Phi(x, y)\, \mathrm{ds}(y). \tag{4.19}$$

Furthermore Green's second formula and the Sommerfeld radiation condition implies that ($x \in B$)

$$\int_{\partial B} u_s(y)\partial_\nu\Phi(x, y)\, \mathrm{ds}(y) - \int_{\partial B} \partial_\nu u_s(y)\Phi(x, y)\, \mathrm{ds}(y) = 0. \tag{4.20}$$

Adding these equations together gives

$$u_s(x) = k^2 \int_{D\setminus\overline{\Omega}} (n - 1)u(y)\Phi(x, y)\, \mathrm{d}y + \int_{\partial\Omega} u(y)\partial_\nu\Phi(x, y)\, \mathrm{ds}(y). \tag{4.21}$$

Finally using the far field pattern of the fundamental solution $\Phi_z(x) = \Phi(x, z)$ which is given by

$$\Phi_z^\infty(\widehat{x}) = \eta_d e^{-ik\widehat{x}\cdot z} \tag{4.22}$$

where the constant η_d is given by $\eta_d = e^{i\frac{\pi}{4}}/\sqrt{8\pi k}$ for $d = 2$ and by $= 1/(4\pi)$ for $d = 3$ is obtained the following integral representation of the far field pattern of u_s:

$$u_s^\infty(\widehat{x}) = \int_{D\setminus\Omega} \eta_d k^2 (n(y)-1) u(y) e^{-ik\widehat{x}y}\,\mathrm{d}y + \int_{\partial\Omega} \eta_d u(y) \partial_{\nu(y)} e^{-ik\widehat{x}y}\,\mathrm{ds}(y). \tag{4.23}$$

We now can see the importance of the second component of H whose adjoint is hence given by

$$H^*(\varphi_1,\varphi_2)(\theta) = \int_{D\setminus\Omega} \varphi_1(x) e^{-ikx\theta}\,\mathrm{d}x + \int_{\partial\Omega} \varphi_2(x) e^{-ikx\theta}\,\mathrm{ds}(x). \tag{4.24}$$

This allows to take into account the second term of (4.23) and after defining the mapping $T : \overline{R(H)} \to L^2(D\setminus\overline{\Omega}) \times L^2(\partial\Omega)$ by

$$T(v,\partial_\nu v) = (k^2(n-1)u_{|D\setminus\overline{\Omega}}, u_{|\partial\Omega}), \tag{4.25}$$

is obtained the following factorization of the far field operator:

$$F = \eta_d H^* T H. \tag{4.26}$$

In the next paragraph are stated the required properties of the newly defined operators.

4.3.2 Properties of the involved operators

In this paragraph we turn our attention to proving the properties of the operators H, G and T which are required for the implementation of the inversion algorithms presented in the next section. In a few words, the operator H will be asked to be injective and compact, G injective with dense range, and T to satisfy a positivity property. The properties of these two last operators depends on the well posedness of a particular boundary value problem called the Interior Transmission Problem (ITP). The latter characterizes the fact that G is injective since the solutions of (ITP) corresponds to elements of the nullspace of G. We now write the corresponding equations of (ITP). Let $v \in Ker(G)$; by definition of G, the far field of the solution u_s of (4.2)-(4.3) is zero. Then Rellich lemma implies that u_s vanishes in $\mathbb{R}^d \setminus \overline{D}$. The regularity of u_s then implies that $u_s = \partial_\nu u_s = 0$ on ∂D. Finally by defining $u := u_s + v$, the pair (u,v) is seen to be satisfying the equations below: find $u \in L^2(D\setminus\overline{\Omega})$, $v \in L^2(D)$ such that $u - v \in H^1(D\setminus\overline{\Omega})$, $\Delta(u-v) \in L^2(D\setminus\overline{\Omega})$ and

$$\left|\begin{array}{rcll} \Delta u + k^2 n\, u &=& 0 & \text{in } D\setminus\overline{\Omega} \\ \Delta v + k^2\, v &=& 0 & \text{in } D \\ \partial_\nu u &=& 0 & \text{on } \partial\Omega. \end{array}\right. \qquad \left|\begin{array}{rcll} u - v &=& 0 & \text{on } \partial D \\ \partial_\nu u - \partial_\nu v &=& 0 & \text{on } \partial D \end{array}\right. \tag{ITP}$$

Note that $v \in \overline{R(H)}$ has been extended to a solution of Helmholtz equation on D in line with Proposition 4.3.3. This problem can be understood as an eigenvalue problem and $k > 0$ is said to be a transmission eigenvalue if there exists a non trivial solution to it. With this terminology G is injective if and only if k is not a transmission eigenvalue. It is shown in Chapter 5 that the set of transmission eigenvalues is empty if n has an imaginary part, otherwise it is shown that it is at most discrete with finite accumulation point. The following lemma will be usefull to show that the range of G is dense.

Lemma 4.3.4. *Let $v_1, v_2 \in \mathscr{H}$ be two incident waves and $w_1, w_2 \in H^2_{loc}(\mathbb{R}^d\setminus\overline{\Omega})$ be the associated scattered fields determined by (4.2)-(4.3). Then we have the following identity,*

$$k^2 \int_{D\setminus\overline{\Omega}} (n-1) v_1 w_2\,\mathrm{d}x + \int_{\partial\Omega} \partial_\nu v_1 w_2\,\mathrm{ds}(x) = k^2 \int_{D\setminus\overline{\Omega}} (n-1) v_2 w_1\,\mathrm{d}x + \int_{\partial\Omega} \partial_\nu v_2 w_1\,\mathrm{ds}(x). \tag{4.27}$$

Proof. w_1 and w_2 satisfies the following equations,

$$\Delta w_1 + k^2 n w_1 = -k^2(n-1)v_1, \quad \Delta w_2 + k^2 n w_2 = -k^2(n-1)v_2 \quad \text{in } \mathbb{R}^d \setminus \overline{\Omega}. \tag{4.28}$$

Multiplying the first equation by w_2 and the second by w_1, then integrating by parts the difference over $B_R \setminus \overline{\Omega}$, where B_R is the open ball of radius R centered at O, we obtain

$$-k^2 \int_{D\setminus\overline{\Omega}} (n-1)(v_1 w_2 - v_2 w_1)\,\mathrm{d}x = \int_{\partial B_R} (\partial_\nu w_1 w_2 - w_1 \partial_\nu w_2)\,\mathrm{ds}(x) + \int_{\partial\Omega} (w_2 \partial_\nu v_1 - w_1 \partial_\nu v_2)\,\mathrm{ds}(x). \tag{4.29}$$

Since w_1 and w_2 satisfies the Sommerfeld radiation condition, the first integral of the right hand side goes to zero when R goes to infinity, indeed

$$\begin{aligned}\left|\int_{\partial B_R} (\partial_\nu w_1 w_2 - w_1 \partial_\nu w_2)\,\mathrm{ds}(x)\right| &\leq \int_{\partial B_R} |\partial_\nu w_1 w_2 - ik w_1 w_2|\,\mathrm{ds}(x) + \int_{\partial B_R} |ik w_1 w_2 - w_1 \partial_\nu w_2|\,\mathrm{ds}(x) \\ &\leq \int_{\partial B_R} |\partial_\nu w_1 - ik w_1|^2\,\mathrm{ds}(x) \int_{\partial B_R} |w_2|^2\,\mathrm{ds}(x) + \int_{\partial B_R} |\partial_\nu w_2 - ik w_2|^2\,\mathrm{ds}(x) \int_{\partial B_R} |w_1|^2\,\mathrm{ds}(x).\end{aligned} \tag{4.30}$$

Consequently taking the limit $R \to +\infty$ in (4.29) gives the desired identity.

□

Proposition 4.3.5. *The operator H is injective and compact. Assume that $k > 0$ is not a transmission eigenvalue. Then the operator $G : \overline{R(H)} \to L^2(\mathbb{S}^{d-1})$ is compact, injective with dense range.*

Proof. The proof of the injectivity of H follows a classical argument based on the Jacobi Anger expansion (apply [29, Lemma 2.1]). The compactness of H results from the fact that H is an integral operator with smooth kernel. The injectivity of G is a consequence of the assumption made on k as discussed before introducing (ITP). The compactness of G is deduced from the equality $G = H^* T$ since H is compact and T is continuous. We now proceed with the proof of the denseness of the range of G. Let ϕ, $g \in L^2(\mathbb{S}^{d-1})$, on the one hand we have from the representation formula (4.23) that

$$\langle G(\overline{H\phi}), g\rangle_{L^2(\mathbb{S}^{d-1})} = k^2 \int_{D\setminus\overline{\Omega}} (n-1)(\overline{v_\phi} + u_s(\phi))\overline{v_g}\,\mathrm{d}x + \int_{\partial\Omega} (\overline{v_\phi} + u_s(\phi))\partial_\nu \overline{v_g}\,\mathrm{ds}(x) \tag{4.31}$$

where $u_s(\phi)$ is the scattered field associated to $\overline{v_\phi}$. On the second hand we have from identity (4.27),

$$\begin{aligned}k^2 \int_{D\setminus\overline{\Omega}} (n-1)(\overline{v_\phi} + u_s(\phi))\overline{v_g}\,\mathrm{d}x + \int_{\partial\Omega} (\overline{v_\phi} + u_s(\phi))\partial_\nu \overline{v_g}\,\mathrm{ds}(x) \\ = k^2 \int_{D\setminus\overline{\Omega}} (n-1)(\overline{v_g} + u_s(g))\overline{v_\phi}\,\mathrm{d}x + \int_{\partial\Omega} (\overline{v_g} + u_s(g))\partial_\nu \overline{v_\phi}\,\mathrm{ds}(x)\end{aligned} \tag{4.32}$$

where $u_s(g)$ is the scattered associated to $\overline{v_g}$. Therefore we obtain the following reciprocity relation

$$\langle G(\overline{H\phi}), g\rangle_{L^2(\mathbb{S}^{d-1})} = \langle G(\overline{Hg}), \phi\rangle_{L^2(\mathbb{S}^{d-1})}. \tag{4.33}$$

Now if $g \in R(G)^\perp$, the reciprocity relation implies that $G(Hg) = 0$. It follows from the injectivity of G and H that g is necessarly zero, hence G has dense range. □

We now turn our attention on the properties of T.

Lemma 4.3.6. *For all $V = (v, \partial_\nu v) \in \overline{R(H)}$, we have the energy identity*

$$\Im\mathfrak{m}(\langle TV, V\rangle_{L^2(D\setminus\overline{\Omega})\times L^2(\partial\Omega)}) = k^2 \int_{D\setminus\overline{\Omega}} \Im\mathfrak{m}(n)|u_s + v|^2 \,\mathrm{d}x + k\|u_s^\infty\|^2_{L^2(\mathbb{S}^{d-1})}, \tag{4.34}$$

where u_s denotes the solution of (4.2)-(4.3) with $u_i = v$.

Proof. Let $(v, \partial_\nu v) \in \overline{R(H)}$, the corresponding u_s satisfies the equation

$$\Delta u_s + k^2 u_s = -k^2(n-1)(u_s + v). \tag{4.35}$$

Let B_R be the centered ball of radius R sufficiently large such that $D \subset B_R$. Multiplying equation (4.35) by $\overline{u_s}$ and integrating by parts over $B_R \setminus \overline{\Omega}$ gives

$$\begin{aligned} &-\int_{B_R\setminus\overline{\Omega}} |\nabla u_s|^2 - k^2|u_s|^2 \,\mathrm{d}x \\ &\qquad + \int_{\partial B_R} \partial_\nu u_s \overline{u_s} \,\mathrm{d}s(x) - \int_{\partial\Omega} \partial_\nu u_s \overline{u_s} \,\mathrm{d}s(x) = -k^2 \int_{D\setminus\overline{\Omega}} (n-1)(u_s+v)\overline{u_s} \,\mathrm{d}x \end{aligned}$$

Using the definition of T (4.25) and the previous relation gives

$$\begin{aligned} \langle TV, V\rangle_{L^2(D\setminus\overline{\Omega})\times L^2(\partial\Omega)} &= k^2 \int_{D\setminus\overline{\Omega}} (n-1)|u_s+v|^2 \,\mathrm{d}x - \int_{B_R} |\nabla u_s|^2 - k^2|u_s|^2 \,\mathrm{d}x \\ &\quad + \int_{\partial\Omega} (v+u_s)\partial_\nu \overline{v} \,\mathrm{d}s(x) - \int_{\partial\Omega} \partial_\nu u_s \overline{u_s} \,\mathrm{d}s(x) + \int_{\partial B_R} \partial_\nu u_s \,\overline{u_s} \,\mathrm{d}s(x). \end{aligned}$$

We now take the imaginary part of this equation, after noticing that

$$\int_{\partial\Omega} v\partial_\nu \overline{v} \,\mathrm{d}s(x) = \int_\Omega |\nabla v|^2 \,\mathrm{d}x - k^2 \int_\Omega |v|^2 \,\mathrm{d}x$$

we obtain

$$\begin{aligned} \Im\mathfrak{m}\langle TV, V\rangle_{L^2(D\setminus\overline{\Omega})\times L^2(\partial\Omega)} &= k^2 \int_{D\setminus\overline{\Omega}} \Im\mathfrak{m}(n)|u_s+v|^2 \,\mathrm{d}x \\ &\quad + \int_{\partial\Omega} \Im\mathfrak{m}(u_s\partial_\nu\overline{v} - \partial_\nu u_s \overline{u_s}) \,\mathrm{d}s(x) + \Im\mathfrak{m} \int_{\partial B_R} \partial_\nu u_s \overline{u_s} \,\mathrm{d}s(x). \end{aligned} \tag{4.36}$$

We observe that the first sum of the second line is zero because of the Neumann condition $\partial_\nu u_s = -\partial_\nu v$ on $\partial\Omega$. Finally the radiation condition (4.3) implies

$$\lim_{R\to\infty} \int_{\partial B_R} \partial_\nu u_s \overline{u_s} \,\mathrm{d}s(x) = ik \int_{\mathbb{S}^{d-1}} |u_s^\infty|^2 \,\mathrm{d}\theta = ik\|GV\|^2_{L^2(\mathbb{S}^{d-1})}. \tag{4.37}$$

As a consequence, letting R to infinity in (4.36) gives the desired identity.

□

Proposition 4.3.7. *Assume that the refractive index satisfies* $1 - \mathfrak{Re}(n) + \alpha\mathfrak{Im}(n) > n_0$ *or* $\mathfrak{Re}(n) - 1 + \alpha\mathfrak{Im}(n) > n_0$ *almost everywhere on* $D \setminus \overline{\Omega}$ *where* α *and* n_0 *are positive constants. Assume furthermore that* k *is not a transmission eigenvalue, then there exists a constant* $\mu > 0$ *such that* $\forall V \in \overline{R(H)}$,

$$|\langle TV, V\rangle_{L^2(D\setminus\overline{\Omega})\times L^2(\partial\Omega)}| \geq \mu \|V\|^2_{L^2(D\setminus\overline{\Omega})\times L^2(\partial\Omega)}. \tag{4.38}$$

Proof. We use a contradiction argument, assume the existence of a sequence $(V_l)_{l\in\mathbb{N}} = (v_l, \partial_\nu v_l)_{l\in\mathbb{N}} \subset \overline{R(H)}$ satisfying

$$\|V_l\|_{L^2(D\setminus\overline{\Omega})\times L^2(\partial\Omega)} = 1 \quad \text{and} \quad \langle TV_l, V_l\rangle_{L^2(D\setminus\overline{\Omega})\times L^2(\partial\Omega)} \underset{l\to\infty}{\longrightarrow} 0. \tag{4.39}$$

Since $(V_l)_{l\in\mathbb{N}}$ is bounded, one can assume that it converges weakly to $V = (v, \partial_\nu v) \in \overline{R(H)}$. Now let $w_l \in H^2_{loc}(\mathbb{R}^d \setminus \overline{\Omega})$ be the solution of the scattering problem (4.2)-(4.3) with $u_i = v_l$. Then classical elliptic regularity implies,

$$\|w_l\|_{H^2(D\setminus\overline{\Omega})} \leq C\|v_l\|_{L^2(D\setminus\overline{\Omega})}. \tag{4.40}$$

Consequently $(w_l)_{l\in\mathbb{N}}$ is bounded in $H^2_{loc}(\mathbb{R}^d \setminus \overline{\Omega})$ and the compact embedding theorem implies that it converges strongly in $L^2(D \setminus \overline{\Omega})$. Denoting $w \in L^2(\mathbb{R}^d \setminus \overline{\Omega})$ the limit, it can be shown using distributionnal limits that w satisfies (4.4)-(4.3) with $u_i = v$. Assumption (4.39) and Lemma 4.3.6 then imply that $GV = 0$. Finally the assumption on k implies that $V = 0$. We now can conclude this proof, from the definition of T and the L^2 scalar product is obtained after regrouping terms,

$$\begin{aligned}\langle TV_l, V_l\rangle_{L^2(D\setminus\overline{\Omega})\times L^2(\partial\Omega)} = k^2 \int_{D\setminus\Omega} (n-1)|v_l|^2 \,\mathrm{d}y \\ + \int_{\partial\Omega} v_l \partial_\nu \overline{v}_l \,\mathrm{ds}(y) + k^2 \int_{D\setminus\Omega} (n-1) w_l \overline{v}_l \,\mathrm{d}y + \int_{\partial\Omega} w_l \partial_\nu \overline{v}_l \,\mathrm{ds}(y).\end{aligned}$$

All the terms of the second line goes to zero as l goes to infinity. Indeed we obtain for the first term after using Lemma 4.3.2 with $\widetilde{\Omega} = \Omega$

$$\int_{\partial\Omega} v_l \partial_\nu \overline{v}_l \,\mathrm{ds}(y) \leq C\|v_l\|^2_{H^2(\Omega)} \leq C\|v_l\|^2_{L^2(D\setminus\overline{\Omega})} \underset{l\to 0}{\longrightarrow} 0. \tag{4.41}$$

This shows the desired result for the first term, the convergence to zero of the two other terms is obvious because of the strong convergence of w_l to zero in $H^2(D \setminus \overline{\Omega})$ resulting from estimation (4.40). To summarize, we have shown that

$$\langle TV_l, V_l\rangle_{L^2(D\setminus\overline{\Omega})\times L^2(\partial\Omega)} = k^2 \int_{D\setminus\Omega} (n-1)|v_l|^2 \,\mathrm{d}y + \underset{l\to\infty}{o}(1).$$

The hypothesis on n and the first assertion of (4.39) implies that

$$\lim_{l\to+\infty} |\langle TV_l, V_l\rangle_{L^2(D\setminus\overline{\Omega})\times L^2(\partial\Omega)}| > c > 0 \tag{4.42}$$

where c is a constant and this is a contradiction to the second assertion (4.39). □

In order to implement the $F_\sharp$ method we also show the following result,

Lemma 4.3.8. *Assume that there exists* $\theta \in [0, \pi]$ *such that* $\mathfrak{Im}(n) \geq 0$ *and* $\mathfrak{Re}(e^{i\theta}(n-1)) > \alpha > 0$ *for some positive constant* α. *We define the operator* $T^\theta := \mathfrak{Re}(e^{i\theta}T) + i\mathfrak{Im}(T)$, *then* T^θ *satisfies*

1. $\Im\mathfrak{m}\langle T^\theta V, V\rangle \geq 0$ *for all* $V \in \overline{R(H)}$.
2. $\Re\mathfrak{e} T^\theta = T_0^\theta + C$ *where* C *is compact on* $\overline{R(H)}$ *and* T_0^θ *satisfies*

$$\langle T_0^\theta V, V\rangle \geq \alpha \|V\|^2 \tag{4.43}$$

for all $V \in \overline{R(H)}$ *and some positive constant* α.

3. $\Im\mathfrak{m}(T^\theta)$ *is injective on* $\overline{R(H)}$.

Proof. We recall the definition of $T : \overline{R(H)} \to L^2(D\setminus\overline{\Omega}) \times L^2(\partial\Omega)$,

$$T(v, \partial_\nu v) = (k^2(n-1)u_{|D\setminus\overline{\Omega}}, u_{|\partial\Omega}). \tag{4.44}$$

with u the solution of (4.1)-(4.3). We introduce the operator

$$T_0^\theta V = (k^2 \Re\mathfrak{e}(e^{i\theta}(n-1))V_1, V_2) \tag{4.45}$$

which is obviously coercive. $\Re\mathfrak{e}(T^\theta - T_0^\theta)$ is compact thanks to the compact embedding from $H^1(D\setminus\overline{\Omega})$ to $L^2(D\setminus\overline{\Omega})$. From identity (4.34) we obtain that $\Im\mathfrak{m}(\langle T^\theta V, V\rangle) = \Im\mathfrak{m}(\langle TV, V\rangle) \geq 0$. Finally since k is not a transmission eigenvalue we can show similarly to the previous proof that $\Im\mathfrak{m}(T^\theta)$ is injective on $\overline{R(H)}$. □

We now have all the ingredients allowing to state the results of the sampling methods which is the subject of the next section.

4.4 Inversion algorithms

This section is split into two paragraphs. In the first one we reconstruct the shape of the scatterer by the use of the GLSM whose justification is straightforward from the results of the previous section. In the second one the original proof of the DLSM is adapted to fit to our setting allowing to detect sound hard defects from differential measurements.

4.4.1 Reconstruction of the background

All the results of the previous section allows to use the $F_\sharp$ method to recover the shape of the background formed by the inhomogeneous media and the sound hard obstacle. Another possibility is to use the GLSM and use the penalty term $\langle F_\sharp g, g\rangle$ since the latter is equivalent to $\|Hg\|$ according to the abstract theorem of the $F_\sharp$ method. We have chosen to rather present the GLSM with the $F_\sharp$ penalty term since it provides approximate solutions to (ITP), a key element required for the DLSM. The main ingredient of GLSM is the following theorem whose proof is classical and can easily be adapted to our setting (see for instance [29, Theorem 2.3]).

Theorem 4.4.1. *Assume that the interior transmission problem* (ITP) *is well-posed. Then*

$$z \in D \qquad \text{if and only if} \qquad \Phi_z^\infty \in R(G).$$

The particularity of the GLSM is to build an approximate solution of the far field equation $Fg \simeq \Phi_z^\infty$, obtained by the least square method with a well chosen penalization term. For the latter are defined the following operators for given $\theta \in \mathbb{R}$,

$$F_\theta = \Re\mathfrak{e}(e^{i\theta}F) + i\Im\mathfrak{m}(F) \tag{4.46}$$

and

$$F_\theta^\sharp := |\mathfrak{Re}(e^{i\theta}F)| + |\mathfrak{Im}(F)| \tag{4.47}$$

Obviously we have

$$F_\theta = H^\star T^\theta H \tag{4.48}$$

where T^θ is defined in Lemma 4.3.8. We then define the following cost functional $J^\alpha(\Phi_z^\infty, \cdot) : L^2(\mathbb{S}^{d-1}) \to \mathbb{R}$ by

$$J^\alpha(\Phi_z^\infty, g) = \alpha\langle F_\theta^\sharp g, g\rangle_{L^2(\mathbb{S}^{d-1})} + \|Fg - \Phi_z^\infty\|^2_{L^2(\mathbb{S}^{d-1})}, \quad \forall g \in L^2(\mathbb{S}^{d-1}), \tag{4.49}$$

Theorem 4.4.2 (GLSM). *Assume that k is not a transmission eigenvalue, that the index n and the parameter θ are as in Lemma 4.3.8. Let $g_z^\alpha \in L^2(\mathbb{S}^{d-1})$ be a minimizing sequence of $J^\alpha(\Phi_z^\infty, \cdot)$ such that*

$$J^\alpha(\Phi_z^\infty, g_z^\alpha) \leq \inf_g J^\alpha(\Phi_z^\infty, g) + p(\alpha), \tag{4.50}$$

where $\lim_{\alpha\to 0} \alpha^{-1}p(\alpha) = 0$. Then

- *$z \in D$ if and only if $\lim_{\alpha\to 0}\langle F_\theta^\sharp g_z^\alpha, g_z^\alpha\rangle_{L^2(\mathbb{S}^{d-1})} < +\infty$.*
- *If $z \in D$ then there exists $h \in \overline{R(H)} = \{(v_{|D\setminus\Omega}, \partial_\nu v_{|\partial\Omega})$ such that $v \in \mathscr{H}\}$ such that $\Phi_z^\infty = Gh$ and Hg_z^α converges strongly to h as $\alpha \to 0$.*

Thus the GLSM, justified by this theorem, offers a way to recover D, that is to identify the perturbation in the reference background. Note that the GLSM, contrary to the LSM, provides an exact characterization of D. However it does not give any information on the location of the obstacle Ω. We also mention that in the case where D is simply connected and $\mathfrak{Im}(n)$ is positive definite in a region of D then one can avoid the assumption on k: indeed it is shown in chapter 5 that the set of transmission eigenvalue is empty in this case.

Proof. We establish this theorem by applying the abstract result of [29, Theorem 2.10]. The latter requires that the following properties hold.

i) $F = GH$ is injective with dense range and G is compact,

ii) $F_\theta^\sharp$ factorizes as $F_\theta^\sharp = H^* T_\theta^\sharp H$ where $T_\theta^\sharp$ satisfies the coercivity property

$$\exists \mu > 0,\ \forall V \in \overline{R(H)}, \qquad |\langle T_\theta^\sharp V, V\rangle_{L^2(D\setminus\Omega)\times L^2(\Omega)}| \geq \mu \|V\|^2_{L^2(D\setminus\Omega)\times L^2(\Omega)}, \tag{4.51}$$

iii) $V \mapsto |\langle T_\theta^\sharp V, V\rangle_{L^2(D\setminus\Omega)\times L^2(\Omega)}|^{1/2}$ is uniformly convex on $\overline{R(H)}$.

Item *i)* results from the properties of G and H Propositon 4.3.5. Item *ii)* is a direct consequence of [29, Theorem 2.31] which requires some assumption on T^θ that are all gathered in Lemma 4.3.8. The last item *iii)* is deduced from *ii)* and from the fact that $T_\theta^\sharp$ is selfadjoint and coercive on $\overline{R(H)}$ (see e.g. [29]). □

Since F is compact, so does the operator $F_\theta^\sharp$ and the penalization term $\langle F_\theta^\sharp g, g\rangle_{L^2(\mathbb{S}^{d-1})}$ is then not a classical regularization term. Consequently, dealing with a noisy version F requires a particular regularization of the cost function J^α which moreover treat the fact that the corresponding $F_\theta^\sharp$ might not have the required factorization. For this aspect, we refer the reader to [10, Section 5.2].

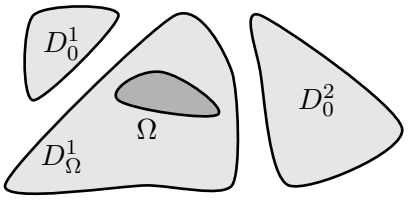

Figure 4.1: We split D into two families of connected components.

4.4.2 Identification of sound hard defects in inhomogeneities

In this paragraph is provided a method allowing to locate the position of a defect Ω, corresponding to a sound hard obstacle, in a penetrable material D. To implement this method, one requires two set of far field data at fixed frequency. The first one is measured from the flawless material and the second one from the damaged material. The theoretical foundation of this method relies on the comparison of the solution v_0 and v of the transmission problems $\mathscr{P}(D)$ and $\mathscr{P}_\Omega(D)$ defined by

$\mathscr{P}(D)$: find u_0, $v_0 \in L^2(D)$ such that $u_0 - v_0 \in H^2(D)$ and

$$\left|\begin{array}{rcll} \Delta u_0 + k^2 n u_0 & = & 0 & \text{in } D \\ \Delta v_0 + k^2 v_0 & = & 0 & \text{in } D \\ u_0 - v_0 & = & \Phi_z^\infty & \text{on } \partial D \\ \partial_\nu u_0 - \partial_\nu v_0 & = & \partial_\nu \Phi_z^\infty & \text{on } \partial D, \end{array}\right.$$

$\mathscr{P}_\Omega(D)$: find u, $v \in L^2(D)$ such that $u - v \in H^1_\Delta(D \setminus \overline{\Omega})$ and

$$\left|\begin{array}{rcll} \Delta u + k^2 n u & = & 0 & \text{in } D \setminus \overline{\Omega} \\ \Delta v + k^2 v & = & 0 & \text{in } D \\ \partial_\nu^+ u & = & 0 & \text{on } \partial\Omega \\ u - v & = & \Phi_z^\infty & \text{on } \partial D \\ \partial_\nu u - \partial_\nu v & = & \partial_\nu \Phi_z^\infty & \text{on } \partial D. \end{array}\right.$$

We distinguish the components of D which contains the obstacle Ω with the following notations: the ones containing obstacles are listed by $(D_\Omega^j)_j$; the other components are listed by $(D_0^j)_j$. We finally set $D_\Omega := \cup_j D_\Omega^j$ and $D_0 := \cup_j D_0^j$ so that $D = D_\Omega \cup D_0$. In figure 4.1 is illustrated an example of setting in the two dimensional case.

Theorem 4.4.3. *Assume that k^2 is not a Neumann eigenvalue for $-n^{-1}\Delta$ in Ω and is such that both $\mathscr{P}(D)$ and $\mathscr{P}_\Omega(D)$ are well-posed.*

i) If $z \in D_0$ then $v = v_0$ in D. *ii) If $z \in D_\Omega$ then $v \neq v_0$ in D_Ω.*

Proof. *i)* Let $z \in D_0$, since the equations for $\mathscr{P}(D)$ and $\mathscr{P}_\Omega(D)$ coincide on D_0 and are uniquely solvable, we deduce that $v = v_0$ in D_0. Moreover the solution to both problems $\mathscr{P}(D)$ and $\mathscr{P}_\Omega(D)$ is given by the pair $(0, -\Phi_z^\infty)$ on D_Ω. Consequently $v = v_0 = -\Phi_z^\infty$ in D_Ω.
ii) Now let $z \in D_\Omega$, we prove the second assertion by using a contradiction argument. Assume that $v = v_0$ in D_Ω. Define U such that $U = u - u_0$ in $D_\Omega \setminus \overline{\Omega}$ and $U = 0$ in $\mathbb{R}^d \setminus D_\Omega$. Since $U = \partial_\nu U = 0$ on ∂D_Ω, from the unique continuation principle, we obtain $U = 0$ in $\mathbb{R}^d \setminus \overline{\Omega}$ and then $\partial_\nu u_0 = \partial_\nu u = 0$ on $\partial\Omega$. Since we assumed that k is not a Neumann eigenvalue for $-n^{-1}\Delta$ in Ω, we deduce that $u_0 = 0$ in Ω, and by unique continuation, $u_0 = 0$ in D_Ω. Thus we must have $v_0 = -\Phi_z^\infty$ in D_Ω which contradicts the fact that $u_0 - v_0 \in H^2(D)$. □

Now we consider a first heterogeneous medium without obstacle with a perturbation of the reference background supported in $\overline{D}$ modeled by some index n, and a second medium with the same refractive index n but with an additional sound hard obstacle inside D. The corresponding far field operators are denoted respectively F_0 and F_1. Then for $j = 0, 1$, let $g_{j,z}^\alpha$ refer to the sequences introduced in the statement of Theorem 4.4.2 with $F_j^\sharp = |\frac{1}{2}(F_j + F_j^*)| + |\frac{1}{2i}(F_j - F_j^*)|$

(corresponding with $\theta = 0$. We also set for $j = 0, 1$

$$\mathcal{A}_j^\alpha(z) = \langle F_j^\sharp g_{j,z}^\alpha, g_{j,z}^\alpha \rangle_{L^2(\mathbb{S}^{d-1})};\ \mathcal{D}_j^\alpha(z) = \langle F_j^\sharp (g_{1,z}^\alpha - g_{0,z}^\alpha), (g_{1,z}^\alpha - g_{0,z}^\alpha) \rangle_{L^2(\mathbb{S}^{d-1})}. \tag{4.52}$$

The combination of Theorem 4.4.2 and 4.4.3 leads to the following result.

Theorem 4.4.4 (DLSM)**.** *Assume that k, n are as in Theorem 4.4.3 and that n also satisfies the assumptions of Theorem 4.4.2. Then for $j = 0$ or 1*

$$\big[\, z \in D_0 \,\big] \Rightarrow \big[\, \lim_{\alpha \to 0} \mathcal{D}_j^\alpha(z) = 0 \,\big] \quad \text{and} \quad \big[z \in D_\Omega \big] \Rightarrow \big[0 < \lim_{\alpha \to 0} \mathcal{D}_j^\alpha(z) < +\infty \big].$$

Proof. As explained in the proof of Theorem 4.4.2, $F_1^\sharp$ admits a factorization of the form $H^* T_1^\sharp H$ where $T_1^\sharp$ is bounded and $\langle T_1^\sharp \cdot, \cdot \rangle$ is coercive. According to the study of obstacle-free inhomogeneous medium a same factorization stands for F_0 involving an operator $T_0^\sharp$ that have the same properties of $T_1^\sharp$. This implies (for $j = 0$ or 1) the existence of two positive constants κ and K such that

$$\kappa \| H(g_{1,z}^\alpha - g_{0,z}^\alpha) \|_{L^2(D)}^2 \le \mathcal{D}_j^\alpha(z) \le K \| H(g_{1,z}^\alpha - g_{0,z}^\alpha) \|_{L^2(D)}^2. \tag{4.53}$$

Now for $z \in D$, if we denote (u_0, v_0) (resp. (u_1, v_1)) the solution of $\mathscr{P}(D)$ (resp. $\mathscr{P}_\Omega(D)$), then Theorem 4.4.2 and the GLSM for the obstacle-free inhomogeneous medium (see the justification in [29]) guarantee that $\lim_{\alpha \to 0} \| H(g_{1,z}^\alpha - g_{0,z}^\alpha) \| = \| H(v - v_0) \|$. Then the result follows from Theorem 4.4.3. □

From Theorems 4.4.2 and 4.4.4, one can design indicators for D and D_Ω.

$$I^{\mathrm{GLSM}}(z) = \lim_{\alpha \to 0} \frac{1}{\mathcal{A}_1^\alpha(z)} \quad \text{and} \quad I^{\mathrm{DLSM}}(z) = \lim_{\alpha \to 0} \frac{1}{\mathcal{A}_0^\alpha(z) \Big(1 + \frac{\mathcal{A}_0^\alpha(z)}{\mathcal{D}^\alpha(z)} \Big)}. \tag{4.54}$$

For these indicators, one can show the following result which allows one to identify the connected components of D in which some obstacles have appeared.

Corollary 4.4.5. *Under the assumptions of Theorem 4.4.4, we have*

- $I^{\mathrm{GLSM}}(z) = 0$ *in* $\mathbb{R}^d \setminus D$ *and* $I^{\mathrm{GLSM}}(z) > 0$ *in* D.
- $I^{\mathrm{DLSM}}(z) = 0$ *in* $\mathbb{R}^d \setminus D_\Omega$ *and* $I^{\mathrm{DLSM}}(z) > 0$ *in* D_Ω.

4.5 Numerical results

To conclude this chapter, we apply the GLSM and the DLSM on synthetic data computed from numerical approximations of the scattering problems. All simulated backgrounds have in the examples below the same shape D constituted of three disjoint disks of radi 0.75 and of refractive index $n = 1.5$. They differ from one to another in the distribution of obstacles inside the disks. For each background we generate a discretization of the far field operator F by solving numerically the direct problem for multiple incident fields $u_i(\theta_p)$ with wave number $k = 4\pi$. Then we compute the matrix $F = (u_s^\infty(\theta_p, \widehat{x_q}))_{p,q}$ for θ_p, $\widehat{x_q}$ in $\{\cos(\frac{2l\pi}{100}), \sin(\frac{2l\pi}{100}),\ l = 1..100\}$ (somehow we discretize $L^2(\mathbb{S}^1)$). Finally, we add random noise to the simulated F and obtain our final synthetic far field data F^δ with $F_{pq}^\delta = F_{pq}(1 + \sigma N)$. Here N is a complex random variable whose real and imaginary parts are uniformly chosen in $[-1, 1]^2$. The parameter $\sigma > 0$ is chosen so that $\| F^\delta - F \| = 0.05 \| F^\delta \|$.

To handle the noise δ added on the far field data, we use a regularized version of the GLSM consisting in finding the minimizers $g_z^{\alpha,\delta}$ of the functional

$$g \mapsto J^{\alpha,\delta}(\Phi_z^\infty, g) = \alpha(|\langle F^{\sharp\delta} g, g\rangle_{L^2(\mathbb{S}^{d-1})}| + \delta\|F^\delta\|\|g\|^2_{L^2(\mathbb{S}^2)}) + \|F^\delta g - \Phi_z^\infty\|^2_{L^2(\mathbb{S}^{d-1})},$$

where $F^{\sharp\delta} := |\frac{1}{2}(F^\delta + F^{\delta *})| + |\frac{1}{2i}(F^\delta - F^{\delta *})|$. We fit α to δ according to [10, Section 5.2]. The new relevant indicator function for the regularized GLSM is then given by

$$I^{\alpha,\delta}_{\mathrm{GLSM}}(z) = \frac{1}{\mathcal{A}^{\alpha,\delta}(z)}$$

where $\mathcal{A}^{\alpha,\delta}(z) = \langle F^{\sharp\delta} g_z^{\alpha,\delta}, g_z^{\alpha,\delta}\rangle_{L^2(\mathbb{S}^{d-1})} + \delta\|F^\delta\|\|g_z^{\alpha,\delta}\|^2_{L^2(\mathbb{S}^{d-1})}$.

Fig. 4.2 shows the results of GLSM indicator function $z \mapsto I^{\alpha,\delta}_{\mathrm{GLSM}}(z)$ for two different configurations where the second one is obtained from the first one by adding a defect to the third component. The two other components contain the same defect. One observes that GLSM is capable of retrieving the domain D for each configuration. We also observe how the behavior of the indicator function is different inside the third component. This is somehow what the DLSM exploits to isolate the component where a defect appears and this is what is discussed next.

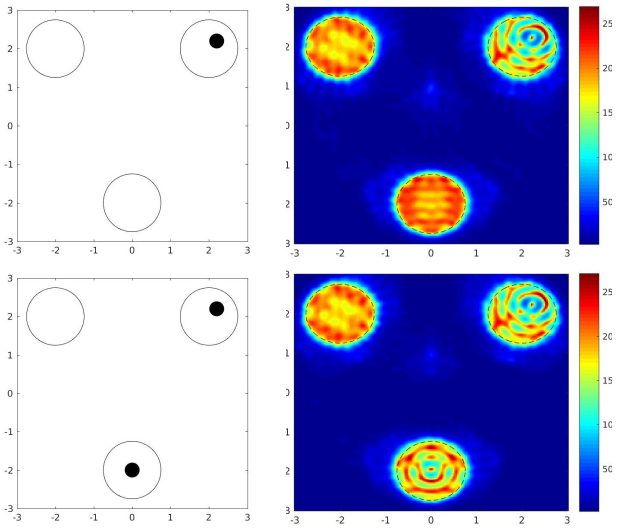

Figure 4.2: Simulated backgrounds on the left and associated GLSM indicator function $z \mapsto I^{\alpha,\delta}_{\mathrm{GLSM}}(z)$ on the right.

Given two far field data F_0^δ and F_1^δ, we respectively define $F_0^{\sharp\delta}$, $g_{0,z}^{\alpha,\delta}$, $\mathcal{A}_0^{\alpha,\delta}(z)$ and $F_1^{\sharp\delta}$, $g_{1,z}^{\alpha,\delta}$, $\mathcal{A}_1^{\alpha,\delta}(z)$ associated to each data as described in the previous paragraph. We also define

$$\mathcal{D}^{\alpha,\delta}(z) = \langle F_0^\sharp(g_{1,z}^{\alpha,\delta} - g_{0,z}^{\alpha,\delta}), (g_{1,z}^{\alpha,\delta} - g_{0,z}^{\alpha,\delta})\rangle_{L^2(\mathbb{S}^{d-1})}.$$

Then, according to (4.54), the DLSM indicator is given by

$$I^{\alpha,\delta}_{\mathrm{DLSM}}(z) = \frac{1}{\mathcal{A}_0^{\alpha,\delta}(z)\left(1 + \frac{\mathcal{A}_0^{\alpha,\delta}(z)}{\mathcal{D}^{\alpha,\delta}(z)}\right)}.$$

The behavior of the DLSM indicator function is illustrated below for several scenarios. In each figure is presented from left to right, the initial background (associated with F_0^δ), the damaged background (associated with F_1^δ) and the DLSM indicator function $z \mapsto I^{\alpha,\delta}_{\mathrm{DLSM}}(z)$. As expected,

the latter allows us to identify for all scenarios the component(s) D_Ω where (additional) defects appeared. We also remark that it slightly accentuates the border of D_0. But this effect is not explained by our theory and it does not contradict it: Our theoretical result does not stipulate that the indicator function is "uniformly" close to 0 outside D_Ω.

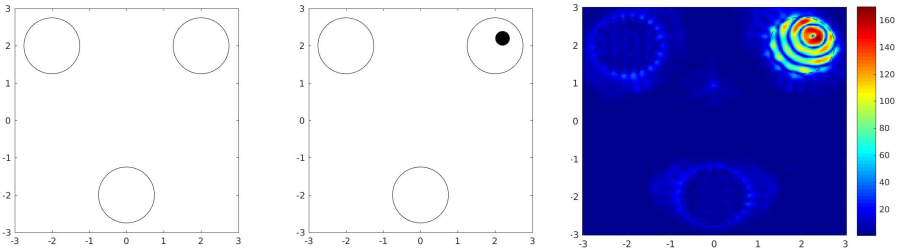

Figure 4.3: A scenario for DLSM simulating the emergence of a defect in one component of a healthy background.

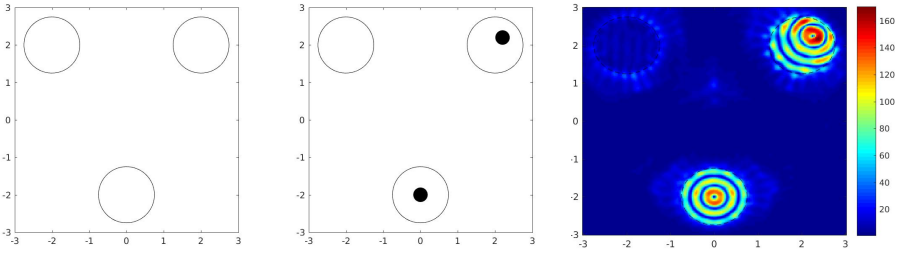

Figure 4.4: A scenario for DLSM simulating the emergence of a defect in two components of a healthy background.

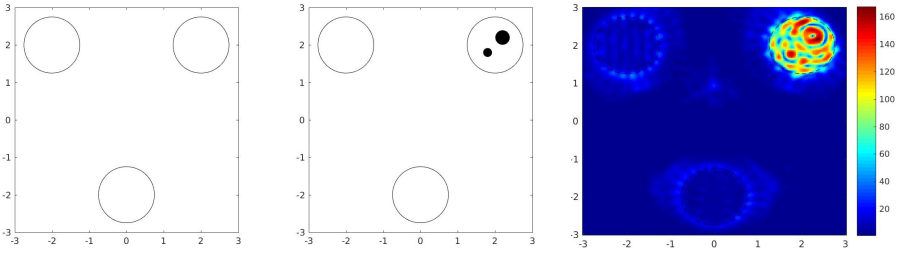

Figure 4.5: A scenario for DLSM simulating the emergence of two defects in one component of a healthy background.

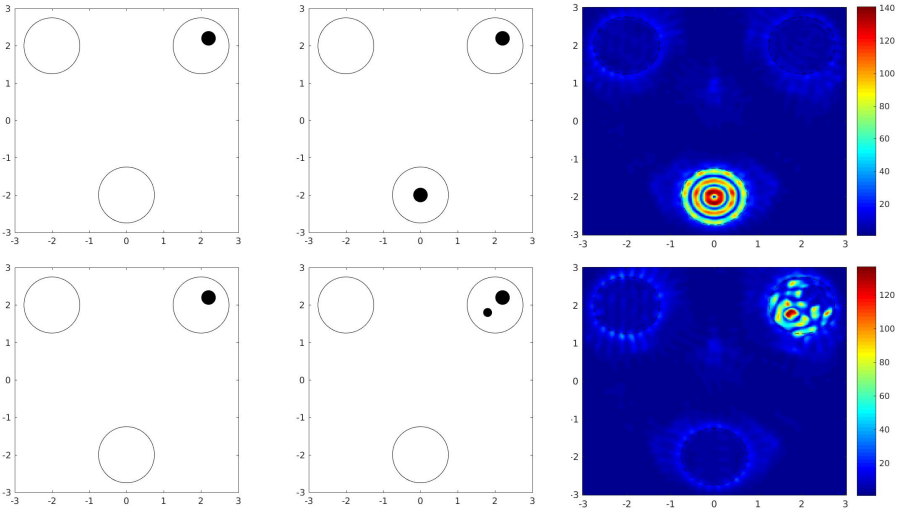

Figure 4.6: Two scenarios for DLSM simulating the emergence of a defect in one component of an already damaged material.

Chapter 5

The interior transmission problem for inhomogeneities with sound hard inclusions

Contents

5.1 Introduction

In this chapter is studied the interior transmission problem for isotropic inhomogeneities containing sound hard obstacles. This chapter differs from chapter 3 in that the obstacles considered are now of non empty interior. We investigate the classical issues related to the study of interior transmission problems that are the Fredholm property, the discreteness of the set of transmission eigenvalues and the existence of positive transmission eigenvalues. The first approach we consider relies a fourth order formulation of the interior transmission problem. This approach has been introduced in [113] for the study of isotropic inhomogeneities and has been successfully used in many other works [33, 34, 104, 32]. However we have encountered several difficulties with this approach. Finding the right weak formulation has not been easy and we have been compelled to set a variational space which depends on the parameter k. We treated this situation by adapting the works [26] which first introduced such formulations when studying the ITP with cavities. We notice that such difficulty did not arise in the study of ITP related to inhomogeneities with

sound soft inclusions inside [32]. The developed framework allows us to prove that the set of TEs is at most discrete, but only if the inclusion is big enough and provided that the refractive index n satisfies $n > 1$. However we could not conclude about the existence of TEs with this framework and we explain why our various attempts failed. We propose another approach in order to relax the assumption on n and remove the condition on the size of the inclusion to obtain the discreteness of the set of TEs. The latter approach relies on the properties of the Dirichlet-to-Neumann operator.

5.2 Setting of the problem and notations

In this section we recall the Interior Transmission Problem (ITP) in the case of an inhomogeneous isotropic medium with Neumann obstacle inside and define a suitable space for the solutions. For more details on the link between the (ITP) and the scattering problem, we refer to chapter 4. We consider an inhomogeneity delimited by a set $D \subset \mathbb{R}^d$, with $d = 2, 3$. The impenetrable obstacle is materialized by a subset $\overline{\Omega} \subset D$. The set D is assumed to be a connected bounded domain of Lipschitz boundary and Ω is a domain of Lipschitz boundary which can possibly be multiply connected. The refractive index n is a complex valued function which is only defined on $D \setminus \overline{\Omega}$. We assume that $n \in L^\infty(D \setminus \overline{\Omega})$ and satisfies $\Im\mathfrak{m}(n) \geq 0$. The ITP is the following: for given $f \in H^{\frac{1}{2}}(\partial D)$ and $g \in H^{-\frac{1}{2}}(\partial D)$, find $(u, v) \in L^2(D \setminus \overline{\Omega}) \times L^2(D)$ with $u - v \in \{\varphi \in H^1(D \setminus \overline{\Omega}) \,|\, \Delta\varphi \in L^2(D \setminus \overline{\Omega})\}$ such that

$$\left|\begin{array}{rcll} \Delta u + k^2 n\, u &=& 0 & \text{in } D \setminus \overline{\Omega} \\ \Delta v + k^2\, v &=& 0 & \text{in } D \\ \partial_\nu u &=& 0 & \text{on } \partial\Omega. \end{array}\right. \qquad \left|\begin{array}{rcll} u - v &=& f & \text{on } \partial D \\ \partial_\nu u - \partial_\nu v &=& g & \text{on } \partial D \end{array}\right. \tag{ITP}$$

The chosen space for u and v is classical since it is known that there exist solutions to ITP which have only L^2 regularity. The one for $w := u - v$ is less classical, but it is the most we can expect from the variational regularity of w. In this chapter, we will use the following notation for a given bounded domain $X \subset \mathbb{R}^d$,

$$H^1_\Delta(X) = \{\varphi \in H^1(X) \,|\, \Delta\varphi \in L^2(X)\}. \tag{5.1}$$

We define ν as the unit outward normal vector to ∂D and $\partial\Omega$. We will be considering traces on both sides of $\partial\Omega$ and introduce the following notation whenever they make sense for a given function ψ,

$$\forall x \in \partial\Omega, \quad \psi^\pm(x) = \lim_{h \to 0^+} \psi(x \pm h\nu(x)) \quad \text{and} \quad \partial_\nu^\pm \psi(x) = \lim_{h \to 0^+} \nu(x).\nabla\psi(x \pm h\nu(x)),$$

so that the upscript $+$ (resp. $-$) corresponds to the outside trace (resp. inside trace) on $\partial\Omega$. We also define the jumps of ψ on $\partial\Omega$ by

$$[\psi] := \psi^+ - \psi^- \quad \text{and} \quad \left[\frac{\partial\psi}{\partial\nu}\right] := \partial_\nu^+\psi - \partial_\nu^-\psi.$$

5.3 The fourth order equation approach

5.3.1 Reformulation of the problem

We now write a weak formulation of (ITP) by deriving a fourth order formulation for w. It consists in rewriting the problem only in terms of $w = u - v$. To do so, we assume from now

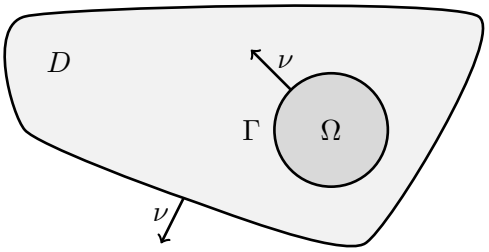

Figure 5.1: Sketch of the domain in $\mathbb{R}^2$.

on that the coefficient n satisfies $\frac{1}{n-1} \in L^\infty(D \setminus \overline{\Omega})$. Then subtracting the second equation from the first in (ITP) gives the following equation for w in $D \setminus \overline{\Omega}$:

$$-\frac{1}{k^2(n-1)}(\Delta + k^2 n)w = v \quad \text{in} \quad D \setminus \overline{\Omega}. \tag{5.2}$$

Then by using the equation on v is derived the fourth order equation, namely

$$(\Delta + k^2)(n-1)^{-1}(\Delta + k^2 n)w = 0 \quad \text{in} \quad D \setminus \overline{\Omega} \tag{5.3}$$

together with the boundary conditions

$$w = f \text{ on } \partial D \qquad \text{and} \qquad \partial_\nu w = g \text{ on } \partial D. \tag{5.4}$$

Note that if w is known in $D \setminus \overline{\Omega}$ then v and u can be retrieved in $D \setminus \overline{\Omega}$ from equations (5.2) and $u = w + v$. Hence it remains to take into account the unknown v in Ω. To this end, let us extend w in Ω by

$$w := -v \text{ in } \Omega.$$

Then w satisfies

$$\Delta w + k^2 w = 0 \text{ in } \Omega, \tag{5.5}$$

and the Neumann boundary conditions on $\partial\Omega$ can be reformulated as

$$\partial_\nu^+ w = \partial_\nu^- w \text{ on } \partial\Omega, \tag{5.6}$$

and the jump conditions $[v] = 0$, $[\partial_\nu v] = 0$ on $\partial\Omega$ can be expressed in terms of w thanks to relation (5.2) as

$$\left(\frac{1}{k^2(n-1)}(\Delta + k^2 n)w\right)^+ = w^- \quad \text{and} \quad \partial_\nu^+ \left(\frac{1}{k^2(n-1)}(\Delta + k^2 n)w\right) = \partial_\nu^- w. \tag{5.7}$$

The derived equations fully describe (ITP) in terms of w; it can be shown that if $w \in H^1_\Delta(D \setminus \overline{\Omega}) \times H^1_\Delta(\Omega)$ is a solution to (5.3)-(5.7), then (u, v) defined by

$$v = \begin{cases} \frac{-1}{k^2(n-1)}(\Delta w + k^2 n w) & \text{in} \quad D \setminus \overline{\Omega} \\ -w & \text{in} \quad \Omega \end{cases} \qquad \text{and} \qquad u = w + v \text{ in } D \setminus \overline{\Omega}, \tag{5.8}$$

is a solution to (ITP).

5.3.2 Variational formulation

The variational formulation we propose is based on the equations (5.3)-(5.7). The need to include (5.5) in the variational space, unlike what has been proposed in the study of the ITP for inhomogeneities with sound soft obstacles [32], is precised below. We define the variational space as follows,

$$V_k = \{\varphi \in H^1_\Delta(D \setminus \overline{\Omega}) \times H^1_\Delta(\Omega) \text{ such that } \Delta\varphi + k^2\varphi = 0 \text{ in } \Omega, \\ \varphi = \frac{\partial \varphi}{\partial \nu} = 0 \text{ on } \partial D \text{ and } [\frac{\partial \varphi}{\partial \nu}] = 0 \text{ on } \partial\Omega\}.$$

Note that V_k depends on k. V_k is equipped with the induced scalar product of $H^1_\Delta(D\setminus\overline{\Omega})\times H^1_\Delta(\Omega)$:

$$\langle \psi, \varphi\rangle_V = \int_D \psi\overline{\varphi}\,\mathrm{d}x + \int_{D\setminus\partial\Omega} \nabla\psi\nabla\overline{\varphi}\,\mathrm{d}x + \int_{D\setminus\partial\Omega} \Delta\psi\Delta\overline{\varphi}\,\mathrm{d}x, \tag{5.9}$$

and is a Hilbert space for the associated norm $\|\cdot\|_V = \sqrt{\langle\cdot,\cdot\rangle_V}$.

To simplify the computations while deriving the variational formulation, we have chosen to start with the equation on v, namely $\Delta v + k^2 v = 0$ on D. The function v will be replaced afterwards by a quantity depending on w given by relation (5.2). Let $\varphi \in V_k$, integrating the mentioned equation for v against $\overline{\varphi}$ and applying Green's second formula gives

$$\begin{aligned} 0 &= \int_{D\setminus\overline{\Omega}} v(\Delta\overline{\varphi} + k^2\overline{\varphi})\,\mathrm{d}x - \int_{\partial\Omega} \partial_\nu^+ v\overline{\varphi}^+\,\mathrm{ds}(x) + \int_{\partial\Omega} v^+\partial_\nu^+\overline{\varphi}\,\mathrm{ds}(x) \\ &= \int_{D\setminus\overline{\Omega}} v(\Delta\overline{\varphi} + k^2 n\overline{\varphi})\,\mathrm{d}x - k^2\int_{D\setminus\overline{\Omega}} (n-1)v\overline{\varphi}\,\mathrm{d}x - \int_{\partial\Omega} \partial_\nu^+ v\overline{\varphi^+}\,\mathrm{ds}(x) + \int_{\partial\Omega} v^+\partial_\nu^+\overline{\varphi}\,\mathrm{ds}(x). \end{aligned} \tag{5.10}$$

We now treat the terms of (5.10) separately. For the first term we use (5.2) to obtain

$$\int_{D\setminus\overline{\Omega}} v(\Delta\overline{\varphi} + k^2 n\overline{\varphi})\,\mathrm{d}x = \int_{D\setminus\overline{\Omega}} \frac{-1}{k^2(n-1)}(\Delta w + k^2 n w)(\Delta\overline{\varphi} + k^2 n\overline{\varphi})\,\mathrm{d}x. \tag{5.11}$$

For the second and third terms of (5.10) we use relation (5.2) and then Green's first formula gives

$$\begin{aligned} -k^2\int_{D\setminus\overline{\Omega}} (n-1)v\overline{\varphi}\,\mathrm{d}x - \int_{\partial\Omega} \partial_\nu^+ v\overline{\varphi^+}\,\mathrm{ds}(x) &= \int_{D\setminus\overline{\Omega}} (\Delta w + k^2 n w)\overline{\varphi}\,\mathrm{d}x - \int_{\partial\Omega} \partial_\nu^+ v\overline{\varphi^+}\,\mathrm{ds}(x) \\ &= -\int_{D\setminus\overline{\Omega}} \nabla w\nabla\overline{\varphi}\,\mathrm{d}x + k^2\int_{D\setminus\overline{\Omega}} nw\overline{\varphi}\,\mathrm{d}x - \int_{\partial\Omega} (\partial_\nu^+ v + \partial_\nu^+ w)\overline{\varphi^+}\,\mathrm{ds}(x). \end{aligned} \tag{5.12}$$

In the previous equation, the last sum on $\partial\Omega$ is zero because of the Neumann boundary conditions $\partial_\nu^+ w + \partial_\nu^+ v = 0$ on $\partial\Omega$. We finally treat the last term of (5.10). It is this term that led us to impose that the test functions satisfy the Helmholtz equation in Ω so one can simplify it as follows,

$$\int_{\partial\Omega} v^+\partial_\nu^+\overline{\varphi}\,\mathrm{ds}(x) = \int_{\partial\Omega} v^-\partial_\nu^-\overline{\varphi}\,\mathrm{ds}(x) = \int_\Omega \nabla v\nabla\overline{\varphi}\,\mathrm{d}x - k^2\int_\Omega v\overline{\varphi}\,\mathrm{d}x. \tag{5.13}$$

As mentioned, we chose to extend the unknown w by $-v$ in Ω. Using this relation in the previous equation gives

$$\int_{\partial\Omega} v^+ \partial_\nu^+ \overline{\varphi}\,\mathrm{ds}(x) = -\int_\Omega \nabla w \nabla\overline{\varphi}\,\mathrm{d}x + k^2\int_\Omega w\overline{\varphi}\,\mathrm{d}x. \tag{5.14}$$

Combining (5.11), (5.12) and (5.14) in (5.10) gives after multiplying by $-k^2$

$$\int_{D\setminus\overline{\Omega}} \frac{1}{n-1}(\Delta w + k^2 n w)(\Delta\overline{\varphi} + k^2 n\overline{\varphi})\,\mathrm{d}x + k^2\int_{D\setminus\partial\Omega} \nabla w\nabla\overline{\varphi}\,\mathrm{d}x - k^4\int_{D\setminus\overline{\Omega}} nw\overline{\varphi}\,\mathrm{d}x - k^4\int_\Omega w\overline{\varphi}\,\mathrm{d}x = 0. \tag{5.15}$$

Now let $\theta \in H^2(D)$ be a lifting function such that $\theta = f$, $\partial_\nu\theta = g$ on ∂D and $\theta = 0$ in a neighborhood of Ω. We moreover choose θ such that

$$\|\theta\|_{H^2(D)} \le C\left(\|f\|_{H^{\frac{3}{2}}(\partial D)} + \quad \|g\|_{H^{\frac{1}{2}}(\partial D)}\right). \tag{5.16}$$

where C is a positive constant. Finally, we obtain the following variational formulation dealing with $w_0 = w - \theta \in V_k$. For given $\theta \in H^2(D)$ compactly supported in $D\setminus\overline{\Omega}$, find $w_0 \in V_k$ such that $\forall\varphi \in V_k$,

$$\begin{aligned}&\int_{D\setminus\overline{\Omega}} (n-1)^{-1}(\Delta w_0 + k^2 n w_0)(\Delta\overline{\varphi} + k^2 n\overline{\varphi})\,\mathrm{d}x + k^2\int_{D\setminus\partial\Omega} \nabla w_0\nabla\overline{\varphi}\,\mathrm{d}x - k^4\int_{D\setminus\overline{\Omega}} nw_0\overline{\varphi}\,\mathrm{d}x - k^4\int_\Omega w_0\overline{\varphi}\,\mathrm{d}x\\ &= \int_{D\setminus\overline{\Omega}} (n-1)^{-1}(\Delta\theta + k^2 n\theta)(\Delta\overline{\varphi} + k^2 n\overline{\varphi})\,\mathrm{d}x + k^2\int_{D\setminus\overline{\Omega}} \nabla\theta\nabla\overline{\varphi}\,\mathrm{d}x - k^4\int_{D\setminus\overline{\Omega}} n\theta\overline{\varphi}\,\mathrm{d}x.\end{aligned} \tag{5.17}$$

The next theorem gives a first result on the equivalence between the well posedeness of (ITP) and the variational formulation. It requires k^2 not to be a Neumann eigenvalue for $-\Delta$ in Ω for relations (5.8) between the weak solution w and the classical solutions (u, v) of (ITP) to be valid. This assumption will be dropped in a second step by adding a correction term in the definition of v.

Theorem 5.3.1.

- *If (u, v) is a solution to (ITP), then w_0 defined by*

$$w_0 = u - v - \theta \quad in \quad D\setminus\overline{\Omega} \qquad and \qquad w_0 = -v - \theta \quad in \quad \Omega \tag{5.18}$$

  is a solution to (5.17).

- *Assume that k^2 is not a Neumann eigenvalue for $-\Delta$ in Ω. Let w_0 be a solution to (5.17) and set $w = w_0 + \theta$. Then (u, v) defined by*

$$v = \begin{cases} \frac{-1}{k^2(n-1)}(\Delta w + k^2 n w) & in \quad D\setminus\overline{\Omega} \\ -w & in \quad \Omega \end{cases} \qquad and \qquad u = w + v \ in\ D\setminus\overline{\Omega}, \tag{5.19}$$

  is a solution to (ITP).

Proof. We only need to prove the second point of the theorem. Let w_0 be a solution of (5.17) and define $w := w_0 + \theta$. Since any $\varphi \in C_c^\infty(D\setminus\overline{\Omega})$ extended by zero in Ω is an element of V_k, we obtain by using this class of test functions in (5.17) that

$$\varphi \in C_c^\infty(D\setminus\overline{\Omega}), \quad \int_{D\setminus\overline{\Omega}} (\Delta + k^2)(n-1)^{-1}(\Delta + k^2 n)w\overline{\varphi}\,\mathrm{d}x = 0.$$

Then w satisfies $(\Delta + k^2)(n-1)^{-1}(\Delta + k^2 n)w = 0$ in $D \setminus \overline{\Omega}$ in the distributional sense. Consequently $v \in L^2(D)$ defined by (5.19) satisfies Helmholtz equation in $D \setminus \overline{\Omega}$ but also in Ω because of the definition of the variational space. We now show that v is a global solution of Helmholtz equation in D. To this end we show that $[v] = 0$ and $[\partial_\nu v] = 0$ on $\partial\Omega$. After integrating by parts in (5.17), it is obtained that for all $\varphi \in V_k$,

$$\left\langle \partial_\nu^+ \left(\frac{1}{n-1}(\Delta w + k^2 n w) \right) - k^2 \partial_\nu^- w, \varphi^+ \right\rangle_{H^{-\frac{1}{2}}(\partial\Omega)\times H^{\frac{1}{2}}(\partial\Omega)} - \left\langle \left(\frac{1}{n-1}(\Delta w + k^2 n w) \right)^+ - k^2 w^-, \partial_\nu^+ \varphi \right\rangle_{H^{\frac{1}{2}}(\partial\Omega)\times H^{-\frac{1}{2}}(\partial\Omega)} = 0. \quad (5.20)$$

With test functions φ satisfying $\varphi_{|\Omega} = 0$ we obtain, since $\partial_\nu \varphi_{|\partial\Omega} = 0$ for such φ, that the first term of (5.20) is zero for arbitrary $\varphi^+ \in H^{\frac{1}{2}}(\partial\Omega)$. Consequently

$$\partial_\nu^- w = \partial_\nu^+ \left(\frac{-1}{k^2(n-1)}(\Delta w + k^2 n w) \right) \text{ on } \partial\Omega. \quad (5.21)$$

Then equation (5.20) becomes

$$\forall \varphi \in V_k, \quad \int_{\partial\Omega} \left\{ \left(\frac{1}{n-1}(\Delta w + k^2 n w) \right)^+ - k^2 w^- \right\} \partial_\nu^+ \overline{\varphi} \, \mathrm{ds}(x) = 0, \quad (5.22)$$

and the hypothesis on k allows one to choose for $\partial_\nu^+ \varphi$ any element of $H^{-\frac{1}{2}}(\partial\Omega)$. As a consequence we obtain

$$w^- = \left(\frac{-1}{k^2(n-1)}(\Delta w + k^2 n w) \right)^+ \text{ on } \partial\Omega. \quad (5.23)$$

Equations (5.21) and (5.23) imply the desired result for v. Then u defined by (5.19) is easily seen to satisfy the equation $\Delta u + k^2 n u = 0$ on $D \setminus \overline{\Omega}$. □

Now we make more precise the second point of Theorem 5.3.1 in the case where k^2 is a Neumann eigenvalue for $-\Delta$ in Ω. We first prove the following lemma.

Lemma 5.3.2. *Assume that k^2 is a Neumann eigenvalue for $-\Delta$ in Ω of multiplicity $N \in \mathbb{N}^*$. The associated basis of eigenfunctions is denoted $\varphi_1, \ldots, \varphi_N \in H^1(\Omega)$. Let $\gamma \in H^{\frac{1}{2}}(\partial\Omega)$ and assume that*

$$\forall \varphi \in H^1(\Omega) \text{ such that } \Delta\varphi + k^2\varphi = 0 \text{ in } \Omega, \ \gamma \text{ satisfies } \int_{\partial\Omega} \partial_\nu \varphi(y)\gamma(y) \, \mathrm{ds}(y) = 0. \quad (5.24)$$

Then $\gamma \in \mathrm{span}(\varphi_{1|\partial\Omega}, \ldots, \varphi_{N|\partial\Omega})$.

Proof. Denoting $\Phi(x, y)$ the fundamental solution to the Helmholtz equation, we consider for $x \in \mathbb{R}^d \setminus \partial\Omega$ the double layer potential

$$w(x) = \int_{\partial\Omega} \partial_\nu \Phi(x, y)\gamma(y) \, \mathrm{ds}(y). \quad (5.25)$$

We recall that the double layer potential satisfies the Helmholtz equation in $\mathbb{R}^d \setminus \partial\Omega$ and the following jump relations [99, Theorem 6.11],

$$[w] = \gamma \quad \text{and} \quad [\partial_\nu w] = 0 \text{ on } \partial\Omega. \tag{5.26}$$

Since for all $x \in \mathbb{R}^d \setminus \overline{\Omega}$, $\Phi(x, \cdot)$ satisfies Helmholtz equation in Ω we deduce with assumption (5.24) that w vanishes in $\mathbb{R}^d \setminus \overline{\Omega}$. Then (5.26) implies that $\partial_\nu w = 0$ on $\partial\Omega$ and therefore w is an eigenfunction of $-\Delta$ in Ω with Neumann boundary condition. Consequently $w \in \text{span}(\varphi_1, \dots, \varphi_N)$ in Ω, and in $\gamma = -w_{|\partial\Omega} \in \text{span}(\varphi_{1|\partial\Omega}, \dots, \varphi_{N|\partial\Omega})$. □

The following theorem is a generalization of Theorem 5.3.1.

Theorem 5.3.3. *Assume that k^2 is a Neumann eigenvalue for $-\Delta$ in Ω. Then with the same notation as in Lemma 5.3.2 we have the following result. Let w_0 be a solution of (5.17) and set $w = w_0 + \theta$. Then there exists $(\alpha_1, \dots, \alpha_N) \in \mathbb{R}^N$ which is uniquely determined such that (u, v) defined by*

$$v = \begin{cases} \frac{-1}{k^2(n-1)}(\Delta w + k^2 n w) & \text{in} \quad D \setminus \overline{\Omega} \\ -w + \sum_{i=1}^{N} \alpha_i \varphi_i & \text{in} \quad \Omega \end{cases} \qquad \text{and} \qquad u = w + v \text{ in } D \setminus \overline{\Omega}, \tag{5.27}$$

is a solution to (ITP).

Proof. We can repeat the proof of Theorem 5.3.1 up to equation (5.22). Applying Lemma 5.3.2 gives the existence of $\alpha_1, \dots, \alpha_N \in \mathbb{R}$ such that

$$\left(\frac{-1}{k^2(n-1)}(\Delta w + k^2 n w) \right)^+ = -w^- + \sum_{i=1}^{N} \alpha_i \varphi_i \text{ on } \partial\Omega \tag{5.28}$$

The α_i are uniquely defined since the $(\varphi_i)_{1 \le i \le N}$ are linearly independent. Since $\partial_\nu \varphi_i = 0$ on $\partial\Omega$, v defined by (5.27) is guaranteed to be a global solution to the Helmholtz homogeneous equation in D. Once again we easily check that u satisfies $\Delta u + k^2 n u = 0$ in $D \setminus \overline{\Omega}$. □

5.3.3 Fredholm property of the interior transmission problem

We now show that the interior transmission problem satisfies the Fredholm property, that is uniqueness of solutions for any (f, g) implies existence of solution for any (f, g). By linearity of the problem (ITP), if (u, v) and (u', v') are solutions then $(u - u', v - v')$ is a solution with zero right hand side (i.e $f = g = 0$), hence with the following definition it is equivalent to say that the problem is injective or that k is not a transmission eigenvalue.

Definition 5.3.4. *Values of $k > 0$ for which the interior transmission problem (ITP) with $f = g = 0$ has non trivial solutions are called transmission eigenvalues.*

Using the Riesz representation theorem we define the two following operators $\mathbb{A}_k$ and $\mathbb{B}_k$ on V_k,

$$\langle \mathbb{A}_k w, \varphi \rangle_V = \int_{D \setminus \overline{\Omega}} \frac{1}{n-1} \Delta w \Delta \overline{\varphi} \, \mathrm{d}x + \int_\Omega \Delta w \Delta \overline{\varphi} \, \mathrm{d}x + k^2 \int_D \nabla w \nabla \overline{\varphi} \, \mathrm{d}x + \int_D w \overline{\varphi} \, \mathrm{d}x, \tag{5.29}$$

and

$$\begin{aligned}\langle \mathbb{B}_k w, \varphi\rangle_V = &\int_{D\setminus\overline{\Omega}} \frac{(k^4-1)n+1}{n-1} w\overline{\varphi}\,\mathrm{d}x + k^2 \int_{D\setminus\overline{\Omega}} \frac{n}{n-1}(\Delta w\overline{\varphi} + w\Delta\overline{\varphi})\,\mathrm{d}x \\ &- (2k^4+1)\int_{\Omega} w\overline{\varphi}\,\mathrm{d}x,\end{aligned} \tag{5.30}$$

for all $\varphi \in V_k$. With these notations, a solution $w_0 \in V_k$ to (5.17) with $\theta = 0$ is equivalently an element of $Ker(\mathbb{A}_k + \mathbb{B}_k)$.

Remark 5.3.5. *The variational formulation is never uniquely solvable when k^2 is a Neumann eigenvalue for $-\Delta$ in Ω. Indeed if we denote by $\varphi_1, \dots, \varphi_N \in V_k$ the corresponding Neumann eigenfunctions to k^2 extended by zero in $D\setminus\overline{\Omega}$. Then all the φ_i are solutions to (5.17) with $\theta = 0$. However, the constructed functions $\varphi_1, \dots, \varphi_N$ obviously do not correspond to transmission eigenvalues. In Lemma 5.3.6, more precision is given on the structure of $Ker(\mathbb{A}_k + \mathbb{B}_k)$, in particular when k is simultaneously a transmission eigenvalue and such that k^2 is a Neumann eigenvalue for $-\Delta$ in Ω.*

Lemma 5.3.6. *Let $k > 0$ such that k^2 is a Neumann eigenvalue of multiplicity $N \in \mathbb{N}^*$ and define $\varphi_1, \dots, \varphi_N \in V_k$ as in Remark 5.3.5. We then have the following results.*

- *If k is not a transmission eigenvalue then $Ker(\mathbb{A}_k + \mathbb{B}_k) = \mathrm{span}(\varphi_1, \dots, \varphi_N)$*
- *If k is a transmission eigenvalue of multiplicity $M \in \mathbb{N}^*$, denote by $(u_1, v_1)\dots(u_M, v_M)$ the corresponding eigenfunctions and define $w_j \in V_k$ by $w_j = u_j - v_j$ in $D\setminus\overline{\Omega}$ and $w_j = -v_j$ in Ω. Then $Ker(\mathbb{A}_k + \mathbb{B}_k)$ is a space of dimension $M + N$ given by*

$$Ker(\mathbb{A}_k + \mathbb{B}_k) = \mathrm{span}(\varphi_1, \dots, \varphi_N) \oplus \mathrm{span}(w_1, \dots, w_M). \tag{5.31}$$

Proof. We begin with the first point. Assume that k is not a transmission eigenvalue and let $w \in Ker(\mathbb{A}_k + \mathbb{B}_k)$. According to Theorem 5.3.3, there exists $(\alpha_1, \dots, \alpha_N) \in \mathbb{R}^N$ such that (u, v) defined by (5.27) is a solution to (ITP) with $f = g = 0$. Since k is not a transmission eigenvalue, $v = 0$ on $D\setminus\overline{\Omega}$. Consequently $\Delta w + k^2 n w = -k^2(n-1)v = 0$ on $D\setminus\overline{\Omega}$ and since the Cauchy data of w is zero on ∂D we deduce that $w = 0$ on $D\setminus\overline{\Omega}$. Finally we deduce thanks to the continuity of the normal derivative of w on $\partial\Omega$ that $\partial_\nu^{\pm}\varphi_{|\partial\Omega} = 0$ and hence $w \in \mathrm{span}(\varphi_1, \dots, \varphi_N)$.

We proceed with the proof of the second point, let k be a transmission eigenvalue of multiplicity $M \in \mathbb{N}^*$. We first prove the direct inclusion, let $w \in Ker(\mathbb{A}_k + \mathbb{B}_k)$. Theorem 5.3.3 implies the existence of $\varphi \in \mathrm{span}(\varphi_1, \dots, \varphi_N)$ such that $w + \varphi \in \mathrm{span}(w_1, \dots, w_M)$. Consequently $w \in \mathrm{span}(\varphi_1, \dots, \varphi_N, w_1, \dots, w_M)$. For the reverse inclusion, it suffices to apply the first point of Theorem 5.3.1 which ensures that $w_j \in Ker(\mathbb{A}_k + \mathbb{B}_k)$. It remains to show that the spaces $\mathrm{span}(\varphi_1, \dots, \varphi_N)$ and $\mathrm{span}(w_1, \dots, w_M)$ are linearly independent. The latter comes from the fact that the φ_j are compactly supported in Ω whereas the w_j cannot vanish on $D\setminus\overline{\Omega}$. □

Theorem 5.3.7. *Assume that there exists $\rho \in]-\frac{\pi}{2}, \frac{\pi}{2}[$ such that $\Re\mathfrak{e}(\frac{e^{i\rho}}{n-1}) > \alpha > 0$ and that $k > 0$ is not a transmission eigenvalue. Then for any pair $(f, g) \in H^{\frac{3}{2}}(\partial D) \times H^{\frac{1}{2}}(\partial D)$, the interior transmission problem (ITP) has a unique solution $(u, v) \in L^2(D\setminus\overline{\Omega}) \times L^2(D)$ and*

$$\|u\|_{L^2(D\setminus\overline{\Omega})} + \|v\|_{L^2(D)} \leq C\left(\|f\|_{H^{\frac{3}{2}}(\partial D)} + \|g\|_{H^{\frac{1}{2}}(\partial D)}\right). \tag{5.32}$$

Proof. Let $\theta \in H^2(D)$ be a function with compact support in $\overline{D}\setminus\overline{\Omega}$. The right hand side of (5.17) defines a function

$$F : \varphi \longmapsto \int_{D\setminus\overline{\Omega}} (n-1)^{-1}(\Delta\theta+k^2n\theta)(\Delta\overline{\varphi}+k^2n\overline{\varphi})\,\mathrm{d}x+k^2\int_{D\setminus\overline{\Omega}}\nabla\theta\nabla\overline{\varphi}\,\mathrm{d}x-k^4\int_{D\setminus\overline{\Omega}} n\theta\overline{\varphi}\,\mathrm{d}x \quad (5.33)$$

which is an antilinear continuous functional on V_k. According to the Riesz representation theorem, there exists a unique $l \in V_k$ such that $F(\varphi) = \langle l, \varphi\rangle_V$ for all $\varphi \in V_k$ and

$$\|l\|_V = \|F\| \leq C\|\theta\|_{H^2(D)}. \quad (5.34)$$

With these notations and definitions (5.29),(5.30), a solutions $w_0 \in V_k$ to (5.17) is equivalently a solution to

$$\mathbb{A}_k w_0 + \mathbb{B}_k w_0 = l \text{ in } V_k. \quad (5.35)$$

The assumption on n implies that for all $\varphi \in V$, $|\langle \mathbb{A}_k\varphi, \varphi\rangle_V| > c\|\varphi\|_V^2$ and therefore by the Lax Milgram theorem, $\mathbb{A}_k$ is an isomorphism on V_k. The operator $\mathbb{B}_k$ is compact. The proof of this is classic. For instance consider the part $\mathbb{B}_k^1$ of the operator $\mathbb{B}_k$ given by the first integral in (5.30), then

$$\forall\varphi \in V_k, \quad \|\mathbb{B}_k^1\varphi\|_{V_k}^2 = \int_{D\setminus\overline{\Omega}} \frac{(k^4-1)n+1}{n-1}\varphi\overline{\mathbb{B}_k^1\varphi}\,\mathrm{d}x \leq C\|\varphi\|_{L^2(D\setminus\overline{\Omega})}\|\mathbb{B}_k^1\varphi\|_{V_k} \quad (5.36)$$

Consequently

$$\forall\varphi \in V_k, \quad \|\mathbb{B}_k^1\varphi\|_{V_k} \leq C\|\varphi\|_{L^2(D\setminus\overline{\Omega})}. \quad (5.37)$$

The compact embedding of $H^1(D\setminus\overline{\Omega})$ in $L^2(D\setminus\overline{\Omega})$ then implies that $\mathbb{B}_k^1$ is compact. We proceed in the same way to show that the other terms of $\mathbb{B}_k$ are compact. We now conclude with the Fredholm alternative [20] by distinguishing two cases.

First assume in addition to the hypothesis on k that k^2 is not a Neumann eigenvalue for $-\Delta$ in Ω, then the operator $(\mathbb{A}_k + \mathbb{B}_k)$ is injective. Consequently there exists a unique solution $w_0 \in V_k$ to equation (5.35) and $\|w_0\|_V \leq C\|l\|_V$. Theorem 5.3.1 implies that there exists a unique solution to (ITP) given by (u, v) defined by (5.19) where $w := w_0 + \theta$. Since u and v can be written with $w, \Delta w$, both of their L^2 norm on D are controlled by $\|w\|_V$. Finally we deduce with (5.34) and (5.16) the desired estimate (5.32).

Now assume that k^2 is a Neumann eigenvalue for $-\Delta$ in Ω of multiplicity N. We define $\varphi_1, \ldots, \varphi_N \in V_k$ as in Lemma 5.3.6. Fredholm alternative implies that equation (5.35) is uniquely solvable since $l \in Ker(\mathbb{A}^\star+\mathbb{B}^\star)^\perp$. Indeed it can be shown from (5.29),(5.30) that $Ker(\mathbb{A}^\star+\mathbb{B}^\star) = \mathrm{span}(\overline{\varphi_1}, \ldots, \overline{\varphi_N})$. As a consequence, any $\psi \in Ker(\mathbb{A}^\star + \mathbb{B}^\star)$ is compactly supported in Ω and by definition of F we obtain $\langle l, \psi\rangle_V = F(\psi) = 0$. We proceed as in the previous paragraph to obtain the estimate (5.32).

□

In the following theorem, it is shown similarly to the classical case of inhomogeities, that if the refractive index has a positive imaginary part then the set of real transmission eigenvalues is empty.

Theorem 5.3.8. *Assume that the index $n \in L^\infty(D\setminus\overline{\Omega})$ is such that $\Im\mathfrak{m}(n) > 0$ a.e. in a subset of non empty interior $D_0 \subset D\setminus\overline{\Omega}$. Then the set of real transmission eigenvalues is empty.*

Proof. Let $k > 0$ and $w_0 \in V_k$ be a solution to (5.17) with $\theta = 0$. After regrouping terms in (5.17), we obtain the following equation for w_0,

$$\int_{D\setminus\overline{\Omega}} (n-1)^{-1}|\Delta w_0 + k^2 w_0|^2 \,\mathrm{d}x + k^2 \int_D |\nabla w_0|^2 \,\mathrm{d}x - k^4 \int_D |w_0|^2 \,\mathrm{d}x \\ + 2k^2 \int_{D\setminus\overline{\Omega}} \mathfrak{Re}\left(w_0(\Delta w_0 + k^2 w_0)\right) \mathrm{d}x = 0.$$

Since $\int_{D\setminus\overline{\Omega}} \mathfrak{Im}(n-1)^{-1}|\Delta w_0 + k^2 w_0|^2$ is the only term having an imaginary part in the above equation and since $\mathfrak{Im}(n-1)^{-1} < 0$ a.e in D_0, we infer that $\Delta w_0 + k^2 w_0 = 0$ in D_0. Let $(u, v$ be the corresponding solution to (ITP) given by (5.19) or (5.27). Then

$$u = -\frac{1}{k^2(n-1)}(\Delta w_0 + k^2 w_0) = 0 \text{ in } D_0. \tag{5.38}$$

The unique continuation principle implies that $u = 0$ in D. Therefore the Cauchy data of u and consequently of v are zero on ∂D. Hence v also vanish in D and k is not a transmission eigenvalue. □

We now turn our attention on the properties of transmission eigenvalues. Because of the above result, it will be assumed from now on that the refractive index is real valued. In addition to that, our approach requires the interior transmission problem to satisfies the Fredholm property. Therefore it is moreover assumed that the refractive index satisfies $n - 1 \geq \alpha > 0$ so that the operator $\mathbb{A}_k$ is coercive.

Assumption 5.3.9. *The refractive index $n \in L^\infty(D)$ is assumed to be a real valued function. With the following notations,*

$$n_* := \inf_{x\in D} n(x) \quad \textit{and} \quad n^* := \sup_{x\in D} n(x)$$

it is moreover assumed that $n_* > 1$.

Under this assumption, we will be discuss the following points in the indicated order: existence of a lower bound for TEs, discreteness of the set of TEs, existence of TEs.

5.3.4 Faber-Krahn inequalities for transmission eigenvalues

In this section, it is shown that $\mathbb{A}_k + \mathbb{B}_k : V_k \to V_k$ is coercive for k sufficiently small. This property will be required to prove the discreteness of the set of TEs. Furthermore a direct consequence of this result is the existence of a non zero lower bound for TEs. We start by proving some useful estimates.

Lemma 5.3.10.

- *There exists $C_P > 0$ independant of k such that*

$$\forall w \in V_k,\ \|w\|_{L^2(D\setminus\overline{\Omega})} \leq C_P \|\nabla w\|_{L^2(D\setminus\overline{\Omega})}. \tag{5.39}$$

The constant is given by

$$C_P = \sup_{w\in V_k\setminus\{0\}} \frac{\|w\|_{L^2(D\setminus\overline{\Omega})}}{\|\nabla w\|_{L^2(D\setminus\overline{\Omega})}}. \tag{5.40}$$

- *Let $k > 0$, and denote by $\mu_2(\Omega)$ the second Neumann eigenvalue for $-\Delta$ in Ω. Then we have*

$$\forall w \in V_k, \quad \|w\|^2_{L^2(\Omega)} \leq \frac{1}{\mu_2(\Omega)}\|\nabla w\|^2_{L^2(\Omega)} + \frac{|D \setminus \overline{\Omega}|}{k^4|\Omega|}\|\Delta w\|^2_{L^2(D\setminus\overline{\Omega})}. \tag{5.41}$$

Proof. One can prove (5.39) by adapting the proof of the classical Poincaré inequality. For the proof of the second estimate we define for all $w \in V_k$, $\underline{w} = \frac{1}{|\Omega|}\int_\Omega w \,\mathrm{d}x$. Since $\langle w - \underline{w}, \underline{w}\rangle_{L^2(\Omega)} = 0$,

$$\|w\|^2_{L^2(\Omega)} = \|w - \underline{w}\|^2_{L^2(\Omega)} + \|\underline{w}\|^2_{L^2(\Omega)}. \tag{5.42}$$

On the one hand, the Poincaré-Wirtinger inequality [59, section 5.8.1] implies

$$\forall w \in V_k, \quad \|w - \underline{w}\|^2_{L^2(\Omega)} \leq \frac{1}{\mu_2(\Omega)}\|\nabla w\|^2_{L^2(\Omega)}. \tag{5.43}$$

On the other hand, the equation $w = -\frac{1}{k^2}\Delta w$ in Ω gives

$$\|\underline{w}\|^2_{L^2(\Omega)} = |\Omega||\underline{w}|^2 = \frac{1}{k^4|\Omega|}\left|\int_\Omega \Delta w \,\mathrm{d}x\right|^2.$$

Then with $[\partial_\nu w]_{|\Omega} = 0$, we obtain after using Green's formula and Cauchy Schwarz inequality

$$\|\underline{w}\|^2_{L^2(\Omega)} = \frac{1}{k^4|\Omega|}\left|\int_{D\setminus\overline{\Omega}} \Delta w \,\mathrm{d}x\right|^2 \leq \frac{|D \setminus \overline{\Omega}|}{k^4|\Omega|}\|\Delta w\|^2_{L^2(D\setminus\overline{\Omega})}. \tag{5.44}$$

Finally the combination of (5.43) and (5.44) in (5.42) gives the result.

□

Theorem 5.3.11. *Assume in addition to Assumption 5.3.9, that*

$$\left(1 - \frac{1}{n^*}\right)|D| < |\Omega|. \tag{5.45}$$

Then there exists a real $K^\star > 0$ such that for all $k \in]0, K^\star[$, $\mathbb{A}_k + \mathbb{B}_k$ is definite positive on V_k.

Proof. From Assumption 5.3.9 on n and definitions of $\mathbb{A}_k$ and $\mathbb{B}_k$ (5.29),(5.30), we first obtain

$$\begin{aligned}
\langle(\mathbb{A}_k + \mathbb{B}_k)w, w\rangle &= \int_{D\setminus\overline{\Omega}} \frac{1}{n-1}|\Delta w|^2 \,\mathrm{d}x + 2k^2 \int_{D\setminus\overline{\Omega}} \frac{n}{n-1}\mathfrak{Re}(\Delta w \overline{w}) \,\mathrm{d}x + k^2 \int_D |\nabla w|^2 \,\mathrm{d}x \\
&\quad + k^4 \int_{D\setminus\overline{\Omega}} \frac{n}{n-1}|w|^2 \,\mathrm{d}x - k^4 \int_\Omega |w|^2 \,\mathrm{d}x \\
&\geq \frac{1}{n^* - 1}\|\Delta w\|^2_{L^2(D\setminus\overline{\Omega})} - 2k^2 C_P \frac{n_*}{n_* - 1}\|\Delta w\|_{L^2(D\setminus\overline{\Omega})}\|\nabla w\|_{L^2(D\setminus\overline{\Omega})} \\
&\quad + k^2\|\nabla w\|^2_{L^2(D)} - k^4\|w\|^2_{L^2(\Omega)}.
\end{aligned}$$

We first use estimate (5.43) to obtain

$$\begin{aligned}
&\langle(\mathbb{A}_k + \mathbb{B}_k)w, w\rangle \geq \\
&\qquad \gamma\|\Delta w\|^2_{L^2(D\setminus\overline{\Omega})} - 2k^2 C_P \frac{n_*}{n_* - 1}\|\Delta w\|_{L^2(D\setminus\overline{\Omega})}\|\nabla w\|_{L^2(D\setminus\overline{\Omega})} + k^2\|\nabla w\|^2_{L^2(D\setminus\overline{\Omega})} \\
&\qquad + \left(k^2 - \frac{k^4}{\mu_2(\Omega)}\right)\|\nabla w\|^2_{L^2(\Omega)}
\end{aligned} \tag{5.46}$$

where the parameter γ is given by

$$\gamma := \frac{1}{n^* - 1} - \frac{|D \setminus \overline{\Omega}|}{|\Omega|}. \tag{5.47}$$

One can show that assumption (5.45) is equivalent to $\gamma > 0$. Indeed

$$\left(1 - \frac{1}{n^*}\right)|D| < |\Omega| \iff \frac{n^*}{n^* - 1} > \frac{|D|}{|\Omega|} \iff \frac{1}{n^* - 1} > \frac{|D|}{|\Omega|} - 1 = \frac{|D \setminus \overline{\Omega}|}{|\Omega|}. \tag{5.48}$$

Now choosing k such that $\gamma k^2 > k^4 C_P^2 (\frac{n_*}{n_* - 1})^2$ implies that the first line of (5.46) is coercive, more precisely there exists $C_1(k) > 0$ such that

$$\begin{aligned}\gamma \|\Delta w\|^2_{L^2(D\setminus\overline{\Omega})} - 2k^2 C_P \frac{n_*}{n_* - 1} \|\Delta w\|_{L^2(D\setminus\overline{\Omega})} \|\nabla w\|_{L^2(D\setminus\overline{\Omega})} + k^2 \|\nabla w\|^2_{L^2(D\setminus\overline{\Omega})} \\ \geq C_1(k)(\|\Delta w\|^2_{L^2(D\setminus\overline{\Omega})} + \|\nabla w\|^2_{L^2(D\setminus\overline{\Omega})}).\end{aligned} \tag{5.49}$$

Consequently if we define

$$K^\star = \min\left(\sqrt{\mu_2(\Omega)}, (1 - \frac{1}{n_*})\frac{\sqrt{\gamma}}{C_P}\right) \tag{5.50}$$

then we obtain from (5.46) that for all $k \in]0, K^\star[$, there exists $C_2(k) > 0$ such that

$$\langle (\mathbb{A}_k + \mathbb{B}_k) w, w \rangle \geq C_2(k)(\|\Delta w\|^2_{L^2(D\setminus\overline{\Omega})} + \|\nabla w\|^2_{L^2(D\setminus\overline{\Omega})} + \|\nabla w\|^2_{L^2(\Omega)}). \tag{5.51}$$

The result is now straightforward since Lemma 5.3.10 implies that the norm $\|w\| = (\|\Delta w\|^2_{L^2(D\setminus\overline{\Omega})} + \|\nabla w\|^2_{L^2(D)})^{\frac{1}{2}}$ is equivalent to the chosen norm $\|\cdot\|_{V_k}$ on V_k.

□

Corollary 5.3.12. *With the same assumptions and notations of Theorem 5.3.11, if $k > 0$ is a transmission eigenvalue then $k > K^\star$.*

5.3.5 Discreteness of transmission eigenvalues

In this section, we show that the set of transmission eigenvalues is at most discrete. As mentioned at the beginning of section 5.3.3, TEs correspond to values of $k > 0$ for which the operator $\mathbb{A}_k + \mathbb{B}_k : V_k \to V_k$ has a non trivial kernel. To show that the latter occurs only for a discrete set of k, we would like to apply the Analytic Fredholm Theorem. But $\mathbb{A}_k$ and $\mathbb{B}_k$ operate on a space depending on k. To overcome this problem, we adapt the approach of [27] where the same difficulty was encountered. A space V which is independent of k and moreover contains every V_k is introduced. Then the operators $\mathbb{A}_k$ and $\mathbb{B}_k$ are extended to operators $\widetilde{\mathbb{A}}_k$ and $\widetilde{\mathbb{B}}_k$ defined on V via a projection like operator $\widetilde{P}_k$. We finally conclude by showing that applying the Analytic Fredholm theorem to this setting implies the desired result.

We introduce the following Hilbert space V, which is obtained by removing the constraint $\Delta\varphi + k^2\varphi = 0$ in Ω of the tests functions in the space V_k:

$$V = \{\varphi \in H^1_\Delta(D \setminus \Omega) \times H^1_\Delta(\Omega) \mid \varphi_{|\partial D} = \partial_\nu \varphi_{|\partial D} = [\frac{\partial \varphi}{\partial \nu}]_{|\partial\Omega} = 0\}. \tag{5.52}$$

Note that V does not depend on k and moreover contains every V_k for $k \in \mathbb{C}$. The space V is equipped with the same scalar product $\langle \cdot, \cdot \rangle_V$ used for the spaces V_k defined at (5.9). We also introduce the operator $\theta_k : V \to V$ which is defined for $w \in V$ by

$$\forall x \in D, \quad \theta_k w(x) = \frac{1}{4} \int_\Omega (\Delta w + k^2 w)(y) Y_0(k|x-y|) \, \mathrm{d}y, \tag{5.53}$$

where Y_0 denotes the Bessel function of second kind of order zero. As shown in [27], θ_k depends analytically on k with $\Re\mathfrak{e}(k) > 0$ and $\theta_k w \in H^2(D)$. Let χ be a smooth function that equals 1 in Ω and 0 outside of D. We define the following continuous operator

$$\begin{array}{rccc} \widetilde{P}_k : & V & \longrightarrow & V \\ & w & \longmapsto & w - \chi \theta_k w. \end{array} \tag{5.54}$$

$\widetilde{P}_k$ also depends analytically on k with positive real part and we observe that

$$\forall w \in V_k, \quad \theta_k w = 0 \quad \text{and} \quad \widetilde{P}_k w = w. \tag{5.55}$$

Furthermore for all $w \in V$, $\Delta \theta_k w + k^2 \theta_k w = \Delta w + k^2 w$ in Ω, and as a consequence

$$\forall w \in V, \quad \widetilde{P}_k w \in V_k. \tag{5.56}$$

We finally define the operators $\widetilde{\mathbb{A}}_k$ and $\widetilde{\mathbb{B}}_k$ which extend the operators $\mathbb{A}_k$ and $\mathbb{B}_k$ on V. They are defined by the use of the Riesz representation theorem such that for all w and φ in V,

$$\begin{aligned} \langle \widetilde{\mathbb{A}}_k w, \varphi \rangle_V &= \langle \mathbb{A}_k \widetilde{P}_k w, \overline{\widetilde{P}_k \overline{\varphi}} \rangle_V + \alpha \langle \theta_k w, \overline{\theta_k \overline{\varphi}} \rangle_V, \\ \langle \widetilde{\mathbb{B}}_k w, \varphi \rangle_V &= \langle \mathbb{B}_k \widetilde{P}_k w, \overline{\widetilde{P}_k \overline{\varphi}} \rangle_V. \end{aligned} \tag{5.57}$$

The parameter α is a sufficiently large positive constant that will be fixed later. The analyticity of $\widetilde{P}_k$ and θ_k, and definitions of $\mathbb{A}_k$ and $\mathbb{B}_k$ (5.29)-(5.30) imply that $\widetilde{\mathbb{A}}_k$ and $\widetilde{\mathbb{B}}_k$ depend analytically on $k \in \mathbb{C}$ with $\Re\mathfrak{e}(k) > 0$. In addition to that, the operators $\widetilde{\mathbb{A}}_k$ and $\widetilde{\mathbb{B}}_k$ respectively coincides with $\mathbb{A}_k$ and $\mathbb{B}_k$ on V_k when k is real. Indeed it can be shown by using (5.55),(5.57) and observing that $\forall v \in V_k$, $\overline{v} \in V_k$, that

$$\forall w \in V_k, \qquad \widetilde{\mathbb{A}}_k w = \mathbb{A}_k w \quad \text{and} \qquad \widetilde{\mathbb{B}}_k w = \mathbb{B}_k w. \tag{5.58}$$

Consequently if $k \in \mathbb{R}$ is such that $\mathbb{A}_k + \mathbb{B}_k : V_k \to V_k$ is not injective implies $\widetilde{\mathbb{A}}_k + \widetilde{\mathbb{B}}_k : V \to V$ is not injective. As a consequence, to prove the discreteness of the set of transmission eigenvalues, it is sufficient to prove that the set of $k > 0$ for which the operator $\widetilde{\mathbb{A}}_k + \widetilde{\mathbb{B}}_k : V \to V$ has a non trivial kernel is at most discrete. We rely on the following theorem, [44, Theorem 8.26]

Theorem 5.3.13 (Analytic Fredholm Theorem)**.** *Let Ω be a domain in $\mathbb{C}$ and let $(\mathbb{T}_z)_{z\in\Omega} \subset \mathcal{L}(E)$ be a family of compact operators such that $z \mapsto \mathbb{T}_z$ is analytic in Ω. Then either*

a) $(I + \mathbb{T}_z)$ is not injective for any $z \in \Omega$ or

b) $(I + \mathbb{T}_z)$ is injective for all $z \in \Omega \setminus S$ where S is a discrete subset of Ω.

To simplify the presentation, we show this intermediate result.

Lemma 5.3.14. *Assume that n satisfies Assumption 5.3.9 and the condition (5.45), and let $K^\star$ be defined by (5.50). Then the operators $\widetilde{\mathbb{A}}_k$ and $\widetilde{\mathbb{B}}_k$ defined by (5.57) satisfies the following,*

- *There exists α independent from k such that for all $k > 0$, $\widetilde{\mathbb{A}}_k$ is coercive on V.*

- *For all $k \in]0, K^\star[$, the operator $\widetilde{\mathbb{A}}_k + \widetilde{\mathbb{B}}_k$ is injective on V.*

Proof. We begin with the first point. After observing that for k real $\overline{\theta_k(\overline{w})} = \theta_k(w)$ and $\overline{\widetilde{P}_k(\overline{w})} = \widetilde{P}_k(w)$, expression of $\widetilde{\mathbb{A}}_k$ simplifies

$$\langle \widetilde{\mathbb{A}}_k w, w\rangle_V = \langle \mathbb{A}_k \widetilde{P}_k w, \widetilde{P}_k w\rangle_V + \alpha \|\theta_k w\|^2. \tag{5.59}$$

On the one hand, from the definition of $\mathbb{A}_k$ (5.29), there exists a $\gamma_k > 0$ given for example by $\gamma_k = min((n^* - 1)^{-1}, k^2, 1/2)$ such that

$$\langle \widetilde{\mathbb{A}}_k w, w\rangle_V \geq \gamma_k \|\widetilde{P}_k w\|_V^2 + \alpha \|\theta_k w\|_V^2.$$

On the other hand we deduce from the expression of $\widetilde{P}_k$ the existence of a constant C_χ depending only on χ such that

$$\|\widetilde{P}_k w\|_V^2 \geq \|w\|_V^2 - 2C_\chi \|w\|_V \|\theta_k w\|_V + \|\chi \theta_k w\|_V^2. \tag{5.60}$$

Hence

$$\langle \widetilde{\mathbb{A}}_k w, w\rangle_V \geq \gamma_k \|w\|_V^2 - 2C_\chi \gamma_k \|w\|_V \|\theta_k w\|_V + \alpha \|\theta_k w\|_V^2.$$

The operator $\widetilde{\mathbb{A}}_k$ is then coercive a soon as α satisfies $\alpha\gamma_k > C_\chi \gamma_k^2$. Since $\gamma_k < 1$, one can fix a valid α independent from k with $\alpha := C_\chi^2$.

We now prove the second assertion. Let $k \in]0, K^\star[$. According to Theorem 5.3.11, $\mathbb{A}_k + \mathbb{B}_k$ is coercive on V_k. Consequently there exists a $\sigma_k > 0$ such that

$$\begin{aligned} \forall w \in V, \quad \langle (\widetilde{\mathbb{A}}_k + \widetilde{\mathbb{B}}_k) w, w\rangle_V &= \langle (\mathbb{A}_k + \mathbb{B}_k) \widetilde{P}_k w, \widetilde{P}_k w\rangle_V + \alpha \|\theta_k w\|_V^2 \\ &\geq \sigma_k \|\widetilde{P}_k w\|_V^2 + \alpha \|\theta_k w\|_V^2. \end{aligned} \tag{5.61}$$

Therefore if $w \in V$ such that $(\widetilde{\mathbb{A}}_k + \widetilde{\mathbb{B}}_k) w = 0$, then $\widetilde{P}_k w = \theta_k w = 0$. We finally conclude from the definition of $\widetilde{P}_k$ that $w = \widetilde{P}_k w + \chi \theta_k w = 0$. □

Theorem 5.3.15. *Assume that n satisfies Assumption 5.3.9 and the condition (5.45). Then the set of transmission eigenvalues is discrete.*

Proof. We show that the set of $k > 0$ such that $\widetilde{\mathbb{A}}_k + \widetilde{\mathbb{B}}_k$ is non injective is discrete. For this purpose we apply Theorem 5.3.13 and use the same notations. Since $\widetilde{\mathbb{A}}_k$ depends analytically on $k \in \mathbb{C}$ and is an isomorphism for $k > 0$, there exists a set $\Omega \subset \mathbb{C}$ containing the positive real axis such that $\widetilde{\mathbb{A}}_k^{-1}$ exists and depends analytically to $k \in \Omega$. Hence the operator $\mathbb{T}_k : V \to V$ defined by $\widetilde{\mathbb{A}}_k^{-1} \widetilde{\mathbb{B}}_k$ also depends analytically to $k \in \Omega$ and is moreover compact because $\widetilde{\mathbb{B}}_k$ is compact. The second point of Lemma 5.3.14 implies the existence of $k \in \Omega$ such that $(I + \mathbb{T}_k)$ is injective. Consequently, the set of $k > 0$ for which $(I + \mathbb{T}_k)$ is injective, or equivalently $\widetilde{\mathbb{A}}_k + \widetilde{\mathbb{B}}_k$, is at most discrete.

□

5.3.6 On the existence of transmission eigenvalues

The main purpose of the framework developed in this section is to prove the existence of transmission eigenvalues since then the variational formulation can be expressed in terms of self-adjoint operators $\mathbb{A}_k$ and $\mathbb{B}_k$. However, it did not allow to conclude about the existence of transmission eigenvalues, and it is explained in this paragraph what are the difficulties that prevented us to conclude in the classical way. In a few words, the result on which we rely allows to give the existence of positive reals k such that $\mathbb{A}_k + \mathbb{B}_k$ is not injective. But this is not sufficient

to conclude about the existence of TEs. According to Lemma 5.3.6, one shall moreover prove that the square of the determined k are not Neumann eigenvalues or otherwise that the dimension of $Ker(\mathbb{A}_k + \mathbb{B}_k)$ is larger than the multiplicity of the Neumann eigenvalue k^2. Proving this last fact requires numerous restrictive conditions on n and Ω that cannot be valid simultaneously.

Before going any further, we place ourselves in a setting that allows us to apply Lemma 5.3.16. Since $\mathbb{A}_k : V_k \longrightarrow V_k$ is definite positive and self-adjoint, the operators $\mathbb{A}_k^{\pm\frac{1}{2}}$ are well defined. Both are self-adjoint, positive definite and satisfies $\mathbb{A}_k^{\frac{1}{2}}\mathbb{A}_k^{\frac{1}{2}} = \mathbb{A}_k$ and $\mathbb{A}_k^{\frac{1}{2}}\mathbb{A}_k^{-\frac{1}{2}} = I_k$ where I_k is the identity on V_k. Obviously, the kernel of $\mathbb{A}_k + \mathbb{B}_k$ is nontrivial if and only if the kernel of the operator

$$I_k + \mathbb{A}_k^{-\frac{1}{2}}\mathbb{B}_k\mathbb{A}_k^{-\frac{1}{2}} : V_k \longrightarrow V_k \tag{5.62}$$

is nontrivial. In order to avoid dealing with function spaces depending on k we introduce the orthogonal projection operator $P_k : V \to V$ and the canonical injection $R_k : V_k \to V$ where the space V is defined as in (5.52). We then consider the (compact) operator $T_k : V \to V$ by

$$T_k := R_k\mathbb{A}_k^{-\frac{1}{2}}\mathbb{B}_k\mathbb{A}_k^{-\frac{1}{2}}P_k. \tag{5.63}$$

Denoting I the identity operator on V, one can easily check that

$$Ker(I + T_k) = \mathbb{A}_k^{\frac{1}{2}} \cdot Ker(\mathbb{A}_k + \mathbb{B}_k). \tag{5.64}$$

Consequently the nullspace of $I + T_k$ and of $\mathbb{A}_k + \mathbb{B}_k$ have the same (finite) dimension and we can equivalently deal with the operator $I + T_k$ to show the existence of TEs. It is shown in [27] that P_k depends continuously on the parameter $k > 0$. Moreover the proof of Corollary 4.6 of this paper can be transposed in our situation to prove that T_k also depends continuously on k. We denote by $\lambda_i(k)$ the i^{th} negative eigenvalue of the compact and self-adjoint operator T_k (ordered in the increasing order). From the max-min we notice that each $\lambda_i(k)$ are continuous functions of k. We then have the following useful result proved in [29]. It gives existence of k for which $Ker(I + T_k)$ is nontrivial, or equivalently existence of k such that $1 + \lambda_i(k) = 0$.

Lemma 5.3.16. *Assume that*

1. *There is a $k_0 > 0$ such that $I + T_{k_0}$ is positive on V.*
2. *There is a $k_1 > k_0$ such that $I + T_{k_1}$ is non positive on a p-dimensional subspace W of V.*

Then the equation $1 + \lambda_i(k) = 0$ has p solutions in $[k_0, k_1]$ counting their multiplicity.

Now let $\epsilon > 0$ be small enough such that $D \setminus \overline{\Omega}$ contains $m(\epsilon) \geq 1$ pairwise disjoint balls of radius ϵ denoted $B_\epsilon^1, \dots B_\epsilon^m$. Assuming that

$$\left(1 - \frac{1}{n^*}\right)|D| < |\Omega|, \tag{5.65}$$

one can easily prove by using Lemma 5.3.16 and (5.64) that equation $1 + \lambda_i(k) = 0$ has $m(\epsilon)$ solutions in $[K^\star, \xi_{n_*}/\epsilon]$, where $K^\star$ is defined by (5.50) and ξ_{n_*} is the first transmission eigenvalue of the interior transmission problem for the unit ball with index n_*. Indeed since the positivity of $\mathbb{A}_k + \mathbb{B}_k$ implies the positivity of $I + T_k$, we infer from Theorem 5.3.11 that the first point of the Lemma is valid for $k_0 = K^\star$. For the second point we denote by $w_\epsilon^j \in H_0^2(B_\epsilon^j)$ the eigenfunction of the transmission eigenvalue problem on $B_\epsilon^1, \dots B_\epsilon^m$ with constant refractive index n_* associated

to the first transmission eigenvalue given by $k_\epsilon = \frac{\xi_{n_*}}{\epsilon}$. We then define $w^j \in V_k$ the continuation by zero of each w^j_ϵ to the whole of $D \setminus \overline{\Omega}$. The family $(w^j)_j$ form an orthogonal family since the w^j are of disjoint compact support. We show that $I + T_k$ is negative on the $m(\epsilon)$-dimensional space $\mathrm{span}(\mathbb{A}_k^{-\frac{1}{2}} w^j)$,

$$
\begin{aligned}
\langle (I + T_{k_\epsilon}) \mathbb{A}_{k_\epsilon}^{-1/2} w^j, \mathbb{A}_{k_\epsilon}^{-1/2} w^j \rangle_V & \\
&= \langle (\mathbb{A}_{k_\epsilon} + \mathbb{B}_{k_\epsilon}) w^j, w^j \rangle_V \\
&= \int_{D\setminus\overline{\Omega}} \frac{1}{n-1} |\Delta w^j + k_\epsilon^2 w^j|^2 \,\mathrm{d}x + 2k_\epsilon^2 \int_{D\setminus\overline{\Omega}} \mathfrak{Re}(\Delta w^j \overline{w^j}) \,\mathrm{d}x \\
&\quad + k_\epsilon^2 \int_D |\nabla w^j|^2 \,\mathrm{d}x + k_\epsilon^4 \int_{D\setminus\overline{\Omega}} |w^j|^2 \,\mathrm{d}x - k_\epsilon^4 \int_\Omega |w^j|^2 \,\mathrm{d}x \\
&= \int_{B_\epsilon^j} \frac{1}{(n-1)} |\Delta w^j + k_\epsilon^2 w^j|^2 \,\mathrm{d}x - k_\epsilon^2 \int_{B_\epsilon^j} |\nabla w^j|^2 \,\mathrm{d}x + k_\epsilon^4 \int_{B_\epsilon^j} |w^j|^2 \,\mathrm{d}x \\
&\leq \int_{B_\epsilon^j} \frac{1}{(n_*-1)} |\Delta w^j + k_\epsilon^2 w^j|^2 \,\mathrm{d}x - k_\epsilon^2 \int_{B_\epsilon^j} |\nabla w^j|^2 \,\mathrm{d}x + k_\epsilon^4 \int_{B_\epsilon^j} |w^j|^2 \,\mathrm{d}x \\
&= 0.
\end{aligned}
$$

We have finally shown the existence of values of $k \in [K^\star, \xi_{n_*}/\epsilon]$ for which $\mathbb{A}_k + \mathbb{B}_k$ is not injective and the cumulative dimension of the nullspaces for these k is equal to $m(\epsilon)$.

To conclude on the existence of transmission eigenvalues one needs to ensure that $m(\epsilon)$ is greater than the number of occurence for k^2 being a Neumann eigenvalue for $k \in [K^\star, \xi_{n_*}/\epsilon]$. The two approaches we tried, and that we explain hereafter were unsuccessful.

First temptative approach using the Weyl asymptotic formula

For $\mu > 0$ we denote by $N_\Omega(\mu)$ the counting function of the Neumann eigenvalues for $-\Delta$ in Ω (counting multiplicities). We recall the Weyl asymptotic formula [121],

$$
N_\Omega(\mu) \underset{\mu\to+\infty}{\sim} \frac{B_d |\Omega| \mu^{d/2}}{(2\pi)^d} \tag{5.66}
$$

where B_d is the d-dimensional measure of the unit ball in $\mathbb{R}^d$. Consequently we have the following estimate,

$$
N_\Omega\left(\frac{\xi_{n_*}^2}{\epsilon^2}\right) \underset{\epsilon\to 0}{\sim} \frac{B_d |\Omega| \xi_{n_*}^d}{(2\pi)^d \epsilon^d}. \tag{5.67}
$$

In addition to this we have that $m(\epsilon) \underset{\epsilon\to 0}{\sim} |D \setminus \Omega|/B_d$. Consequently, asking that n and Ω to satisfy in addition to (5.65),

$$
\frac{|D \setminus \Omega|}{B_d} > \frac{B_d |\Omega| \xi_{n_*}^d}{(2\pi)^d} \tag{5.68}
$$

would imply the existence of infinitely many transmission eigenvalues. However the condition (5.68) is equivalent to

$$
|D| \left(1 + \frac{B_d^2 \xi_{n_*}^d}{(2\pi)^d}\right)^{-1} > |\Omega| \tag{5.69}
$$

and asking for this condition together with condition (5.65) necessitates at least that

$$\left(1+\frac{B_d^2\xi_{n_*}^d}{(2\pi)^d}\right)\left(1-\frac{1}{n^*}\right)<1. \tag{5.70}$$

Numerical simulations in the two dimensional case show that the latter is not valid in general.

Second temptative approach for the existence of at least one transmission eigenvalue in $(\mathbf{0},\sqrt{\mu_2})$

We now discuss the possibility of finding at least one transmission eigenvalue k such that $k^2\leq\mu_2$. To this end we fix ϵ such that $k_\epsilon^2=\mu_2$, and define $\varphi_j\in V_{k_\epsilon}$ the Neumann eigenfunctions that have been extended by zero to D. We know that the φ_j are in the nullspace of $\mathbb{A}_{k_\epsilon}+\mathbb{B}_{k_\epsilon}$. Now if we can include a ball B_ϵ in $D\setminus\overline{\Omega}$ then similarly to above we could show that the element $w_\epsilon\in V_{k_\epsilon}$ defined as the continuation by zero to D of the eigenfunction of the first transmission eigenvalue for the ball B_ϵ of constant refractive index n_*. Lemma 5.3.16 would then imply the existence of a transmission eigenvalue in $]0,\sqrt{\mu_2}]$. The existence of such a ball $B_\epsilon\subset D\setminus\overline{\Omega}$ requires since $\epsilon=\xi_{n_*}/\sqrt{\mu_2}$

$$|B_\epsilon|+|\Omega|=\frac{B_d\xi_{n_*}^d}{\mu_2^{d/2}}+|\Omega|<|D|, \tag{5.71}$$

or equivalently

$$\frac{B_d\xi_{n_*}^d}{\mu_2^{d/2}|\Omega|}+1<\frac{|D|}{|\Omega|}. \tag{5.72}$$

This together with the condition (5.65) requires to ask for the following condition,

$$\left(1+\frac{B_d\xi_{n_*}^d}{\mu_2^{d/2}|\Omega|}\right)\left(1-\frac{1}{n^*}\right)<1. \tag{5.73}$$

Once again, numerical simulations in the two dimensional case shows that the latter is not valid in general.

5.4 Discreteness of transmission eigenvalues via the Dirichlet-to-Neumann approach

Proving the discreteness of the set of TEs with the previous developed framework required an unusual constraint on the size of the impenetrable obstacle Ω (5.45). This condition does not have any physical meaning to our knowledge. The purpose of this section is to establish the discreteness result by removing this condition.

5.4.1 Main analysis

Let $D\subset\mathbb{R}^d$, $d\geq 2$, be a domain with smooth boundary. Let ω be a domain with Lipschitz boundary such that $\overline{\omega}\subset D$. We shall denote $\Omega:=D\setminus\overline{\omega}$ and we assume that D is connected. In the present note, we are interested in the following interior transmission problem

$$\begin{array}{l}\text{Find } (u,v)\in \mathrm{L}^2(\Omega)\times\mathrm{L}^2(D) \text{ such that}\\ \begin{array}{rcll}\Delta u-\lambda n u &=& 0 & \text{in } \Omega\\ \Delta v-\lambda v &=& 0 & \text{in } D\\ \partial_\nu u &=& 0 & \text{on } \partial\omega\end{array}\qquad\qquad \begin{array}{rcll}u-v &=& 0 & \text{on } \partial D\\ \partial_\nu u-\partial_\nu v &=& 0 & \text{on } \partial D.\end{array}\end{array} \tag{5.74}$$

Here $n \in \mathrm{L}^\infty(\Omega)$ is a real valued function such that $n \geq C > 0$ in Ω. We shall say that λ is a transmission eigenvalue if there is $(u, v) \neq (0, 0)$ solving (5.74). Our goal is to prove that the set of eigenvalues is discrete in the complex plane. To proceed, we shall mix some ideas from [114, 88, 76, 103]. In our analysis, we shall assume that there is a connected open set $\mathcal{V} \subset \Omega$ with $\partial D \subset \overline{\mathcal{V}}$ and $\mathcal{V} \cap \overline{\omega} = \emptyset$ such that $n \in \mathrm{W}^{1,\infty}(\mathcal{V})$. Moreover, we shall assume that we have either

$$n - 1 \geq C > 0 \text{ in } \mathcal{V} \qquad \text{or} \qquad 1 - n \geq C > 0 \text{ in } \mathcal{V}.$$

Introduce some function $\tilde{n} \in \mathrm{L}^\infty(D)$ such that $\tilde{n} = n$ in $\mathcal{V}$ and such that, according to the assumption made on n, we have either $\tilde{n} - 1 \geq C > 0$ in D or $1 - \tilde{n} \geq C > 0$ in D.

For $\lambda \in \mathbb{C} \setminus \mathscr{S}$, where $\mathscr{S}$ is a discrete set of $(-\infty; 0)$, we define the Dirichlet-to-Neumann maps $\Lambda_n(\lambda)$, $\Lambda_{\tilde{n}}(\lambda)$, $\Lambda(\lambda) : \mathrm{H}^{-1/2}(\partial D) \to \mathrm{H}^{-3/2}(\partial D)$ such that for $g \in \mathrm{H}^{-1/2}(\partial D)$

$$\Lambda_n(\lambda)g = \partial_\nu u, \qquad \Lambda_{\tilde{n}}(\lambda)g = \partial_\nu \tilde{u}, \qquad \Lambda(\lambda)g = \partial_\nu v$$

where $u \in \mathrm{L}^2(\Omega)$, $\tilde{u} \in \mathrm{L}^2(D)$, $v \in \mathrm{L}^2(D)$ are the functions which solve

$$\left| \begin{array}{rcll} \Delta u - \lambda n u &=& 0 & \text{in } \Omega \\ u &=& g & \text{on } \partial D \\ \partial_\nu u &=& 0 & \text{on } \partial\Omega \end{array} \right| \quad \left| \begin{array}{rcll} \Delta \tilde{u} - \lambda \tilde{n} \tilde{u} &=& 0 & \text{in } D \\ \tilde{u} &=& g & \text{on } \partial D \end{array} \right| \quad \left| \begin{array}{rcll} \Delta v - \lambda v &=& 0 & \text{in } D \\ v &=& g & \text{on } \partial D. \end{array} \right. \tag{5.75}$$

For $\lambda \in \mathbb{C} \setminus (\mathscr{S} \cup \{0\})$, define the operators

$$\mathrm{A}(\lambda) := \frac{\Lambda_n(\lambda) - \Lambda(\lambda)}{\lambda} \qquad \text{and} \qquad \tilde{\mathrm{A}}(\lambda) := \frac{\Lambda_{\tilde{n}}(\lambda) - \Lambda(\lambda)}{\lambda}. \tag{5.76}$$

Lemma 5.4.1. *Assume that $\lambda \in \mathbb{C} \setminus (\mathscr{S} \cup \{0\})$. Then λ is a transmission eigenvalue if and only if* $\ker \mathrm{A}(\lambda) \neq \{0\}$.

Proof. Assume that $\lambda \in \mathbb{C} \setminus (\mathscr{S} \cup \{0\})$ is a transmission eigenvalue. Set $g := u = v$ where (u, v) is an eigenpair for (5.74). Clearly, we have $g \not\equiv 0$ otherwise we would have $u \equiv v \equiv 0$ which is impossible because $\lambda \notin \mathscr{S}$. According to (5.74) there holds $\mathrm{A}(\lambda)g = 0$ which shows that $\ker \mathrm{A}(\lambda) \neq \{0\}$.
Now if $g \in \ker \mathrm{A}(\lambda) \setminus \{0\}$. Define u and v as in (5.75). Then $(u, v) \neq (0, 0)$ solves (5.74). □

Lemma 5.4.2. *For all $\lambda \in \mathbb{C} \setminus (\mathscr{S} \cup \{0\})$, the operators $\mathrm{A}(\lambda)$, $\tilde{\mathrm{A}}(\lambda)$ are bounded from $\mathrm{H}^{-1/2}(\partial D)$ in $\mathrm{H}^{+1/2}(\partial D)$.*

Proof. We show the result for $\mathrm{A}(\lambda)$, the proof is completely similar for $\tilde{\mathrm{A}}(\lambda)$. Pick some $g \in \mathrm{H}^{-1/2}(\partial D)$ and introduce the functions u, v as in (5.75). We have $\mathrm{A}(\lambda)g = \partial_\nu w$ where $w := \lambda^{-1}(u - v)$ in Ω. Since $w \in \mathrm{L}^2(\Omega)$ satisfies $w = 0$ on ∂D and $\Delta w - \lambda n w = (n - 1)v$ in Ω, results of interior regularity (see e.g. [96]) guarantee that $w \in \mathrm{H}^2(\mathcal{V})$ with $\|w\|_{\mathrm{H}^2(\mathcal{V})} \leq C \|v\|_{\mathrm{L}^2(\Omega)}$. Since we have $\|v\|_{\mathrm{L}^2(\Omega)} \leq \|v\|_{\mathrm{L}^2(D)} \leq C \|g\|_{\mathrm{H}^{-1/2}(\partial D)}$, we can write

$$\|\mathrm{A}(\lambda)g\|_{\mathrm{H}^{1/2}(\partial D)} = \|\partial_\nu w\|_{\mathrm{H}^{1/2}(\partial D)} \leq C \|w\|_{\mathrm{H}^2(\mathcal{V})} \leq C \|v\|_{\mathrm{L}^2(\Omega)} \leq C \|g\|_{\mathrm{H}^{-1/2}(\partial D)}. \tag{5.77}$$

This shows that $\mathrm{A}(\lambda)$ is bounded from $\mathrm{H}^{-1/2}(\partial D)$ to $\mathrm{H}^{+1/2}(\partial D)$. □

Now we state three propositions that we will combine in order to get the main result of the note. The proofs will be given in the Section 5.4.2 below.

Proposition 5.4.3. *There is $\lambda_0 \geq 0$ such that for all $\lambda \geq \lambda_0$, the operator $\tilde{\mathrm{A}}(\lambda) : \mathrm{H}^{-1/2}(\partial D) \to \mathrm{H}^{1/2}(\partial D)$ is an isomorphism.*

Proposition 5.4.4. *For all $\lambda \in \mathbb{C} \setminus (\mathscr{S} \cup \{0\})$, the operator $\mathrm{A}(\lambda) - \tilde{\mathrm{A}}(\lambda_0) : \mathrm{H}^{-1/2}(\partial D) \to \mathrm{H}^{1/2}(\partial D)$ is compact.*

Proposition 5.4.5. *There is $\lambda_1 \geq 0$ such that for all $\lambda \geq \lambda_1$, the operator $\mathrm{A}(\lambda) : \mathrm{H}^{-1/2}(\partial D) \to \mathrm{H}^{1/2}(\partial D)$ is injective.*

We can now prove the main theorem of this note.

Theorem 5.4.6. *Assume that the coefficient $n \in \mathrm{L}^\infty(\Omega)$, with $n \in \mathrm{W}^{1,\infty}(\mathcal{V})$, is such that we have either*

$$n - 1 \geq C > 0 \text{ in } \mathcal{V} \qquad \text{or} \qquad 1 - n \geq C > 0 \text{ in } \mathcal{V}.$$

Then the set of transmission eigenvalues for Problem (5.74) is discrete in $\mathbb{C}$.

Proof. According to Lemma 5.4.1, in order to prove this result, it suffices to show that the set of $\lambda \in \mathbb{C} \setminus (\mathscr{S} \cup \{0\})$ such that $\mathrm{A}(\lambda)$ has a non zero kernel is discrete. Let us write

$$\mathrm{A}(\lambda) = I + K(\lambda) \qquad \text{with} \quad I := \tilde{\mathrm{A}}(\lambda_0) \quad \text{and} \quad K(\lambda) := \mathrm{A}(\lambda) - \tilde{\mathrm{A}}(\lambda_0).$$

Proposition 5.4.3 ensures that $I : \mathrm{H}^{-1/2}(\partial D) \to \mathrm{H}^{1/2}(\partial D)$ is an isomorphism. Moreover, Proposition 5.4.4 guarantees that $K(\lambda) : \mathrm{H}^{-1/2}(\partial D) \to \mathrm{H}^{1/2}(\partial D)$ is compact. Since $\lambda \mapsto K(\lambda)$ is analytic and since $\mathrm{A}(\lambda_1)$ is injective (Proposition 5.4.5), we deduce from the analytical Fredholm theorem that $\mathrm{A}(\lambda)$ is invertible for all $\lambda \in \mathbb{C} \setminus (\mathscr{S} \cup \{0\})$, except maybe for a discrete set of λ. □

In the remaining part of the note, we show the intermediate results needed in the above analysis.

5.4.2 Proof of the intermediate results

Proof of Proposition 5.4.3. For $h \in \mathrm{H}^{1/2}(\partial D)$, let us introduce the following interior transmission problem

$$\left|\begin{array}{l} \text{Find } (\tilde{u}, v) \in \mathrm{L}^2(D) \times \mathrm{L}^2(D) \text{ such that} \\ \Delta \tilde{u} - \lambda \tilde{n} \tilde{u} = 0 \quad \text{in } D \qquad\qquad \tilde{u} - v = 0 \quad \text{on } \partial D \\ \Delta v - \lambda v = 0 \quad \text{in } D \qquad\qquad \partial_\nu \tilde{u} - \partial_\nu v = h \quad \text{on } \partial D. \end{array}\right. \tag{5.78}$$

Due the features of $\tilde{n}$, the analysis of (5.78) is relatively simple. More precisely, since we have either $\tilde{n} - 1 \geq C > 0$ in D or $1 - \tilde{n} \geq C > 0$ in D, it is now well-known that (5.78) admits a unique solution for $\lambda \geq \lambda_0 \geq 0$. Since $\tilde{\mathrm{A}}(\lambda) : \mathrm{H}^{-1/2}(\partial D) \to \mathrm{H}^{1/2}(\partial D)$ is bounded (Lemma 5.4.2), this is enough to show that $\tilde{\mathrm{A}}(\lambda) : \mathrm{H}^{-1/2}(\partial D) \to \mathrm{H}^{1/2}(\partial D)$ is an isomorphism for $\lambda \geq \lambda_0$. □

Proof of Proposition 5.4.4. Let us prove that $\mathrm{A}(\lambda) - \tilde{\mathrm{A}}(\lambda_0) : \mathrm{H}^{-1/2}(\partial D) \to \mathrm{H}^{1/2}(\partial D)$ is a compact operator for all $\lambda \in \mathbb{C} \setminus (\mathscr{S} \cup \{0\})$. Denote u_0, $\tilde{u}_0$, v_0 the solutions of (5.75) with $\lambda = \lambda_0$. In Ω, set $w := \lambda^{-1}(u - v)$ and $\tilde{w}_0 := \lambda_0^{-1}(\tilde{u}_0 - v_0)$. Since $n = \tilde{n}$ in $\mathcal{V}$, these functions satisfy

$$\Delta w - \lambda n w = (n-1)v \text{ in } \mathcal{V} \qquad \text{and} \qquad \Delta \tilde{w}_0 - \lambda_0 n \tilde{w}_0 = (n-1)\tilde{v}_0 \text{ in } \mathcal{V}.$$

Introduce the function e such that $e = w - \tilde{w}_0$ in $\mathcal{V}$. We have

$$(\mathrm{A}(\lambda) - \tilde{\mathrm{A}}(\lambda_0))g = \partial_\nu e. \tag{5.79}$$

A direct calculation gives

$$\Delta e - \lambda n e = (n-1)(v - \tilde{v}_0) + (\lambda - \lambda_0) n \tilde{w}_0 \quad \text{in } \mathcal{V}. \tag{5.80}$$

Note that to obtain the equation (5.80), it was crucial in the definition of $A(\lambda)$, $\tilde{A}(\lambda)$ (see (5.76)) to divide by λ. Let us prove that the right hand side of (5.80) is in $H^1(\mathcal{V})$. We have $v - \tilde{v}_0 = 0$ on ∂D and $\Delta(v - \tilde{v}_0) - \lambda(v - \tilde{v}_0) = (\lambda - \lambda_0)\tilde{v}_0$ in D. Therefore, results of elliptic regularity ensure that $v - \tilde{v}_0 \in H^2(D)$ with

$$\|v - \tilde{v}_0\|_{H^2(D)} \leq C \|\tilde{v}_0\|_{L^2(D)} \leq C \|g\|_{H^{-1/2}(\partial D)}.$$

Using the equivalent of estimate (5.77) for $\tilde{w}_0$, we can write (here we use the assumption that $n \in W^{1,\infty}(\mathcal{V})$)

$$\|(n-1)(v - \tilde{v}_0) + (\lambda - \lambda_0) n \tilde{w}_0\|_{H^1(\mathcal{V})} \leq C \|g\|_{H^{-1/2}(\partial D)}. \tag{5.81}$$

Introduce $\mathcal{O} \subset \mathcal{V} \subset \Omega$ a neighbourhood of ∂D such that $(\overline{\mathcal{O}} \cap \Omega) \subset \mathcal{V}$. Since $e = 0$ on ∂D, from (5.80), (5.81), we obtain $e \in H^3(\mathcal{O})$ with $\|e\|_{H^3(\mathcal{O})} \leq C \|g\|_{H^{-1/2}(\partial D)}$. From (5.79), we infer that $A(\lambda) - \tilde{A}(\lambda_0)$ is a bounded operator from $H^{-1/2}(\partial D)$ to $H^{3/2}(\partial D)$. This is enough to conclude that $A(\lambda) - \tilde{A}(\lambda_0) : H^{-1/2}(\partial D) \to H^{1/2}(\partial D)$ is compact. □

Proof of Proposition 5.4.5. Let $g \in H^{-1/2}(\partial D)$ be in the kernel of $A(\lambda)$. Define the functions u, v as in (5.75). Introduce a smooth cut-off function ζ such that $\zeta = 1$ in $\mathcal{O}$ (the domain $\mathcal{O}$ is the one introduced after (5.81)) and $\zeta = 0$ in $D \setminus \overline{\mathcal{V}}$. Set $\mathfrak{u} := \zeta u$ (we extend u by zero in ω). Since $n = \tilde{n}$ on the support of ζ, we have

$$\left| \begin{array}{lcll} \Delta \mathfrak{u} - \lambda \tilde{n} \mathfrak{u} & = & \mathfrak{f} & \text{in } D \\ \Delta v - \lambda v & = & 0 & \text{in } D \\ (\mathfrak{u}, v) \in L^2(D) \times L^2(D) \text{ with } \mathfrak{e} := \mathfrak{u} - v \in H_0^2(D), & & & \end{array} \right. \tag{5.82}$$

where $\mathfrak{f} := 2\nabla u \cdot \nabla \zeta + u \Delta \zeta$. Results of interior regularity guarantee that $\mathfrak{f} \in L^2(D)$. Moreover, using the Lemma 5.4.7 below, one can prove the estimate

$$\|\mathfrak{f}\|_{L^2(D)} \leq C\, e^{-c\lambda} \|u\|_{L^2(\mathcal{O})}. \tag{5.83}$$

Here $c > 0$ is a constant independent of λ. Working from (5.82), we find

$$\left| \begin{array}{ll} \Delta \mathfrak{e} - \lambda \tilde{n} \mathfrak{e} = \mathfrak{f} + \lambda(\tilde{n} - 1) v & \text{in } D \\ \Delta \mathfrak{e} - \lambda \mathfrak{e} = \mathfrak{f} + \lambda(\tilde{n} - 1) \mathfrak{u} & \text{in } D. \end{array} \right.$$

Multiplying by $\overline{\mathfrak{e}}$ and integrating by parts, we deduce

$$\left| \begin{array}{l} \displaystyle\int_D |\nabla \mathfrak{e}|^2 + \tilde{n}\lambda |\mathfrak{e}|^2 \, dx = \int_D \mathfrak{f}\, \overline{\mathfrak{e}} \, dx + \lambda \int_D (1 - \tilde{n}) v \overline{\mathfrak{e}} \, dx \\ \displaystyle\int_D |\nabla \mathfrak{e}|^2 + \lambda |\mathfrak{e}|^2 \, dx = \int_D \mathfrak{f}\, \overline{\mathfrak{e}} \, dx + \lambda \int_D (1 - \tilde{n}) \mathfrak{u} \overline{\mathfrak{e}} \, dx. \end{array} \right.$$

Replacing $\mathfrak{e}$ by $\mathfrak{u} - v$ in the right hand sides, we obtain

$$\left| \begin{array}{l} \displaystyle\int_D |\nabla \mathfrak{e}|^2 + \tilde{n}\lambda |\mathfrak{e}|^2 \, dx + \lambda \int_D (1 - \tilde{n}) |v|^2 \, dx = \int_D \mathfrak{f}\, \overline{\mathfrak{e}} \, dx + \lambda \int_D (1 - \tilde{n}) v \overline{\mathfrak{u}} \, dx \\ \displaystyle\int_D |\nabla \mathfrak{e}|^2 + \lambda |\mathfrak{e}|^2 \, dx + \lambda \int_D (\tilde{n} - 1) |\mathfrak{u}|^2 \, dx = \int_D \mathfrak{f}\, \overline{\mathfrak{e}} \, dx - \lambda \int_D (1 - \tilde{n}) \mathfrak{u} \overline{v} \, dx. \end{array} \right. \tag{5.84}$$

Now multiplying the equation $\Delta v - \lambda v = 0$ in D by $\overline{\mathfrak{e}}$ and integrating twice by part, we get

$$0 = \int_D (\Delta v - \lambda v) \overline{\mathfrak{e}} \, dx = \int_D v (\Delta \overline{\mathfrak{e}} - \lambda \overline{\mathfrak{e}}) \, dx = \int_D v\, \overline{\mathfrak{f}} \, dx + \lambda \int_D (\tilde{n} - 1) v \overline{\mathfrak{u}} \, dx. \tag{5.85}$$

Using (5.85) in (5.84), we deduce that, for $\lambda > 0$,

$$\left| \begin{array}{l} \displaystyle\int_D |\nabla \mathfrak{e}|^2 + \tilde{n}\lambda|\mathfrak{e}|^2\,dx + \lambda\int_D (1-\tilde{n})|v|^2\,dx = \int_D \mathfrak{f}\,\overline{\mathfrak{e}}\,dx + \int_D v\,\overline{\mathfrak{f}}\,dx \\ \displaystyle\int_D |\nabla \mathfrak{e}|^2 + \lambda|\mathfrak{e}|^2\,dx + \lambda\int_D (\tilde{n}-1)|\mathfrak{u}|^2\,dx = \int_D \mathfrak{f}\,\overline{\mathfrak{e}}\,dx - \int_D \overline{v}\,\mathfrak{f}\,dx. \end{array} \right. \tag{5.86}$$

Now, thanks to (5.83), we can write

$$\begin{array}{rcl} \left| \displaystyle\int_D \mathfrak{f}\,\overline{\mathfrak{e}}\,dx + \int_D v\,\overline{\mathfrak{f}}\,dx \right| & \leq & C\,e^{-c\,\lambda}\|\mathfrak{u}\|_{\mathrm{L}^2(\mathcal{O})}\big(\|\mathfrak{e}\|_{\mathrm{L}^2(D)} + \|v\|_{\mathrm{L}^2(D)}\big) \\ & \leq & C\,e^{-c\,\lambda}\|\mathfrak{e}+v\|_{\mathrm{L}^2(\mathcal{O})}\big(\|\mathfrak{e}\|_{\mathrm{L}^2(D)} + \|v\|_{\mathrm{L}^2(D)}\big) \\ & \leq & C\,e^{-c\,\lambda}\big(\|\mathfrak{e}\|^2_{\mathrm{L}^2(D)} + \|v\|^2_{\mathrm{L}^2(D)}\big). \end{array} \tag{5.87}$$

Using (5.87) in the first identity of (5.86), we conclude that $\mathfrak{e} = v = 0$ in D for $\lambda > 0$ large enough when $1 - \tilde{n} \geq C > 0$ in D. This implies also $u = 0$ in Ω (by unique continuation), $g = 0$ on ∂D and shows that $\mathrm{A}(\lambda)$ is injective. Adapting (5.87) and using the second identity of (5.86), we prove similarly that $\mathrm{A}(\lambda)$ is injective for $\lambda > 0$ large enough when $\tilde{n}-1 \geq C > 0$ in D.□

Below, we state a classical result. Its proof can be found e.g. in [55, Lem. 3.1] or in [103, Lem. 2].

Lemma 5.4.7. *Let $\mathcal{U}$, $\mathcal{U}_{\mathrm{int}}$, be two domains with Lipschitz boundary such that $\overline{\mathcal{U}_{\mathrm{int}}} \subset \mathcal{U}$. Let $\gamma \in \mathrm{L}^\infty(\mathcal{U})$ be a function such that $\gamma \geq C > 0$ in $\mathcal{U}$. Then there are constants $C > 0$, $c > 0$ such that for any $\varphi \in \mathrm{L}^2(\mathcal{U})$ satisfying $\Delta\varphi - \lambda\gamma\varphi = 0$ in $\mathcal{U}$, for λ large enough, we have*

$$\|\varphi\|_{\mathrm{H}^1(\mathcal{U}_{\mathrm{int}})} \leq C\,e^{-c\,\lambda}\|\varphi\|_{\mathrm{L}^2(\mathcal{U}\setminus\mathcal{U}_{\mathrm{int}})}.$$

Chapter 6

Local estimates of crack densities in crack networks

Contents

6.1 Introduction

In inverse scattering theory, the main procedure which is followed while probing objects is simple: incident waves are sent to the object and information on the latter are deduced from the measured far field of the resulting scattered fields. When the obstacle is penetrable, many inversion algorithms, in particular the Sampling Methods (e.g. Linear Sampling Method (LSM) [47], Factorization Method (FM) [80], Generalized Linear Sampling Method (GLSM) [10]) require to avoid particular wavenumbers, called Transmission Eigenvalues. These values correspond to the spectrum of the Interior Transmission Problem (ITP), a boundary value problem defined on the support of the obstacle which combines two partial differential equations. The physical interpretation of TEs is that for such wavenumbers, an incident wave for which the resulting far field is arbitrarily small can be found. Because of the failure of the Sampling Methods at TEs, showing that they form at most a discrete set was imperative. This property has been proved in a general case [43, 113]. However, the importance of TEs recently increased as a result to a series of papers. It has been shown in [28, 31, 25] that TEs can be computed from far field data, and moreover that the knowledge of these can be used to infer qualitative information on the material [22, 31, 63, 66]. However, recovering sharp information from TEs is not an easy task.

The main difficulty relies in the fact that they cannot be viewed as the spectrum of a selfadjoint operator. To overcome this difficulty, recent works [6, 30, 5, 41] suggested to rather consider a modified spectrum that we refer to as Relative Transmission Eigenvalues (RTEs) and that can still be computed from far field data. The original proposed idea consists in the introduction of an artificial background that can be chosen by the observer. This time RTEs correspond to the spectrum of a new transmission problem, the Relative Transmission Problem(RTP), which indicates that for such wavenumbers there exists an incident field such that the far field resulting from the effective background and the one resulting from the artificial background are arbitrarily close. The advantage of using RTEs is that they depend on the artificial background which can be fit as desired, in accordance with the problem under consideration. Hence choosing the appropriate setting for the artificial obstacle, such as the position, the geometry, whether the obstacle is penetrable or not and the corresponding refractive index or boundary conditions, can greatly simplify the link between the RTEs and the parameters of interest. In this chapter we shall adapt these ideas for crack monitoring perspectives.

We consider the problem of identifying a set of cracks Γ embedded in some homogeneous background from measured far field data at multiple frequencies generated by acoustic waves. First of all we point out that this framework do not allow to define usual TEs since a crack has empty interior. Working with an artificial sound-soft (resp. sound-hard) obstacle Ω, we show that it is possible to define RTEs. The latter mainly correspond to the Dirichlet eigenvalues (DEs) (resp. Neumann eigenvalues (NEs)) for the Laplace operator in Ω, with the exception that the corresponding eigenfunction u satisfies the additional condition $\sigma(u) = 0$ on Γ, where σ denotes the boundary conditions on Γ. Hence, each RTE is a perturbation $\delta(\Omega, \Gamma)$ of a DE (resp. NE) which encodes the additional condition satisfied by the associated eigenfunction. In addition to this, we show that RTEs can be determined from the data. For this purpose, we adapt the framework of the use of GLSM to compute TEs [10]. Consequently, it is possible to measure the difference $\delta(\Omega, \Gamma)$ between the computed RTEs and the known DEs (resp. NEs). In the case of sound-soft cracks, sound-hard cracks or impedance cracks, we prove that $\Gamma \mapsto \delta(\Omega, \Gamma)$ is monotonous with respect to $\Gamma \cap \Omega$ for the inclusion order. This result led us to use $\delta(\Omega, \Gamma)$ as an estimator of $|\Gamma \cap \Omega|$: we refer this quantity to the localized crack density in Ω. At last, an indicator function of the local crack density at each point is obtained by repeating this process and computing $(\delta(\Omega + t, \Gamma))_t$ for a collection of artificial backgrounds $(\Omega + t)_{t \in A \subset \mathbb{R}^3}$, made of translations of Ω, which scans the probed area. The resolution of this method is fixed by the size of Ω. Numerical simulations carried in the a two dimensional setting validates expected behavior of this indicator function.

A weak point to the method described above is the high numerical cost of the computations of the RTEs associated to one artificial background. Since increasing the resolution (reduce the size of Ω) requires to increase the number of considered artificial backgrounds, imaging with high resolution may be prohibitive. To bypass this drawback, we suggest another method which requires to deal with far field data at only one fixed frequency. This alternative approach mix the notion of artificial background with the ideas of the Differential Linear Sampling Method [9]. Indeed we consider the same Ω of the previous paragraph and compare two functions u and $\widetilde{u}$ which are the solutions of two different problems. $\widetilde{u}$ is the solution of the Helmholtz equation in Ω whereas u is the solution of RTP, which is the Helmholtz equation on $\Omega \setminus \overline{\Gamma}$. On the one hand, $\widetilde{u}$ can be computed independently to the data. On the other hand, we show that when the wavenumber is not a RTE, the GLSM can be used to approximate u. Consequently it is possible to detect the presence of the crack by computing the difference between u and $\widetilde{u}$ which is non zero when $\Gamma \cap \Omega \neq \emptyset$. Repeating this procedure for a collection of artificial backgrounds allow in principle to determine the position of the crack. On the presented numerical simulation, it seems that this indicator moreover reveals the crack density of the probed medium.

After having introduced the notation in a first section, the inversion method using RTEs, and the one inspired by the DLSM are treated in two separate sections. In view of the preexisting works related to crack detection [11, 87, 19, 23], our method makes more sense when it comes to quantifying crack networks or aggregates of small cracks.

6.2 Setting of the problem

We consider a set of cracks $\Gamma \subset \mathbb{R}^d$, with $d = 2$ or 3, embedded in a homogeneous background. The cracks are modeled by non intersecting open arcs/surfaces which are a portion of the boundary of a Lipschitz domain A. The unit normal vector ν on Γ is chosen to be outward to A.

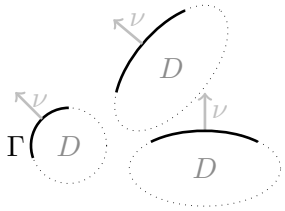

Figure 6.1: Example of setting in $\mathbb{R}^2$.

In this setting, the modeling of the scattering problem with the Helmholtz equation for the total field $u \in H^1_{loc}(\mathbb{R}^d \setminus \overline{\Gamma})$ reads

$$\left| \begin{array}{rcll} \Delta u + k^2 u & = & 0 & \text{in } \mathbb{R}^d \setminus \overline{\Gamma} \\ \sigma(u) & = & 0 & \text{on } \Gamma \end{array} \right. \tag{6.1}$$

where $k > 0$ is the wave number and $\sigma(u)$ a boundary operator that will be precised later. Given an incident field u_i, the scattered field $u_s := u - u_i$ then satisfies

$$\left| \begin{array}{rcll} \Delta u_s + k^2 u_s & = & 0 & \text{in } \mathbb{R}^d \setminus \overline{\Gamma} \\ \sigma(u_s) & = & -\sigma(u_i) & \text{on } \Gamma. \end{array} \right. \tag{6.2}$$

We select the outgoing solution of (6.2) which satisfies the Sommerfeld radiation condition,

$$\lim_{r \to +\infty} r^{\frac{d-1}{2}} \left(\frac{\partial u_s}{\partial r} - iku_s \right) = 0, \tag{6.3}$$

uniformly with respect to $x/|x|$. As a consequence, u_s has the following expansion

$$u_s(x) = e^{ik|x|} |x|^{-\frac{d-1}{2}} \left(u_s^\infty(\widehat{x}) + O(1/|x|) \right), \tag{6.4}$$

as $|x| \to +\infty$, uniformly in $\widehat{x} = x/|x| \in \mathbb{S}^{d-1}$, where $\mathbb{S}^{d-1}$ denotes the unit sphere of $\mathbb{R}^d$. The function $u_s^\infty : \mathbb{S}^{d-1} \to \mathbb{C}$, is called the far field pattern associated with u_i. We are interested in far field patterns associated with a particular class of incident waves called Herglotz wave functions defined for $g \in L^2(\mathbb{S}^{d-1})$ by

$$v_g := \int_{\mathbb{S}^{d-1}} g(\theta) e^{ik\theta \cdot x} \, \mathrm{ds}(\theta). \tag{6.5}$$

We denote by $u_s^\infty(\theta, \widehat{x})$ the far field pattern associated to $u_i(\theta, \cdot) := e^{ik\theta \cdot x}$ for $\theta \in \mathbb{S}^{d-1}$ (incident plane wave of direction θ). Thanks to the linearity of the scattering problem (6.2)-(6.3), the far field pattern associated to the Herglotz wave v_g is given by

$$(Fg)(\widehat{x}) = \int_{\mathbb{S}^{d-1}} g(\theta)\, u_s^\infty(\theta, \widehat{x})\, \mathrm{ds}(\theta). \tag{6.6}$$

This defines the so called far field operator $F : L^2(\mathbb{S}^{d-1}) \to L^2(\mathbb{S}^{d-1})$ which constitutes the data of the inverse scattering problem where one is interested in recovering qualitative information on the crack Γ.

In this chapter we propose two methods relying on the concept of artificial backgrounds to retrieve the position of the crack. The first approach which is a quite straightforward adaptation of the work in [6], where TEs with artificial backgrounds is introduced, is developed in the next section. The described method allows us to isolate the crack but also to quantify small crack aggregates. Nevertheless this technique requires data at multiple frequencies and its implementation is quite expensive. To overcome this issue we propose in a final section an alternative method inspired by the Differential Linear Sampling Method which requires only data at fixed frequency and fewer computations.

6.3 Quantification of crack density using relative transmission eigenvalues

The perturbation of measured far field data with far fields generated by an artificial background in order to simplify the transmission eigenvalue problem has been developed in [6] for isotropic inhomogeneities. In our setting, the use of artificial backgrounds is especially interesting because it allows to define a transmission problem which usually does not exist for scatterers of empty interior. After defining the relative far field operator, we will derive an associated boundary eigenvalue problem whose spectrum is shown to carry straightforward information on the cracks. Furthermore it will be shown that the spectrum can be computed from collected far field data at multiple frequencies. The possibility to quantify small crack aggregates with this spectrum will be illustrated with some numerical simulations.

6.3.1 The relative far field operator for cracks embedded in free space

We introduce an impenetrable obstacle $\Omega \subset \mathbb{R}^d$ of smooth boundary. We can freely choose the shape and the position of Ω but also the prescribed boundary condition on $\partial\Omega$ which will be generally denoted by an operator $\mathcal{B}$. For the latter, we will consider in our study two possibilities, either the Dirichlet boundary condition $\mathcal{B}w = w_{|\partial\Omega}$, or the Neumann boundary condition $\mathcal{B}w = \partial_\nu w_{|\partial\Omega}$. We will also denote by $\mathcal{B}^*$ the adjoint operator of $\mathcal{B}$. For a given incident wave u_i, we consider the exterior scattering problem to Ω: find $\widetilde{u}_s \in H^1_{loc}(\mathbb{R}^d \setminus \overline{\Omega})$ such that

$$\left|\begin{array}{rcll} \Delta\widetilde{u}_s + k^2\widetilde{u}_s & = & 0 & \text{in } \mathbb{R}^d \setminus \overline{\Omega} \\ \mathcal{B}\widetilde{u}_s & = & -\mathcal{B}u_i & \text{on } \partial\Omega \\ \lim\limits_{r\to+\infty} r^{\frac{d-1}{2}} \left(\dfrac{\partial\widetilde{u}_s}{\partial r} - ik\widetilde{u}_s\right) & = & 0. & \end{array}\right. \tag{6.7}$$

Similarly to the previous section, we define the far field operator $\widetilde{F} : L^2(\mathbb{S}^{d-1}) \to L^2(\mathbb{S}^{d-1})$ associated to problem (6.7). Note that $\widetilde{F}$ can be computed numerically independently from F. The relative far field operator $F^{rel} : L^2(\mathbb{S}^{d-1}) \to L^2(\mathbb{S}^{d-1})$ is finally defined by

$$F^{rel} := F - \widetilde{F}. \tag{6.8}$$

We now give a factorization of the relative far field operator. For $g \in L^2(\mathbb{S}^{d-1})$, let u_s^g and $\widetilde{u}_s^g$ be respectively the outgoing solutions of (6.2) and (6.7), for the same given incident field $u_i = v_g$. We define the quantity

$$w = \begin{cases} u_s^g - \widetilde{u}_s^g & \text{in } \mathbb{R}^d \setminus \overline{\Omega} \\ u_s^g + v_g & \text{in } \Omega \end{cases} \tag{6.9}$$

so that $w^\infty = F^{rel} g$. The function $w \in H^1_{loc}(\mathbb{R}^d \setminus \{\overline{\Omega} \cup \overline{\Gamma}\}) \times H^1(\Omega \setminus \overline{\Gamma})$ and satisfies

$$\left| \begin{array}{rcll} \Delta w + k^2 w & = & 0 & \text{in } \mathbb{R}^d \setminus \{\overline{\Omega} \cup \overline{\Gamma}\} \\ \sigma(w) & = & 0 & \text{on } \Gamma \cap \Omega \\ \lim\limits_{r \to +\infty} r^{\frac{d-1}{2}} & (& \frac{\partial w}{\partial r} - ikw) = 0 & \end{array} \right. \qquad \left| \begin{array}{rcll} [\mathcal{B}^* w] & = & -\psi_1 & \text{on } \partial\Omega \\ \sigma(w) & = & -\psi_2 & \text{on } \Gamma \cap \Omega^c \\ [\mathcal{B} w] & = & 0 & \text{on } \partial\Omega \end{array} \right. \tag{6.10}$$

where $\psi_1 = \mathcal{B}^*(v_g + \widetilde{u}_s^g)$ and $\psi_2 = \sigma(v_g + \widetilde{u}_s^g)$. We define the intermediate operators

$$\begin{array}{rccc} H_{\partial\Omega} : & L^2(\mathbb{S}^{d-1}) & \longrightarrow & X^*(\partial\Omega) \\ & g & \longmapsto & \mathcal{B}^*(v_g + \widetilde{u}_s^g) \end{array} \qquad \begin{array}{rccc} \Psi_\Gamma : & L^2(\mathbb{S}^{d-1}) & \longrightarrow & Y(\Gamma \cap \Omega^c) \\ & g & \longmapsto & \sigma(v_g + \widetilde{u}_s^g) \end{array} \tag{6.11}$$

where the spaces $X(\partial\Omega)$ and $Y(\Gamma \cap \Omega^c)$ correspond to Sobolev spaces on $\partial\Omega$ and $\Gamma \cap \Omega^c$ whose definition depends on the boundary conditions $\mathcal{B}$ and σ. We choose the usual ones, $H^{\frac{1}{2}}$ for Dirichlet boundary conditions and $H^{-\frac{1}{2}}$ for impedance boundary conditions. Furthermore, the space $X^*(\partial\Omega)$ denotes the dual space of $X(\partial\Omega)$. We then define

$$\begin{array}{rccc} H^{rel} : & L^2(\mathbb{S}^{d-1}) & \longrightarrow & X^*(\partial\Omega) \times Y(\Gamma \cap \Omega^c) \\ & g & \longmapsto & (H_{\partial\Omega} g, \Psi_\Gamma g), \end{array} \tag{6.12}$$

and

$$\begin{array}{rccc} G^{rel} : & X^*(\partial\Omega) \times Y(\Gamma \cap \Omega^c) & \longrightarrow & L^2(\mathbb{S}^{d-1}) \\ & (\psi_1, \psi_2) & \longmapsto & w^\infty, \end{array} \tag{6.13}$$

where w is the solution of (6.10). The following factorization of F^{rel} is then straightforward,

$$F^{rel} = G^{rel} H^{rel}. \tag{6.14}$$

6.3.2 Relative transmission eigenvalues

We are interested in numbers $k \in \mathbb{C}$ for which the nullspace of G^{rel} is not trivial. For such a k there exists a non trivial element $(\psi_1, \psi_2) \in X^*(\partial\Omega) \times Y(\Gamma \cap \Omega^c)$ such that the solution $w \in H^1_{loc}(\mathbb{R}^d \setminus \{\overline{\Omega} \cup \overline{\Gamma}\}) \times H^1(\Omega \setminus \overline{\Gamma})$ of (6.10) satisfies $w^\infty = 0$. The Rellich Lemma then implies that w vanishes in $\mathbb{R}^d \setminus \overline{\Omega}$. Consequently, we deduce from (6.10) that w satisfies

$$\left| \begin{array}{rcll} \Delta w + k^2 w & = & 0 & \text{in } \Omega \setminus \overline{\Gamma} \\ \mathcal{B} w & = & 0 & \text{on } \partial\Omega \\ \sigma(w) & = & 0 & \text{on } \Gamma \cap \Omega. \end{array} \right. \tag{6.15}$$

Definition 6.3.1. *$k > 0$ is a Relative Transmission Eigenvalue (RTE) if there exists a non trivial solution $w \in H^1(\Omega \setminus \overline{\Gamma})$ to (6.15).*

We make a first simple observation: if the chosen artificial background Ω is such that $\Omega \cap \overline{\Gamma} = \emptyset$, then the relative transmission eigenvalues correspond to the spectrum of the following problem,

$$\left| \begin{array}{rcll} \Delta w + k^2 w & = & 0 & \text{in } \Omega \\ \mathcal{B} w & = & 0 & \text{on } \partial\Omega \end{array} \right. \tag{6.16}$$

which can be computed independently from the data (we recall that Ω is chosen independently from Γ). It will be shown in the next paragraph that the spectrum of (6.15) can be computed from far field data. Consequently it is possible to determine whether $\Omega \cap \Gamma$ is empty or not by comparing the computed spectrum of (6.15) with the spectrum of (6.16). Furthermore, for particular boundary values $\sigma(w)$, we can be more precise: the values $\tau = k^2$ for which there exists a non trivial solution to (6.15) are monotonous with respect to $\Gamma \cap \Omega$ (for the inclusion order). Such a result gives a justification of the quantification of the amount of cracks contained in the localized area Ω. We now enumerate the different possibilities for the boundary operator σ which fits to this framework and show the monotonous result for the eigenvalues in each case. We also choose $\mathcal{B}w = w_{|\partial\Omega}$ in the study but one can easily adapt the results for the Neumann boundary conditions.

Sound soft cracks

The variational formulation of the following problem: $w \in H^1(\Omega \setminus \overline{\Gamma})$ such that for a given data $f \in L^2(\Omega)$

$$\left| \begin{array}{rcll} \Delta w & = & f & \text{in } \Omega \setminus \overline{\Gamma} \\ w & = & 0 & \text{on } \Gamma \\ w & = & 0 & \text{on } \partial\Omega \end{array} \right. \tag{6.17}$$

is, $w \in E^D(\Omega, \Gamma) := \{u \in H^1(\Omega) \mid u = 0 \text{ on } (\Gamma \cap \Omega) \cup \partial\Omega\}$ such that

$$\forall \varphi \in E^D(\Omega, \Gamma), \quad \int_\Omega \nabla w \nabla \overline{\varphi} \, \mathrm{d}x = \int_\Omega f \overline{\varphi} \, \mathrm{d}x. \tag{6.18}$$

Consequently if $\sigma(w) = w$ on Γ, the spectrum of (6.15) is made of positive reals $0 < \tau_0^D(\Omega, \Gamma) \leq \tau_1^D(\Omega, \Gamma) \leq \cdots \leq \tau_p^D(\Omega, \Gamma) \leq \ldots$ that satisfy the following min max principle [92],

$$\tau_j^D(\Omega, \Gamma) = \min_{W \subset U_j^D(\Gamma)} \max_{w \in W \setminus \{0\}} \frac{\displaystyle\int_\Omega |\nabla w|^2 \, \mathrm{d}x}{\displaystyle\int_\Omega |w|^2 \, \mathrm{d}x} \tag{6.19}$$

where $U_j^D(\Gamma)$ denotes the sets of the j-dimensional subspaces of $E^D(\Omega, \Gamma)$. Now consider two sets of cracks Γ_1 and Γ_2 such that $\Omega \cap \Gamma_1 \subset \Omega \cap \Gamma_2$. Since $U_j^D(\Gamma_1)$ contains all the j-dimensional subspaces of $\{w \in H^1(\Omega) \mid u = 0 \text{ on } \Gamma_2 \cap \Omega\}$, we deduce the following monotonicity result,

$$(\Omega \cap \Gamma_1) \subset (\Omega \cap \Gamma_2) \implies \forall j \in \mathbb{N}, \quad \tau_j^D(\Omega, \Gamma_1) \leq \tau_j^D(\Omega, \Gamma_2). \tag{6.20}$$

Sound hard cracks

Similarly, it can be shown that if $\sigma(w) = 0$ is replaced by the Neumann boundary conditions $\partial_\nu^\pm w = 0$ on Γ, then the spectrum of (6.15) is made of positive reals $0 < \tau_0^N(\Omega, \Gamma) \leq \tau_1^N(\Omega, \Gamma) \leq \cdots \leq \tau_p^N(\Omega, \Gamma) \leq \ldots$ that satisfy the following min max principle,

$$\tau_j^N(\Omega,\Gamma) = \min_{W\subset U_j^N(\Gamma)} \max_{w\in W\setminus\{0\}} \frac{\displaystyle\int_\Omega |\nabla w|^2\,\mathrm{d}x}{\displaystyle\int_\Omega |w|^2\,\mathrm{d}x} \tag{6.21}$$

where $U_j^N(\Gamma)$ denotes the set of the j-dimensional subspaces of $E^N(\Omega,\Gamma) := \{u \in H^1(\Omega\setminus\overline{\Gamma}) \,|\, u = 0 \text{ on } \partial\Omega\}$. Now consider two sets of cracks Γ_1 and Γ_2 such that $\Omega\cap\Gamma_1 \subset \Omega\cap\Gamma_2$. Since $U_j^N(\Gamma_2)$ contains all the j-dimensional subspaces of $E^N(\Omega,\Gamma_1)$, we deduce the following monotonicity result,

$$(\Omega\cap\Gamma_1)\subset(\Omega\cap\Gamma_2) \implies \forall j\in\mathbb{N},\quad \tau_j^N(\Omega,\Gamma_1)\geq\tau_j^N(\Omega,\Gamma_2). \tag{6.22}$$

Impedance boundary conditions

We consider the following impedance boundary conditions on the crack, $\sigma(w) = \partial_\nu^\pm w \mp \lambda^\pm w^\pm$ on Γ where $\lambda^\pm$ are non negative functions. We define the two following operators $\mathbb{A}$, $\mathbb{B}$ on $E^N(\Omega,\Gamma)$ by the use of the Riesz representation theorem:

$$\langle \mathbb{A}\phi,\psi\rangle = \int_\Omega \nabla\phi\overline{\nabla\psi}\,\mathrm{d}x + \int_\Gamma (\lambda^+\phi^+\overline{\psi^+} + \lambda^-\phi^-\overline{\psi^-})\,\mathrm{d}s(x) + \tau_0\int_\Omega \phi\overline{\psi}\,\mathrm{d}x \tag{6.23}$$

and

$$\langle \mathbb{B}\phi,\psi\rangle = \int_\Omega \phi\overline{\psi}\,\mathrm{d}x \tag{6.24}$$

for all $\phi,\psi\in E^N(\Omega,\Gamma)$. The τ_0 has to be chosen so that the $\mathbb{A}$ is coercive. With these notations, τ is in the spectrum of (6.15) if and only if there exists a non trivial element $w\in E^N(\Omega,\Gamma)$ such that $\mathbb{A}w = (\tau+\tau_0)\mathbb{B}w$. Consequently, the spectrum of (6.15) is made of reals $-\tau_0 \leq \tau_0^I(\Omega,\Gamma) \leq \tau_1^I(\Omega,\Gamma)\leq\cdots\leq\tau_p^I(\Omega,\Gamma)\leq\ldots$ which again satisfy the min max principle [29, Theorem 4.3]

$$\tau_j^I(\Omega,\Gamma)+\tau_0 = \min_{W\subset U_j^N(\Gamma)} \max_{w\in W\setminus\{0\}} \frac{\langle \mathbb{A}w,w\rangle}{\langle \mathbb{B}w,w\rangle}. \tag{6.25}$$

Hence we obtain the same result as for the case of sound hard cracks, that is for two given sets of cracks Γ_1 and Γ_2 we have

$$(\Omega\cap\Gamma_1)\subset(\Omega\cap\Gamma_2) \implies \forall j\in\mathbb{N}\quad \tau_j^I(\Omega,\Gamma_1)\geq\tau_j^I(\Omega,\Gamma_2). \tag{6.26}$$

6.3.3 Computation of the relative transmission eigenvalues from the data

In this section we show that the RTEs can be computed from the data. The method we use is similar to the one used for the characterization of classical transmission eigenvalues from the failure of the Linear Sampling Method for particular wavenumbers k [28]. In our case, it relies on the fact that when k is a RTE, the approximate solution of the far field equation

$$F^{rel}g = \Phi_z^\infty \tag{6.27}$$

cannot be associated with Herglotz waves with finite norm for z in a subset $U\subset\Omega$ of non empty interior, where Φ_z^∞ is the far field of $\Phi(z,\cdot)$, the outgoing solution of the equation

$$\Delta\Phi(z,\cdot)+k^2\Phi(z,\cdot) = -\delta_z. \tag{6.28}$$

We also add to our method the same improvement provided by the Generalized Linear Sampling Method [**?**]. Instead of approximating the solution of (6.27) by the Tikonov regularization, we rather use a penalization which controls the quantity $\|H^{rel}g\|$, which blows up when k is a RTE. We begin with the simple but fundamental following result.

Lemma 6.3.2. *Assume that k is not a RTE. Then $\Phi_z^\infty \in R(G^{rel})$ if and only if $z \in \Omega$.*

Proof. Assume that k is not a RTE and let $z \in \Omega$. The assumption on k implies that the following problem of seeking $w \in H^1(\Omega \setminus \overline{\Gamma})$ for given $f \in H^{\frac{1}{2}}(\partial\Omega)$ such that

$$\left| \begin{array}{rcll} \Delta w + k^2 w & = & 0 & \text{in } \Omega \setminus \overline{\Gamma} \\ \sigma(w) & = & 0 & \text{on } \Gamma \cap \Omega \\ \mathcal{B}w & = & f & \text{on } \partial\Omega. \end{array} \right. \tag{6.29}$$

is well posed. Let w_{int} be the solution of this problem with $f = \mathcal{B}\Phi_{z|\partial\Omega}$. We define $w \in H^1_{loc}(\mathbb{R}^d \setminus \overline{\Omega}) \times H^1(\Omega \setminus \overline{\Gamma})$ with $w = w_{int}$ in Ω and $w = \Phi_z$ in $\mathbb{R}^d \setminus \{\overline{\Omega} \cup \overline{\Gamma}\}$. Then w is a solution to (6.10) with $\psi_1 = \mathcal{B}^*(\Phi_z - w_{int})$ and $\psi_2 = \sigma(\Phi_z)$.

Now let $z \in \mathbb{R}^d \setminus \overline{\Omega}$. Assume that there exists $(\psi_1, \psi_2) \in X^*(\partial\Omega) \times Y(\Gamma \cap \Omega^c)$ such that $G(\psi_1, \psi_2) = \Phi_z^\infty$. By the Rellich's Lemma we deduce that $w = \Phi_z$, where w is the solution to (6.10). This gives a contradiction since $w \in H^1_{loc}(\mathbb{R}^d \setminus \overline{\Omega})$ whereas $\Phi_z \notin H^1_{loc}(\mathbb{R}^d \setminus \overline{\Omega})$ because of its singularity at z. □

In the following lemma we show the possibility to define a penalization term P from the data which controls both $\|H_{\partial\Omega}g\|$ and $\|\Psi_\Gamma g\|$. (We recall that $\|\cdot\|$ denotes the norm in the arrival space of each mapping).

Lemma 6.3.3. *Assume that k is not an eigenvalue of (6.16). For $g \in L^2(\mathbb{S}^{d-1})$ define*

$$P(g) := \langle F^\sharp g, g\rangle + \langle \widetilde{F} g, g\rangle \tag{6.30}$$

where $F^\sharp = |\Re\mathrm{e} F| + \Im\mathrm{m} F$ and $\widetilde{F}^\sharp = |\Re\mathrm{e}\widetilde{F}| + \Im\mathrm{m}\widetilde{F}$. Then there exists a constant $C > 0$ such that

$$\forall g \in L^2(\mathbb{S}^{d-1}), \quad P(g) \geq C\|H^{rel}g\|^2_{X^*(\partial\Omega)\times Y(\Gamma\cap\Omega^c)} \tag{6.31}$$

Proof. We introduce the following operators

$$S_k : \begin{array}{ccc} H^{-\frac{1}{2}}(\Gamma) & \longrightarrow & H^{\frac{1}{2}}(\Gamma) \\ \varphi & \longmapsto & \int_\Gamma \Phi(x,y)\varphi(y)ds(y) \end{array} \quad \text{and} \quad N_k : \begin{array}{ccc} H^{\frac{1}{2}}(\Gamma) & \longrightarrow & H^{-\frac{1}{2}}(\Gamma) \\ \varphi & \longmapsto & \partial_\nu \int \varphi(y)\partial_\nu\Phi(x,y)ds(y). \end{array}$$

All the properties of $\widetilde{F}$, S_k and N_k used in the following can be found in [83, Theorems 1.15 & 1.26 and Lemma 1.14]. The operator $\widetilde{F}$ satisfies a first factorization of the form

$$\widetilde{F} = H^\star_{\partial\Omega}\widetilde{T}_1 H_{\partial\Omega} \tag{6.32}$$

where $\widetilde{T}_1 = -S_k^\star$ in case of the Dirichlet boundary condition for $\mathcal{B}$ and $\widetilde{T}_1 = -N_k^\star$ in the case of the Neumann boundary condition for $\mathcal{B}$. The coercivity property of $S_i^\star$ and $N_i^\star$ and the compactness of $S_k^\star - S_i^\star$ and $N_k^\star - N_i^\star$ implies that

$$\widetilde{F}^\sharp = H^\star_{\partial\Omega}\widetilde{T}_1^\sharp H_{\partial\Omega} \tag{6.33}$$

where $\widetilde{T}_1^\sharp$ is coercive provided that k is not an eigenvalue of (6.16). Therefore

$$\forall g \in L^2(\mathbb{S}^{d-1}), \quad \langle \widetilde{F}^\sharp g, g\rangle = \langle \widetilde{T}_1^\sharp H_{\partial\Omega}g, H_{\partial\Omega}g\rangle \geq c\|H_{\partial\Omega}g\|^2_{X^*(\partial\Omega)}. \tag{6.34}$$

This shows that $P(g)$ controls $\|H_{\partial\Omega} g\|^2_{X^*(\partial\Omega)}$. We now show that it also controls $\|\Psi_\Gamma g\| = \|\sigma(\widetilde{u}_s + v_g)\|$ where $\widetilde{u}_s$ is the solution of (6.7) with $u_i = v_g$. It can be shown that $\widetilde{F}$ satisfies a second factorization in the form

$$\widetilde{F} = H^\star \widetilde{T}_2 H \tag{6.35}$$

where $H : g \mapsto \mathcal{B} v_g$ and $\widetilde{T}_2$ satisfies properties similar as $\widetilde{T}_1$. Therefore,

$$\langle \widetilde{F}^\sharp g, g\rangle = \langle \widetilde{T}_2^\sharp H g, Hg\rangle \geq c\|\mathcal{B} v_g\|^2_{X(\partial\Omega)}. \tag{6.36}$$

It is known that problem (6.7) is well posed and that all the derivatives of the solution on bounded subsets of $\mathbb{R}^d \setminus \overline{\Omega}$ depends continuously on the boundary data $\mathcal{B} v_{g|\partial\Omega}$ [44, Theorems 3.11 & 3.12]. Consequently (6.36) implies

$$\langle \widetilde{F}^\sharp g, g\rangle \geq \|\sigma(\widetilde{u}_s)\|^2_{Y(\Gamma\cap\Omega^c)}. \tag{6.37}$$

It remains to control $\sigma(v_g)$ on $\Gamma \cap \Omega^c$, the latter is ensured by the properties of $F^\sharp$ that can be found in the literature. For instance in the case of impedance boundary condition on the cracks, it is shown in [18] that $F^\sharp$ satisfies the following factorization

$$F^\sharp = H_\Gamma^\star T^\sharp H_\Gamma \tag{6.38}$$

where $H_\Gamma : g \mapsto \sigma(v_g)$ and $T^\sharp$ also satisfies a coercivity property similar to $\widetilde{T}_1^\sharp$. Consequently

$$\langle F^\sharp g, g\rangle = \langle T^\sharp H_\Gamma g, H_\Gamma g\rangle \geq c\|\sigma(v_g)\|^2. \tag{6.39}$$

Finally by using estimates (6.34),(6.37) and (6.39) we conclude that

$$\exists C > 0, \quad \forall g \in L^2(\mathbb{S}^{d-1}), \quad P(g) \geq C\left(\|\mathcal{B}^*(v_g + \widetilde{u}_s)\|^2_{X^*(\partial\Omega)} + \|\sigma(v_g + \widetilde{u}_s)\|^2_{Y(\Gamma\cap\Omega^c)}\right). \tag{6.40}$$

□

We now have all the ingredients to show that RTEs can be determined from the data. Define

$$J_z^\alpha(g) := \alpha P(g) + \|F^{rel} g - \Phi_z^\infty\|^2_{L^2(\mathbb{S}^2)}. \tag{6.41}$$

We denote by j_z^α the infimum of J_z^α:

$$j_z^\alpha = \inf_{g \in L^2(\mathbb{S}^{d-1})} J^\alpha(g) \tag{6.42}$$

and define a sequence $g_z^\alpha \in L^2(\mathbb{S}^2)$ such that

$$J_z^\alpha(g_z^\alpha) \leq j_z^\alpha + C\alpha^\eta, \quad \eta > 2. \tag{6.43}$$

Roughly speaking, the quantity $\lim_{\alpha\to 0} P(g_z^\alpha)$ is shown to blow up only when k is a RTE. We proceed in two steps and begin with the following result,

Theorem 6.3.4. *Assume that k is not a RTE. Then $\forall z \in \Omega$, $\limsup_{\alpha\to 0} P(g_z^\alpha) < +\infty$.*

Proof. Let $z \in \Omega$. From the definition of J_z^α, g_z^α and j_z^α, there holds

$$\alpha P(g_z^\alpha) \leq J_\alpha(g_z^\alpha) \leq j_z^\alpha + C\alpha^\eta. \tag{6.44}$$

According to Lemma 6.3.2, there exists $\varphi_z = (\varphi_1^z, \varphi_2^z) \in X^*(\partial\Omega) \times Y(\Gamma \cap \Omega^c)$ such that $G^{rel}(\varphi_1^z, \varphi_2^z) = \Phi_z^\infty$. Let $g_0 \in L^2(\mathbb{S}^{d-1})$ be such that $\|H^{rel} g_0 - \varphi_z\| < \alpha$. Estimate (6.44) gives

$$\alpha P(g_z^\alpha) \leq \alpha P(g_0) + \|G^{rel} H^{rel} g_0 - \Phi_z^\infty\| + C\alpha^\eta. \tag{6.45}$$

The continuity of G^{rel} then implies,

$$\begin{aligned} \alpha P(g_z^\alpha) &\leq \alpha P(g_0) + \|G^{rel}\| \|H^{rel} g_0 - \varphi_z\| + C\alpha^\eta \\ &\leq \alpha P(g_0) + \alpha \|G^{rel}\| + C\alpha^\eta. \end{aligned} \tag{6.46}$$

Hence $\limsup_{\alpha \to 0} P(g_z^\alpha) < +\infty$. □

The final step allowing one to compute RTEs is the following result complementary to the previous one.

Theorem 6.3.5. *Assume that k is a RTE. Assume furthermore that k^2 is not an eigenvalue of (6.16) and that F^{rel} has dense range. Then for all subdomain $A \subset \Omega$ such that $(\Gamma \cap \Omega) \subset A$, the function $z \mapsto \liminf_{\alpha \to 0} P(g_z^\alpha)$ does not belong to $L^\infty(\Omega \setminus \overline{A})$.*

Proof. We proceed by using a contradiction argument. Assume that

$$\exists M > 0 \text{ such that } \liminf_{\alpha \to 0} P(g_z^\alpha) \leq M \text{ for a.e } z \in \Omega \setminus \overline{A}. \tag{6.47}$$

Let $z \in \Omega \setminus \overline{A}$. The result of Lemma 6.3.3 (which requires that k^2 is not an eigenvalue of (6.16)) implies the existence of a subsequence $\psi_z^n := H^{rel} g_z^{\alpha_n}$ such that ψ_z^n converges weakly to a limit denoted $\psi_z \in X^*(\partial\Omega) \times Y(\Gamma \cap \Omega)$. Furthermore the assumption on the denseness of the range of F^{rel} implies that $F^{rel} g_z^\alpha \to \Phi_z^\infty$ when $\alpha \to 0$. Then the compactness of G^{rel} implies that $G^{rel}\psi_z = \Phi_z^\infty$. Now by definition of G^{rel}, there exists a solution $w_z \in H^1_{loc}(\mathbb{R}^d \setminus \{\overline{\Omega} \cup \overline{\Gamma}\}) \times H^1(\Omega \setminus \overline{\Gamma})$ of (6.10) such that $w_z^\infty = \Phi_z^\infty$. The Rellich's Lemma implies that w_z satisfies the following equations,

$$\left| \begin{array}{rcll} \Delta w_z + k^2 w_z & = & 0 & \text{in } \Omega \setminus \overline{\Gamma} \\ \sigma(w_z) & = & 0 & \text{on } \Gamma \cap \Omega \\ \mathcal{B} w_z & = & \mathcal{B}\Phi_z & \text{on } \partial\Omega. \end{array} \right. \tag{6.48}$$

We have shown the existence of a solution $w_z \in H^1(\Omega \setminus \overline{\Gamma})$ for all $z \in \Omega \setminus \overline{A}$ to equation (6.48). We now show that this is not compatible with the fact that k is a RTE. Indeed let w_0 be an eigenfunction of (6.15). Then multiplying the first equation of (6.48) with w_0 and using Green's second formula gives

$$\begin{aligned} 0 = &\int_{\partial\Omega} (\partial_\nu w_0 w_z - w_0 \partial_\nu w_z)\, \mathrm{ds}(x) \\ &+ \int_{\Gamma \cap \Omega} \left(\partial_\nu^- w_0^- w_z^- - w_0^- \partial_\nu^- w_z\right) \mathrm{ds}(x) - \int_{\Gamma \cap \Omega} \left(\partial_\nu^+ w_0 w_z^+ - w_0^+ \partial_\nu^+ w_z\right) \mathrm{ds}(x). \end{aligned} \tag{6.49}$$

Since $\sigma(w_0) = \sigma(w_z) = 0$ on Γ, the sum on Γ in the above equation is zero whatever the choice for σ (Dirichlet, Neumann or impedance boundary condition). Consequently, since $\mathcal{B} w_0 = 0$ and $\mathcal{B} w_z = \mathcal{B}\Phi_z$ on $\partial\Omega$, we have shown

$$\forall z \in \Omega \setminus \overline{A}, \quad \int_{\partial\Omega} (\partial_\nu w_0 \Phi_z - w_0 \partial_\nu \Phi_z)\, \mathrm{ds}(x) = 0. \tag{6.50}$$

The Green's representation theorem together with this last equation imply that

$$\forall z \in \Omega \setminus \overline{A}, \quad w_0(z) \quad = \int_{\Gamma\cap\Omega} [w_0]\partial_\nu \Phi_z \,\mathrm{ds}(x) - \int_{\Gamma\cap\Omega} [\partial_\nu w_0]\Phi_z \,\mathrm{ds}(x). \tag{6.51}$$

The function $\widetilde{w}_0(z) \in H^1_{loc}(\mathbb{R}^d \setminus \overline{A})$ defined by

$$\widetilde{w}_0(z) := \int_{\Gamma\cap\Omega} [w_0]\partial_\nu \Phi_z \,\mathrm{ds}(x) - \int_{\Gamma\cap\Omega} [\partial_\nu w_0]\Phi_z \,\mathrm{ds}(x) \tag{6.52}$$

is an outgoing solution to Helmholtz equation and coincides with w_0 on $\Omega \setminus \overline{A}$. We observe from (6.51) that $\mathcal{B}\widetilde{w}_0 = \mathcal{B}w = 0$ on $\partial\Omega$, consequently $\widetilde{w}_0 = 0$ on $\mathbb{R}^d \setminus \overline{\Omega}$ [29, corollary 1.3]. The unique continuation principle then implies that $\widetilde{w}_0 = 0$ on $\Omega \setminus \overline{A}$. This implies that $w_0 = 0$ which gives a contradiction to (6.47). □

Remark 6.3.6. *Theorems 6.3.4 and 6.3.5 suggest that RTEs corresponds to values of k for which peaks are observed in the curve*

$$f : k \mapsto \int_{\Omega\setminus\overline{A}} P(g_z^\alpha)\, \mathrm{d}z \tag{6.53}$$

for small values of α and any subdomain A of Ω - but only provided that k^2 is not simultaneously an eigenvalue of (6.16). However, as it will be mentioned in the numerical algorithm, this latter restriction can be easily removed.

6.3.4 Description of the inversion algorithm

Crack detection in a localized area

Let $(F(k))_{k\in[k_m,k_M]}$ be the far field operators for wavenumbers $k \in [k_m, k_M]$ associated to a material made of cracks embedded in an homogeneous background. A first idea of using RTE to perform crack monitoring is to determine from the data $(F(k))_{k\in[k_m,k_M]}$ if there are cracks in a neighborhood of a point $t \in \mathbb{R}^d$. Set $\Omega := B(t, r)$ where $r > 0$ is somehow related to the resolution of the method. The procedure we shall describe is simple and requires to consider only the first RTE $\tau_0(\Omega, \Gamma)$. We first compute the relative far field operators $(F^{rel}(k))_{k\in[k_m,k_M]}$ with formula (6.8), then for all $k \in [k_m, k_M]$ approximate the far field equation $F^{rel}(k)g = \Phi_z^\infty$ by computing $g_z^\alpha(k)$ which is given by (6.43) for small values of α. Then compute $\tau_0(\Omega, \Gamma) = k^2$ which corresponds to the first peak in the curve

$$\mathcal{E}_\Omega \mapsto \int_{\Omega\setminus\overline{A}} P(g_z^\alpha(k))\, \mathrm{d}z. \tag{6.54}$$

Let $\tau_0(\Omega, \emptyset)$ be the first eigenvalue of (6.16) that can be computed independently from the data $(F(k))_{k\in[k_m,k_M]}$. Since $\tau_0(\Omega, \Gamma)$ is a perturbation of $\tau_0(\Omega, \emptyset)$, we precise at this point that k_m and k_M should be chosen such that $\tau_0(\Omega, \emptyset) \subset [k_m, k_M]$. We then have the following result,

$$|\tau_0(\Omega, \Gamma) - \tau_0(\Omega, \emptyset)| \neq 0 \implies \Gamma \cap \Omega \neq \emptyset. \tag{6.55}$$

This result is not satisfactory since it may be possible to have $\Gamma \cap \Omega \neq \emptyset$ and $\tau_0(\Omega, \Gamma) = \tau_0(\Omega, \emptyset)$, in which case the possbility to compute $\tau_0(\Omega, \Gamma)$ is not even covered by the theory (see Remark 6.3.6). We propose a solution to overcome this issue as follows.

The crack location can be identified by repeating the previous procedure for many artificial backgrounds which scans an a priori known location of the crack $U \subset \mathbb{R}^d$. Define the collection of artificial backgrounds $(\Omega_t)_{t\in U} = (B(t,r))_{t\in U}$ and denote with $\tau_0(\Omega_t, \Gamma)$ the computed first RTE associated to each Ω_t. We observe that

$$|\tau_0(\Omega_t, \Gamma) - \tau_0(\Omega_0, \emptyset)| \neq 0 \implies \Gamma \cap \Omega_t \neq \emptyset. \tag{6.56}$$

Then defining the following indicator function,

$$I(t) = \int_{B(t,r)} |\tau_0(\Omega_x, \Gamma) - \tau_0(\Omega_0, \emptyset)| \, \mathrm{d}x, \tag{6.57}$$

we expect the existence of $x \in B(t,r)$ such that $\tau_0(\Omega_x, \Gamma) \neq \tau_0(\Omega_0, \emptyset)$ which implies the equivalence $I_\Gamma(t) = 0 \iff \Gamma \cap \Omega_t = \emptyset$. A rigorous proof of this statement is under study.

Crack densities

It has been shown in section 6.3.2 that if we have an a priori information of the boundary condition σ (Dirichlet, Neumann or impedance), then for a fixed artificial background Ω, the quantity $\tau_0(\Omega, \Gamma)$ is monotonous with respect to $\Gamma \cap \Omega$ for the inclusion order. Consequently, for fixed t, the function

$$\Gamma \cap \Omega_t \mapsto I_\Gamma(t) \tag{6.58}$$

is a monotonous function for the inclusion order. Although it is not true, we extrapolate this result and assume the following:

the quantity $I_\Gamma(t)$ depends only on $|\Gamma \cap \Omega_t|$,
furthermore the function $|\Gamma \cap \Omega_t| \mapsto I_\Gamma(t)$ is monotonous.

Under this assumption, we expect that if $I_\Gamma(t_1) \leq I_\Gamma(t_2)$ for $t_1, t_2 \in \mathbb{R}^d$, then $|\Gamma \cap \Omega_{t_1}| \leq |\Gamma \cap \Omega_{t_2}|$. In other words, the indicator function $I_\Gamma(t)$ does not only give information on the position of the crack but also a qualitative information on $|\Gamma \cap \Omega_t|$. In the next section we test this indicator function in a two dimensional setting for sound hard cracks.

6.3.5 Numerical validation of the algorithm

Data generation and computation of the relative far field operator

We conclude this section by applying the indicator function (6.57) to simulated backgrounds made of sound hard crack networks. For a given wavenumber k, a discretization of the far field operator F is generated by solving numerically the direct problem (6.2) for multiple incident fields $u_i(\theta_p, x) = e^{-ikx\cdot\theta_p}$. Then we compute the matrix $F = (u_s^\infty(\theta_p, \widehat{x_q}))_{p,q}$ for θ_p, $\widehat{x_q}$ in $\{\cos(\frac{2l\pi}{100}), \sin(\frac{2l\pi}{100}),\ l = 1..100\}$ (somehow we discretize $L^2(\mathbb{S}^1)$). We then add random noise to the simulated F and obtain a noisy far field data F^δ defined by $F^\delta_{pq} = F_{pq}(1 + \eta N)$. Here N is a complex random variable whose real and imaginary parts are uniformly chosen in $[-1, 1]^2$. The parameter $\eta > 0$ is chosen so that $\|F^\delta - F\| \leq \delta$. We repeat this process for multiple wavenumbers $k \in [k_m, k_M]$ to obtain a collection of noisy far field data $(F^\delta(k))_{k\in[k_m,k_M]}$.

We have chosen the ball for the geometry of the artificial obstacles $\Omega_t = B(t,r)$ because it is the only geometry for which an analytic expression of the far field pattern associated to problem (6.7) is known. As described next, this considerably accelerates the computation of the relative far field operators $F_t^{rel}(k)$ associated to the background Ω_t from the given data $F(k)$. Furthermore we have chosen to prescribe the Dirichlet boundary conditions $\mathcal{B}w = w_{|\partial\Omega_t}$ on the

boundary of the artificial backgrounds. Consequently k_m ad k_M have been chosen such that $[k_m, k_M]$ contains the first Dirichlet eigenvalue of $B(0,r)$. Now let $u_i(\theta, x) = e^{ikx\cdot\theta}$ and consider the solution $\widetilde{u}_s(\cdot,\theta,k,t)$ of (6.7) with $\Omega = \Omega_t$. Firstly for $t = 0$, the scattered field $\widetilde{u}_s(\theta,k,t)$ can be easily expressed as a sum of Hankel functions. Then it can be shown by using the asymptotic behavior of the Hankel functions that

$$\widetilde{u}_s^\infty(\theta,\widehat{x},k,t=0_{\mathbb{R}^2}) = e^{-\frac{i\pi}{4}}\sqrt{\frac{2}{\pi k}}\sum_{m\in\mathbb{Z}} -\frac{J_m(kr)}{H_m(kr)}e^{im(\widehat{x}-\theta)}. \tag{6.59}$$

From the translation formula [44, equation 5.3], the solution of (6.7) where Ω is replaced by Ω_t, has the following far field pattern,

$$\widetilde{u}_s^\infty(\theta,\widehat{x},k,t) = e^{ikt\cdot(\theta-\widehat{x})}\widetilde{u}_s^\infty(\theta,\widehat{x},0_{\mathbb{R}^2}). \tag{6.60}$$

Consequently if we define the two matrix $T(k)$ and $\widetilde{F}(k)$ by

$$T_{p,q}(k) = e^{ikt\cdot(\theta_p-\widehat{x}_q)} \quad \text{and} \quad \widetilde{F}_{p,q}(k) = \widetilde{u}_s^\infty(\theta_p,\widehat{x}_q,0_{\mathbb{R}^2}). \tag{6.61}$$

Then the relative far field operators $F_t^{rel}(k)$ are given by

$$F_t^{rel}(k) = F^\delta(k) - \widetilde{F}_t(k). \tag{6.62}$$

where $\widetilde{F}_t(k)$ is the component wise multiplication of $T(k)$ with $\widetilde{F}(k)$.

Regularization of $\mathbf{J}_\mathbf{z}^\alpha$

To handle the noise δ added on the data, we use a regularized version of the cost function J_z^α defined by (6.41). It consists in finding the minimizer $g_z^{\alpha,\delta}(k,t)$ of the functional

$$J_z^{\alpha,\delta}(g,k,t) = \alpha\left(P^\delta(g,k,t) + \delta\|g\|^2_{L^2(\mathbb{S}^2)}\right) + \|F_t^{rel}(k)g - \Phi_z^\infty\|^2_{L^2(\mathbb{S}^{d-1})}, \tag{6.63}$$

where $P^\delta(g,k,t) = \langle F_\sharp^\delta(k)g, g\rangle + \langle \widetilde{F}_t^\sharp g, g\rangle$. Following [10, Section 5.2], we fit α to δ as follows,

$$\alpha(\delta,t,k) = \frac{\alpha_{LSM}(t,k)}{\|F_\sharp^\delta(k)\| + \|\widetilde{F}_t^\sharp(k)\| + \delta} \tag{6.64}$$

where $\alpha_{LSM}(k,t)$ is the regularization parameter given by the Morozov discrepancy principle in the Tikonov regularization of the equation $F_t^{rel}(k)g = \Phi_z^\infty$.

Indicator of the crack density

From the computed $g_z^{\alpha,\delta}(k,t)$, we compute the RTEs $\tau_0(\Gamma,\Omega_t)$ as described in the previous section.

We first illustrate the indicator function $I(t)$ on a neat example (figure 6.2). We also presented the plot of the curve $\mathcal{E}_\Omega$ defined by (6.54) for two different artificial disks Ω_{t_1} (figure 6.3) and Ω_{t_2} (figure 6.4) so one can appreciate how the first eigenvalue of (6.15), determined by the first peak of the curve $\mathcal{E}_t$, deviates from the first eigenvalue of (6.16) when Ω_t intersects the crack. In figure 6.5, we decreased the artificial disks radii to $r = 0.1$ to recover the crack with a better resolution.

Finally, we implement the method to less academical situations in figure 6.6. It gives quite good results in the sense that it allows to identify highly damaged areas. However, this method is quite expensive in computations to allow a better resolution of the image. This is why we propose another approach in the next section, which requires only measurements at one fixed frequency and whose implementation is less costly.

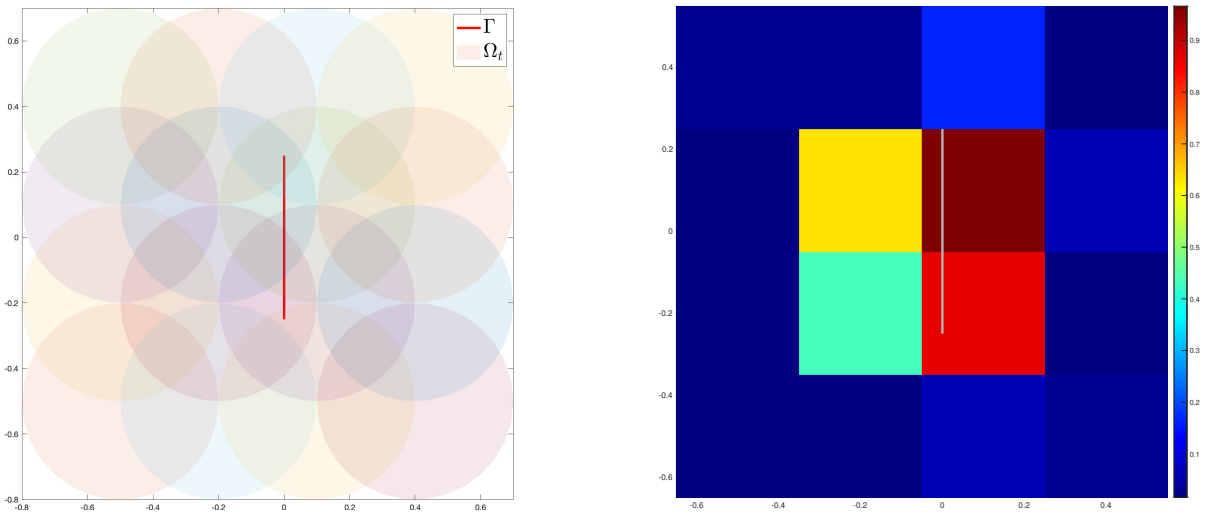

Figure 6.2: Left: collection of artificial disks of radii $r = 0.3$ used to identify a single crack of length 0.5. Right: results of the reconstruction provided by the indicator I.

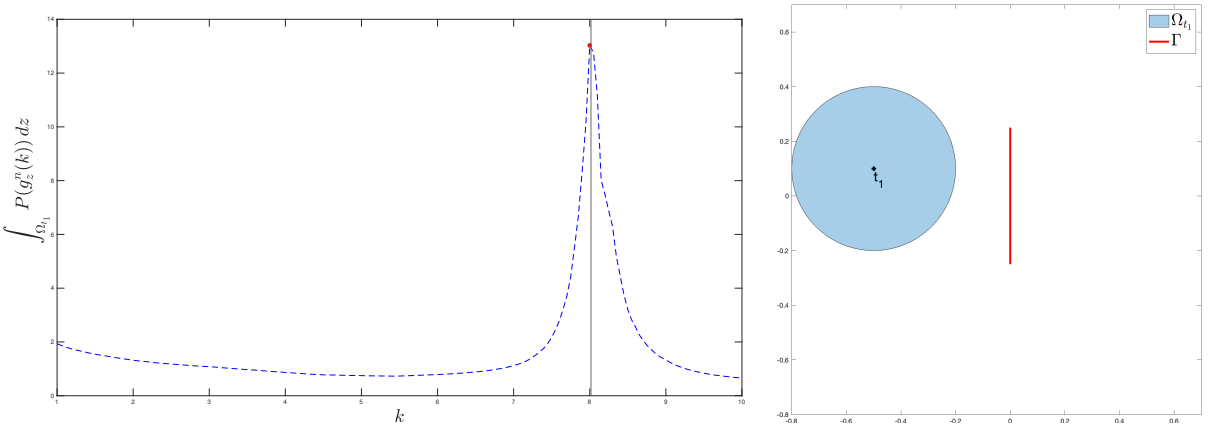

Figure 6.3: Plot of the curve $\mathcal{E}_{t_1}$ (left) defined by (6.54) computed with the artificial background Ω_{t_1} represented on right. The peak of the curve is reached at $k^* \approx \sqrt{\tau_0(\Omega_0, \emptyset)}$, the latter quantity being indicated by a vertical bar. Consequently, it is obtained that $I(t_1) = |\tau_0(\Omega_0, \emptyset) - (k^*)^2| \approx 0$.

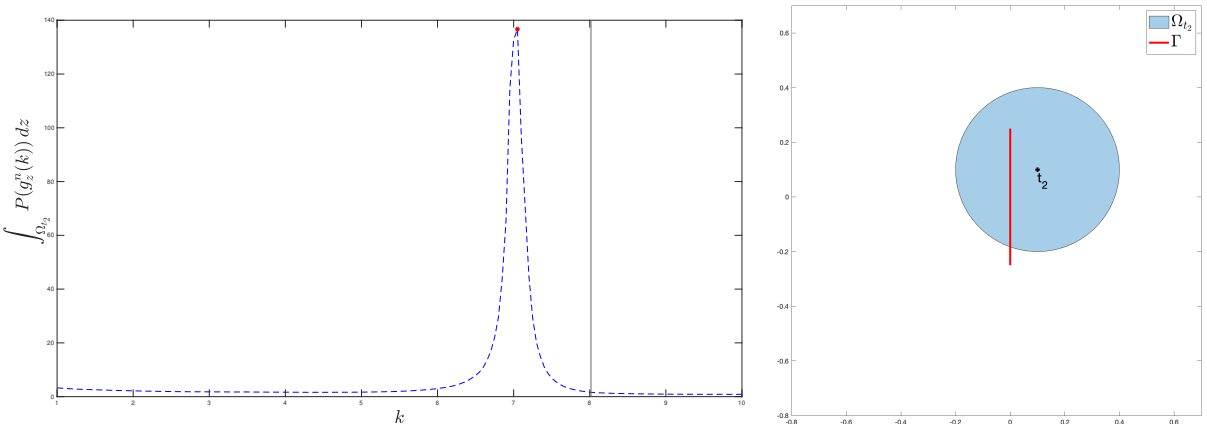

Figure 6.4: Plot of the curve $\mathcal{E}_{t_2}$ (left) defined by (6.54) computed with the artificial background Ω_{t_2} represented on right. The peak of the curve is reached at $k^* < \sqrt{\tau_0(\Omega_0, \emptyset)}$, the latter quantity being indicated by a vertical bar. Consequently, it is obtained that $I(t_2) = |\tau_0(\Omega_0, \emptyset) - (k^*)^2| \gg 0$.

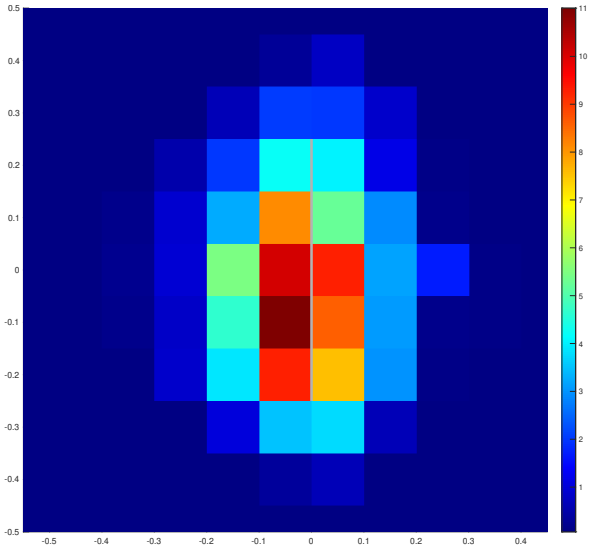

Figure 6.5: Results of the reconstruction provided by the indicator I to recover a single crack. The method is carried with artificial disks of radii $r = 0.1$.

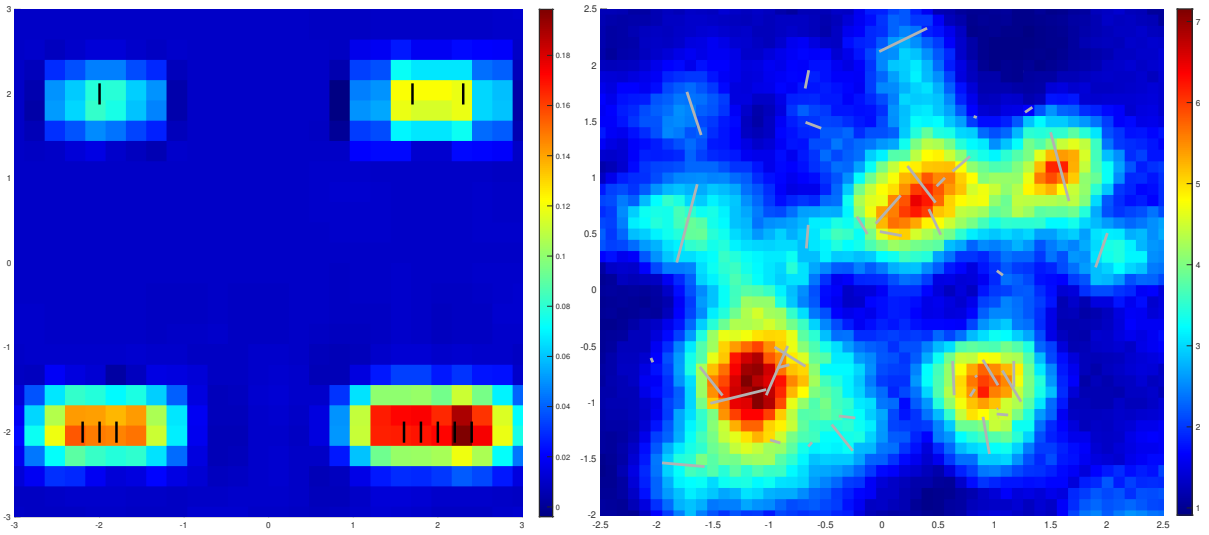

Figure 6.6: Use of the indicator I to image simulated damaged backgrounds. Left: 11 vertical cracks of length 0.25 arranged in 4 damaged areas with different degrees of damage, the radius of the artificial backgrounds is $r = 0.25$. Right: 40 cracks of different lengths arranged randomly, the radius of the artificial backgrounds is $r = 0.1$. The data is corrupted with 1% of noise.

6.4 An alternative method using measurements at one fixed frequency

In this section we try to define an indicator function which would allow to quantify small crack aggregates similarly to $I(t)$ but which requires only far field measurements at one fixed frequency. The method we propose is inspired by the Differential Linear Sampling Method [9], but we precise that we do not require differential measurements. In fact, the idea of our method is that for a given far field operator F, we compare the two solutions of the transmission problem (6.15) which arises for two different artificial backgrounds $\Omega_1 \neq \Omega_2$, with Ω_1 disjoint from the crack and Ω_2 intersecting the crack. The new proposed indicator allows us to isolate the crack but there is no theoretical justification for the quantification of crack networks. However numerical simulations show that it gives good results for this perspective.

6.4.1 Solution of the far field equation

In this section we give a characterization of the solution to equation $G^{rel}\psi_z = \Phi_z^\infty$. It will be shown that when k is not a RTE, the solution can be approximated by optimizing the cost functional (6.41) for small values of α. Let w be a solution of (6.10) such that $w^\infty = \Phi_z^\infty$. Rellich's lemma implies that $w = \Phi_z$ on $\mathbb{R}^d \setminus (\Omega \cup \Gamma)$. Consequently $\psi_2 = -\sigma(\Phi_z)$ on $\Gamma \cap \Omega^c$ and $\psi_1 = \mathcal{B}^*(w_i - \Phi_z)$ where w_i is given by the solution of

$$\left|\begin{array}{rcll} \Delta w_i + k^2 w_i & = & 0 & \text{in } \Omega \setminus \overline{\Gamma} \\ \sigma(w_i) & = & 0 & \text{on } \Gamma \cap \Omega \\ \mathcal{B} w_i & = & \mathcal{B}\Phi_z & \text{on } \partial\Omega. \end{array}\right. \tag{6.65}$$

Theorem 6.4.1. *Assume that F^{rel} has dense range and that k is such that (6.15) and (6.16) are well posed. Then $\forall z \in \Omega$, there exists a unique solution $(\psi_1, \psi_2) \in X^*(\partial\Omega) \times Y(\Gamma \cap \Omega^c)$ to equation $G^{rel}(\psi_1, \psi_2) = \Phi_z^\infty$. Furthermore the sequence g_z^α defined by (6.43) is such that*

the sequence $H_{\partial\Omega} g_z^\alpha$ converges strongly to $\psi_1 = \mathcal{B}^*(w_i - \Phi_z)$ where w_i is the unique solution of (6.65).

Proof. Uniqueness of the solution to equation $G(\psi_1, \psi_2) = \Phi_z^\infty$ comes from the well posedeness of (6.15) and the characterization $\psi_1 = \mathcal{B}^*(w_i - \Phi_z)$ has been established in the above discussion. We now show that $H_{\partial\Omega} g_z^\alpha$ converges to ψ_1. According to Theorem 6.3.4, the sequence $(P(g_z^\alpha))_{\alpha>0}$ is bounded and Lemma 6.3.3 then implies that the sequence $H^{rel} g_z^\alpha$ is bounded. Up to extracting subsequences, we assume that $H^{rel} g_z^\alpha$ converges weakly.

On the one hand, the compactness of G^{rel} implies that $G^{rel} H^{rel} g_z^\alpha$ converges strongly to Φ_z^∞ in $L^2(\mathbb{S}^{d-1})$ when $\alpha \to 0$. On the other hand, since F^{rel} has dense range, we also have that $F^{rel} g_z^\alpha \to \Phi_z^\infty$ when $\alpha \to 0$. Then the injectivity of G^{rel} implies that the only possible weak limit for $H^{rel} g_z^\alpha$ is (ψ_1, ψ_2). We now show the strong convergence of $H_{\partial\Omega} g_z^\alpha$ to ψ_1. Firstly, from the definition of j_z^α,

$$j_z^\alpha \leq \inf_{(h_1,h_2)\in R(H^{rel})} \alpha \langle \widetilde{T}_1^\sharp h_1, h_1\rangle + \alpha \langle T^\sharp h_2, h_2\rangle + \|G_m(h_1,h_2) - \Phi_z^\infty\|^2 \tag{6.66}$$

where $\widetilde{T}_1^\sharp$ and $T^\sharp$ appears in factorizations (6.33) and (6.38) then choosing $(h_1, h_2) = (\psi_1, \psi_2)$ in the above estimation gives

$$j_z^\alpha \leq \alpha \langle \widetilde{T}_1^\sharp \psi_1, \psi_1\rangle + \alpha \langle T^\sharp \psi_2, \psi_2\rangle. \tag{6.67}$$

Finally from the definition of g_z^α (6.43),

$$\limsup_{\alpha\to 0} \left(\langle \widetilde{T}_1^\sharp H_{\partial\Omega} g_z^\alpha, H_{\partial\Omega} g_z^\alpha\rangle + \langle T^\sharp H_\Gamma g_z^\alpha, H_\Gamma g_z^\alpha\rangle \right) \leq \langle \widetilde{T}_1^\sharp \psi_1, \psi_1\rangle + \langle T^\sharp \psi_2, \psi_2\rangle. \tag{6.68}$$

Thanks to the coercivity properties of $\widetilde{T}_1^\sharp$, we can write

$$\begin{aligned} c_1 \|H_{\partial\Omega} g_z^\alpha - \psi_1\|^2 &\leq \langle \widetilde{T}_1^\sharp (H_{\partial\Omega} g_z^\alpha - \psi_1^z), H_{\partial\Omega} g_z^\alpha - \psi_1\rangle \\ &\leq \langle \widetilde{T}_1^\sharp H_{\partial\Omega} g_z^\alpha, H_{\partial\Omega} g_z^\alpha\rangle - \langle \widetilde{T}_1^\sharp H_{\partial\Omega} g_z^\alpha, \psi_1\rangle - \langle \psi_1, H_{\partial\Omega} g_z^\alpha - \psi_1\rangle, \end{aligned} \tag{6.69}$$

and similarly,

$$c_2 \|H_\Gamma g_z^\alpha - \psi_2\|^2 \leq \langle T^\sharp H_\Gamma g_z^\alpha, H_\Gamma g_z^\alpha\rangle - \langle T^\sharp H_\Gamma g_z^\alpha, \psi_2\rangle - \langle \psi_2, H_\Gamma g_z^\alpha - \psi_2\rangle. \tag{6.70}$$

By adding (6.69), (6.70) together and using (6.68) we obtain

$$\lim_{\alpha\to 0} c_1 \|H_{\partial\Omega} g_z^\alpha - \psi_1\|^2 + c_2 \|H_\Gamma g_z^\alpha - \psi_2\|^2 = 0, \tag{6.71}$$

and hence $\lim_{\alpha\to 0} H_{\partial\Omega} g_z^\alpha = \psi_1$. □

6.4.2 Comparison of two transmission problems revealing the presence of cracks

We consider the following boundary value problems,

$\mathscr{P}^z$: find $w \in H^1(\Omega)$ such that

$$\left| \begin{array}{rcll} \Delta w + k^2 w &=& 0 & \text{in } \Omega \\ \mathcal{B} w &=& \mathcal{B}\Phi_z & \text{on } \partial\Omega \end{array} \right.$$

$\mathscr{P}_\Gamma^z$: find $w_\Gamma \in H^1(\Omega \setminus \overline{\Gamma})$ such that

$$\left| \begin{array}{rcll} \Delta w_\Gamma + k^2 w_\Gamma &=& 0 & \text{in } \Omega \setminus \overline{\Gamma} \\ \sigma(w_\Gamma) &=& 0 & \text{on } \Gamma \cap \Omega \\ \mathcal{B} w_\Gamma &=& \mathcal{B}\Phi_z & \text{on } \partial\Omega. \end{array} \right. \tag{6.72}$$

Of course if $\Gamma \cap \Omega = \emptyset$ the two problems above are the same. Moreover we have the following result,

Lemma 6.4.2. *Assume that k^2 is not an eigenvalue of problem (6.16) and let w^z, w^z_Γ be the solutions of $(\mathscr{P})$ and $(\mathscr{P}_\Gamma)$ respectively. Then we have*

1. *$\forall z \in \Omega$, the functions $\Im\mathfrak{m}(w^z)$ and $\Im\mathfrak{m}(\Phi_z)$ coincide on Ω.*
2. *If $\Gamma \cap \Omega \neq \emptyset$, the set of $z \in \Omega$ such that the functions $\Im\mathfrak{m}(\mathcal{B}^* w^z_\Gamma)$ and $\Im\mathfrak{m}(\mathcal{B}^* \Phi_z)$ of $X^*(\partial\Omega)$ coincide is of empty interior.*

Proof. We begin with the first point. The fundamental solution of Helmholtz equation is given by the following formulas,

$$\Phi_z(x) = \frac{i}{4}(J_0(k|x-z|) + iY_0(k|x-z|)) \text{ if } d = 2 \qquad \text{and} \qquad \Phi_z(x) = \frac{1}{4\pi}\frac{e^{ik|x-z|}}{|x-z|} \text{ if } d = 3 \quad (6.73)$$

where J_0 and Y_0 are respectively the Bessel functions of order zero of first kind and of second kind. We have that $\Im\mathfrak{m}(\Phi_z) \in H^1(\Omega)$ thanks to the smoothness of J_0 for $d = 2$ and the smoothness of $x \mapsto \sin(x)/x$ for $d = 3$. As a consequence, the unique solution of the following problem

$$\left| \begin{array}{rcll} \Delta w + k^2 w & = & 0 & \text{in } \Omega \\ \mathcal{B} w & = & \Im\mathfrak{m}(\mathcal{B}\Phi_z) & \text{on } \partial\Omega \end{array} \right. \quad (6.74)$$

is given by $\Im\mathfrak{m}(\Phi_z)$. We observe that $\Im\mathfrak{m}(w^z)$ is also a solution of (6.74), hence $\Im\mathfrak{m}(w^z) = \Im\mathfrak{m}(\Phi_z)$ on Ω.

We prove the second point by using a contradiction argument. Assume that there exists a subset $U \subset \Omega$ of non empty interior such that the functions $\Im\mathfrak{m}(\mathcal{B}^* w^z_\Gamma)$ and $\Im\mathfrak{m}(\mathcal{B}^* \Phi_z)$ coincide. Since $\Im\mathfrak{m}(w_z)$ and $\Im\mathfrak{m}(\Phi_z)$ satisfy the same Cauchy conditions on $\partial\Omega$ we first deduce that they coincide on $\Omega \setminus \overline{\Gamma}$. Therefore we have shown that

$$\forall z \in U, \quad \sigma(\Im\mathfrak{m}(\Phi_z)) = 0 \text{ on } \Gamma. \quad (6.75)$$

We now show that the above result leads to a contradiction. For two given real valued functions α, $\beta \in L^2(\Omega)$, we define the following function defined on $\Omega \setminus \overline{\Gamma}$,

$$f(z) = \int_\Gamma \alpha(x)\Phi(x,z)\,\mathrm{ds}(x) + \int_\Gamma \beta(x)\partial_{\nu(x)}\Phi(x,z)\,\mathrm{ds}(x). \quad (6.76)$$

The function f satisfies the Helmholtz equation on $\mathbb{R}^d \setminus \overline{\Gamma}$ and the Sommerfeld radiation condition. We first treat the case when σ corresponds to the Dirichlet boundary conditions on Γ. We set $\beta = 0$ and choose for α any nonzero (real valued) element of $L^2(\Gamma)$. Assumption (6.75) first implies $\Im\mathfrak{m}(f) = 0$ in U. Then the unique continuation principle implies that $\Im\mathfrak{m}(f)$ vanishes in $\mathbb{R}^d$. Furthermore a real valued solution of Helmholtz equation which satisfies the Sommerfeld radiation condition is necessarily zero. Hence $f = 0$ in $\mathbb{R}^d$. The latter contradicts the jump properties of the single layer potential which states that $[\partial_\nu f] = \alpha$ on Γ. The cases of the Neumann and impedance boundary conditions for σ are treated similarly. For the Neumann boundary conditions, set $\alpha = 0$ and choose for β any nonzero (real valued) function of $L^2(\Gamma)$. For the impedance condition $\lambda\Phi_z + \partial_\nu \Phi_z = 0$, set $\alpha = \lambda$ and $\beta = 1$. □

Theorem 6.4.3. *Assume that k^2 is not an eigenvalue of problem (6.15) nor an eigenvalue of problem (6.16). For $z \in \Omega$, let g^α_z be the sequence defined by (6.43). Then we have the two following characterizations of $\Gamma \cap \Omega = \emptyset$,*

1. $\Gamma \cap \Omega = \emptyset$ *iff* $\| \lim_{\alpha\to 0}(H_{\partial\Omega} g_z^\alpha) - \mathcal{B}^*(w^z - \Phi_z)\|_{X^*(\partial\Omega)} = 0$ *for a.e* z *in* Ω.

2. $\Gamma \cap \Omega = \emptyset$ *iff* $\|\Im\mathfrak{m}(\lim_{\alpha\to 0} H_{\partial\Omega} g_z^\alpha)\|_{X^*(\partial\Omega)} = 0$ *for a.e* z *in* Ω.

where w^z *is the solution of* $\mathscr{P}^z$ (6.72).

Proof. We denote by w_Γ^z the solution of $\mathscr{P}_\Gamma^z$ (6.72) (where $\Gamma \cap \Omega$ is eventually empty) and by w^z the solution of $\mathscr{P}^z$ (6.72). Theorem 6.4.1 implies that

$$\lim_{\alpha\to 0} H_{\partial\Omega} g_z^\alpha = \mathcal{B}^*(w_\Gamma^z - \Phi_z). \tag{6.77}$$

It suffices to observe that

$$\| \lim_{\alpha\to 0}(H_{\partial\Omega} g_z^\alpha) - \mathcal{B}^*(w^z - \Phi_z)\|_{X^*(\partial\Omega)} = \|\mathcal{B}^*(w_\Gamma^z - w^z)\|_{X^*(\partial\Omega)}. \tag{6.78}$$

and

$$\|\Im\mathfrak{m}(\lim_{\alpha\to 0} H_{\partial\Omega} g_z^\alpha)\|_{X^*(\partial\Omega)} = \|\Im\mathfrak{m}(\mathcal{B}^* w_\Gamma^z - \mathcal{B}^*\Phi_z)\|_{X^*(\partial\Omega)}. \tag{6.79}$$

The two results of the theorem are then a direct consequence of Lemma 6.4.2. □

Note that the quantity w^z and the operator $H_{\partial\Omega}$ can be computed numerically independently from the data. Similarly to the previous section, we propose to detect the position of the crack by considering a collection of artificial backgrounds $\Omega_t = B(t, r)$. Then $\Gamma \cap \Omega_t$ is identified by comparing the solutions of $\mathscr{P}(\Omega_t)$ and $\mathscr{P}_\Gamma(\Omega_t)$. Therefore, in view of Theorem 6.4.3 we define the following indicator functions,

$$J_1^\alpha(t) = \int_{A\subset\Omega_t} \|H_{\partial\Omega_t} g_z^\alpha(t) - \mathcal{B}^*(w_z(t) - \Phi_z)\|_{X^*(\partial\Omega_t)}\, \mathrm{d}z \tag{6.80}$$

and

$$J_2^\alpha(t) = \int_{A\subset\Omega_t} \|\Im\mathfrak{m}(H_{\partial\Omega_t} g_z^\alpha(t))\|_{X^*(\partial\Omega_t)}\, \mathrm{d}z. \tag{6.81}$$

We then have for $i = 1, 2$

$$\forall t \in \mathbb{R}^d, \quad \Gamma \cap \Omega_t = \emptyset \text{ iff } \lim_{\alpha\to 0} J_i^\alpha(t) = 0. \tag{6.82}$$

The indicators J_i^α can then be used to identify the crack location.

Remark 6.4.4. *We point out here that the indicator* J_2^α *is weaker than* J_1^α. *Indeed, for* $z \in \Omega$, $\Im\mathfrak{m} w_z = \Im\mathfrak{m}\,\Phi_z$ *on* Ω. *Consequently,*

$$\forall z \in \Omega, \quad \Im\mathfrak{m}(H_{\partial\Omega} g_z^\alpha - \partial_\nu^+(w_z - \Phi_z)) = \Im\mathfrak{m}(H_{\partial\Omega} g_z^\alpha) \text{ on } \partial\Omega.$$

From the definitions of J_1^α *and* J_2^α, *we deduce*

$$\forall t \in \mathbb{R}^d, \quad J_2^\alpha(t) \le J_1^\alpha(t).$$

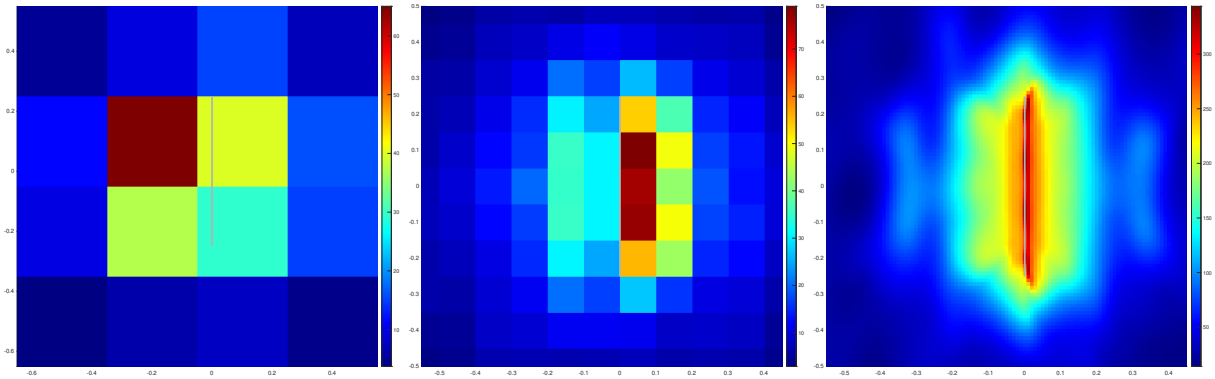

Figure 6.7: Reconstruction of a single crack with the indicator J_1 from given far field data generated at frequency $k = 15$. The resolution of the image is set by the radii of the used artificial disks: $r = 0.3$ (left), $r = 0.1$ (middle), $r = 0.01$ (right). The data is corrupted with 1% of noise.

6.4.3 Numerical results and comparison with the multiple frequencies approach

Similarly to what has been done in the previous section, we generate the far field data from a simulated background, but this time only data for a single wave number k is required. We prescribe on the artificial backgrounds $\Omega_t = B(t, r)$ the Dirichlet boundary conditions $\mathcal{B}w = w_{|\partial\Omega_t}$. Once again the choice for k depends on the desired resolution r. Since k^2 must be different from the eigenvalues of (6.15) and (6.16), it suffices to take k^2 smaller than the first Laplace Dirichlet eigenvalue for $B(0, r)$. For the chosen k, the matrix $F^\delta(k)$ and $F_t^{rel}(k)$ are then defined similarly to the previous section by (6.62). For a sample of $t \in \mathbb{R}^d$ we then compute $g_z^\alpha(t)$ by solving the regularized version of the far field equation (6.63).

Again, we begin with the neat example of the single crack. In figure 6.7, the crack is recovered with different resolutions using the indicator $J_1(t)$. Then we take advantage of this simple example to highlight the behavior of the indicator $J_1(t)$ in figures 6.8-6.9. In figure 6.8 is provided the plots of the quantities $H_{\partial\Omega_t} g_z^\alpha$ and $\partial_\nu(w_z - \Phi_z)$ for a particular $z \in \Omega_t$ when Ω_t does not intersect the crack. We provide the plots of the same quantities when Ω_t intersects the crack in figure 6.9.

Since the implementation of this present method is quite fast, we have been able to image the backgrounds treated in figure 6.6 with a higher resolution. The results are given in figures 6.10-6.11 where we also provided the result obtained with the indicator J_2. In figure 6.11, it can be observed that the indicator J_1 offers a better contrast than J_2. This behavior is explained in remark 6.4.4.

Finally in figures 6.12-6.15, we compared the three different indicators I, J_1 and the Factorization Method (FM) to increasingly damaged materials. In these last examples, the data used to compute the indicators J_1 and FM were generated at the same wavelength $\lambda = 0.15$. The distance dz between sampling points when computing the FM indicator is equal to the radii of the artificial disks used for the indicator J_1: $r = dz = 0.01$. For the indicator I, we used data generated for a sample of wavelengths between $\lambda_{min} = 0.15$ and $\lambda_{max} = 0.42$. For this indicator, the radii of the artificial backgrounds are set to $r' = 0.1$. With this setting, $k = 2\pi/\lambda$ with $\lambda = 0.16$ or $\lambda = 0.26$ correspond to the two first eigenvalues of problem (6.16).

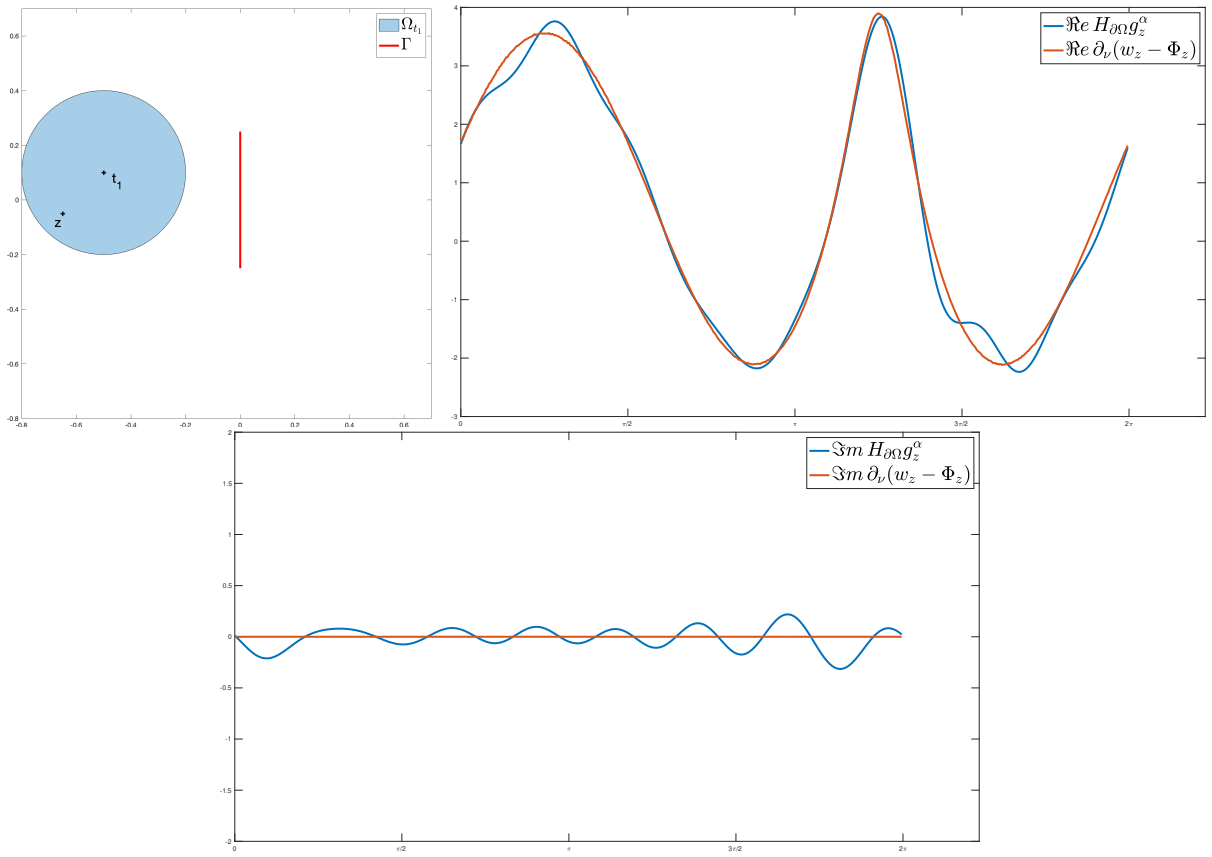

Figure 6.8: Consider the artificial background Ω_{t_1} and the crack Γ (top left). Since Ω_{t_1} does not intersect Γ, for any $z \in \Omega_{t_1}$, the quantities $H_{\partial\Omega_{t_1}} g_z^\alpha$ and $\partial_\nu(w_z - \Phi_z)$ are expected to be close in $H^{-1/2}(\partial\Omega)$. The real part and the imaginary part of the two latter quantities for a particular $z \in \Omega_{t_1}$ are respectively plotted on the top right graph and the bottom graph.

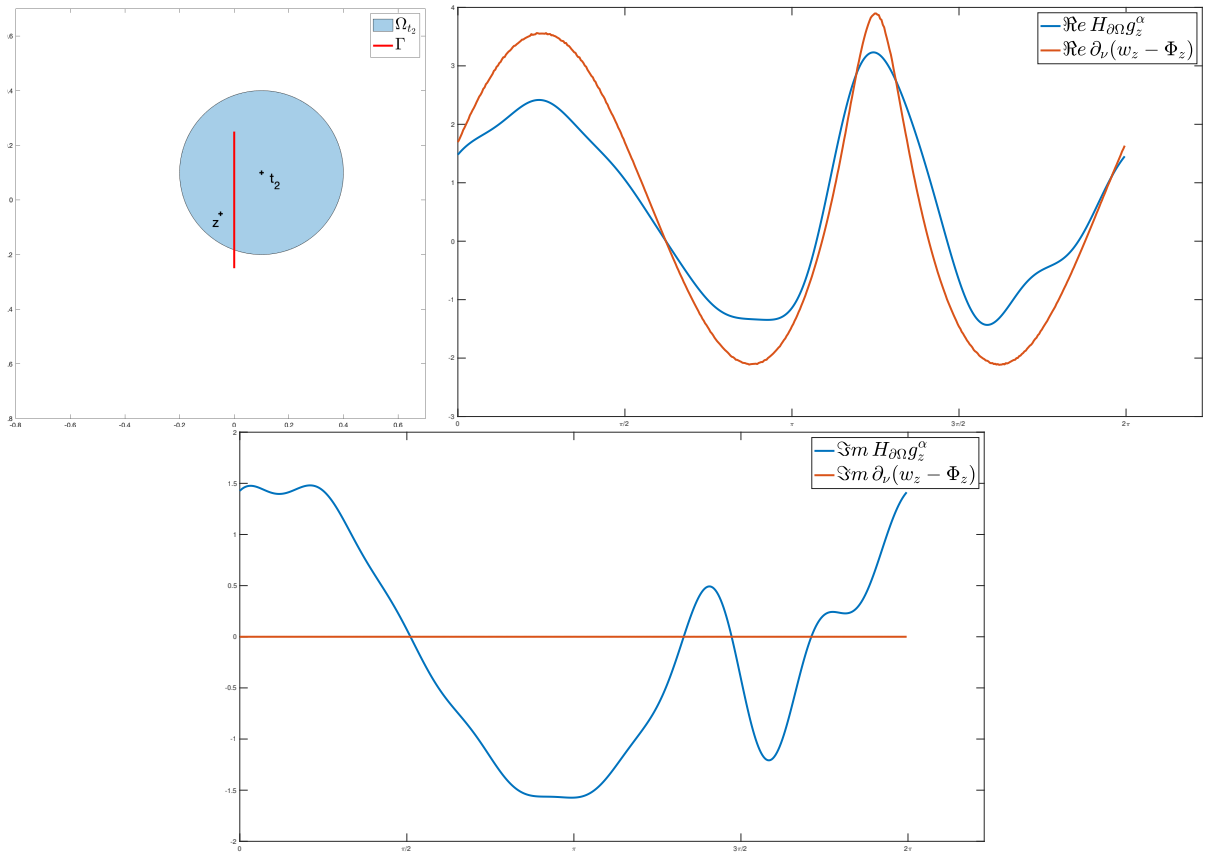

Figure 6.9: Consider the artificial background Ω_{t_2} and the crack Γ (top left). Since Ω_{t_2} intersects Γ, for any $z \in \Omega_{t_1}$, the quantities $H_{\partial\Omega_{t_1}} g_z^\alpha$ and $\partial_\nu(w_z - \Phi_z)$ are expected to be different in $H^{-1/2}(\partial\Omega)$ in general. The real part and the imaginary part of the two latter quantities for a particular $z \in \Omega_{t_2}$ are respectively plotted on the top right graph and the bottom graph.

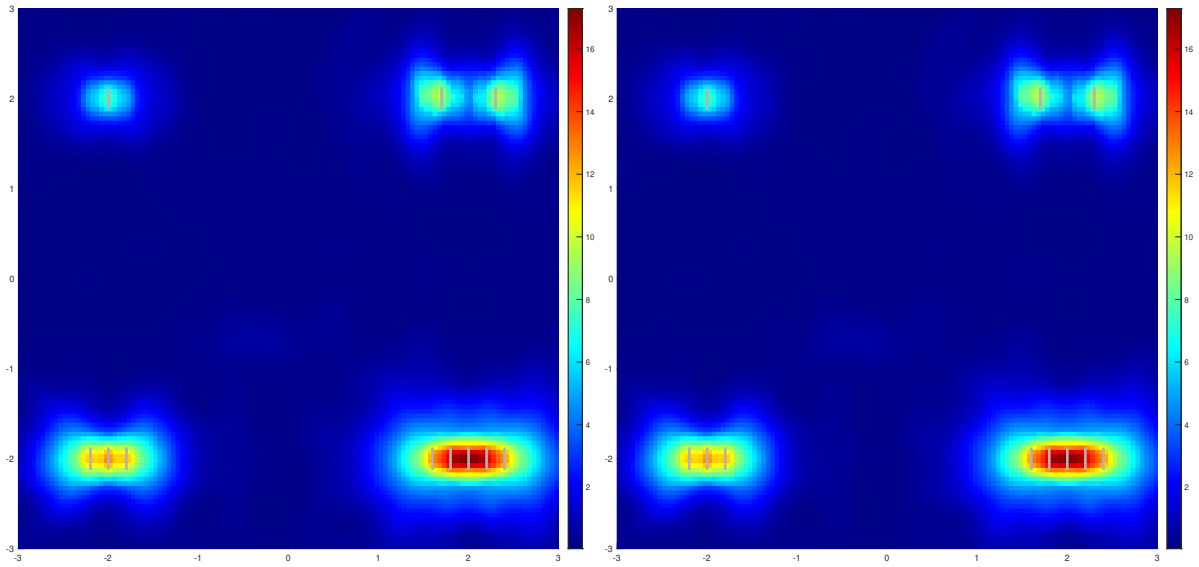

Figure 6.10: Use of the indicators J_1 (left) and J_2 (right) to image a simulated damaged background made of 11 vertical cracks of length 0.25 arranged in 4 damaged areas with different degrees of damage. The radius of the artificial backgrounds is $r = 0.25$. The radius of the artificial backgrounds is $r = 0.1$. The data is corrupted with 1% of noise.

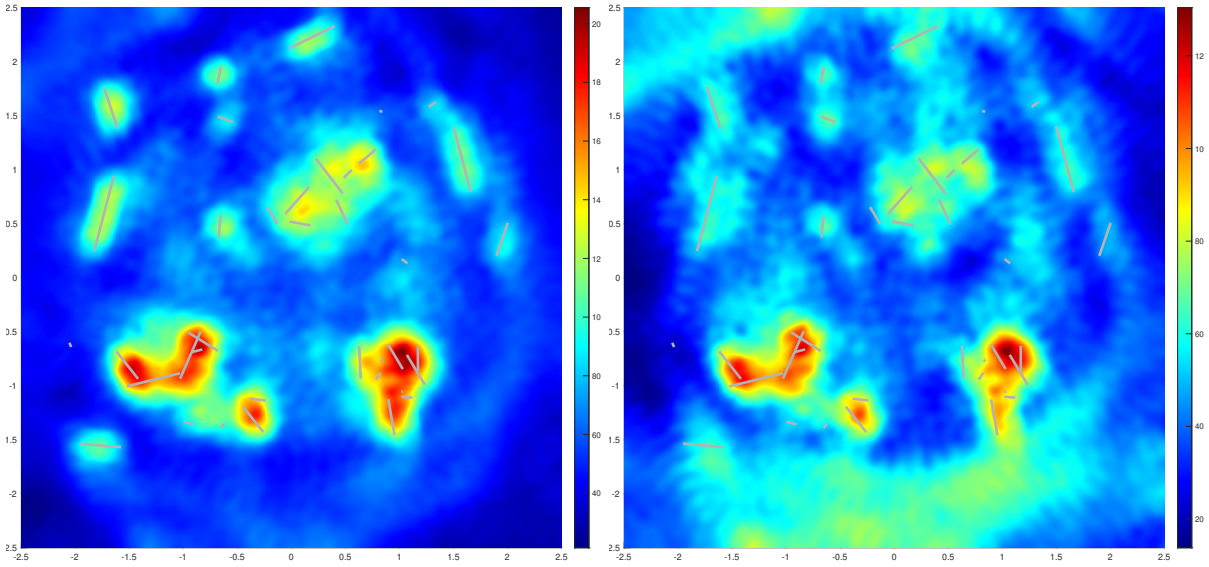

Figure 6.11: Use of the indicators J_1 (left) and J_2 (right) to image a simulated damaged background made of 40 cracks of different lengths arranged randomly. The radius of the artificial backgrounds is $r = 0.1$. The data is corrupted with 1% of noise.

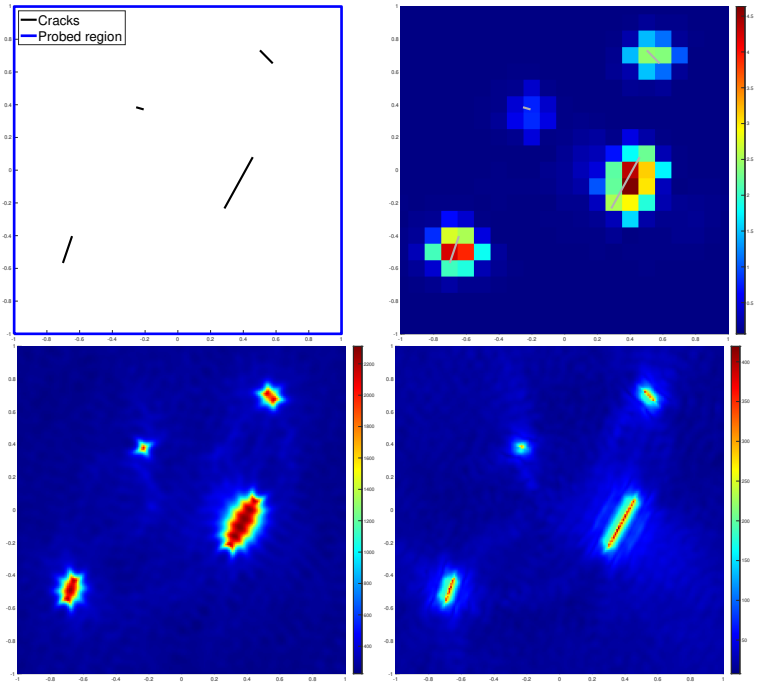

Figure 6.12: Use of indicators I (top right), J_1 (bottom right), and FM (bottom left) to recover a set of 4 sound hard cracks. The data is corrupted with 1% of noise.

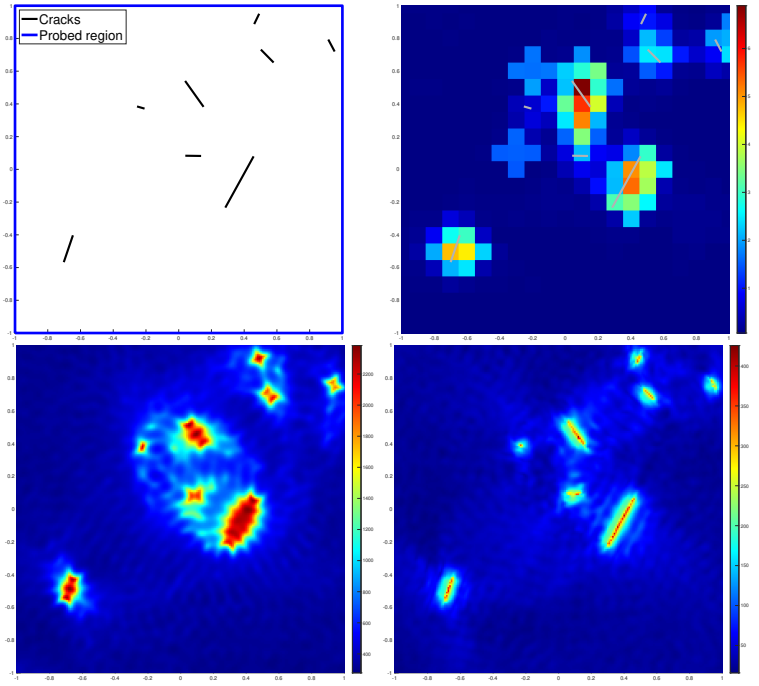

Figure 6.13: Use of indicators I (top right), J_1 (bottom right), and FM (bottom left) to recover a set of 8 sound hard cracks. The data is corrupted with 1% of noise.

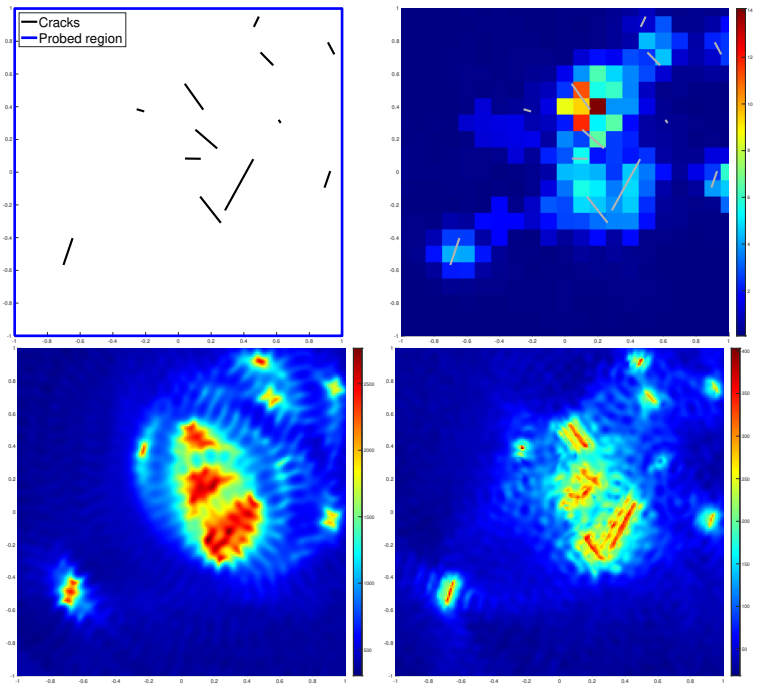

Figure 6.14: Use of indicators I (top right), J_1 (bottom right), and FM (bottom left) to recover a set of 12 sound hard cracks. The data is corrupted with 1% of noise.

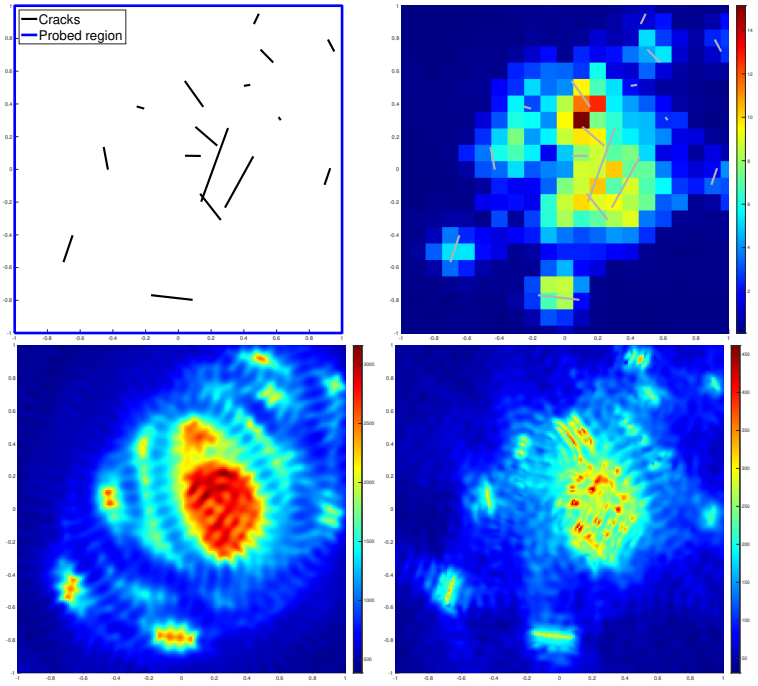

Figure 6.15: Use of indicators I (top right), J_1 (bottom right), and FM (bottom left) to recover a set of 16 sound hard cracks. The data is corrupted with 1% of noise.

Conclusion

In this chapter, we synthesize the results obtained during the thesis. In doing so, we will also mention the main difficulties that have not been solved and suggest, when available, solutions that might be addressed. Finally, we enumerate some possible perspectives.

In chapter 1, we illustrated the LSM, FM and the GLSM in a simple case where the obstacle is a circular inhomogeneous medium of constant refractive index. In this setting we were able to describe the spectral properties of the far field operator precisely. As a consequence, we could easily compute the indicator functions of the shape of the inhomogeneity provided by the sampling methods. We then conducted some numerical experiments allowing to compare the efficiency of these indicator functions and more particularly their respective behavior across the boundary of the inhomogeneity. Since in this setting, the TEs correspond to zeros of known quantities which involve Bessel functions, their values can be approximated as accurately as desired. Consequently, we were able to perform some numerical experiments that test the reliability of the GLSM for the determination of TEs from far field data. We tested both the precision of the method with respect to the noise level on the far field data and the precision with respect to the size of the scattering matrix (which depends on the number of receivers used to collect the far field data). These few numerical results are a first step before a theoretical analysis of this issue which seems challenging but also increasingly important for the use of TEs in solving inverse problems [22, 31, 63, 66, 32]. Estimates on the error made while approximating TEs can be useful for instance to choose an optimal sampling of frequencies when collecting the data or to estimate the error being made when using TEs in inversion algorithms. We also gave a lower bound on the rate of convergence of the sequence of the regularized solutions of the far field equation provided by the GLSM to the predicted limit (which is the solution of a transmission problem). This result is important for a deeper understanding of the DLSM which relies on approximations of ITP solutions.

In chapters 2 and 4, we respectively considered the problem of detecting emergence of sound-hard cracks or sound-hard obstacles in some non-homogeneous background. We extended the results of the DLSM which requires two different factorization of the far field operator. The study of each type of defects, cracks or obstacles, have presented some particularities. Indeed the validity of the DLSM for the detection of a crack requires the crack to be defined as a part of the boundary of a bounded domain with analytic boundary. For an obstacle Ω, only a Lipschitz regularity is required for its boundary, but in counterpart the wavenumber is required to be different from Neumann eigenvalues for the Laplace operator in Ω. We notice that the established factorizations of the far field operator have also extended the use of FM to image isotropic inhomogeneities containing sound-hard cracks or obstacles. In view of using FM in practical situations, it would be interesting to study more complex backgrounds, by considering for instance inhomogeneous media containing inclusions with different boundary conditions altogether.

In chapter 3, we investigated the interior transmission problem for istropic inhomogeneities containing sound-hard cracks. Provided that the refractive index satisfies $n > 1$, we showed the

existence of infinitely many real TEs with no finite accumulation point. We also derived Faber-Krahn type inequalities for the TEs. It could be interesting to understand the behaviour of the TEs with respect to the size of the crack or its distance to the boundary of the inhomogeneity in view of using TEs in crack monitoring.

In chapter 5, we studied the interior transmission problem for isotropic inhomogeneities containing sound-hard inclusions. We relied on the properties of the Dirichlet-to-Neumann operator to prove that the set of transmission eigenvalues is at most discrete, provided that the sign contrast is fixed in a vicinity of the boundary of the support of the medium. In order to prove the existence of TEs, we developed a variational formulation similar to the one used in [33] and which is based on a fourth order equation. From the weak formulation arose many technical difficulties that we believe are independent from the existence of TEs. For instance the spectrum of the weak problem includes all Neumann eigenvalues for the Laplace operator in the support of the inclusion. Furthermore, the weak and the strong formulations cannot be proved to be equivalent when k corresponds to a Neumann eigenvalue. Therefore, proving the existence of TEs with the approach used in [33] necessitates to be more cautious by ensuring that the exhibited elements of the weak spectrum do not correspond to the Neumann eigenvalues. Our various efforts to answer this question were not successful. A first obvious theoretical perspective is to answer this open question. One can also ask the question of existence of complex transmission eigenvalues for which following the approach by Robbiano [112] would be a natural way to investigate.

In chapter 6, we proposed two different techniques to locally quantify small crack aggregates embedded in some homogeneous background from far field data. Our results are valid for either sound-hard cracks, sound-soft cracks or cracks with impedance boundary conditions. The first method we proposed rely on transmission eigenvalues with artificial backgrounds. More precisely, we made use of an artificial impenetrable obstacle localized in a chosen bounded area Ω inside the probed domain. We show that the Relative Transmission Eigenvalues which correspond to the spectrum of a PDE defined on Ω, namely the Relative Transmission Problem, can be computed with the GLSM. Since the solutions of RTP satisfy some boundary conditions on the crack, the RTEs carry information on the latter. More precisely, we show the possibility to deduce the presence of the crack in Ω by comparing the computed RTEs to the spectrum of the Laplace operator in Ω. Furthermore, we showed that the difference between these two spectra are monotonous with respect to the crack size inside Ω for the inclusion order. The latter justifies the possibility to define and to quantify a crack density in Ω. Finally, a quantification of the crack density is obtained at each point by repeating this process for various positions of Ω along the probed area. However, this method requires a large amount of data and numerical computations. To circumvent these drawbacks, we propose an alternative approach using far field data at fixed frequency. The second method we propose consists in comparing the solutions of the two mentioned PDEs instead of comparing their spectrum. The computation of the solution of RTP is also provided by the GLSM and we prove that its difference with the solution of the Helmholtz equation allows to characterize the presence of the crack in Ω. Hence the crack can be identified by varying the position of Ω. This alternative method is more attractive because it requires less computations than the first one. Nevertheless, there is no theoretical guarantee for this method provides a quantification of the crack density. Providing the necessary theoretical elements to justify the use of the second method to quantify crack density would be desirable. On the numerical side, it would be informative to carry out extensive numerical experiments on optimal choices and interplay between the different parameters of the method: size of the probing artificial object and sampling size in space (related to the experiment frequency), number of the transmission eigenvalues used in the criterion evaluation, other ways to compare the numerical spectra for crack free obstacle and the spectra computed from the data, etc. Analytical studies

may be helpful for the cases where cracks are replaced with circular Neumann obstacles. One can also explore the use of different backgrounds and experiment the methods on more realistic configurations.

In addition to the possible perspectives mentioned above, we propose a few others that are a bit more general:

- Concerning the determination of transmission eigenvalues for cracks in artificial media, it would also be interesting to explore other methods, like the inside-outside duality. This method has been extended to the case where the artificial background is made dielectric media [7]. The cases where the artificial background is made of obstacles is still open.
- Extend the methodologies to time dependent data with limited number of sources/receivers is another interesting perspective. For a multifrequency framework, combining the use of the frequencies in a multi-resolution approach is a desirable path to follow in order to perform better in terms of inversion cost. Defining this type of methodology requires a better understanding of the parameters in the previous point.
- Finally, a natural extension of our work would be to study other models (electromagnetism, elastodynamics) and consider realistic applicative settings.

Bibliography

[1] Milton Abramowitz and Irene A. Stegun. *Handbook of mathematical functions: with formulas, graphs, and mathematical tables*, volume 55. Courier Corporation, 1965. (page 26.)

[2] Richard A. Albanese, Richard L. Medina, and John W. Penn. Mathematics, medicine and microwaves. *Inverse Problems*, 10(5):995, 1994. (pages 1 and 9.)

[3] Tilo Arens. Why linear sampling works. *Inverse Problems*, 20(1):163–173, 2003. (page 23.)

[4] Tilo Arens and Armin Lechleiter. The linear sampling method revisited. *The Journal of Integral Equations and Applications*, pages 179–202, 2009. (page 23.)

[5] Lorenzo Audibert, Fioralba Cakoni, and Houssem Haddar. New sets of eigenvalues in inverse scattering for inhomogeneous media and their determination from scattering data. *Inverse Problems*, 33(12):125011, 2017. (pages 5, 13, and 102.)

[6] Lorenzo Audibert, Lucas Chesnel, and Houssem Haddar. Transmission eigenvalues with artificial background for explicit material index identification. *Comptes Rendus Mathematique*, 356(6):626–631, 2018. (pages 5, 13, 102, and 104.)

[7] Lorenzo Audibert, Lucas Chesnel, and Houssem Haddar. Inside-outside duality with artificial backgrounds. working paper or preprint, April 2019. (page 129.)

[8] Lorenzo Audibert, Lucas Chesnel, Houssem Haddar, and Kevish Napal. Detecting sound hard cracks in isotropic inhomogeneities. In *International Conference on Acoustics and Vibration*, pages 61–73. Springer, 2018. (pages 3 and 11.)

[9] Lorenzo Audibert, Alexandre Girard, and Houssem Haddar. Identifying defects in an unknown background using differential measurements. *Inverse Problems & Imaging*, 9(3), 2015. (pages 3, 5, 8, 11, 14, 15, 17, 38, 39, 64, 102, and 116.)

[10] Lorenzo Audibert and Houssem Haddar. A generalized formulation of the linear sampling method with exact characterization of targets in terms of farfield measurements. *Inverse Problems*, 30(3):035011, 2014. (pages 3, 4, 7, 8, 11, 13, 16, 17, 20, 25, 39, 45, 47, 52, 64, 73, 76, 101, 102, and 113.)

[11] Fahmi Ben Hassen, Yosra Boukari, and Houssem Haddar. Application of the linear sampling method to identify cracks with impedance boundary conditions. *Inverse Problems in Science and Engineering*, 21(2):210–234, 2013. (page 103.)

[12] Fahmi Ben Hassen, Klaus Erhard, and Roland Potthast. The singular sources method for 3d inverse acoustic obstacle scattering problems. *IMA journal of applied mathematics*, 75(1):1–16, 2009. (pages 2 and 10.)

[13] Eemeli Blåsten, Lassi Päivärinta, and John Sylvester. Corners always scatter. *Communications in Mathematical Physics*, 331(2):725–753, 2014. (page 25.)

[14] Norman Bleistein. *Mathematical methods for wave phenomena*. Academic Press, 2012. (pages 2 and 10.)

[15] Oleksandr Bondarenko, Andreas Kirsch, and Xiaodong Liu. The factorization method for inverse acoustic scattering in a layered medium. *Inverse problems*, 29(4):045010, 2013. (pages 3, 11, 39, and 63.)

[16] Brett Borden. *Radar Imaging of Airborne Targets: A primer for applied mathematicians and physicists*. CRC Press, 1999. (pages 2 and 10.)

[17] Christoph Börgers and Frank Natterer. *Computational radiology and imaging: Therapy and diagnostics*, volume 110. Springer Science & Business Media, 2012. (pages 1 and 9.)

[18] Yosra Boukari and Houssem Haddar. The factorization method applied to cracks with impedance boundary conditions. 2013. (page 109.)

[19] Laurent Bourgeois and Eric Lunéville. On the use of the linear sampling method to identify cracks in elastic waveguides. 2013. (page 103.)

[20] Haim Brezis. *Functional analysis, Sobolev spaces and partial differential equations*. Springer Science & Business Media, 2010. (page 87.)

[21] Martin Burger and Stanley J. Osher. A survey on level set methods for inverse problems and optimal design. *European journal of applied mathematics*, 16(2):263–301, 2005. (pages 2 and 10.)

[22] Fioralba Cakoni, Mehmet Çayören, and David Colton. Transmission eigenvalues and the nondestructive testing of dielectrics. *Inverse Problems*, 24(6):065016, 2008. (pages 5, 13, 52, 101, and 127.)

[23] Fioralba Cakoni and David Colton. The linear sampling method for cracks. *Inverse problems*, 19(2):279, 2003. (page 103.)

[24] Fioralba Cakoni and David Colton. Qualitative methods in inverse scattering theory interaction of mechanics and mathematics: An introduction. 2006. (page 40.)

[25] Fioralba Cakoni, David Colton, and Houssem Haddar. The computation of lower bounds for the norm of the index of refraction in an anisotropic media from far field data. *The Journal of Integral Equations and Applications*, pages 203–227, 2009. (pages 4, 12, 51, and 101.)

[26] Fioralba Cakoni, David Colton, and Houssem Haddar. The interior transmission problem for regions with cavities. *SIAM Journal on Mathematical Analysis*, 42(1):145–162, 2010. (pages 4, 8, 12, 16, and 79.)

[27] Fioralba Cakoni, David Colton, and Houssem Haddar. The interior transmission problem for regions with cavities. *SIAM Journal on Mathematical Analysis*, 42(1):145–162, 2010. (pages 90, 91, and 93.)

[28] Fioralba Cakoni, David Colton, and Houssem Haddar. On the determination of dirichlet or transmission eigenvalues from far field data. *Comptes Rendus Mathematique*, 348(7-8):379–383, 2010. (pages 4, 12, 51, 101, and 107.)

[29] Fioralba Cakoni, David Colton, and Houssem Haddar. *Inverse scattering theory and transmission eigenvalues*, volume 88. SIAM, 2016. (pages 22, 24, 37, 41, 44, 45, 46, 66, 69, 72, 73, 75, 93, 107, and 111.)

[30] Fioralba Cakoni, David Colton, S Meng, and Peter Monk. Stekloff eigenvalues in inverse scattering. *SIAM Journal on Applied Mathematics*, 76(4):1737–1763, 2016. (pages 5, 13, and 102.)

[31] Fioralba Cakoni, David Colton, and Peter Monk. On the use of transmission eigenvalues to estimate the index of refraction from far field data. *Inverse Problems*, 23(2):507, 2007. (pages 4, 5, 12, 13, 51, 52, 101, and 127.)

[32] Fioralba Cakoni, Anne Cossonnière, and Houssem Haddar. Transmission eigenvalues for inhomogeneous media containing obstacles. *Inverse Probl. Imaging*, 6(3):373–398, 2012. (pages 5, 7, 8, 13, 15, 16, 52, 79, 80, 82, and 127.)

[33] Fioralba Cakoni, Drossos Gintides, and Houssem Haddar. The existence of an infinite discrete set of transmission eigenvalues. *SIAM Journal on Mathematical Analysis*, 42(1):237–255, 2010. (pages 4, 7, 8, 12, 15, 16, 51, 52, 54, 79, and 128.)

[34] Fioralba Cakoni and Houssem Haddar. On the existence of transmission eigenvalues in an inhomogeneous medium. *Applicable Analysis*, 88(4):475–493, 2009. (pages 8, 16, 54, and 79.)

[35] Fioralba Cakoni, Houssem Haddar, Shixu Meng, et al. Boundary integral equations for the transmission eigenvalue problem for maxwell's equations. *Journal of Integral Equations and Applications*, 27(3):375–406, 2015. (pages 4, 13, and 52.)

[36] Margaret Cheney. A mathematical tutorial on synthetic aperture radar. *SIAM review*, 43(2):301–312, 2001. (pages 2 and 10.)

[37] Lucas Chesnel. Interior transmission eigenvalue problem and t-coercivity. (pages 4, 13, and 51.)

[38] Lucas Chesnel. *Étude de quelques problèmes de transmission avec changement de signe. Application aux métamatériaux.* PhD thesis, 2012. (pages 4 and 12.)

[39] Weng Cho Chew. *Waves and fields in inhomogeneous media*. IEEE press, 1995. (pages 2 and 10.)

[40] Weng Cho Chew, Eric Michielssen, JM Song, and Jian-Ming Jin. *Fast and efficient algorithms in computational electromagnetics*. Artech House, Inc., 2001. (pages 1 and 9.)

[41] S Cogar, D Colton, S Meng, and P Monk. Modified transmission eigenvalues in inverse scattering theory. *Inverse Problems*, 33(12):125002, 2017. (pages 5, 13, and 102.)

[42] David Colton and Andreas Kirsch. A simple method for solving inverse scattering problems in the resonance region. *Inverse Problems*, 12(4):383–393, aug 1996. (page 21.)

[43] David Colton, Andreas Kirsch, and Lassi Päivärinta. Far-field patterns for acoustic waves in an inhomogeneous medium. *SIAM Journal on Mathematical Analysis*, 20(6):1472–1483, 1989. (pages 4, 12, 23, and 101.)

[44] David Colton and Rainer Kress. *Inverse acoustic and electromagnetic scattering theory*, volume 93. Springer Science & Business Media, 2012. (pages 19, 21, 22, 91, 109, and 113.)

[45] David Colton and Rainer Kress. *Integral equation methods in scattering theory*, volume 72. SIAM, 2013. (page 19.)

[46] David Colton and Peter Monk. A novel method for solving the inverse scattering problem for time-harmonic acoustic waves in the resonance region. *SIAM journal on applied mathematics*, 45(6):1039–1053, 1985. (pages 2, 3, 10, and 11.)

[47] David Colton and Peter Monk. The inverse scattering problem for time-harmonic acoustic waves in an inhomogeneous medium. *The Quarterly Journal of Mechanics and Applied Mathematics*, 41(1):97–125, 1988. (pages 3, 4, 12, 51, and 101.)

[48] David Colton and Peter Monk. A linear sampling method for the detection of leukemia using microwaves. *SIAM Journal on Applied Mathematics*, 58(3):926–941, 1998. (pages 1 and 9.)

[49] Anne Cossonnière and Houssem Haddar. The electromagnetic interior transmission problem for regions with cavities. *SIAM Journal on Mathematical Analysis*, 43(4):1698–1715, 2011. (pages 4, 13, and 52.)

[50] Marion Darbas and Stephanie Lohrengel. Review on mathematical modelling of electroencephalography (eeg). *Jahresbericht der Deutschen Mathematiker-Vereinigung*, 121(1):3–39, 2019. (pages 1 and 9.)

[51] Maya De Buhan and Marion Darbas. Numerical resolution of an electromagnetic inverse medium problem at fixed frequency. *Computers & Mathematics with Applications*, 74(12):3111–3128, 2017. (pages 2 and 10.)

[52] Anthony J Devaney. *Mathematical foundations of imaging, tomography and wavefield inversion*. Cambridge University Press, 2012. (pages 2 and 10.)

[53] Anne-Sophie Bonnet-Ben Dhia, Lucas Chesnel, and Patrick Ciarlet Jr. T-coercivity for the maxwell problem with sign-changing coefficients. *Communications in Partial Differential Equations*, 39(6):1007–1031, 2014. (pages 4, 13, and 52.)

[54] Anne-Sophie Bonnet-Ben Dhia, Lucas Chesnel, and Sergei A Nazarov. Non-scattering wavenumbers and far field invisibility for a finite set of incident/scattering directions. *Inverse Problems*, 31(4):045006, 2015. (pages 5 and 13.)

[55] Anne-Sophie Bonnet-Ben Dhia, Lucas Chesnel, and Sergei A Nazarov. Non-scattering wavenumbers and far field invisibility for a finite set of incident/scattering directions. *Inverse Problems*, 31(4):045006, 2015. (page 99.)

[56] Mouez Dimassi and Vesselin Petkov. Upper bound for the counting function of interior transmission eigenvalues. *arXiv preprint arXiv:1308.2594*, 2013. (pages 4 and 13.)

[57] O Dorn, H Bertete-Aguirre, JG Berryman, and GC Papanicolaou. A nonlinear inversion method for 3d electromagnetic imaging using adjoint fields. *Inverse problems*, 15(6):1523, 1999. (pages 2 and 10.)

[58] Johannes Elschner and Guanghui Hu. Uniqueness in inverse transmission scattering problems for multilayered obstacles. *Inverse problems and Imaging*, 5(4):793–813, 2011. (pages 2 and 10.)

[59] Lawrence C. Evans. *Partial differential equations*. American Mathematical Society, Providence, R.I., 2010. (page 89.)

[60] Melvin Faierman. The interior transmission problem: spectral theory. *SIAM Journal on Mathematical Analysis*, 46(1):803–819, 2014. (pages 4 and 13.)

[61] David Finch and Kyle S Hickmann. Transmission eigenvalues and thermoacoustic tomography. *Inverse Problems*, 29(10):104016, 2013. (pages 4 and 12.)

[62] Watson George Neville. *A Treatise on the Theory of Bessel Functions*. Cambridge University Press, 1966. (pages 26 and 27.)

[63] Giovanni Giorgi and Houssem Haddar. Computing estimates of material properties from transmission eigenvalues. *Inverse Problems*, 28(5):055009, 2012. (pages 5, 13, 52, 101, and 127.)

[64] Semion Gutman and Michael Klibanov. Iterative method for multi-dimensional inverse scattering problems at fixed frequencies. *Inverse Problems*, 10(3):573, 1994. (pages 2 and 10.)

[65] Martin Haas, Wolfgang Rieger, Wolfgang Rucker, and Günther Lehner. Inverse 3d acoustic and electromagnetic obstacle scattering by iterative adaptation. In *Inverse Problems of Wave Propagation and Diffraction*, pages 204–215. Springer, 1997. (pages 2 and 10.)

[66] Houssem Haddar. The interior transmission problem for anisotropic maxwell's equations and its applications to the inverse problem. *Mathematical methods in the applied sciences*, 27(18):2111–2129, 2004. (pages 5, 13, 52, 101, and 127.)

[67] P Hahner. Acoustic scattering. *Scattering*, 2001. (pages 2 and 10.)

[68] Thorsten Hohage. Logarithmic convergence rates of the iteratively regularized gauss-newton method for an inverse potential and an inverse scattering problem. *Inverse problems*, 13(5):1279, 1997. (pages 2 and 10.)

[69] Thorsten Hohage. Convergence rates of a regularized newton method in sound-hard inverse scattering. *SIAM Journal on Numerical Analysis*, 36(1):125–142, 1998. (pages 2 and 10.)

[70] Thorsten Hohage. *Iterative methods in inverse obstacle scattering: regularization theory of linear and nonlinear exponentially ill-posed problems*. PhD thesis, Johannes-Kepler-Universitat Linz, 1999. (pages 2 and 10.)

[71] Guanghui Hu, Andreas Kirsch, and Tao Yin. Factorization method in inverse interaction problems with bi-periodic interfaces between acoustic and elastic waves. *Inverse Probl. Imaging*, 10(1):103–129, 2016. (pages 3 and 11.)

[72] Guanghui Hu, Yulong Lu, and Bo Zhang. The factorization method for inverse elastic scattering from periodic structures. *Inverse Problems*, 29(11):115005, 2013. (pages 3 and 11.)

[73] Masaru Ikehata. Reconstruction of an obstacle from the scattering amplitude at a fixed frequency. *Inverse Problems*, 14(4):949, 1998. (pages 2 and 10.)

[74] W Imbriale and Raj Mittra. The two-dimensional inverse scattering problem. *IEEE Transactions on Antennas and Propagation*, 18(5):633–642, 1970. (pages 2 and 10.)

[75] Victor Isakov. On uniqueness in the invese transmission scattering problem. *Communications in Partial Differential Equations*, 15(11):1565–1586, 1990. (pages 2 and 10.)

[76] A. Kirsch. A note on Sylvester's proof of discreteness of interior transmission eigenvalues. *C. R. Math. Acad. Sci. Paris*, 354(4):377–382, 2016. (page 96.)

[77] Andreas Kirsch. The denseness of the far field patterns for the transmission problem. *IMA journal of applied mathematics*, 37(3):213–225, 1986. (pages 3, 12, and 51.)

[78] ANDREAS Kirsch. The domain derivative and two applications in inverse scattering theory. *Inverse problems*, 9(1):81, 1993. (pages 2 and 10.)

[79] Andreas Kirsch. Characterization of the shape of a scattering obstacle using the spectral data of the far field operator. *Inverse problems*, 14(6):1489, 1998. (pages 3, 11, and 63.)

[80] Andreas Kirsch. Factorization of the far-field operator for the inhomogeneous medium case and an application in inverse scattering theory. *Inverse problems*, 15(2):413, 1999. (pages 3, 11, 23, 63, and 101.)

[81] Andreas Kirsch. The music-algorithm and the factorization method in inverse scattering theory for inhomogeneous media. *Inverse problems*, 18(4):1025, 2002. (pages 3, 11, and 63.)

[82] Andreas Kirsch. *An introduction to the mathematical theory of inverse problems*, volume 120. Springer Science & Business Media, 2011. (page 32.)

[83] Andreas Kirsch and Natalia Grinberg. *The factorization method for inverse problems*, volume 36. Oxford University Press, 2008. (pages 3, 11, 19, 39, 63, and 108.)

[84] Andreas Kirsch and Rainer Kress. Uniqueness in inverse obstacle scattering (acoustics). *Inverse problems*, 9(2):285, 1993. (pages 2 and 10.)

[85] Andreas Kirsch and Armin Lechleiter. The inside–outside duality for scattering problems by inhomogeneous media. *Inverse Problems*, 29(10):104011, 2013. (pages 4, 13, and 52.)

[86] Andreas Kirsch and Xiaodong Liu. Direct and inverse acoustic scattering by a mixed-type scatterer. *Inverse Problems*, 29(6):065005, 2013. (pages 3, 11, 39, and 63.)

[87] Andreas Kirsch and Stefan Ritter. A linear sampling method for inverse scattering from an open arc. 2000. (page 103.)

[88] E. Lakshtanov and B. Vainberg. Applications of elliptic operator theory to the isotropic interior transmission eigenvalue problem. *Inverse Problems*, 29(10):104003, 2013. (page 96.)

[89] Evgeny Lakshtanov and Boris Vainberg. Applications of elliptic operator theory to the isotropic interior transmission eigenvalue problem. *Inverse Problems*, 29(10):104003, 2013. (pages 4 and 13.)

[90] Evgeny Lakshtanov and Boris Vainberg. Sharp weyl law for signed counting function of positive interior transmission eigenvalues. *SIAM Journal on Mathematical Analysis*, 47(4):3212–3234, 2015. (pages 4 and 13.)

[91] Karl J Langenberg. Applied inverse problems for acoustic, electromagnetic and elastic waves. *Basic methods of tomography and inverse problems*, 1987. (pages 2 and 10.)

[92] PD Lax. Functional analysis wiley. 9, 2002. (pages 60 and 106.)

[93] Armin Lechleiter and Stefan Peters. Determining transmission eigenvalues of anisotropic inhomogeneous media from far field data. *Commun. Math. Sci*, 13(7):1803–1827, 2015. (pages 4, 13, and 52.)

[94] Armin Lechleiter and Stefan Peters. The inside-outside duality for inverse scattering problems with near field data. *Inverse Problems*, 31(8):085004, 2015. (pages 4, 13, and 52.)

[95] Armin Lechleiter and Marcel Rennoch. Inside-outside duality and the determination of electromagnetic interior transmission eigenvalues. *SIAM Journal on Mathematical Analysis*, 47(1):684–705, 2015. (pages 4, 13, and 52.)

[96] J.-L. Lions and E. Magenes. *Problèmes aux limites non homogènes et applications*. Dunod, 1968. (page 96.)

[97] Xiaodong Liu, Bo Zhang, and Guanghui Hu. Uniqueness in the inverse scattering problem in a piecewise homogeneous medium. *Inverse Problems*, 26(1):015002, 2009. (pages 2 and 10.)

[98] Pierluigi Maponi, Maria Cristina Recchioni, and Francesco Zirilli. The use of optimization in the reconstruction of obstacles from acoustic or electromagnetic scattering data. In *Large-Scale Optimization with Applications*, pages 81–100. Springer, 1997. (pages 2 and 10.)

[99] William McLean. *Strongly Ellyptic Systems and Boundary Integral Equations*. Cambridge University Press, 2000. (page 84.)

[100] K Miller. Efficient numerical methods for backward solution of parabolic problems with variable coefficients. *Improperly Posed Boundary Value Problems, Res. Notes Math*, 1:54–64, 1975. (pages 1 and 9.)

[101] Adrian I Nachman, Lassi Päivärinta, and Ari Teirilä. On imaging obstacles inside inhomogeneous media. *Journal of Functional Analysis*, 252(2):490–516, 2007. (page 63.)

[102] Jean-Claude Nédélec. *Acoustic and electromagnetic equations: integral representations for harmonic problems*. Springer Science & Business Media, 2001. (pages 1 and 9.)

[103] H.-M. Nguyen and Q.-H. Nguyen. Discreteness of interior transmission eigenvalues revisited. *Calc. Var. Partial Differential Equations*, 56(2):51, 2017. (pages 96 and 99.)

[104] Lassi Päivärinta and John Sylvester. Transmission eigenvalues. *SIAM journal on Mathematical Analysis*, 40(2):738–753, 2008. (pages 4, 8, 12, 16, 51, 54, 60, and 79.)

[105] Vesselin Petkov and Georgi Vodev. Asymptotics of the number of the interior transmission eigenvalues. *arXiv preprint arXiv:1403.3949*, 2014. (pages 4 and 13.)

[106] Vesselin Petkov and Georgi Vodev. Localization of the interior transmission eigenvalues for a ball. *arXiv preprint arXiv:1603.04604*, 2016. (pages 4 and 13.)

[107] David L Phillips. A technique for the numerical solution of certain integral equations of the first kind. *Journal of the ACM (JACM)*, 9(1):84–97, 1962. (pages 1 and 9.)

[108] Roland Potthast. *Point sources and multipoles in inverse scattering theory*. Chapman and Hall/CRC, 2001. (pages 2 and 10.)

[109] Roland Potthast. A survey on sampling and probe methods for inverse problems. *Inverse Problems*, 22(2):R1, 2006. (pages 2 and 11.)

[110] Michael Reed and Barry Simon. *Methods of modern mathematical physics. vol. 1. Functional analysis*. Academic San Diego, 1980. (page 60.)

[111] Luc Robbiano. Counting function for interior transmission eigenvalues. *arXiv preprint arXiv:1310.6273*, 2013. (pages 4 and 13.)

[112] Luc Robbiano. Spectral analysis of the interior transmission eigenvalue problem. *Inverse Problems*, 29(10):104001, 2013. (pages 4, 13, 51, and 128.)

[113] BP Rynne and BD Sleeman. The interior transmission problem and inverse scattering from inhomogeneous media. *SIAM journal on mathematical analysis*, 22(6):1755–1762, 1991. (pages 4, 7, 12, 16, 54, 79, and 101.)

[114] J. Sylvester. Discreteness of transmission eigenvalues via upper triangular compact operators. *SIAM J. Math. Anal.*, 44(1):341–354, 2012. (page 96.)

[115] John Sylvester and Gunther Uhlmann. A global uniqueness theorem for an inverse boundary value problem. *Annals of mathematics*, pages 153–169, 1987. (pages 2 and 10.)

[116] Albert Tarantola. *Inverse problem theory and methods for model parameter estimation*, volume 89. siam, 2005. (pages 2 and 10.)

[117] Andrei Nikolaevich Tikhonov. On the regularization of ill-posed problems. In *Doklady Akademii Nauk*, volume 153, pages 49–52. Russian Academy of Sciences, 1963. (pages 1 and 9.)

[118] Andrei Nikolaevich Tikhonov. On the solution of ill-posed problems and the method of regularization. In *Doklady Akademii Nauk*, volume 151, pages 501–504. Russian Academy of Sciences, 1963. (pages 1 and 9.)

[119] Andrei Nikolaevich Tikhonov, AV Goncharsky, VV Stepanov, and Anatoly G Yagola. *Numerical methods for the solution of ill-posed problems*, volume 328. Springer Science & Business Media, 2013. (page 20.)

[120] VH Weston and WM Boerner. An inverse scattering technique for electromagnetic bistatic scattering. *Canadian Journal of Physics*, 47(11):1177–1184, 1969. (pages 2 and 10.)

[121] Hermann Weyl. Über die asymptotische verteilung der eigenwerte. *Nachrichten von der Gesellschaft der Wissenschaften zu Göttingen, Mathematisch-Physikalische Klasse*, 1911:110–117, 1911. (page 94.)

[122] Jiaqing Yang, Bo Zhang, and Haiwen Zhang. The factorization method for reconstructing a penetrable obstacle with unknown buried objects. *SIAM Journal on Applied Mathematics*, 73(2):617–635, 2013. (pages 3, 11, 39, and 63.)

université PARIS-SACLAY | École doctorale de mathématiques Hadamard (EDMH)

Titre : Sur l'utilisation de méthodes d'échantillonnages et des signatures spectrales pour la résolution de problèmes inverses en diffraction

Mots clés : analyse spectrale, problèmes inverses, analyse fonctionnelle, analyse numérique, diffraction

Résumé : Cette thèse est une contribution aux problèmes inverses en diffraction acoustique. Nous nous intéressons plus précisément au contrôle non destructif de matériaux hétérogènes tels que les matériaux composites. Surveiller l'état de ce type de matériaux en milieu industriel présente un enjeu majeur. Cependant leurs structures complexes rendent cette tâche difficile. Les méthodes dites d'échantillonnage semblent très prometteuses pour répondre à cette problématique. Nous développons ces techniques pour détecter l'apparition de défauts à partir de données de champs lointains. Les défauts considérés sont des obstacles impénétrables de type Neumann. Nous en distinguons deux catégories qui nécessitent chacune un traitement particulier : les fissures et les obstacles d'intérieur non vide.
Grâce à deux factorisations complémentaires de l'opérateur de champ lointain que nous établissons, nous montrons qu'il est possible d'approcher la solution du Problème de Transmission Intérieur (PTI) à partir des données. Le PTI est un système d'équations différentielles qui met en jeu les paramètres physiques du matériau sondé. Nous montrons qu'il est alors possible de détecter une anomalie en comparant les solutions de deux PTI différents, l'un associé aux mesures faites avant l'apparition du défaut et l'autre associé aux mesures faites après. La validité de la méthode décrite nécessite d'éviter des fréquences particulières correspondant au spectre du PTI pour lequel ce problème est mal posé. Nous montrons que ce spectre est un ensemble infini, dénombrable et sans point fini d'accumulation.
Dans le dernier chapitre, nous utilisons la notion récente de milieux artificiels pour imager des réseaux de fissures au sein d'un milieu homogène. Cette approche permet le design du problème de transmission intérieur par le choix du milieu artificiel, par exemple composé d'obstacle impénétrables. Le spectre associé est alors sensible à la présence de fissures à l'intérieur de l'obstacle artificiel. Ceci permet de quantifier localement la densité de fissure. Cependant, le calcul du spectre nécessite des données pour un intervalle de fréquence et est très coûteux en temps de calcul. Nous proposons une alternative n'utilisant qu'une seule fréquence et qui consiste à travailler avec les solutions du PTI plutôt qu'avec son spectre.

Title : On the use of sampling methods and spectral signatures for the resolution of inverse scattering problems

Keywords : spectral analysis, inverse problems, functional analysis, numerical analysis, scattering theory

Abstract : This thesis is a contribution to inverse scattering theory. We are more specifically interested in the non-destructive testing of heterogeneous materials such as composite materials by using acoustic waves. Monitoring this type of materials in an industrial environment is of major importance, but their complex structure makes this task difficult. The so-called sampling methods seem very promising to address this issue. We develop these techniques to detect the appearance of defects from far field data. The defects considered are impenetrable Neumann obstacles. We distinguish two categories of them, each requiring a specific treatment: cracks and obstacles with non empty interior.
Thanks to the two complementary factorizations of the far field operator that we establish, we show that it is possible to approach the solution of the Interior Transmission Problem (ITP) from the data. The ITP is a system of partial differential equations that takes into account the physical parameters of the material being surveyed. We show that it is then possible to detect an anomaly by comparing the solutions of two different ITPs, one associated with measurements made before the defect appeared and the other one associated with measurements made after. The validity of the described method requires avoiding particular frequencies, which are the elements of the ITP spectrum for which this problem is not well posed. We show that this spectrum is an infinite set, countable and without finite accumulation points.
In the last chapter, we use the recent notion of artificial backgrounds to image crack networks embedded in a homogeneous background. This approach allows us to design a transmission problem with the choice of the artificial background, for instance made of an obstacle. The associated spectrum is then sensitive to the presence of cracks inside the artificial obstacle. This allows to quantify locally the crack density. However, the computation of the spectrum requires data at several frequencies and is expensive in terms of calculations. We propose an alternative method using only data at fixed frequency and which consists in working with the solutions of the ITP instead of it's spectrum.

Université Paris-Saclay
Espace Technologique / Immeuble Discovery
Route de l'Orme aux Merisiers RD 128 / 91190 Saint-Aubin, France